Birkbeck
UNIVERSITY OF LONDON

The Interactions between Fungi and British Heritage Buildings: The Effects

of Fungal Growth on Organic Collections and Conservation Implications

Thesis submitted by

Sophie Downes

For the degree of

Doctor of Philosophy

School of Science

Department of Biological Science

Birkbeck, University of London

September 2017

Declaration

I hereby confirm that this thesis is my own work and that the material from other sources in this work has been appropriately and fully acknowledged.

Sophie Downes

Dedication

The Richard, Jane and my family, thank you for putting up with me throughout this whole process and to Sheila, for starting me along this road.

Abstract

Heritage tourism is an important part of the economy of the United Kingdom with a wide range of historic buildings and integral collections open to the public. One of the main attractions to these properties is the immersive experience of walking through rooms with objects in-situ and on open display. This however creates issues regarding the conservation of these structures due to the increase in opening hours, limited environmental control and increased exposure of collections to external elements.

The National Trust and English Heritage each provided ten heritage properties to survey, in order to determine the species of fungi present in the air and colonising collections during the four seasons. Environmental readings and condition surveys were conducted in order to assess the potential influence of the building envelope, geographical location, furnishing and collections of a property on the number of colony forming units (CFU/m^3) and the species encountered. Accurate identities of cultures were obtained using morphologically typing before the use of polymerase chain reactions to obtain RAPD (random amplified polymorphic DNA) barcodes and Sanger sequencing of the ribosomal internal transcribed spacer region. Knowing the abundance and identity of spores will enable the development of risk management systems.

The physical, chemical and mechanical implications of the growth of the three most abundant fungi on a range of proteinaceous and cellulosic materials were assessed.

A novel method for the mounting of live fungi in-situ on materials and visualisation using confocal fluorescence laser scanning microscopy informed the way in which fungi grow into substrates to a potential depth of 150μm. Spectrodensitometry was also employed to determine the permanent colour alterations that can be expected from intense fungal growth.

Attenuated total reflectance Fourier transform infrared spectroscopy enabled the assessment of surface chemical changes to organic materials as a result of fungal growth

High performance liquid chromatography and mass spectrometry (HPLC-MS) was used to analyse crude solvent extracts from growth substrates after incubation with fungi in order to determine the level of volatile/non-volatile organic compounds produced by each species. Synthetic enzyme assays were also conducted on model heritage substrates in order to assess the potential of fungi to utilise a range of nutritional sources.

The tensile properties of growth substrates were assessed to indicate any mechanical alterations to the fibres as a result of fungal growth.

The effectiveness of remedial conservation treatments relating to fungi were assessed, along with the implications of the use of biocides. Anti-fungal compounds were isolated from plant based sources and identified by HPLC-MS. A methodology for the safe introduction of these compounds is discussed along with future proposals for the treatment, display and storage of organic historic objects.

Experimental results have been used to generate potential risk models and inform preventive and remedial conservation recommendations.

Acknowledgements

Contents

Figures

Tables

Equations

1. Introduction

Since the late 18th century tourists have been paying to view the interiors of Britain's great houses. Cultural tourism is now a recognised industry which now contributes a significant portion to the gross domestic product (GDP) of some countries and is the primary source of revenue for some local communities. The heritage industry represented about 28% of all tourism within the United Kingdom during the 1990s (Garrod & Fyall 2000). In 2015 heritage tourism contributed £20.2 billion to the UK GDP, equating to 192 million heritage motivated trips (Oxford Economics, 2016). This economy is driven by both domestic and foreign visitors with an 18% increase in international visitors to heritage attractions since the last report published in 2013 (Beyrouty & Tessler, 2013; Oxford Economics, 2016). With the financial impact of maintaining historic buildings, cuts to government funded projects and the potentially significant income generated by cultural tourism; the focus of heritage organisations has now necessarily shifted from one of passive guardianship, to a more economic exercise in making the properties and their resources available to the public (Janiskee 1996). With the increased access to properties, through free flowing tourist routes and increased opening hours, properties and their collections are at increasing risk of damage, with fewer dedicated conservation resources.

This research aims to look into the risk of opportunistic fungi to historic interiors, with particular focus on organic materials commonly found within collections. Sponsored by two of the largest heritage organisations in the UK (The National Trust and English Heritage), the project looks in detail at 20 varied heritage buildings, their environment and the fungi found within them over the course of one year (autumn 2013 – summer 2014). Post survey, the most commonly encountered fungi were assessed for their damage potential to organic materials and how effective conservation cleaning methods were at their removal. Potential preventive and remedial treatments for fungal growth on collections were then evaluated.

1.1 Historic buildings in the UK

The title of historic building can sometimes be misleading as it can refer to many different build structures, not to mention the geographical location and climatic conditions (Camuffo et al. 2013). Within the UK there is a broad range of listed buildings, deemed to be of national, historic of architectural importance and therefore protected. The building types extend to industrial sites, wartime bunkers, cottages, castles, mansions and palaces. This makes a comparison of environments and fungal loads difficult, unless common features can be found and a building classification system created, as was done with the Climate for Culture project and microclimate

modelling for museum buildings (Leissner et al. 2015; Martens 2012). Alterations to historic structures also need to be considered, with the introduction of modern amenities (internal kitchens, bathrooms and washing facilities, central heating etc.), all of which can contribute to a higher atmospheric moisture content within buildings that were not designed with such ventilation requirements. Increasing visitor numbers will also have an impact on the internal environment, with increased humidity and an impact on soiling and particle levels, including spores (Camuffo et al. 2001).

1.1.1 Climatic conditions

The environment in which collections are stored can be critical to prevent mechanical, physical and biological damage to collections. As historic buildings are open to the public and objects are ordinarily on open display, it is difficult to maintain a stable environment and due to the high air exchange rate with the exterior (promoted by visitor access) the collections are often affected by the external climate (Lankester & Brimblecombe 2012b). Although a lot of properties now have integrated radiotelemetric systems to monitor the environment within rooms, the sensors are not always located in the best position to reflect the true conditions of the room (Sterflinger 2010) and so specific microclimates and changes in specific regions are not always recorded. Within buildings, there will also be varying conditions due to differences in the building envelope (thicker walls can help to buffer environmental changes), air exchange, exposure to solar heat and light, external features and the tourist route through the property (Camuffo et al. 2001). Therefore some spaces will be more vulnerable to climatic changes and the formation of microclimates. The use of environmental control mechanisms within properties does help to mitigate the worst conditions that can occur. However, it is the fluctuation of conditions that heating, ventilation and air conditioning systems (HVAC) really help to moderate.

With the effects of global warming already becoming apparent, it is clear that historic buildings will be vulnerable. There have been numerous projects investigating the potential effects and working on predictive models so that properties can be prepared and act in advance.

Lankester & Brimblecombe (2012a), highlight the fact that the effects of climate change may already have been experienced elsewhere so the solutions to problems will already be available. This is true to a certain degree when looking at specific events like flooding or increased rainfall. It does not, however, take into account the increased variability and extremes in weather that we are likely to experience. Future variations in weather may promote unfavourable internal microclimates and potentially cause structural and collection based damage (Huijbregts et al.

2012). This has already been witnessed during snow melts, intense rainfall and flooding within properties involved in this project.

Over the past few years, flooding of properties has increased and will likely continue to do so. According to Taylor et al., (2011) flood management will be moving from "prevention towards resilience". Flooding can dramatically increase fungal growth in a property and have far reaching effects, with increased internal fungal presence (in comparison to the external) even 3 months after treatment (Taylor et al. 2011).

Although extreme climate differences, like flooding, cannot be predicted some environmental forecast models do have some very positive points. Huijbregts et al., (2012) used external environmental data and weather forecast to predict the moisture content of interiors. However, due to the complex variables of historic interiors, not everything can be taken into account and although this model considers the effect furnishings may have on buffering the environment, visitor impact is not included. This factor may be accounted for in the 10% variation between predicted and actual conditions (Huijbregts et al. 2012).

Another model represents the predicted fungal growth within buildings based on climate forecasts (Huijbregts et al. 2012). This is based on the work of Sedlbauer (Sedlbauer 2001; krus et al. 2007; Martens 2012) and represents the likelihood of fungal growth occurring on materials according to the moisture content, based on laboratory studies. This project aims to create a similar predictive tool based on observed growth within historic buildings.

1.1.2 Collections and display

Due to the extreme range of different historic buildings found within the UK, it is difficult to define the collections that may be encountered. With regards to fungi, it is the organic materials that are vulnerable to degradation by their growth, although it is possible for them to colonise surface coatings, adhesives and dust associated with inorganic structures. Non-residential buildings tend to have the lowest concentration of vulnerable materials, although the potential for fungi to colonise dust and surface coatings was still present. This could be detrimental to metals and certain stone types, due to the acidic and volatile metabolic products of fungal growth (Kowalik 1984). Buildings with a high degree of organic furnishings are likely to be more vulnerable to fungal colonisation due to the increased surface area for deposition, the hygroscopic nature of some materials, the creation of microclimates and the availability of nutrients. Historic objects that have already undergone degradation as part of their natural life (mechanical wear, light and humidity damage, chemical degradation) may be more vulnerable

to fungi, due to the potential for a weakened state of fibres and a reduction in the complexity of structures.

From interview with property staff, it is clear that they believe the growth of mould on objects is increasing. Although this may be due to better education and a greater awareness of the problem, Lankester & Brimblecombe (2012b) also support this observation.

This work aimed to evaluate the different conditions that can be encountered within twenty historic buildings, both in terms of the internal climate and the collections. By categorising the buildings according to geographical and landscaping features, building envelope, the function of the building, the furnishings and collections, it was hoped that the most important features associated with a high internal fungal load and whether growth would occur could be determined. This would enable more effective risk assessments for buildings and collections, enabling staff to prioritise time and resources and potentially mitigate the effect of features that pose a specific threat.

1.2 Fungi found within buildings

Some fungi are opportunistic and their presence within buildings, whether as airborne spores/particles, as a result of active growth or transported in by human movement, is a given. The majority of fungal matter should come from an external source (World Health Organization 2009), but there are a lot of complex variables and the source of spores is not always clear (Sterflinger 2010; Mandrioli & Saiz-Jimenez 1997).

The particle concentration of fungal spores within buildings is recommended to be between 10^3-10^4 /m^3 but this can be severely affected by the external climatic conditions (Mandrioli & Saiz-Jimenez 1997). The fungal load can also be influenced by the housekeeping regime of the property since fungal spores of between 3-30μm can have a settling velocity of 0.05-2.00cm/s^{-1} (Mandrioli & Saiz-Jimenez 1997), supporting the view that a large proportion of dust is formed of fungal spores. It has been noted that dust and soiling are colonised by fungi, in particular *Aspergillus* species, and that this substrate acts as a source of nutrition (Haleem Khan & Mohan Karuppayil 2012; Taylor et al. 2011). The furnishings of a location can also influence the fungal content of a space with carpeted areas of a museum containing 10 times the spores of an uncarpeted area (Camuffo et al. 2001). This is likely also to be true of historic houses with carpet, and this phenomenon may be amplified by the level of furnishings, also on open display.

The most common way of determining fungal load is through air sampling, which can give an indication of the viable fungal material, fungal particles and volatile chemicals of fungal origin

(World Health Organization 2009; Górny et al. 2002; Cabral 2010; Green et al. 2005). The fungal load from surfaces and dust can also give an indication of the health of environments (Haleem Khan & Mohan Karuppayil 2012; Karbowska-Berent et al. 2011).

1.2.1 Identification

The fungi that are likely to be encountered within an indoor sample occur in three phyla; *Ascomycota, Basidiomycota* and *Zygomycota*, the most common of which being the *Ascomycota*. It has been reported that humans may be associated with 600 fungal species, but fewer than 50 are commonly identified during studies on indoor air quality (Haleem Khan & Mohan Karuppayil 2012). Spores from *Cladosporium* species are believed to be the most abundant fungal isolates from the air (Bensch et al. 2005; Flannigan 1997). There has been little published work specifically on the species of fungi that are found within the British historical property. Most of the results have to be isolated from papers on specific objects (see Chapter 2) and are mostly published from data collected outside of the UK.

1.2.2 Growth requirements

When materials are colonised, there may be a hierarchy of fungi able to germinate and grow based on available nutrients, but primarily water availability. Water availability was found to be the most important factor associated with indoor air quality in Canadian homes (Li & Kendrick 1996). Fungi are considered to significantly contribute to the biodeterioration of heritage collections through utilising moisture collected in microclimates; which may be formed due to building structure flaws, condensation stagnant air and stored water in materials (Sterflinger & Pinzari 2012).

Xerophytes, able to grow in conditions of lower water availability (below $0.8a_w$) such as *Aspergillus* and *Penicillium* (Pitt 1975) are deemed to be primary colonisers of indoor environments (Fog Nielsen 2002). It has also been noted that the more biodegradable the substrate is, the less water that is required by fungi (Sterflinger 2010). This indicated that historic collections are likely to be vulnerable.

1.2.3 Impact on collections

The growth of fungi on a substrate can cause significant damage due to enzymatic activity, the release of metabolic products and their ability to adapt and grow on materials with different nutritional and water contents; a fact which is however often not adequately communicated to heritage professionals (Sterflinger 2010). Historic objects will routinely have fungal matter on

their surfaces, but only under conditions favourable to growth will they cause damage to these substrates (Dornieden et al. 2001).

Damage to the structure of buildings is largely due to the action of Basidiomycetes on timber (Tiano 2001). This can also be the case for wooden items within the building, although the hygroscopic and nutrient rich nature of furniture glue, waxes, sizes and coatings have been observed to be more common sources of fungal colonisation (Kowalik 1984). This phenomena is also noticed in relation to books, paintings, leather, textiles and paper ephemera that may have adhesives or coatings, including those used during the course of conservation.

Libraries are often affected by fungal growth and it has long been reported that this growth becomes embedded within the leather of bindings, alters the texture and stains the surface of the book (Blades 2013). Species of *Aspergillus*, *Penicillium*, *Cladosporium*, *Paecilomyces and Trichoderma* have been found to grow on adhesives; *Aspergillus*, *Alternaria*, *Cladosporium*, *Fusarium*, *Gliomastix*, *Paecilomyces, Penicillium* and *Scopulariopsis* were found to colonies wax; whilst *Penicillium*, *Aspergillus* and *Paecilomyces* have even been found to develop on inks.

Textiles are also vulnerable to colonisation by fungi, regardless of their composition (cellulosic or proteinaceous). Proteinaceous textiles, parchment and leather are vulnerable, depending on the amino acid composition and form of protein. Keratin, found in wool, has been colonised by *Chaetomium*, *Aspergillus*, *Fusarium*, *Penicillium* and *Trichoderma* species (Kowalik 1980). Fibroin, found in silk, is thought to be more resistant to fungal growth; even after the protective, amorphous seracin protein has been removed (through degumming). Cellulosic materials, including paper and wood are more or less vulnerable depending on the other fibre components (lignin, pectin, waxes hemicelluloses etc.); the greater the lignin content, the more resistant to fungal growth a textile is (Kowalik 1980). If lignin is chemically removed, as with some papers, then the material will be less resistant to fungi. The most prevalent species of fungi that attack cellulosic materials are *Chaetomium*, *Stachybotrys*, *Fusarium*, *Alternaria*, *Trichoderma*, *Trichodadium*, *Gliomastix*, *Scopulariopsis*, *Paecilomyces*, *Aspergillus* and *Penicillium*. There is also evidence that the *Zygomycetes Mucor* and *Rhizopus* can colonise textiles (Kowalik 1980). Wood is the most resistant to fungal attack due to the high lignin content and depending on the species of tree, wood can be between 4-10 times more resistant than the other cellulosic fibre components. Excluding the *Basidiomycetes,* fungi that have been found to colonise wood include *Cladosporium*, *Chaetomium, Alternaria, Trichoderma and Aureobasidium.*

Aside from the structural damage that can be done to objects, there is also the risk of aesthetic damage (Sterflinger & Pinzari 2012) and a visual distortion created by active growth and metabolic products such as pigments and volatile chemicals (Tiano 2001).

There are other organisms that can be associated with fungal growth that may also have a detrimental effect on collections as secondary colonisers; bacteria and a wide variety of insects have been linked with fungal colonies and insects may be a potential route for the spread of spores (Trovão et al. 2013; Fog Nielsen 2002).

1.2.4 Impact on human health

The concentration of spores and volatile metabolic compounds from fungi growing within an indoor environment are potentially greater than those found outside. The severity of reaction to fungal products (spores, fragments and chemicals) will depend on the individual and exposure time, but humans can potentially suffer from irritation to producing an allergic, toxic or infectious response; in order of severity (Górny et al. 2002): fungal glycoproteins, (1,3)-β-D-glucans, microbial volatile organic compounds (MVOCs) and mycotoxins (Fog Nielsen 2002; World Health Organization 2009).

This study of the twenty historic properties included air sampling both internally and externally in order to assess the fungal load and create a representative population for historic buildings. This was achieved by using random cultures from at least four locations at each property four times in one year (autumn, winter, spring & summer). The cultures were morphologically typed and then molecular techniques used to sort by barcoding and then process for Sanger sequencing. Identification was performed by BLAST, of the ITS region sequences, to published examples in Genbank. The fungal population was then analysed in relation to the environmental survey data and key build features identified as fungal load and growth risk factors.

The risk to different organic substrates present within collections was also evaluated by using the most abundant fungal species found during the survey and the biofilm that naturally occurred on the surface of each material. Physical, chemical and mechanical changes to whole materials were assessed, along with the species potential for enzyme and secondary metabolic production. The aim of this section was to quantify the damage that fungi can inflict and highlight the risks to specific materials within collections and inform about the potential damage that can be expected and potential modes of cleaning.

By creating an easy method to interpret fungal growth in properties, staff would be able to determine whether building environments had a safe fungal content, if there were species that

were potentially hazardous and whether it was likely that there was an internal source of spores. This could save both time and money for the property as well as improving the health and safety of the building.

1.3 The removal and prevention of growth in buildings

1.3.1 Past treatments

There have been many methods for the removal and prevention of fungal growth and the treatment of historic objects has involved using techniques and materials from many other industries. Some of the earliest recorded treatments for the home were by herbalists (Pechey 1694; Culpeper 1653; Gerard 1597) and involved the use of plants; treatments which are still used today by some (Hatfield 2009). Plants such as basil, bay, garlic liquorice, marjoram, juniper, oregano, sage and thyme were used for the treatment of clothes, furnishings and floor coverings and contain different, potentially fungicidal, volatile compounds including terpenes, ketones, flavonols, phenols, to name a few. As a response to antibiotic resistance and the constant search for effective biocides, there has been a revival of plant based natural products as specific fungicides, which will be discussed in Chapter 6.

It has always been known that ventilation and air flow were important to prevent fungal growth and general building health. There are many buildings that have ornate ventilation panes in their windows and there are records of residents feeling a breeze through the house, due to open windows (Sackville-West 1998). Housekeeping records and domestic manuals also document and recommend the cleaning (removal of dirt & dust, laundry and cleansing of pests) and ventilation of properties. Mrs Beeton recommends the introduction of air bricks and vents for the ventilation of rooms, not just those with an outside wall (Beeton 1890). Archivists were also aware of this, Bernard Simon (1761-1781) recommended ventilation and cleaning within archives, Blades (1881) noted that fungal growth is facilitated by a lack of ventilation and Count Stanislaw Dunin-Borkowski (1827) noted that damp should be driven out of libraries, certain woods were more efficacious for preventing pests and that binding adhesives could be doctored with pest preventing additions, such as bitter herbs and pepper (Simon 2013; Dunin-Borkowski 2013; Blades 2013).

Previously within curated collections, environmental and volatile treatments were used in the removal of pests. The use of moist heat treatments, such as an autoclave were recommended, after testing, rapid drying of objects and radiation treatment were suggested for textile objects; along with ethylene oxide, quaternary ammonium compounds, salicylanilide, P-

dichlorobenzene, pentachlorophenol, formaldehyde, thymol and others (Leene 1972). Within collections in other parts of the world, plant based volatile compounds have been used effectively (Agrawal 1981), including neem leaves and camphor.

1.3.2 Present treatments

Preventive conservation can be one of the most cost effective ways of managing collections and is widely used throughout the heritage sector. Vulnerable materials are ideally displayed within environmental parameters that reduce the rate of degradation and increase the time for which these collections can be enjoyed. This is particularly pertinent for organic materials such as textiles, paper and leather, which are displayed at an ambient temperature with a relative humidity of below 65% (believed to be the threshold for preventing microbiological growth), reduced light and prevention of pollution and dust build up. Within historic buildings, the context of the collection is a key factor and that visitors can view objects within an original setting, without the visual distortion of display cases. However, this method of display makes the management of environments very difficult. Although mediations in the form of conservation heating, dehumidification and air flow management are made, with the sheer volume of objects often within a space and often irregular building envelopes to contend with, microclimates can still form in which fungi can grow. There is also reduced access for heritage professionals to collections for cleaning and monitoring due to the increase in opening times and the shortening of the housekeeping season.

During preliminary work, it was shown that the various remedial conservation treatments of textiles have little effect on the removal of viable spores which can then germinate after less than a month of being returned to the same environment (Downes 2013). This may be due to the fact that large numbers of spores and mycelium become embedded within the surface of textured materials (Kowalik 1984) and some treatments may in fact contribute to activating dormant, viable spores that may not have been removed (Florian 2007a).

1.3.3 Future treatments

Fungal contamination is an issue to many other industries, aside from conservation and there have been innovative solutions that may be applicable to the heritage sector.

The medical sector has produced coatings and products to reduce the spread of contamination, disease prevention and the treatment of antibiotic resistant microbes. There is a wide range of material treatments that have been developed including both solid and flexible surfaces, which could be potentially adapted for use within conservation. This has in fact already been tested in

the case of copper, zinc and silver nano-particles, although these metals are not always effective biocides against fungi (Kowalik 1984). There are also many mechanisms for the controlled release of compounds and targeted drug delivery that could be adapted for use within a heritage setting.

Many potentially volatile, anti-microbial compounds are used within the cosmetics industry for the control of skin colonisation. Oxidised natural products from plants like tea tree and eucalyptus are toxic to humans, but can be microencapsulated for controlled release. This technology shows potential for use in conservation adhesives and coatings that would otherwise be vulnerable to fungal colonisation.

The spoilage of food is a worldwide problem and there have been numerous attempts to mitigate the growth of fungi in stored goods and to improve the shelf life of pre-packaged food products; some of which may be applicable to objects packaged for long term storage and archival settings.

1.4 Outline and objectives

This study aims to characterise the airborne fungi found within heritage buildings with the United Kingdom and determine whether there are common building features that impact the growth of fungi in general the presence of specific species and high colony forming unit counts that could lead to colonisation of objects and risks to human health (Chapter 2).

It is assumed that fungi cause damage to organic heritage materials. This will be evaluated through experimental work into the effect that common fungi have on the physical, chemical and mechanical properties during growth (Chapters 3-5).

The effectiveness of selected conservation cleaning methods against common fungi and on a range of organic substrates were evaluated. The potential of disinfection and growth prevention methods were assessed along with the fungicidal potential of plant natural products and methods of deployment (Chapter 6).

Fungi are ubiquitous, it is hoped that this work will provide information and practical advice on how to manage their growth and treatment on historic objects on open display.

2. The Fungi of Historic Buildings within the United Kingdom

An exploratory survey of 20 English Heritage and National Trust case study properties is undertaken and the data collected analysed in regards to forming a predictive tool for property risk management. The collection and identification of a representative airborne fungal population, using high throughput molecular techniques, is introduced and the results represented using biodiversity indices. The environmental and building survey data was modelled to assess the significant features affecting the quantity and identity of fungi found, and risk factors for human health and collection safety.

2.1 The fungal load in air

Air is the most common method of dispersal employed by fungi (Li & Kendrick, 1995). When considering indoor environments, such as heritage buildings, sources of fungal material could be external, internal or influenced by the human visitor flow (Camuffo *et al*., 2001; Kalogerakis *et al.*, 2005; Korpi *et al.*, 1997; Li & Kendrick, 1996; Stetzenbach, 1998).

One of the most frequent reasons for studying air quality has been for assessing potential health implications from both the quantity and specific species of airborne fungal material (Kalogerakis et al. 2005; Haleem Khan & Mohan Karuppayil 2012). The data from studies like these can be applied to heritage buildings as reference populations.

According to Cabral, for normal buildings the majority of fungal species recorded should come from an outside source, in addition to the total indoor count being lower than the exterior (Cabral 2010). The most abundant fungal constituent of external air is reported to be *Cladosporium* (Bensch *et al.*, 2005; Ingold, 1953) with lower numbers of *Penicillium*, *Alternarium*, *Epicoccum* and *Aspergillus*.

The abundance and species recorded are seasonal and their dispersal is largely affected by meteorological patterns (Ingold, 1953; Li & Kendrick, 1995). Ingold also stated that there would be higher concentrations of spores during the summer and autumn but relatively few in the winter, which corresponds to the seasonal development of fungi. The previously mentioned species are all light weight spores produced from *Ascomycete,* species that are easily dispersed in the air. Rao *et al*. (1996) conducted a literature review of government and health organisations into safe quantitative standards for airborne fungi (Rao *et al.,* 1996). There was no clear consensus on indoor levels of colony forming units (CFU) m^3 but The World Health

Organisation (WHO) summarised that there are likely to be few, up to several thousand viable colonies in indoor air depending on the conditions and air exchange but 500 CFU/m^3 has been used as a limit in indoor winter samples (World Health Organization 2009). Sedlbauer (Sedlbauer 2001) suggests, based on work conducted by Senkpiel (in Germany), that counts inside buildings could safely be 100CFU/m^3 over that of the outside. The CFUm^3 of both indoor and outdoor air will be calculated as part of this study as well as the biodiversity of samples collected so it will be possible to gauge the quality of air within properties.

2.1.1 Indoor air quality

Indoor air quality has been studied for both residential and occupational environments so there is literature available regarding the species that could be encountered and relative abundance (Khan & Karuppayil, 2012; Kalogerakis *et al.*, 2005; Korpi *et al.*, 1997; Lee *et al.*, 2006; Pei-chih & Chia-yin, 2000). However, a large proportion of these studies have been conducted abroad and in buildings with different environmental parameters to those being considered during this study.

Biological sampling across all fields requires the study of a small section of the total population that can provide generalisations about the community as a whole. In order to create a quantified and statistically viable model population for heritage properties, a stratified random sampling method was adopted. It was hoped that this would provide data regarding the biodiversity of fungi encountered in fundamentally different heritage buildings as well as the environmental conditions and potential modes of nutrition in each sampling location (McDonald 1997; Marshall 1996).

2.1.2 Fungal populations

Fungal populations have been identified in specific heritage locations such as libraries and archives (Borrego *et al.*, 2010; Karbowska-Berent *et al.*, 2011) with the most abundant genera being *Penicillium*, followed by *Cladosporium*, *Alternaria* and *Aspergillus*. However, a representative population has not yet been proposed for buildings in general and most of the studies were again, performed outside of the UK.

Other fungal populations isolated relate to specific objects and surfaces such as paper based objects (Florian & Manning 2000; Arai 2000; Corte et al. 2003), wood (Blanchette, 2000; Koziróg *et al.*, 2014), painted surfaces (Garg et al. 1995) and textiles (Kavkler & Demšar, 2012; Pangallo *et al.*, 2013). The fungi isolated have all selectively colonised the host material, most likely from

an airborne source. The most commonly isolated species included *Penicillium*, *Alternaria*, *Aspergillus*, *Cladosporium, Chaetomium, Epicoccum* and *Eurotium.*

The consensus of the most abundant airborne genera recorded in literature are *Cladosporium*, *Penicillium, Aspergillus, Alternaria, Fusarium* and *Epicoccum* (Ingold, 1953; Li & Kendrick, 1995; Li & Kendrick, 1996; Scott, 2001; Shelton *et al.*,2002) Through morphological typing and molecular techniques, the collected historic house population will be identified to determine whether the same genera are isolated and their relative abundance.

2.1.3 Methods of identification

Previous methods of identification for taxonomic studies have relied on extensive morphological analysis. This is very time consuming, labour intensive and often unreliable due to limitations in cultural and morphological characteristics (Wu & Hsiang 2000; Johannesson et al. 2000; Stummer et al. 2000; Schmidt & Moreth 2000).

The accurate identification of fungi from morphology alone also requires a high degree of experience and expertise (Flannigan 1997). Flannigan also surmises that in order to counteract the problem of no one technique being adequate to assess the indoor air quality, one sampling technique should be used to collect the sample and then further culture and analytical techniques applied. That is the methodology that this study will adopt.

In order reduce the margin of error involved in morphological interpretation, this project will largely rely on the use of molecular techniques for the identification of the fungal population collected.

The extraction of DNA from fungi has often had a varied approach, from the very simple homogenisation of mycelium in water (Schmidt & Moreth 2000) to the complex processes involving thermo-cycling in a lysis buffer and then extraction with volatile chemicals (Johannesson et al. 2000; Kong et al. 2000), a process that can take up to 4 hours.

Bioline Reagents Ltd were in the process of developing a fungal DNA extraction buffer for direct PCR and donated a lot of time and resources to this project which would test the capabilities of this new methodology. Unfortunately, as this product is in the process of production, it is not possible to discuss the composition of the extraction buffer.

The development of fungal molecular biology has largely relied on the rDNA regions between the 18S SSU gene, the 5.8S gene and the 28S LSU gene. These two regions (ITS 1 and ITS 2) are highly variable compared to the more conserved genes that they separate (Martin & Rygiewicz 2005).

The primers used to test the PCR capabilities of the Bioline kit were the primer pair of ITS4 (reverse) and ITS5 (forward). The use of ITS regions for fungal "barcoding" is a widely used practice (Schoch et al. 2012). ITS4 amplifies the 28s rDNA in region 2 and ITS5 amplifies the 18s rDNA of region 1.

More commonly than ITS 4 and ITS5 as a primer pair, ITS1 and ITS4 are used (Martin & Rygiewicz 2005; Held et al. 2005; Arenz & Blanchette 2011; Duncan et al. 2010; Shehata, Mukherjee, Aboulatta, et al. 2008; Pangallo et al. 2013). However, in a study analysing PCR bias in ITS primers, it was determined that ITS5 was generally more reliable than ITS1 under strict PCR conditions (Bellemain et al. 2010). ITS5 also amplified a higher proportion of *Basidiomycetes* than ITS1. As ITS4 is biased towards *Ascomycetes*, this pair combination covers the majority of fungal Phyla. In addition, this primer pair also amplified the greatest proportion of non-dikarya (not *Basidiomycete* or *Ascomycete*) sequences (Bellemain et al. 2010). Although this experiment was carried out *in-silico*, it does support the findings of this mycology group, who have been using this primer pair for some time with great success. This combination does also seem to offer the greatest reliability of amplification for what is a very mixed population study.

The use of microsatellite primers to create random amplified polymorphic DNA (RAPD) profiles is a useful way of determining similar species that was hoped would be more reliable than the morphological comparisons of isolates (Wu & Hsiang 2000; Shehata, Mukherjee, Aboulatta, et al. 2008; Cogliati et al. 2007). The short repetitive primer section binds randomly to DNA with the same motif to produce different polymorphic bands after PCR (Schmidt & Moreth 2000). These banding patterns can distinguish different genera but can produce rather homologous results for different isolates of the same species (Schmidt & Moreth 2000).

This study will use the microsatellite GACA$_4$, as it has been proven to be effective over a wide range of fungal species and should offer a good degree of success for an unknown population (Shehata, Mukherjee, Aboulatta, et al. 2008; Cogliati et al. 2007; López-ribot et al. 2000; Faggi et al. 2001; Cardinali et al. 2002).

Using an ITS primer pair is a widely accepted methodology for identification of fungal isolates by sequencing (Schabereiter-Gurtner et al. 2001; Möhlenhoff et al. 2001; Nilsson et al. 2009; Wu & Hsiang 2000; Schoch et al. 2012). This study will utilise this technique for the cultures that have individual banding patterns. Post Sanger sequencing, aligned, contiguous sequences can then be compared to published fungal nucleotides stored in Genbank using the NCBI BLASTn suite (Arenz & Blanchette 2011; Ortiz et al. 2014; Duncan et al. 2010).

2.1.4 Diversity indices

No one diversity index can fully describe a population over a wide range of variable. To enable a broad spectrum of analysis and to avoid "erroneous conclusions", a number of indices should be applied to the data (Beisel et al. 2003).

Species richness is the commonly adopted expression for the number of species in a given population. This richness can be investigated further with the use of a species evenness calculation such as E_{var} (Smith & Wilson 1996) that looks at the evenness of species distribution within a population.

The Shannon Wiener diversity index (H') has been used in other fungal isolation studies (Trovão et al. 2013; Humphrey et al. 2000) to represent biodiversity, taking into account the species richness, abundance and their distribution through the population.

The above methods will help to inform on the structure of the fungal population isolated from historic buildings and indicate whether there are any seasonal and location based variations in biodiversity.

2.1.5 Environmental conditions

Utilising the environmental data readings and building characteristics has been used extensively throughout the Climate for Culture project (Antretter 2013) and for evaluating the future risks to buildings and collections from climate change (Lankester & Brimblecombe 2012 a & b). Hydrothermal data from buildings have also been used to develop predictive models for indicating the potential germination and growth rate of fungi (Sedlbauer 2001; Sedlbauer et al. 2001; krus et al. 2007). Largely, these models are based on isopleths generated from laboratory experiments and climate guidelines based on figures published by ASHRAE (Huijbregts et al. 2012).

The present study aimed to generate a predictive model based on data collected from case study properties and whether fungal growth was visibly growing on objects within specific environments.

2.1.6 Objectives

- Identify and quantify the fungi found within heritage buildings

- Assess geographical, building and environmental features that may contribute to the presence of fungi within a historic room

- Determine the building features that significantly influence whether a space will have fungal growth on collections and if the air will have a high colony forming unit count

2.2 Materials and Methods

2.2.1 Sampling methods

Heritage buildings from The National Trust and English Heritage were profiled for the project and the 20 most suitable selected for the survey phase (Figure 2.1). The buildings were classified and an assessment matrix created based on the work of Martens in European museums (Martens 2012). A categorical grading of the local geography, building features and collections

| Belsay Hall |
| Bolsover Castle |
| Brodsworth Hall |
| Dover Wartime Tunnels |
| Gainsborough Old Hall |
| Great Yarmouth Row Houses |
| Kenwood House |
| Osborne House |
| Stokesay Castle |
| York Cold War Bunker |
| Anglesey Abbey |
| Arlington Court and Carriage Museum |
| Castle Coole |
| Charlecote Park |
| Claydon House |
| Dyffryn House and Gardens |
| Hardwick Hall |
| Knole |
| Lanhydrock House |
| Sudbury Hall |

Figure 2.1- The geographical distribution of the historic buildings surveyed over the course of the year

was created based on the features detailed in Table 2.1, to enable statistical analysis and modelling.

At least four locations per property were selected for survey. With the assistance of building staff, inside rooms were to include any areas of the building that may have had fungal growth in the past as well as ensuring that the different wings and floors of the property were represented as far as possible. An outside apace was also sampled in order to calibrate the indoor samples.

The environmental conditions within the spaces (temperature and relative humidity) were recorded using a calibrated thermo-hygrometer in 5 locations; 4 walls and the centre of the room. The sensor was left to equilibrate for 10 minutes prior to readings being recorded.

Variable	Example
Geographical location	Latitude, longitude, Elevation (m)
Surrounding Geography	Soil type (1-22), water drainage (1-11), landscaping (1-6), water features (1-7),
Building type	Building classification (1-5), quality of envelope (1-4)
Survey location	Room classification (1-8), volume (m^3), floor level
Location features	Windows/doors/fireplaces (1-5)
Level of control	No control to active conservation heating (0-3)
Furnishing	From empty space to soft furnishings (0-5)
Organic collections	Collections on open display: nothing to fully furnished room (0-5)

Table 2.1- Categorical data collected as part of the building survey to enable the statistical representation of buildings and features

Triplicate air samples were taken at the centre of each room and within 3m of the building for outdoor, using a Biotest RCS Plus with Hycon YM agar strips (Merck Millipore). The strips were incubated with the agar surface face up for 7 days at 20°C with limited light. The viable colony forming units (CFU) were then counted using a plate reader and the CFU m^3 was calculated. This sampling was only able to detect viable fungal spores but enabled the culturing of random colonies could be identified to create a representative population of fungi that could potentially colonise historic substrates. Any instances of fungal growth on collections was also recorded and swabs taken to assess viability and the species identified.

In addition to the samples taken and categorical variables recorded during the building survey, mean external environmental data was sourced from weather stations local to the case studies for the survey seasons (http://www.metoffice.gov.uk/public/weather/climate-historic/#?tab=climateHistoric). The longitude and latitude were determined using Google Maps

(https://www.google.co.uk/maps) and the elevation above sea level found using these (https://www.freemaptools.com/elevation-finder.htm). The soil type and water drainage was sourced from The National Soil Resources Institute, Cranfield University (https://www.cranfield.ac.uk/centres/cranfield-soil-and-agrifood-institute/research-groups/national-soil-resources-institute). Psychrometric properties were also calculated from the elevation above sea level, relative humidity and temperature data using the Dayton ASHRAE platform which uses ASHRAE Standard 41.6 method for Standard Method for Measurement of Moist Air Properties in SI (http://www.daytonashrae.org/psychrometrics_si.html).

Figure 2.2-The grid system used to randomly sample the air strips after incubation. Samples were generated from the cultures growing in B1-17 and T1-17 with both the letter & number of the location code generated using a random number function. For this, B=1 & T=2

2.2.2 Sample Processing

In order to create a statistically representative population for heritage buildings, colonies from the triplicate air samples for each location were sampled using random number generation to represent the grip structure of the agar strips. An example of the grid system used to mark up the agar wells on a strip in shown in Figure 2.2. Ten colonies from each sample location were determined in this way for each of the seasonal surveys to give a population of around 4000 colonies.

The selected colonies were isolated from the agar strips using sterile disposable loops and inoculated on potato dextrose agar (PDA) plates prior to incubation at 20°C. All culture techniques were performed within a Class II safety cabinet to reduce contamination and comply with COSSH protocols.

The morphology of cultures were compared to the original isolation strips using microscopy to confirm successful inoculation of the target. Any contamination caused by the close proximity of colonies on the sample strips was removed by further sub-culturing and streaking to purity. The fungal colonies isolated from growth on collections and the building fabric were also cultured to confirm viable growth.

2.2.3 Morphological typing

To group samples and reduce the number of molecular techniques, samples were primarily grouped according to macro morphology and colour and then micro-morphology and conidiophore shape. This enabled the formation of seven classifications (*Penicillium*, *Aspergillus*, black backed cultures, white cultures, coloured cultures & yeasts) and meant that like cultures
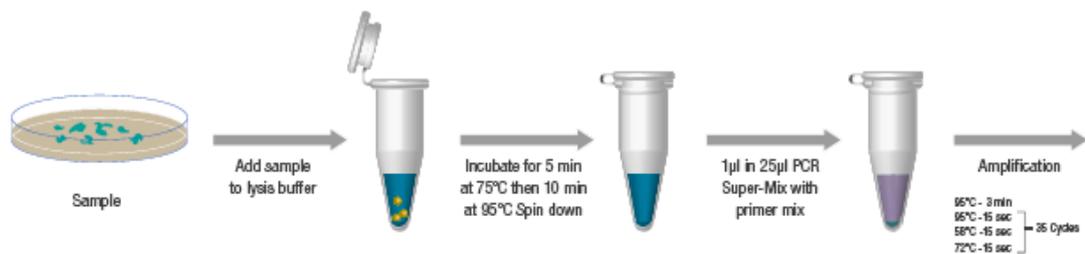
Figure 2.3-Work flow diagram for the Bioline DNA extraction and direct PCR methodology (S.Downes, A.M.Calcagno, J.Faull, F.Chang-Pi-Hin and S.Baker 2015)

could be more easily identified, recorded and all but one representative removed from future identification methodologies.

As potential yeast cultures were identified, antibacterial Rose Bengal with 0.05% Chloramphenicol media was used to isolate these and slides were made to determine whether any cultures were bacteria. This enabled the selective culturing of yeasts onto Sabouraud dextrose agar (SDA) and the ability to discount bacterial cultures from the study. Abundance and location were recorded prior to disposal.

2.2.4 Molecular typing

The typed cultures were freshly sub-cultured and incubated for 7 days before DNA extraction directly from the plate culture using the work flow protocol in Figure 2.3.

Approximately 200 cells (determined by haemocytometer) were removed from the perimeter of the desired culture with a disposable loop and transferred to the lysis extraction buffer before thermo-cycles at 75°C and 95°C for 5 and 10 minutes respectively. Some culture extracts, usually highly pigmented required a cleaning stage to provide usable genomic DNA. The Genomic DNA Clean & Concentrator from Zymo Research was used where necessary, following the manufacturers protocol for genomic DNA cleaning. All subsequent PCR reactions were prepared in a UV filtered PCR hood.

Step	Temperature (°c)	Time	Cycle Number
Initial denaturation	95	3 min	1
Denaturation	95	15 sec	
Annealing	55	15 sec	35
Extension	72	15 sec	

Table 2.3- Optimised PCR conditions for use with GACA4 during RAPD reactions

The fungal microsatellite primer, GACA$_4$ (see Table 2.2 for sequence) was used to create RAPD barcodes for species differentiation between the cultures. PCR was performed using 12.5 µl MyTaq Blood PCR kit (Bioline), 11 µl of molecular grade water and 0.5µl of 20pmol GACA$_4$ (Eurofins) per reaction. DNA supernatant (1 µl) was added to the reaction buffer before PCR cycling using the conditions detailed in Table 2.3.

Products were visualised with 1.5% agarose gel with 4 µl ethidium bromide per 100ml of 1% TAE. The electrophoresis buffer used was also 1% TAE and Hyperladder I (Bioline) molecular weight marker and 5x loading buffer (Bioline) for each gel.

Gels were run for 60 minutes at 60v before visualisation using a Syngene gel doc with the Genesnap program (Syngene).

After capture, the images could be processed using Genetools (Syngene) to compare the barcode profiles using the Hyperladder I lane to calibrate product size.

Individual barcode patterns were processed for sequencing whilst duplicates were removed

Step	Temperature (°c)	Time	Cycle Number
Initial denaturation	95	3 min	1
Denaturation	95	30 sec	
Annealing	43.8	1 min	35
Extension	72	1 min	

Table 2.4- Optimised PCR conditions used for ITS 4 and ITS5 reactions to amplify fungal rDNA, ITS regions 1 and 2

from the sample pool.

Primer	Sequence 5'	Tm (°c)	Binding region
ITS 4	TCCTCCGCTTATTGATATGC	53	ITS 2
ITS 5	GGAAGTAAAAGTCGTAACAAGG	61	ITS 1
GACA4	GACAGACAGACAGACA	43.8	

Table 2.2- The primers used during PCR reactions with their sequences, Tm and DNA binding region. All Primers sourced from Eurofins and diluted to 20pmol working concentration with molecular grade water.

The primer pair ITS4 and ITS5 (see Table 2.2 for sequences) were used for universal amplification of fungal. The PCR reaction buffer used was the same as previously mentioned but using a 20pmol ITS4 and ITS5 diluted primer mix, the PCR conditions are detailed in Table 2.4.

Products were visualised to confirm amplification using the same procedure as above but with a 1% agarose gel for 30 minutes at 80v.

The PCR products were then processed for sequencing using the Quaigen PCR spin column clean-up kit to remove the salts and any residual products that might inhibit the sequencing process, following the manufacturers instructions.

Source Bioscience overnight speed read service was used for Sanger sequencing. Results were supplied in an Applied Biosystems file format for reading with the Sequence Scanner 2 program. Primers were provided with the PCR products, ITS4 and ITS5 both diluted to 3.2pm.

2.2.5 Sequence alignment

After base conformation, the ITS4 & ITS5 sequences were then aligned using Multalin (http://www-archbac.u-psud.fr/genomics/multalin.html) and the resultant contiguous sequence truncated to eliminate any single sequence regions, insertions and deletions. Any bases that were not in agreement were located in sequence scanner and the base from the sequence with the best base called probability used to generate the final alignment.

This alignment was entered into the NCBI BLASTn suite and the sequence compared to published fungal nucleotide sequences.

Only alignment results that exceeded 95% identity scores with low error values were considered as reliable identification matches. The sequence annotations were also checked to determine the origins of the sample, sequence regions and strain number.

2.2.6 Biodiversity indices

To analyse the fungal heritage building populations, the species richness (number of species), species evenness (E_{var}) and Shannon Wiener diversity (H') scores were calculated for each property and season.

2.2.7 Predictive models

The building location and environments were expressed in either scale measurements or ordinal categories for analysis of fungal growth and high internal CFU predictors. Due to the presence of categorical and ordinal data collected, logistic regression was selected as the data set would not violate the model assumptions and has been previously utilised in the prediction of whether species would be present within a certain environment (Vaskainen *et al*. 2010; Pearce & Ferrier 2000). This model can be used to predict whether fungal growth may occur on objects within specific environmental parameters and could be used to inform conservation risk assessments.

In order to accurately determine whether variables within buildings can contribute to the fungal load in the air, the difference between the CFU/m^3 must be taken into account. A similar logistic regression model was created was created using any locations with CFU counts that were over 100 units after the external CFU had been accounted for.

The data was cleaned, with any samples missing values removed from the set. The outcome variables (whether viable growth occurred on objects or if a high internal CFU/m^3 count was found) were categorised to create a binary data set returning a 0 for no growth or safe CFU (100 or less CFUs than that found outside) or a 1 for growth found and a high CFU count (100 CFU or more over the number found outside).

Binary logistic regression and model fitting was performed on training data, randomly generated using the select cases function (75% of the data set), with a backward-stepwise selection for generating the most parsimonious model, without causing a significant change in significant deviation (*p=0.05*), using SPSS based on the protocol of Field (Field 2009). Final model validation was reviewed on the test data set and assessments made on the overall performance.

The validation of the data set was made using leverage scores, Cook's Distance and the chi square standardised residuals. The model was assessed using the calculated odds ratio and Wald statistics with the B coefficient generated being used in Equation 2.3, in order to enable predictions of high internal CFU counts and fungal growth on objects in other buildings. A binary result of yes or no will be delivered from the equation depending on whether the result is closer to 0 or 1. All statistical calculations and data processing was performed in SPSS and Microsoft Excel.

$$P(Y) = \frac{1}{1 + e^\wedge - (\boldsymbol{b}0 + \boldsymbol{b1} * \boldsymbol{x}1i + \boldsymbol{b}2 * \boldsymbol{x}2i + \cdots \boldsymbol{b}n * \boldsymbol{xni})}$$

Equation 2.2.1- The generated equation for binary logistic regression in SPSS. The values for the statistically relevant predictor variables can be inserted into the equation, in order to predict whether there will be a high internal CFU in a property or whether fungal growth is likely to occur on organic materials. Results are delivered in a binary format, either yes or no. P(Y) – Probability of Y happening; E – base of logn; b0 – Y intercept; bn – gradient of the line; xn – value of the predictor variable

2.3 Results

2.3.1 Indoor fungal population

During the four seasonal surveys, over 4000 viable cultures were isolated from aerial samples within historic buildings. These were typed and sorted according to their macromorphology and unique cultures were further processed using molecular techniques to determine their identity to species level, in most cases.

More barcode profiles were observed than anticipated for the number of suspected species. Through test sequencing batches, it was found that this technique was in fact sensitive enough to differentiate at sub-species level. However, for this study, this sensitivity was not required.

Figure 2.4 shows the inverted electrophoresis gel of RAPD products for 47 *Penicillium* cultures from survey 2. The coloured squares show the confirmed identities from the ITS sequencing. For *P. brevicompactum*, it is particularly clear that there are four distinct patterns which represent different strains.
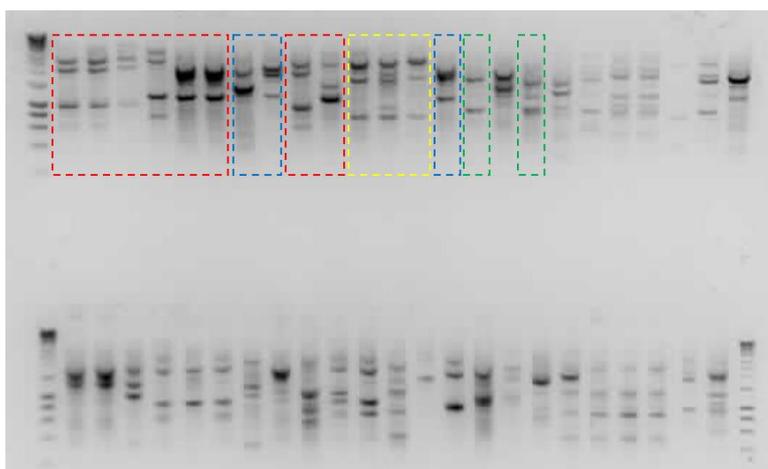
Figure 2.4- Inverted electrophoresis gel for RAPD PCR products of 47 Penicillium *cultures. The coloured groupings represent ITS sequence results: red=* P. brevicompactum*, blue=* P. jugoslavicum*, yellow=* P. spathulatum *& green=* P. commune

After the initial screen of the amplified ITS region (Figure 2.5) and the purification and concentration process, the samples sent for sequencing were of a high quality and it was possible to identify over 95% of the cultures to genus level and 82% of those to a species.

Even with the use of the Zymo Research DNA cleaning kit, it was not possible to obtain viable DNA for all cultures. Any of these that could not be morphologically identified were removed from the data set for the later analysis. There were also a number of unidentified Basidiomycota that were matched to un-cultured environmental samples. As so little taxanomic data could be attributed to these cultures, they were also removed from the sample set.

Figure 2.5- Electrophoresis gel of rDNA amplified by PCR reaction with the primer pair ITS4 and ITS5 for morphologically typed Penicillium *samples 1-83 with 1Kb HyperladderI molecular weight marker (Bioline)*

Despite the presence of Chloramphenicol in both the original isolation agar strips and the Rose Bengal used to sub-culture the yeasts, 3% of the identified population have been confirmed as bacteria. Further identification and classification of these cultures will not be undertaken as it does not fall under the remit of this study.

Table 2.5 shows the taxonomic classifications of the organisms that have been identified and their abundance across the seasons. The three phyla accounted for are Ascomycota, Basidiomycota and Zygomycota which represent 95%, 5% and 1% of the population respectively. These percentages are however skewed due to the high proportion of unidentified Basidiomycota published in GenBank.

Domain	*Kingdom*	*Subkingdom*	*Phylum*	*Subphylum*	*Class*	*Subclass*	*Order*	*Family*	*Genus*	*Species*
2	2	2	3	8	13	20	23	43	76	120

Table 2.5- The taxonomic classifications of organisms identified so far during this study and their abundance. From subkingdom to Family, only fungi have been recorded as the identification of bacteria was not possible beyond this point.

Figure 2.6 shows the abundance of each phyla throughout the year of data collection. Whereas all of the properties have had examples of *Ascomycota* and *Basidiomycota*, only half of the properties contained *Zygomycota* in their populations and the frequencies were very low, likely due to a lack of simple nutrients found within heritage collections.

The most abundant class are the *Eurotiomycetes* which are featured in all case study populations and represent 41% of the total classes. The *Eurotiomycetes* represented in this survey are mostly

the *Penicillium sp.* and their telemorphs, followed by *Aspergillus* and four less abundant genera. More of this class were recorded during the spring and summer surveys.
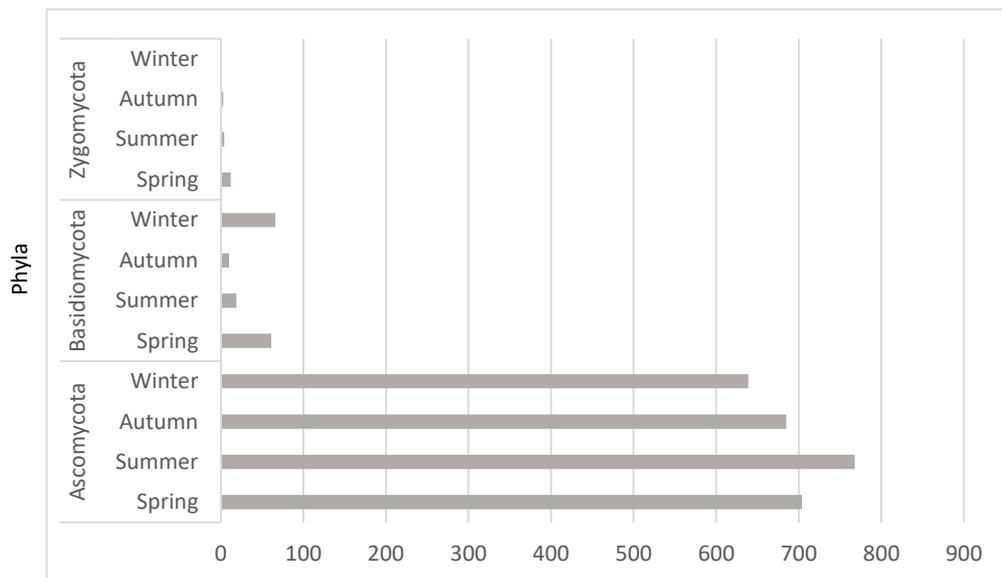
Figure 2.6- The three phyla (Asomycota, Basidiomycota & Zygomycota) and their abundance during the seasonal surveys.

The next most abundant are the *Dothideomycetes* at 39% of the identified population. The fungi of this class are some of the most diverse *Ascomycota*, some of the most common being plant pathogens. They include *Cladosporium sp.*, their telemorph *Davidiella*, *Alternaria sp.* and in lower magnitudes, *Epicoccum nigrum.* This class was more abundant during the autumn and winter survey.

The *Sordariomycetes*, representing 20% of the population are found during all of the seasons and include plant, animal and myco pathogens. This class is one of the most diverse in the genera that it contains but the most predominant are the *Sarocladium, Fusarium, Metacordyceps* and *Engyodontium* species. The abundance of this class is higher during the colder seasons (winter and spring).

The most significant other class, is the *Agaricomycetes.* These *Basidiomycota* are predominantly plant pathogens and decomposers responsible for the decay of lignin based forest matter and include *Bjerkandera adusta* (by far the most abundant), *Heterobasidium abietinum* and *Thanatephorous cucumeris* (only found during the winter and spring).

The genera observed during each season vary in both richness and abundance. The winter and spring have a greater diversity than the summer and autumn surveys. The spring and summer has higher frequencies though, followed by the spring autumn and winter. This indicates that

the summer has fewer genera but a greater abundance of those recorded and the winter has a greater variety of genera but these are found in low numbers.

None of the buildings surveyed had a representative of each genus in the cultures collected. For every property, with the exception of Dyffryn House, 50% or less of the total genera have been recorded. Figure 2.7 contains the genera that represent the top 75% of the identified population.
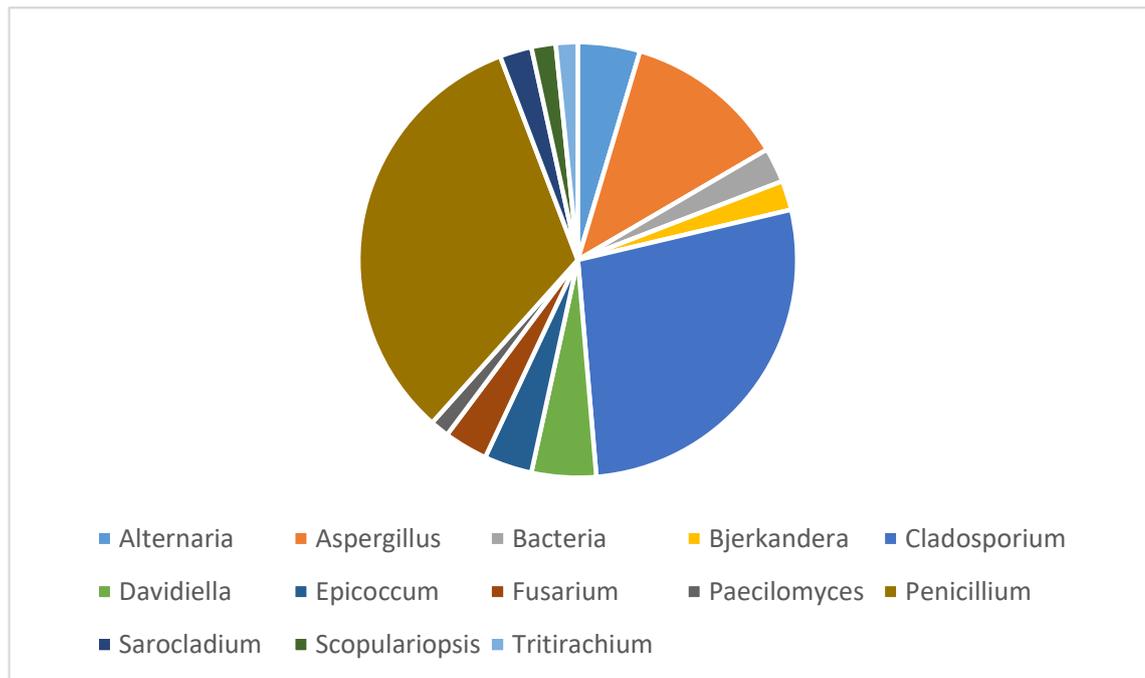
Figure 2.7- The genera that represent 75% of the total identified indoor airborne population

For all properties, the most abundant genera is the *Penicillium*, closely followed by the *Cladosporium* and then *Aspergillus*. Although certain properties have a greater richness of genera, the relative abundance of these is low in comparison to the three greatest contributors. Within each genera, there is a great difference in richness of species. There have been far more *Penicillium* recorded than any other, with 33 individual species identified. Within most of these species, there have also been several strains identified, *P. brevicompactum* having the most at 8 strains. The other two most abundant genera have far fewer species recorded with 9 *Aspergillus* and only 3 *Cladosporium*. Of these three genera, the most abundant species were *P. brevicompactum*, *C. cladosporiodes* and *A. versicolor*.

Due to the large number of species recorded, this data was investigated with biodiversity indices, as a means of data reduction.

2.3.2 Biodiversity indices

From the culture population, it was possible to calculate the species richness (number of species recorded), evenness (E_{var}) and Shannon Wiener index to analyse the biodiversity observed at each property during each season. As the Shannon Wiener Index (H') takes into account the species richness and abundance, only this index will be reported and it can therefore be assumed that the greater the H' score, the greater the number of species that were recorded and the more even the distribution of these.

The ANOVA calculated from the Shannon Wiener index shows that there is a significant difference (*p=0.001*) in diversity in each season at the case study properties. Spring is the most diverse season, followed by the autumn (Figure 2.8).
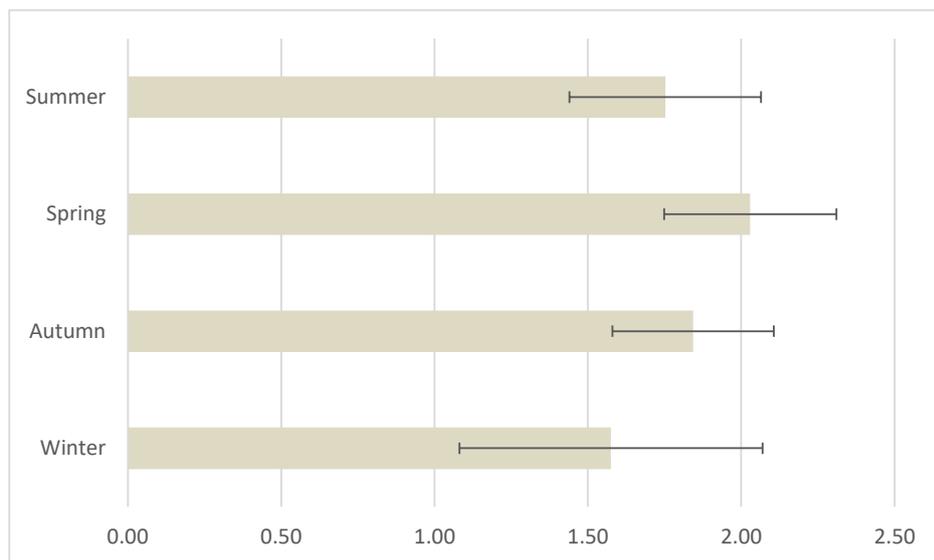
Figure 2.8- The mean Shannon Wiener index for fungi recorded in the survey properties during each season. Error bars: SD

The mean seasonal Shannon Wiener is shown in Figures 2.9a-d. The properties that have a high mean score have a high species richness and evenness which would indicate low abundance of a range of different species. Properties with lower scores will have fewer species recorded and the abundance will not be evenly distributed. This can represent a particular location that has a high abundance of one particular species, such as Knole having high *Trichoderma* and Gainsborough having high *Aspergillus* levels during the winter in one location, with few other species accounted for. This is also shown by the high standard deviations.
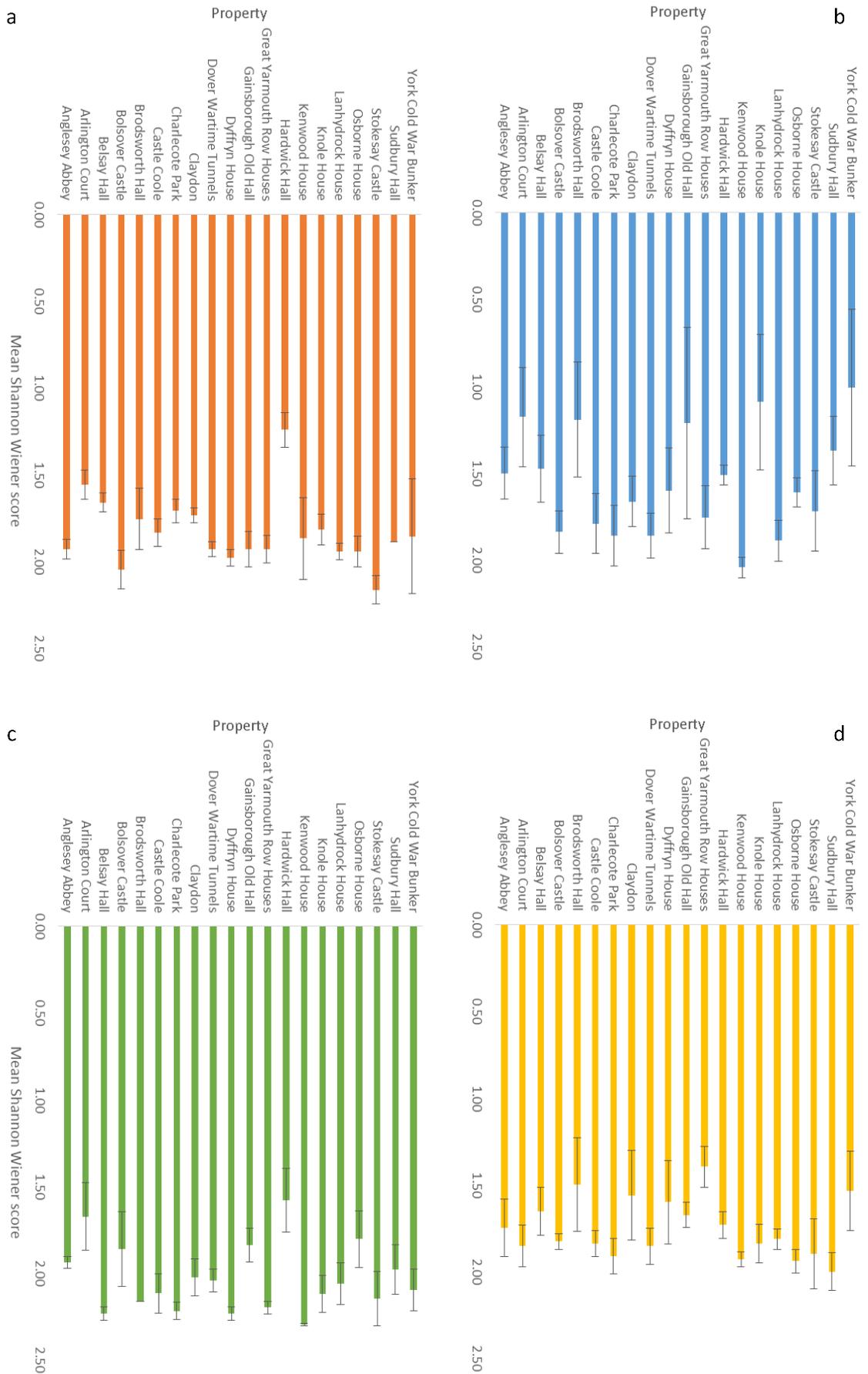
Figure 2.9 a-d- The mean Shannon Wiener index for fungal populations in each property during the seasonal surveys. a= Autumn, b= Winter, c= Spring & d= Summer, error bars: SD

2.3.3 Colony forming units

In addition to the population data, the colony forming units for each location were calculated. From Figure 2.10, it is clear that the peak season for high CFU counts is the summer, but there is a high level of variation seen across the average counts for the properties and locations with a number of extreme outliers. The lowest colony forming units were recorded during the winter.

Some of the indoor results show very high levels of fungi which are well above the 500 CFUm^3 which The World Health Organisation indicate to be a safe threshold. It was assumed that the indoor air sample was influenced by the external so the data was normalised accordingly. Figure 2.11 shows the instances of locations having an internal CFU of 100 or greater than the outside count, as used by Sedlbauer, based on the work of Senkpiel (Sedlbauer 2001). From this it can be seen that low CFU counts outside during the winter highlight locations that may have been considered safe, if just considering the indoor count. Figure 2.11 also reflects the high CFU counts seen externally during the other seasons and only really highlights areas where an internal fungal source may be causing the high count.
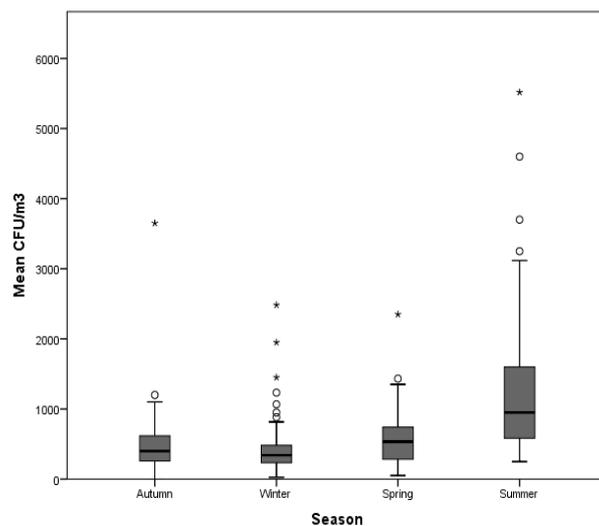
Figure 2.10- The mean internal CFU m^3 counts recorded during each season within survey properties. Circles and stars indicate outliers and their extremity.
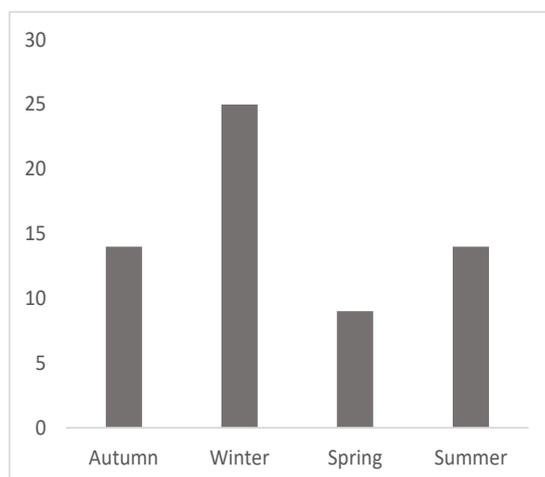
Figure 2.11- The frequency of CFU counts in each season where the internal value is 100 or greater than the outdoor CFU m^3

2.3.4 Environmental modelling

From the viable fungal growth swabs and the case study building and environmental data, it was possible to determine the features that contribute to the likelihood of fungal growth occurring on collections. The training data set was evaluated using the residual statistics requested from the SPSS output. The Cook's distance was less than 1 for all but one case but when analysed using 4/(n), there were 18 outliers, all of which were during the autumn and may have influence over the model. Only 0.8% of cases had a significant z-score (*p=0.05*). There were however a number of cases which had a high DF Beta score (change in the regression coefficient due to the inclusion of a particular case in the model). These tended to be from locations with unusual environments.

Although there were found to be cases that unduly influenced the model, the overall predictive power was reduced when these were removed. As historic environments are very varied, and some places far more likely to have fungi growing it was decided that for integrity, it was more accurate to include all cases in the analysis. Variables that significantly contribute to the likelihood of fungal growth are detailed in Table 2.6.

Table 2.6- Variables included within the binary logistic regression model for the likelihood of fungal growth occurring within an interior (19th iteration). R^2=0.5 (Nagelkerke).B – The beta coefficient; SE – Standard error; Wald – The Wald statistic; Sig – Significance of result (p); Exp(B) – The odds ratio; CI – Confidence interval

Variable	B	SE	Wald	Sig	Exp(B)	95% C.I.for EXP(B)	
						Lower	Upper
Survey	2.167	0.484	20.047	0.000	8.734	3.382	22.554
Elevation	-0.012	0.004	10.389	0.001	0.988	0.981	0.995
Location Classification	-0.596	0.195	9.374	0.002	0.551	0.376	0.807
Level of furnishing	-0.531	0.303	3.078	0.079	0.588	0.325	1.064
Organic collections	0.592	0.303	3.832	0.050	1.808	0.999	3.272
Absolute humidity	0.344	0.139	6.147	0.013	1.410	1.075	1.851
Mean Ex Temp Min	-0.652	0.177	13.608	0.000	0.521	0.369	0.737
Floor level	-1.159	0.322	12.958	0.000	0.314	0.167	0.590
Constant	0.494	1.801	0.075	0.784	1.638		

To assess the fit of the model, the initial -2 log-likelihood of the model (only containing the constant) was 251.245, indicating information not explained by the model. Using a backward stepwise modelling method, after the 19th iteration, the -2 log-likelihood was 187.446 showing that the variables included increase the amount of information explained by the model. The coefficient of determination calculated as R^2=0.5 (Nagelkerke) meaning that 50% of variance is

explained by the new model. Based on the training data set, the model predicts the correct outcome 74% of the time, an improvement from the 58% of the original.

The Wald statistic has a chi-square distribution and shows whether the B coefficient of a variable is significantly different from 0. All of the variables are significant to *p=0.05* with the exception of the level of furnishing (*p=0.08*). The decision to leave this predictor in the model was made, as the variance explained significantly decreased without the level of furnishing included. This shows that the variables with a high Wald score are making a significant contribution the prediction of whether fungal growth might occur. The time of year (season), the external temperature, the level of the building (where data was recorded) and the height above sea level (elevation) are the most influential variables in determining whether fungal growth may occur on collections (*p=0.001*). The type of room (location classification), absolute humidity of the room and the level of organic collections stored in the space are less significant (*p=0.05*). The residual chi-squared statistic for the variables not in the model do not have significant coefficients (*p=0.85*) so would not improve the model if included.

The ExpB, or odds ratio, shows the change in odds resulting from one unit of change in the predictor. All of the predictor variables have a positive ExpB value which indicates that as the input values for the predictor increases, the odds of fungal growth occurring on collections also increases. The B coefficients are inserted into Equation 2.1 to create a predictive algorithm for whether fungal growth is likely to occur on collections in a given environment. When the test data was applied to the model, the model was 84% accurate when compared to observed values.

From the normalised indoor-outdoor CFU/m^3 and the case study building and environmental data, it was possible to determine the features that contribute to the likelihood of high internal viable fungal loads. The training data set was evaluated using the residual statistics requested. The Cook's distance was less than 1 for all cases but when analysed using 4/(n), there were multiple outliers. Some 3% of cases had a significant z-score (*p=0.05*) which is within the 5% limit and there were no DFBeta values over the threshold, which was reached by calculating 2/√(n). Although there were found to be cases with a leverage (35 cases over the expected (k+1)/n)) that could unduly influence the model, the overall predictive power was reduced when these were removed. As historic environments are very varied, and some places far more likely to have fungi growing it was decided that for integrity, it was more accurate to include all cases in the analysis

Variables that significantly contribute to the likelihood of an internal count greater by 100 than the outdoor are detailed in Table 2.7.

Table 2.7- Variables included within the binary logistic regression model for the likelihood of high internal CFUm³ occurring (19th iteration). R2=0.6 (Nagelkerke) B – The beta coefficient; SE – Standard error; Wald – The Wald statistic; Sig – Significance of result (p); Exp(B) – The odds ratio; CI – Confidence interval

Variable	B	SE	Wald	Sig	Exp(B)	95% C.I.for EXP(B)	
						Lower	Upper
Elevation	0.011	0.005	5.340	0.021	1.011	1.002	1.021
Water features	0.541	0.161	11.257	0.001	1.717	1.252	2.355
Building classification	-0.754	0.250	9.081	0.003	0.470	0.288	0.768
Floor level	0.620	0.282	4.846	0.028	1.859	1.070	3.229
Windows	-0.574	0.276	4.338	0.037	0.563	0.328	0.967
Mean Ex Temp Max	-0.309	0.083	13.801	0.000	0.734	0.624	0.864
Mean CFU m3	0.003	0.001	23.820	0.000	1.003	1.002	1.004
Fungal growth observed	1.209	0.535	5.102	0.024	3.350	1.173	9.562
Constant	-0.043	1.552	0.001	0.978	0.958		

To assess the fit of the model, the initial -2 log-likelihood of the model (only containing the constant) was 198.890, indicating information not explained by the model. Using a backward stepwise modelling method, after the 15th iteration, the -2 log-likelihood was 114.426 showing that the variables included increase the amount of information explained by the model. The coefficient of determination calculated as R^2=0.6 (Nagelkerke) meaning that 60% of variance is explained by the new model. Based on the training data set, the model predicts the correct outcome 89% of the time, an improvement from the 84% of the original.

The Wald statistic has a chi-square distribution and showed that all of the variables have coefficients significantly to 0 (*p=0.05*). The mean CFU count of the location, mean minimum external temperature and whether or not there are water features in close proximity to the property are the most influential variables (p=0.001). The type of building, the height above sea level, whether or not fungal growth was observed, the floor level of the location and the amount/size of windows are less significant contributors to the model (*p=0.05*). All of the predictor variables have a positive ExpB value which indicates that as the input values for the predictor increases, the odds of fungal growth occurring on collections also increases.

The residual chi-squared statistic for the variables not in the model do not have significant coefficients (*p=0.90*) so would not improve the model if included.

The B coefficients were inserted into Equation 2.1 to create a predictive algorithm for whether a high internal CFU/m³ is likely to occur on collections in a given environment. When the test data was applied to the model, the model was 94% accurate when compared to observed values.

The algorithms created for both models were inserted into an Excel user form to create a user interface that can be used easily by property staff for risk management and data interpretation (Appendices – Chapter 2). A clearly defined list of ordinal data will be provided to assist data entry, as the score given to property features will influence the model.

2.4 Discussion

2.4.1 Molecular identification

This work has produced the largest representative airborne seasonal population of fungi found within heritage buildings in the United Kingdom. Some cultures could not be adequately classified due to an inability to obtain a viable PCR product or through a lack of published identities for sequence comparison. Work is ongoing with Bioline to improve the ability of the DNA lysis buffer and PCR protocol in order to expand the scope of compatible fungi. The *Basidiomycetes* that do not currently have any taxonomic information, beyond their nucleotide sequences, were described as "Uncultured Basidiomycetes" from environmental samples in Genbank, an issue also identified by Schoch *et al* (Schoch et al. 2012). This study has proved that they can be cultured, which can be annotated to sequences. However, it will most likely not be within the scope of this project to complete their identification to anything below *Phylum* level. Methods to complete this work would include the amplification of an additional region. The large and small sub units of the mitochondrial DNA and the region coding for the βTubulin gene have been widely used in fungal taxonomic studies (Bellemain *et al*., 2010; Palacios *et al*, 2014) and so there may be a wider range of classified organisms for comparison. If this were to be unsuccessful, then another technique like restriction fragment length polymorphism analysis (Martin & Rygiewicz 2005) could be utilised.

In the future, there should also be work concerning the bacteria found in heritage properties. This group represents approximately 3% of the total population and are present throughout all of the seasons. Bacteria have been found to cause biodeterioration of both organic and inorganic cultural heritage (Szostak-Kotowa 2004; Warscheid & Braams 2001) but this is an area that needs more research, particularly within the context of the historic interior.

2.4.2 The fungal population

The same ratio of Phyla recorded during this study, correlates with other published work (Rittenour et al. 2014).

Whereas the most common genus isolated from air samples is usually *Cladosporium* of the Class *Dothideomycetes* (Ingold 1953)*,* this survey has found that the most dominant Class found in indoor air has been the *Eurotiomycetes* largely consisting of the Genera *Penicillium* and *Aspergillus* with a greater abundance of *Penicillium,* results that were also observed in indoor environments by Korpi (Korpi et al. 1997). There was however a greater abundance of *Cladosporium* in the outside air sample and locations with a high air exchange rate (more windows, doors and fireplaces).

Other studies concerned with seasonal variations in viable airborne fungi have also found that a greater abundance of colonies were found during the summer (Medrela-Kuder 2003), with the outdoor concentrations being greater than the indoor. Similar findings were recorded during this study although, once the external CFU levels had been taken into account, it was in fact the winter that had the greater internal fungal load. This may be due to increased heating levels, for the comfort of staff, and the creation of microclimates that are conducive to fungal growth.

The lowest biodiversity score in properties was recorded during the winter. Outdoor CFU counts are usually lower during the winter due to unfavourable growth conditions (Li & Kendrick 1996) and is reflected by the lowest levels of *Cladosporium*, of *Epicoccum* and no *Alternaria* (plant degraders all commonly found in external air samples) recorded during this season (Ingold 1953). The winter usually represents the closed season for properties and is when the majority of the conservation and cleaning occurs. This could account for the elevated indoor fungal load as dust is disturbed during cleaning and case covers usually applied, which would limit the settling of spores. Scott found *Cladosporium*, *Epicoccum* and *Alternaria* to be some of the most abundant constituents of household dust (Scott 2001). There was also a reduction in *Aspergillus* and *Penicillum* during this season, likely due the impact of cleaning on these common indoor fungi. This means that properties may display higher CFU counts, but these will be made up of fewer species and they will not be evenly distributed, with some species being found in high numbers.

An interesting increase in *Agaricomycetes* abundance also occurs over the winter season and into the spring. These are predominantly decay *Basidiomycetes* involved in the degradation of lignin (Hibbett et al. 2014). This increase over the colder seasons is mirrored in the outside findings, however the indoor headings are higher. The could be due to increased indoor growth of these fungi due to the favourable conditions of reduced airflow, increased relative humidity and conservation heating employed in some buildings. These results are in contradiction with Pitkäranta *et al*. who found the lowest levels of *Agaricomycetes* in dust during the winter season (Pitkäranta et al. 2008). However, this study was conducted in Finland so the result is most likely

to be different in the more temperate climate of the UK. Pitkäranta et al. also recorded an increase in the abundance of the *Basidiomycetous* yeast *Cryptococcus* during the winter and sping season, a finding also observed during this work.

The winter was the only season in which there were no *Zygomycota* recorded outside and only one instance inside. Members of this Phylum are saprobic and often associated with soil and decaying plant or animal matter or as pathogens (White et al. 2006). As there will be restricted air flow to buildings and cleaning will have taken place, there would not be as many opportunities for *Zygomycota* to contribute to airborne particles. It is also recorded that they prefer warmer conditions than those recorded during the winter so may not be producing reproductive bodies at this time. The growth of *Mucor* and *Rhizopus*, both *Zygomycetous* Genera recorded during this work, was positively correlated by Scott (2001) in culturable house dust. As neither were found during the winter it supports the conclusion that their lifecycles are highly seasonal and dependant on available nutrients.

The autumn season had the second greatest biodiversity score but second lowest CFUs recorded. During this season, some properties were closed or on reduced opening hours which accounts for the lower levels of *Cladosporium* observed in Indoor air, in comparison to the spring and summer (Li & Kendrick, 1995; Li & Kendrick, 1996).

The abundance of *Penicillium* is greatest during this season. This was not found by Medrela-Kuder (2003) who found a greater abundance of *Penicillium* during the summer and winter in Poland. However, Trovão et al. (2013) found high instances of this Genera in an Italian historic location during both the autumn and summer.

The autumn also had the greatest abundance of Bacteria observed. This is likely due to the presence of visitors over the open season (the period during the year in which the property is open to the general public), with minimal cleaning being conducted (Camuffo *et al*., 2001).

The summer, despite having the highest average CFU isolated, had the second lowest biodiversity which was not found in other studies (Trovão et al. 2013). The largest proportion of *Dothideomycetes* were recorded during this survey. This is most likely due to the high throughput of visitors resulting in a greater air exchange with the exterior environment. Therefore a greater abundance of plant pathogens and decay agents were recorded. Similar patterns were also observed by Li *et al* (1996) and Pitkäranta *et al* (2008). With an increase in airflow and temperature within properties, it is likely that a lot of the Genera recorded in the richer, damper seasons would not have enough available water to continue to grow so have not been detected during this survey, such as the *Agaricomycetes*.

Significant correlations (although weak) between the genera found and the case study properties showed a link between closely related groups and similar environmental conditions, noticeably the *Dothideomycetes* and the *Eurotiomycetes* are grouped.

The *Dothideomycetes* are likely to be found in higher abundance during the warmer, peak plant growth seasons in locations with a higher air exchange rate, temperature and available moisture (dewpoint and absolute humidity). They are more likely in areas with a high CFU count and *Cladosporium* and *Epicoccum* are slightly more likely to be abundant with lower rainfall. This is due to the high external spore loads during the summer affecting the internal conditions. The higher levels of these genera in areas of lower rainfall may be due to a lack of deposition of small spores by precipitation (Ingold 1953), so they therefore remain airborne for longer.

The *Eurotiomycetes* exhibit some unusual trends, in that they statistically more likely to be present in abundance during the spring and summer. This is due to the way the season data was coded (autumn=1, winter=2, spring=3, summer=4), in the order of the data collection and the relative abundance of both species all year. Although the season seem to have the greatest influence over this group (0.30 & 0.21), the correlation is not strong and the figures are also likely to be affected by niche species within the genera. Although the correlation is weaker (0.16) this group are more accurately represented by the level of sunshine and the external temperature. The lower it is, the more likely they are to be abundant.

The Sordariomycetes (*Scopulariopsis, Tritirachium & Sarocladium*) are slightly more likely to be found in locations that have a higher rainfall and have a poorer building structure. *Tritirachium* is also more likely to be found in basement levels with a lower air exchange rate (fewer doors and windows, higher quality of envelope).

The basidiomycota, *Bjerkandura* is more likely to be found in locations where there are external water features and a higher air exchange with the outside air (windows). Cooler temperatures and higher rainfall are also preferable.

The Fusarium levels could also not be predicted from building features. It was however weakly correlated with the presence of *Paecilomyces*, *Scopulariopsis* or *Tritirachium* within a location.

In all properties, the Genera with the greatest abundance were *Penicillium*, *Cladosporium* and *Aspergillus* respectively. The most common Species in each were *P. brevicompactum*, *C. cladosporioides* and *A. versicolor*, species that have been isolated from other historic locations (Trovão et al. 2013). These were isolated from all properties and are some of the most common

species to be identified from culturable swabs. As the most abundant Species from the three most represented Classes, these will be the fungi used to culture organic materials to study their potential effect. This will be discussed in a Chapters 4 & 5.

2.4.3 Environmental modelling

Binary logistic regression models were created for the likelihood of a visual presence of fungal growth on collections and the internal CFU count being significantly higher (100 CFU) than that of the outdoor. The selection of this method was made due to the binary nature of response to these questions, yes (1) or no (0). A similar experimental protocol was used for modelling the effect of climate change on the habitat of butterfly species.

This method was attempted during this work for the presence or absence of the top 75% of the fungal population within buildings but significant models could only be produced for genera that represented over 2.4%, which was only 7 out of 76 genera recorded. This was likely due to the wide variety of environments that were encountered in the case study properties and the difficulty in cleaning the data set of influential variables whilst maintaining a representative pool. This issue was not encountered by Wilson *et al.* due the data set being recorded externally, the use of range brackets for elevation and species abundance recorded within a limited geographical range (Wilson et al. 2005). Their model was however not sensitive to small changes due to the bracketing of data. One of the other difficulties was that there are a broad range of species within each genera which may inhabit different environmental parameters. For example, *Aspergillus* species are usually found within more temporal indoor environments, but *A. ocraceus* was only found in damp, poor building environments which will skew the data set.

It has also been noted that the modelling of species distribution within environments cannot be accurately predicted without taking into account the species-species interactions that can effect habitation boundaries (Davis et al. 1998). The distribution of species will not be explored in this thesis but will be investigated for publication using species interaction as one of the parameters and considering the input of environmental data to improve model accuracy but still maintaining predictive function. Vaskainen *et al.* use logistic regression to model species co-occurrence. This study also found that models would not significantly represent all interactions and that parameter changes could have an effect on the overall fit. It was also found that the model could under and overestimate the occurrence of species (Vaskainen et al. 2010). This issue was also encountered within models generated within this work.

The prediction of visible growth in properties is both under and over-predicted throughout the year, with a trend for over- prediction in the summer and winter (with a few extreme

environments being under, building types 1-3). One of the key issues with fungal detection in properties is the ability to see growth without magnification in subdued lighting and without regular monitoring. This would be assisted by *in-vitro* experiments to determine thresholds for growth on different materials, under a range of conditions in order to create a dose response (Isaksson et al. 2010). Even then, studies into the detection of fungal growth *in-situ* would also need to be conducted in order to improve the accuracy of determining whether it is occurring, even if not visible.

This model was created using spot readings so will only ever be able to represent a fleeting snapshot of a very complex environment, but unlike many models, it was conducted *in-situ* and accounted for more variables. Despite the error of prediction, the model could still accurately discriminate whether fungal growth would occur in 84% of cases which is a valuable tool for property staff and targeted risk management.

The prediction of high inter CFU counts, and therefore a potential internal fungal source was a more successful model (94% on test data), likely due to the measured values of the outcome variable, prior to binning. This model under-predicts buildings categorised 1-3, but over predicts those that are 4-5 (mansions and palaces) during the autumn, the reverse is so in summer and all prediction errors in the winter were under. This is likely due to the higher building categories having lower internal CFU scores and the lower building categories having a tendency to higher CFU counts. This model can be used, with caution, by property staff in the interpretation of air samples, which are now being conducted more regularly. All high counts are often seen as an issue and are investigated. This tool should help to determine whether the indoor environment is an expression of the external air or whether further investigation is needed to determine the high fungal load indoors.

Both models can give useful insight into the occurrence of fungi within buildings, but the mathematical outcome generated by the model is not evidence of direct interaction between these fungi and their environment (Vaskainen et al. 2010), this work is designed to create an initial hypothesis for further investigation.

This work has provided a baseline fungal population for heritage buildings in the United Kingdom through random sampling of collected fungal cultures and evaluation of the built environment. Some of the variables that can influence the airborne fungal populations found have been highlighted, along with conditions that may determine whether fungal growth will occur on collections and if high CFU counts are likely to be from an internal source.

3. Physical changes cause by fungal growth on organic materials

Fungal growth can leave irreversible damage in the form of discolouration, staining and loses to materials which alter the physical appearance and aesthetic properties of historic objects (Sterflinger 2010). Growth has been observed in a wide range of contexts on many different, often nutritionally complex substrates and environments (Zyska 1997; Sato et al. 2014; Was-Gubala & Salerno-Kochan 2000; Duncan et al. 2008; Pangallo et al. 2013; Garg et al. 1995).

This chapter aims to assess the level of growth that common ascomycete fungi are capable of on a range of organic materials that are commonly encountered, in order to determine the physical changes that can be observed as a result. The methods used will evaluate the overall colour change, the levels of growth observed in the substrate and any physical changes to the morphology. This will inform the assessment of historic objects and may influence decision making and prioritisation of treatment in a heritage environment. Non-destructive analytical techniques were used to ensure repeatability in a heritage context, colorimetry and microscopy.

3.1 Introduction

Colorimetry and spectrodensitometry have been used within a heritage context as this is a non-destructive technique which measures colour by reflectance of the surface at different wavelengths or by measuring the density of colour of a surface. The use of spectrodensitometry to monitor the colour change in paper was used by Menart to monitor the effect of pollution (Menart et al. 2011), fibroin degradation (M.A. Koperska et al. 2015) and Abdel-Kareem to monitor the effect of artificial ageing on linen textile (Abdel-Kareem 2005). This is a simple method that can give qualitative data on three dimensional colour using the CIE L*a*b* system (X-rite 2007; Sharma et al. 2005). This methodology has also been used to monitor colour change due to fungal growth on materials (Błyskal 2015; Bicchieri et al. 2002). In this study, the use of the CIE L*a*b* system will be used as quantitative method of classifying fungal growth on different materials by calculating the ΔE colour difference using untreated reference material as the baseline colour.

The visual damage caused to objects by fungi is not always limited to one area and the way in which growth can spread over a seemingly solid material is not well understood. This work aims to study the growth of selected fungi on solid substrates from germination to maturation, in order to assess the penetration of hyphae into materials and the growth of colony features.

Destructive methods of sampling, such as scanning electron microscopy have previously been used to assess fungal growth on organic objects (Florian & Manning 2000; Błyskal 2015; Naumann et al. 2005; Kavkler et al. 2015). This technique however, does not preserve the viability of the sample, cannot show what is occurring below the material surface and does not offer the ability to easily discern fungal hyphae from material fibres.

Confocal laser scanning fluorescence microscopy has been utilised for the imaging of fungi in plant substrates (Hickey et al. 2004; Dickson & Kolesik 1999), enabling the viewing of growth structures *in-situ*. Fluorescent probes were used to highlight different fungal cell features in order to obtain scan sequences which represent optical slices through a sample, for the potential 3D reconstruction of growth structures. Although Hickey *et al*. had success with thin slices of mycorrhizal fungi in plant matter, Dickson *et al*. show that it is possible to mount live fungal cultures on solid agar, in order to view live cells and growth over a period of time. Using an adaptation of these techniques, this study will visualise viable fungal growth by co-staining with the endocytosis membrane dye FM4-64 and the acid red stain Eosin Y.

3.2 Methods

A range of organic substrates were chosen to represent the object materials that could be at risk from fungal colonisation within a historic collection. Cotton and linen are examples of staple and bast cellulosic fibres respectively. Silk and wool represent the other significant fibres found and primarily consist of the proteins fibroin and keratin. Two paper examples were chosen to represent paper production from the 18th century onward; those made from textile (cotton and linen) and wood fibres (lignin free beech wood). Leather and parchment represent two preservation methods for animal skins (collagen) and are a key component of library collections and furniture. Veneer cuts of pine and oak were also selected as common soft and hardwoods found in furniture and building structures.

Artificial ageing of the test samples was not attempted because a uniform method, suitable for all materials could not be found. It would also not be possible to adequately relate the fibre changes to a time of ageing with any precision. Therefore all tests are performed on modern materials that would be found within collections and may be used within the conservation process of objects. Any changes recorded can be related to heritage collections but assume that the damage caused would be increased due to the potentially degraded state of historic materials.

The following preparations for organic samples also apply to the tests performed in Chapters 4 & 5 where the chemical and mechanical effects of growth are investigated.

3.2.1 Preparation of growth substrates

The fibres selected for use were in as natural a way as possible. Textiles remained in loomstate or for dyeing and were unbleached, finished or sized. All textiles were also of a plain weave to ensure a comparable surface and texture for fungal growth and to establish size and orientation during the mechanical analysis. Details of suppliers can be found in Appendices – Chapter 3.

As the samples were subjected to multiple non-destructive analytical methods before the final, destructive tensile strength tests the dimensions were dictated by the requirements for the tensile tests.

3.2.1.1 Dimensions

Each sample strip was cut to approx. 115mm by 10mm in the warp direction. The paper, parchment, leather and wood were measured with a steel engineering ruler and cut with an 11 blade scalpel. The samples were all cut in the same orientation. The paper samples were cut from the length of the sheet, the wood along the tangential grain and the parchment and leather were cut from the nose to tail axis of the hide. The average warp and weft counts within the dimensions was calculated for the textiles using a dissection microscope. Threads were then pulled to mark up the textile and the strips cut using specialist scissors.

The dimensions selected were determined by preliminary test conditions for the tensile strength machine and the size of petri dish that was available for incubation.

Prior to further treatment, all of the strips were measured in three locations using digital callipers to determine average dimensions to be used for the interpretation of mechanical testing. Table 3.1 gives the average sizes of each material at the time of preparation. All cutting and measurements were performed under ambient conditions in the same location and stored in sealed Petri dishes until sterilisation.

Table 3.1- Average dimensions of test strips prior to incubation and analysis. Measurements were taken at ambient temperature and relative humidity and subsequently stored in the same conditions, with low light, until sterilisation. Standard error of mean was calculated

Material	Average height (mm)	Standard error	Average width (mm)	Standard error	Average depth (mm)	Standard error
Cotton	115.88	0.06	9.45	0.07	0.19	0.004
Linen	114.02	0.17	10.85	0.03	0.17	0.004
Silk	115.59	0.08	9.56	0.14	0.13	0.01
Wool	115.53	0.23	9.83	0.13	0.23	0.01
Cotton and linen paper	114.72	0.05	9.79	0.02	0.10	0.002
Lignin free beech paper	114.74	0.04	9.79	0.03	0.14	0.002
Pine	114.79	0.13	9.89	0.13	0.61	0.01
Oak	114.83	0.15	9.91	0.26	0.59	0.02
Leather	115.18	0.19	10.10	0.22	1.59	0.78
Parchment	115.05	0.09	9.98	0.11	0.43	0.04

Sterilisation methods were investigated prior to work commencing to ensure that biofilm growth was that of the target species. The use of an autoclave (moist heat) and microwave irradiation were effective at sterilising the materials but caused significant mechanical damage to fibres (data not shown), which was deemed to be too destructive and could affect the results of analytical tests. Ultraviolet radiation was also trialled but found to be ineffective on textured surfaces such as textiles (Merka-Richards 2015). Ethylene oxide would have caused minimal damage to the materials fibres but was deemed to be unsuitable for use due to the highly reactive and toxic nature of the compound and the health and safety implications. Sterilisation with ethanol, methanol and industrial methylated spirits was also trialled. Saturation with ethanol after vacuum suction removal of fungal matter was found to be the most effective sterilisation of the strips and did not prevent any subsequent growth by the target organisms. This method of sterilisation had no detrimental effects to the physical and mechanical properties of all materials.

The strips were prepared to the correct dimensions and then saturated in a shallow bath of ethanol for 5 minutes. The strips were then removed from the bath and laid out to dry within a UV sterilised laminar flow hood for 24 hours. Care was taken during the laying out of the strips to ensure that the correct orientation of fibres was maintained and no deformations were introduced.

3.2.1.2 Inoculation and incubation

A dry inoculation method was used to introduce spores to the materials. This was aimed to simulate a direct contact transference of spores which can often happen within a historic setting. This method also did not introduce any free water to the incubation set up as a spore suspension would and artificial cementing of spores within the fibre structure was prevented.

The cultures selected were highlighted as the most common airborne spores and were found within each of the survey properties. They were also commonly isolated from objects with fungal growth. For more details on the species, please refer to the chapter 2. The three cultures, *Penicillium brevicompactum*, *Aspergillus versicolor* and *Cladosporium cladosporiodes*, were grown for 10 days at 20°C on potato dextrose agar (PDA) prior to use.

The materials were introduced to 11.5cm^2 disposable Petri dishes containing 50ml of set 1% purified agar (Oxoid) without nutritional supplement. The set gel was to ensure that a water activity (a_w) suitable for germination was achieved and that the materials did not dehydrate over the time of the study but without being in contact with free water. This represents a microclimate that could be found within a historic building with a poor internal environment. Airflow was not considered as a variable during this work so dishes were sealed post inoculation with Parafilm to prevent contamination and dehydration during incubation.

Identical 1cm wide, flat acrylic artist brushes were used to collect spores from a plate of the target culture. Each side of the brush was lightly touched to the surface of the fungal growth. The brush was then lightly spread over the surface of the strips from end to end. This was repeated with the opposite side of the brush and the other end of the strip to ensure even coverage. Figure 3.1 shows a scheme of the inoculation process. In addition to the fungal inoculated strips, there was also a set of strips incubated without sterilisation so that the effect of the natural biofilm of the materials could also be observed.
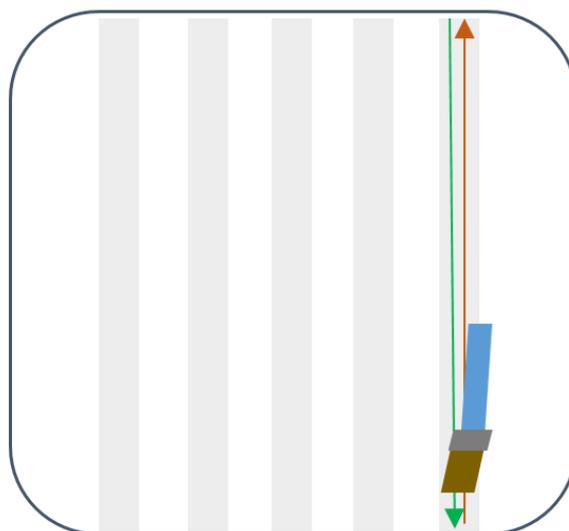
Figure 3.1- Diagrammatic representation of the organic material within the 11.5cm square Petri dish. The arrows represent the movement of the brush over the substrate surface and the distribution of spores. Green is the initial movement, followed by red.

All fungal culture work was performed inside a category II laminar flow hood to ensure the containment of any dry spores and reduce the risk of contamination from non-target organisms.

After inoculation, the Petri dishes were sealed with Parafilm and incubated at 20°C with minimal light for either 1 ,2, 3, 4, 6, 8, 10 or 12 weeks. The samples for each test week were additionally sealed within polythene bags prior to incubation to reduce the influence of the outside environment as the incubator was in regular use.

After the incubation time had elapsed, the dishes were returned to the laminar flow hood, and the strips carefully removed from the agar surface after photography and recording growth.

3.2.1.3 Post growth sterilisation

The post growth sterilisation of the strips was also used to record chemical information about the natural products produced by the fungi on different growth substrates (Chapter 4). The strips were placed into sterile 15ml falcon tubes containing 12ml of ethanol and shaken for 2 hours to extract natural products and ensure complete saturation. The strips were then removed from the tubes and the ethanol extracts retained for analysis by HPLC-MS. The strips were then laid out in the correct orientation on absorbent laboratory paper within the laminar flow hood to dry for 48 hours. After this time, any residual particulate matter was cleaned from the strips using a portable micro-vacuum with low suction and a soft brush. The strips were then saturated again with a 70% ethanol spray and left to dry for a further 24 hours.

3.2.2 Assessment of post growth substrate change

The previous methodology was used for samples to determine the change in colour of the substrate. Individual samples for live cell confocal microscopy were prepared (as in 3.2.1) with the post growth sterilisation phase omitted.

3.2.2.1 Spectrodensitometer readings

Changes in the colour space of materials was measured using an X-rite 500 series spectrodensitometer (DB26; 044570) in L*a*b* mode. Figure 3.2 illustrates the colour dimensions of L*a*b* and the chromatic implications of changes to the L, a and b values. The equipment was calibrated using a white ceramic standard after each set of strips from a fungal group. Measurements were all taken in the same location under ambient conditions.
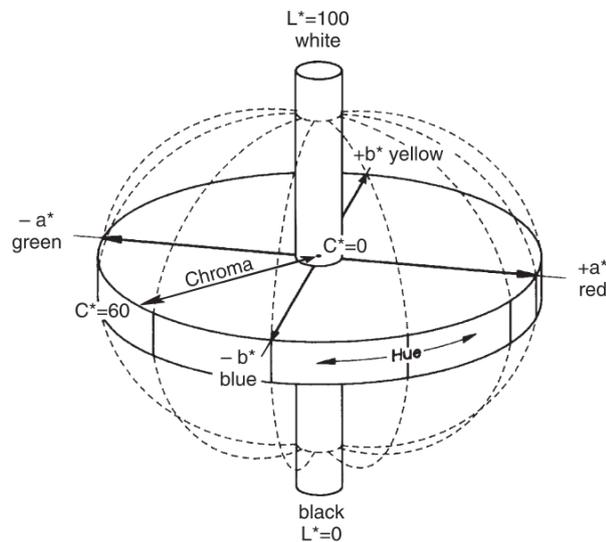
Figure 3.2- Representation of the CIE L*a*b* colour measurement showing the hue, chroma and lightness (X-rite 2007). In this colour space, L represents the lightness, a is how red/green and b is how blue/yellow a sample is.

All strips were measured in the same orientation with the machine facing in the warp direction. The initial reading was taken in the centre of the strip 5mm from the top. The subsequent two measurements were a further 5mm down the strip in the centre. Data was exported using Tool Crib and stored in Excel where statistical analysis was performed.

The total colour change of materials was expressed using untreated control samples to calculate the total colour change, ΔE shown in Equation 3.1.

Equation 3.2.1- ΔE equation using the L*a*b* readings for an untreated control and after fungal growth to express the change in colour within the L, a and b dimensions.

$$\Delta E = [(\Delta L)^2 + (\Delta a)^2 + (\Delta b)^2]^{0.5}$$

3.2.2.2 Confocal laser scanning fluorescence microscopy

Due to the necessity of fluorophores for this technique, separate samples of organic materials were prepared for microscopy analysis measuring $1cm^2$ using the previously described method. A thinner layer of agar was used for this methodology, approximately 4mm thick, and prior to inoculation, the organic substrate was gently pressed into the agar surface using a spatula. This ensured that after incubation, the agar and substrate could be removed together for mounting and reduced the depth of the sample to be measured. Mounting methodologies and dye protocols were adapted from Hickey *et al*. (Hickey et al. 2004).

The fluorescent dyes selected were chosen based on the available lasers for the Leica SP5 confocal microscope to be used and ensuring that the excitation and emission of the dyes did not overlap. The membrane selective probe FM4-64 was selected for the fungi as it indicated cell viability (the dye enters cells through endocytosis) and this amphiphilic styryl dye will only fluoresce in hydrophobic environments. This meant that this dye could be applied as a first stain and not affect the largely hydrophilic growth substrate. Under the 633nm laser, this dye will give a red emission.

Eosin Y was found to successfully label all of the organic substrates to be used using the 543nm laser. During testing, this dye did not overlap with the emission on the FM4-64 and created a green emission, enabling the clear distinction of fungal and material features. This dye also labelled fungal matter that was not stained by the FM4-64 so that the extent of growth could be seen, even if not viable at the time of imaging.

An inverted agar mounting method was developed which used the agar and liquid medium (containing the dyes and deionised water) to seal the slide and cover slip. Figure 3.3 details this methodology with the substrate indented within the agar.
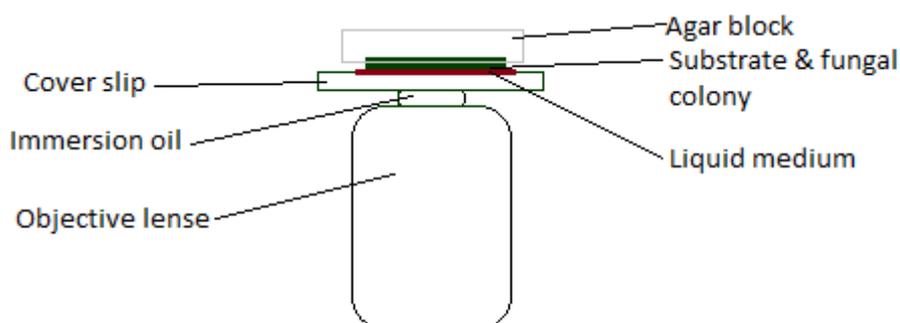
Figure 3.3- The inverted agar method of mounting (developed from Hickey et al., 2004) showing the top section of slides (slide not included). The agar and liquid medium effectively seal the slide and coverslip, leaving the substrate and fungal growth suspended in the liquid layer. A x40 oil immersion objective on a Leica SP5 microscope was used for imaging.

A 15mm section of agar was incised from the incubation dish around the sample on the day on imaging and places in the centre of a glass slide, within a sealed holder. After optimisation, it was found that 100μl of 100μM FM4-64 (in deionised water) applied 1 hour before 100μl of 1% Eosin Y (w/v in deionised water) and a subsequent 20 minute incubation provided the best imaging results. Prior to the cover slip, 50μl of deionised water was added to the agar surface to create a liquid layer and ensure a good fix of the agar, slide and cover slip. Clear nail varnish was applied to the coverslip corners to secure before inversion.

Slides were imaged using a x40 oil immersion lens and image quality was adjusted using the laser intensity and gain. All images were captured as 1024x1024, at a speed of 400 Hz and scanning between frames. Image stacks were recorded in the z-plane with a step size of 0.5μm. Image stacks were exported and processed using ImageJ.

3.3 Results

The results of the physical material changes, determined by colourimetry and confocal laser scanning microscopy investigations, are recorded below and organised by technique, then material.

3.3.1 Spectrodensitometer results

Unfortunately, due to variations in the surface of the wood and parchment samples (grain and follicle patters) and equipment availability, it was not possible to determine the colour change by colourimetry. It should be noted however that there was a visible colour change with the *Cladosporium* growth after 2 weeks of incubation and the *Aspergillus* and *Penicillium* formed more distinct colonies, affecting smaller surface areas. The natural biofilm of the wood samples contained a number of darkly pigmented fungi, whereas that of the parchment formed some bright yellow and red pigments.

3.3.1.1 Total colour change

Table 3.2 summarises the total colour change of each material (post cleaning) which would be indicative of a permanent visual distortion if applied to a historic object. The large standard deviations that can be seen indicate the materials on which fungi formed distinct, highly pigmented colonies rather than a more uniform covering of mycelium. Colour change was not linear over the 12 weeks of the trial for any of the conditions.

The most significant permanent changes were seen for the beech wood paper and the wool, followed by the silk and cotton; all materials commonly found within collections and used during

conservation. The average colour change across the 12 weeks shows that proteinaceous materials have the greatest colour change, with the exception of the materials inoculated with *Cladosporium*, which caused the greatest colour change on all materials (although this change was not significant for the leather and linen, both dense materials). The *Penicillium*, *Aspergillus* and natural biofilms had a much lesser effect on the permanent colour change of materials. Although in the case of the natural biofilm, this was dependant on the species that were cultivated. A summary of the species naturally occurring on each material can be seen in Table 3.3.

3.3.1.2 Natural biofilm cultures

The fungi was the most prevalent kingdom, which represented largely Ascomycota. Most of those cultured were common environmental airborne, with the exception of *Embellisia abundans* (not found during any of the survey work, see Chapter 2) and *Neonectria punicea* (only found during the summer season at 3 properties in south England, all with a latitude of 51). Also found were the teleomorphs (sexual reproductive stage) of *Alternaria* and *Aspergillus*, *Lewia* and *Eurotium* respectively. Teleomorphs have been very uncommon during the study of airborne spores in historic buildings (only *Talaromyces* (*Penicillium*) and *Davidiella* (*Cladosporium*) were cultured from air samples), but more common when cultured from swabs of solid surfaces. The different species grown from the materials, their abundance and their ability to grow effectively all influenced the colour change of the materials.

Table 3.2- The mean colour change (post cleaning), represented as ΔE, over 12 weeks of incubation with different fungal inoculums ±standard deviation. P-value of ANOVA shows significant colour change with fungi marked as * p=<0.05 & ** p=<0.01.

Material	Fungi	Mean colour change (ΔE) Weeks of incubation								p-value
		1	2	3	4	6	8	10	12	
Cotton	Aspergillus*	4.86±2.17	5.54±1.65	5.95±1.81	3.65±1.65	2.68±0.73	3.59±0.64	6.18±2.99	6.38±2.06	0.02
	Cladosporium**	37.68±1.75	38.91±2.76	36.55±2.63	31.73±2.63	30.32±2.07	28.22±3.51	26.44±8.00	35.49±4.07	<0.01
	Natural biofilm*	2.39±0.83	3.36±2.44	3.36±0.64	3.31±0.85	4.75±1.46	7.29±2.58	7.26±3.87	6.54±5.26	0.03
	Penicillium*	2.96±0.76	6.10±2.04	3.88±3.23	5.48±1.60	3.68±0.92	4.16±1.21	5.65±2.36	10.32±7.62	0.02
Linen	Aspergillus	1.13±0.95	3.27±1.55	3.35±0.69	2.28±1.22	3.29±0.71	3.02±1.23	4.73±3.69	3.64±1.58	>0.05
	Cladosporium	4.56±2.52	7.69±2.32	5.54±1.69	9.11±1.63	8.00±2.73	7.59±2.06	9.75±1.90	6.71±2.84	>0.05
	Natural biofilm*	2.41±0.74	2.32±0.66	2.47±0.77	3.44±0.36	2.26±0.24	2.29±1.21	3.45±0.82	3.40±0.87	0.02
	Penicillium	3.42±0.95	6.17±2.58	5.30±4.01	5.40±2.66	3.45±1.26	3.83±1.25	4.00±0.81	5.93±2.39	>0.05
Cotton and linen paper	Aspergillus*	2.27±2.28	6.75±8.48	1.80±0.47	1.07±0.65	1.21±0.65	5.07±3.29	6.74±1.59	6.73±2.59	0.02
	Cladosporium*	17.12±3.27	16.87±3.39	16.83±6.02	24.54±7.53	15.31±3.83	22.24±2.91	22.13±3.00	19.96±4.34	0.03
	Natural biofilm	1.77±0.30	1.34±0.83	1.61±0.72	1.04±0.16	1.39±0.75	1.22±0.42	1.28±0.47	1.01±0.19	>0.05
	Penicillium*	0.85±0.12	5.11±3.15	6.50±6.99	5.35±1.94	1.87±0.57	3.45±3.74	3.63±2.30	8.13±1.96	0.03
Beech wood paper	Aspergillus**	2.29±0.96	4.20±1.79	4.00±1.70	2.80±1.14	4.17±3.27	8.70±2.70	5.60±2.10	6.06±0.77	<0.01
	Cladosporium**	15.28±2.74	17.58±2.08	18.56±3.22	26.08±3.84	19.58±2.37	26.52±4.17	25.30±4.36	26.83±2.63	<0.01
	Natural biofilm**	0.92±0.20	1.02±0.31	0.97±0.36	3.19±2.36	2.28±0.97	1.58±0.36	1.67±0.87	2.60±0.71	0.01
	Penicillium**	2.33±1.38	4.80±1.59	5.74±2.65	5.12±2.20	5.60±2.87	9.17±3.35	2.49±1.51	11.21±4.51	<0.01
Silk	Aspergillus**	4.25±1.09	12.66±2.81	10.96±1.58	3.73±0.98	3.30±0.78	7.65±2.32	11.39±2.28	9.73±1.50	<0.01
	Cladosporium**	32.39±1.17	32.22±5.73	32.93±3.55	27.9±5.69	23.56±3.10	22.48±5.39	21.45±1.64	44.52±2.26	<0.01
	Natural biofilm**	0.96 ± 0.39	1.60±0.48	2.86±1.60	1.95±0.84	5.33±4.34	5.07±3.67	3.99±1.12	4.48±2.48	0.03
	Penicillium	2.88±1.00	9.81±6.98	3.37±2.49	10.06±7.07	6.06±1.80	6.56±2.82	5.88±3.11	8.25±2.64	>0.05
Wool	Aspergillus**	3.51±1.59	7.25±2.65	7.57±1.96	2.64±0.73	3.79±0.92	5.89±1.01	4.73±1.55	6.24±1.33	<0.01
	Cladosporium**	22.97±2.76	25.23±1.47	29.29±1.73	22.31±3.25	18.22±1.93	19.75±2.73	20.87±2.41	34.48±2.16	<0.01
	Natural biofilm**	1.96±1.64	7.03±5.17	9.56±4.29	8.64±4.22	12.61±4.86	19.00±2.09	7.32±2.84	13.71±1.42	<0.01
	Penicillium**	2.17±0.90	7.44±4.44	4.37±2.97	6.10±2.51	8.52±1.67	3.79±2.13	5.45±1.41	5.97±2.11	<0.01
Leather	Aspergillus**	4.36±1.18	5.16±2.46	3.68±0.30	11.35±3.89	5.14±2.81	14.17±3.42	11.81±5.87	15.88±4.29	<0.01
	Cladosporium	5.11±2.08	6.01±2.61	15.06±6.22	11.17±4.03	13.35±3.28	10.91±4.52	11.75±1.65	20.08±18.51	>0.05
	Natural biofilm	5.09±2.00	6.06±3.65	6.67±5.12	7.96±4.70	4.55±2.92	4.82±1.76	4.92±2.61	4.52±2.48	>0.05
	Penicillium**	4.29± 1.74	6.22± 2.52	12.54± 2.68	12.11± 6.01	13.57± 4.58	7.64±3.08	14.90±2.71	12.24±2.16	<0.01

Table 3.3- The species cultivated from PDA press plates of each material. Plates prepared from unsterilized materials in their original packaging by pressing 50mm2 squares into the centre and then discarding the material. Plates incubated for 7 days prior to counting and sub-culturing individual cultures for identification (culture collection comparison and Sanger sequencing of ITS regions).

Material	Kingdom	Phylum	Genera	Species	Frequency
	Bacteria	*Actinobacteria*	*Actinomycete*	-	2
	Fungi	*Ascomycota*	*Cladosporium*	*cladosporiodes*	2
Cotton	Fungi	*Ascomycota*	*Toxicocladosporium*	*irritans*	1
	Fungi	-	-	Unknown yeast	1
	Fungi	*Ascomycota*	*Lewia*	*infectoria*	1
	Fungi	*Ascomycota*	*Aspergillus*	*versicolor*	2
	Fungi	*Zygomycota*	*Mucor*	-	2
	Fungi	*Ascomycota*	*Aspergillus*	*fumigatus*	1
Linen	Fungi	*Ascomycota*	*Aspergillus*	versicolor	1
	Fungi	-	-	Unknown yeast	1
	Fungi	*Ascomycota*	*Cladosporium*	-	3
	Bacteria	-	-	-	2
Cotton and	Fungi	*Ascomycota*	*Lewia*	*infectoria*	1
linen paper	Fungi	*Ascomycota*	*Sarocladium*	*kiliense*	1
	Fungi	-	-	Unknown yeast	2
	Bacteria	-	-	-	1
	Fungi	*Ascomycota*	*Aspergillus*	*versicolor*	1
Beech wood	Fungi	*Ascomycota*	*Cladosporium*	*cladosporiodes*	1
paper	Fungi	*Ascomycota*	*Penicillium*	*vancouverense*	3
	Fungi	*Ascomycota*	*Embellisia*	*abundans*	1
	Fungi	*Ascomycota*	*Cladosporium*	*cladosporiodes*	15
	Fungi	*Ascomycota*	*Penicillium*	*expansum*	4
	Fungi	*Ascomycota*	*Penicillium*	*chrysogenum*	2
Pine	Fungi	*Ascomycota*	*Penicillium*	*sp.*	2
	Fungi	*Ascomycota*	*Aspergillus*	*versicolor*	1
	Fungi	*Ascomycota*	*Eurotium*	*sp.*	1
	Fungi	*Ascomycota*	*Fusarium*	*sporotrochiodes*	1
	Fungi	-	-	Unknown yeast	1
	Fungi	*Ascomycota*	*Trichoderma*	*atroviride*	3
	Fungi	*Ascomycota*	*Epicoccum*	*nigrum*	13
Oak	Fungi	*Ascomycota*	*Penicillium*	*brevicompactum*	4
	Fungi	*Ascomycota*	*Trichoderma*	*atroviride*	5
	Fungi	*Ascomycota*	*Trichoderma*	*atroviride*	4
	Fungi	*Ascomycota*	*Cladosporium*	*allicinum*	2
	Bacteria	*Actinomycete*	-	-	3
	Fungi	*Ascomycota*	*Cladosporium*	*herbarum*	2
	Fungi	*Ascomycota*	*Cladosporium*	*cladosporiodes*	1
Silk	Fungi	*Ascomycota*	*Sarocladium*	-	1
	Fungi	*Ascomycota*	*Lewia*	*infectoria*	1
	Fungi	*Ascomycota*	*Alternaria*	*infectoria*	1
	Fungi	*Ascomycota*	*Alternaria*	-	1
	Fungi	*Ascomycota*	*Cladosporium*	*cladosporiodes*	7
	Fungi	*Ascomycota*	*Penicillium*	*commune*	1
	Fungi	*Ascomycota*	*Penicillium*	*chrysogenum*	1
Wool	Fungi	*Ascomycota*	*Penicillium*	*brevicompactum*	1
	Fungi	*Ascomycota*	*Lewia*	*infectoria*	2
	Fungi	*Ascomycota*	*Aspergillus*	*versicolor*	2
	Fungi	*Ascomycota*	*Aspergillus*	-	1

	Fungi	*Ascomycota*	*Epicoccum*	*nigrum*	1
	Fungi	*Ascomycota*	*Neonectria*	*punicea*	1
	Fungi	-	-	Unknown yeast	1
Leather	Fungi	*Ascomycota*	*Cladosporium*	*herbarum*	1
	Bacteria	-	-	-	1
	Bacteria	-	-	-	1
	Bacteria	-	-	-	1
	Fungi	*Ascomycota*	*Penicillium*	*brevicompactum*	1
	Fungi	*Ascomycota*	*Aspergillus*	*niger*	1
Parchment	Fungi	*Ascomycota*	*Alternaria*	*sp.*	3
	Fungi	-	-	Unknown yeast	1
	Bacteria	*Actinomycete*	-	-	1
	Bacteria	-	-	-	1

3.3.1.3 Dimensional colour change

The specific colour change of samples could be analysed by looking at the different dimensions of the L*a*b colour space; lightening/darkening, red/green and yellow/blue.

Figures 3.4a-d show the specific permanent colour change of cotton after incubation over the 12 weeks of the study. With *A. versicolor* (Figure 3. 4a) there is a linear increase in the redness of the cotton (R^2=0.89) and a yellowing effect that occurs over the first 3 weeks of incubation. However the darkening of the cotton is the most visible difference. The greatest change in colour dimension after *C. cladosporiodes* growth was in the darkening of cotton (Figure 3.4b), as can be seen by the strong correlation between the ΔE and ΔL values; τ= 0.99, *p*=< 0.001. There is also an increase in the level of blue, again correlated significantly to the ΔE value, but not so strongly as the darkening effect (τ= 0.37, *p*=< 0.001). This staining was not limited to colony margins and was spread over the full surface of the material. There is also a linear trend for the increase of red in the cotton after incubation (*J (120)* =4697, *r*= 0.65, *P*<0.001). For cotton, the *Penicillium* and *Aspergillus* show a similar staining pattern, in that the permanent colour changes were predominantly located around the colony perimeters. Over the 12 weeks the *Penicillium* caused a general darkening of the cotton and an increase in red (*R^2*=0.83). There was largely a reduction in the level of yellow, favouring and increase in blue, until week 12 when there was an increase towards yellow (Figure 3.4c). Due to the species diversity of the natural biofilm, there was significant colour change of the cotton, associated with colony boundaries. Figure 3.4d shows that there was a linear darkening of the cotton (R^2=0.71) with an increase in blue and a slight reddening of the material.
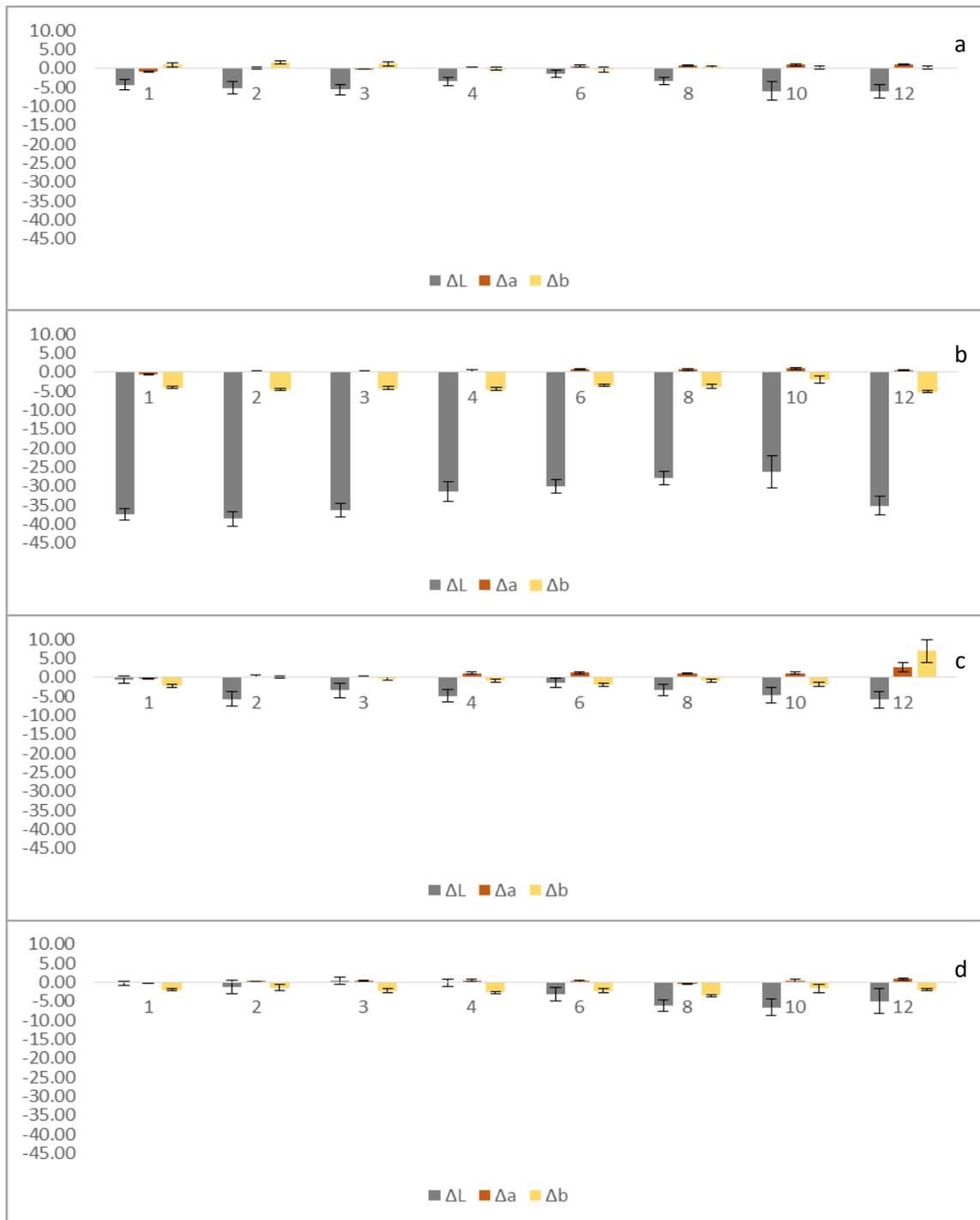
Figure 3.4- a-d- The mean ΔL*a*b* readings for cotton cultivated with inoculums of Aspergillus versicolour *(a),* Cladosporium cladosporiodes *(b),* Penicillium brevicompactum *(C) and the natural biofilm. All were incubated for up to 12 weeks at 20℃, cleaned/sterilised before an average of 5 colorimeter readings calculated. The changes in colour dimensions are represented as ΔL=Lightening/darkening Δa=Red/greening Δb=Yellow/blueing. Error bars represent the calculated standard error.*

The changes in the colour of linen after incubation were far less than those of other materials, with only the natural biofilm having a significant effect on the physical appearance of the material (Table 3.2). Although not significantly altered, the L*a*b* colour space changes for linen after incubation with *Aspergillus* indicate that there is a slight increase in the yellow and

red hues and a darkening of the material. *Cladosporium* caused slight increases in the green and blue of the material and an overall darkening of the fibres, while *Penicillium* increased in the yellow and red of the material and an overall darkening of the fibres. The natural biofilm of linen was the only incubation condition to cause significant alterations to the fabric appearance (*p*=0.02), although this was due to the extreme changes in colour associated with the different colonies that formed (Table 3.3).

Figures 3.5a-c show the significant changes in colour for cotton and linen paper which include the three fungal inoculums, but not the natural biofilm (Table 3.2). *Aspergillus* caused a linear increase in the redness of the paper over the 12 weeks (R^2=0.79) with a yellowing and darkening that were more prominent over the beginning and end weeks of incubation (Figure 3.5a).
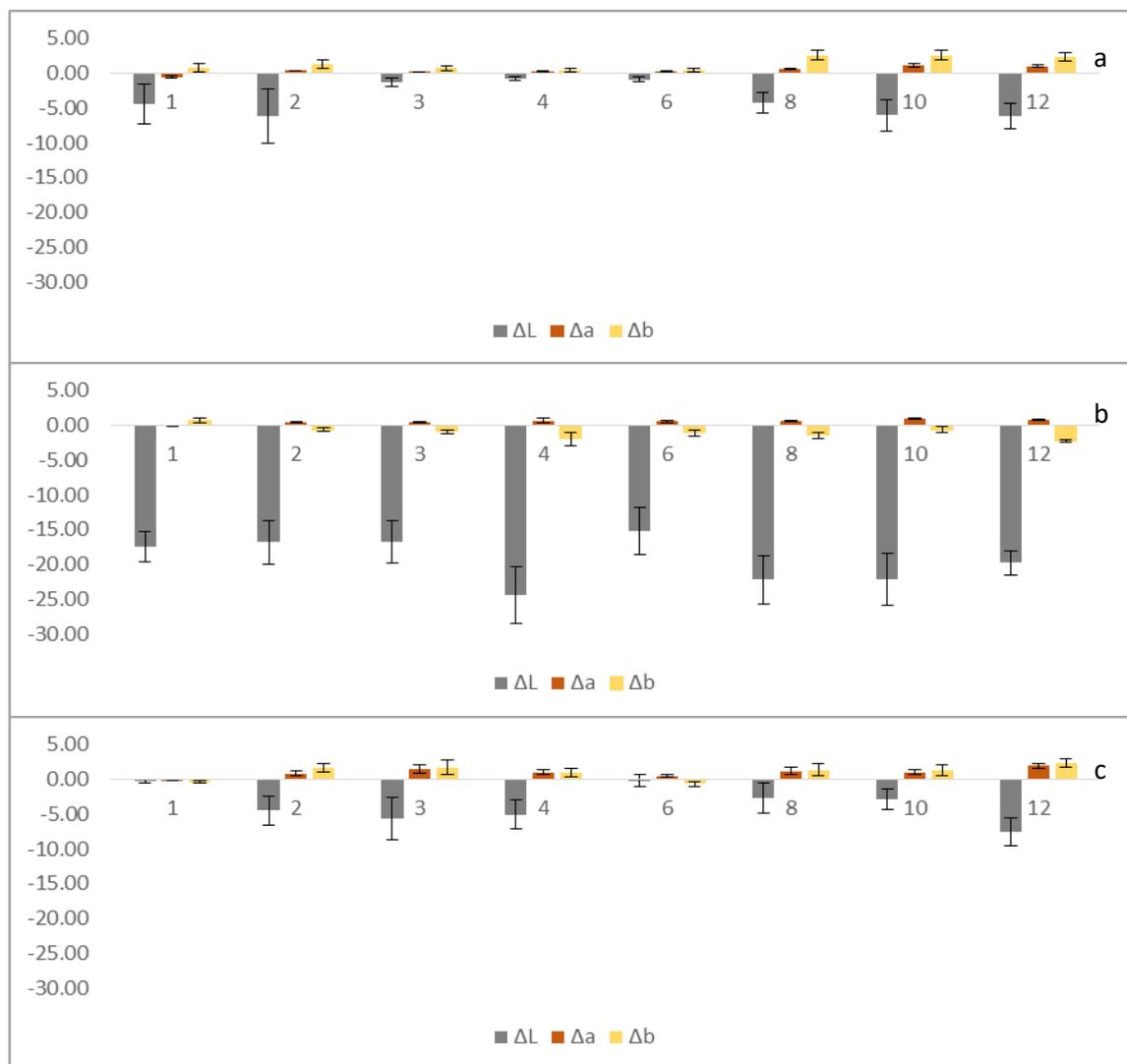
Figure 3.5 a-c- The mean ΔL*a*b* readings for cotton and linen paper cultivated with inoculums of Aspergillus versicolour *(a),* Cladosporium cladosporiodes *(b),* Penicillium brevicompactum *(C) and the natural biofilm. All were incubated for up to 12 weeks at 20°C, cleaned/sterilised before an average of 5 colorimeter readings calculated. The changes in colour dimensions are represented as ΔL=Lightening/darkening Δa=Red/greening Δb=Yellow/blueing. Error bars represent the calculated standard error.*

The *Cladosporium* had the greatest darkening effect on the paper with an increase in red and blue (Figure 3.5b). After an initial slight darkening of the paper (increase of blue/green) *Penicillium* caused an increase in yellow & red and a darkening of the paper during the beginning and latter weeks of the trial (Figure 3.5c). There was only a slight change in the appearance of the samples from week 6.

The beech wood paper had different changes in colour to the cotton and linen with a more intense and significant colour change across all of the fungal incubations. The paper inoculated with *Aspergillus* showed a linear increase of red in the material (R^2= 0.92) with an increase in yellow, although this is curvilinear in trend with a lesser effect seen in weeks 4 and 6 (Figure 3.6a). There is a general darkening effect seen on the paper, the peak of which was during week 8, but there is a general trend for the greater effects being seen after the longer incubation times (R^2= 0.53). *Cladosporium* caused, as in most cases, the greatest darkening effect on the paper (Figure 3.6b) which tends to increase, the longer the fungi is left to incubate (R^2=0.73). There is an initial yellowing of the paper, but this decreases after longer periods of growth and the increase in red can only be seen during weeks 2, 6, 8 and 10. The beech wood paper inoculated with *Penicillium* generally yellowed with an increase in red over the 12 weeks, although this is not the case for the samples of week 10 (Figure 3.6c). The paper also becomes darker the longer it is left to incubate (R^2=0.73). The natural biofilm of beech wood paper caused a darkening of the fibres with a slight increase in blue and red, although this was not a linear effect (Figure 3.6d).

The change in appearance of the proteinaceous materials was generally greater than those of the cellulosic materials. Silk inoculated with *Aspergillus* showed a steady increase in the level of red over the incubation period (R^2=0.89). As the level of yellow increased, the lightness of the silk decreased and vice versa (r=-0.94). This indicates that the level of yellow colour is the significant factor in whether the material will look lighter or darker (Figure 3.7a). After incubation, *Cladosporium* again showed the greatest darken effect on the substrate with a slight increase of yellow and red (Figure 3.7b). *Penicillium* also caused an increase in yellow and red in the silk, although after initial fluctuations, this levelled off after week 4 of the incubation (Figure 3.7c). The silk also became darker, the effect of which was again similar after the readings of week 4 and was largely dependent on whether there was an established colony in the vicinity of the sample location. The natural biofilm again increased the level of yellow and red with an overall darkening of the silk, although the colonies of different species did not make for an even effect (Figure 3.7d).
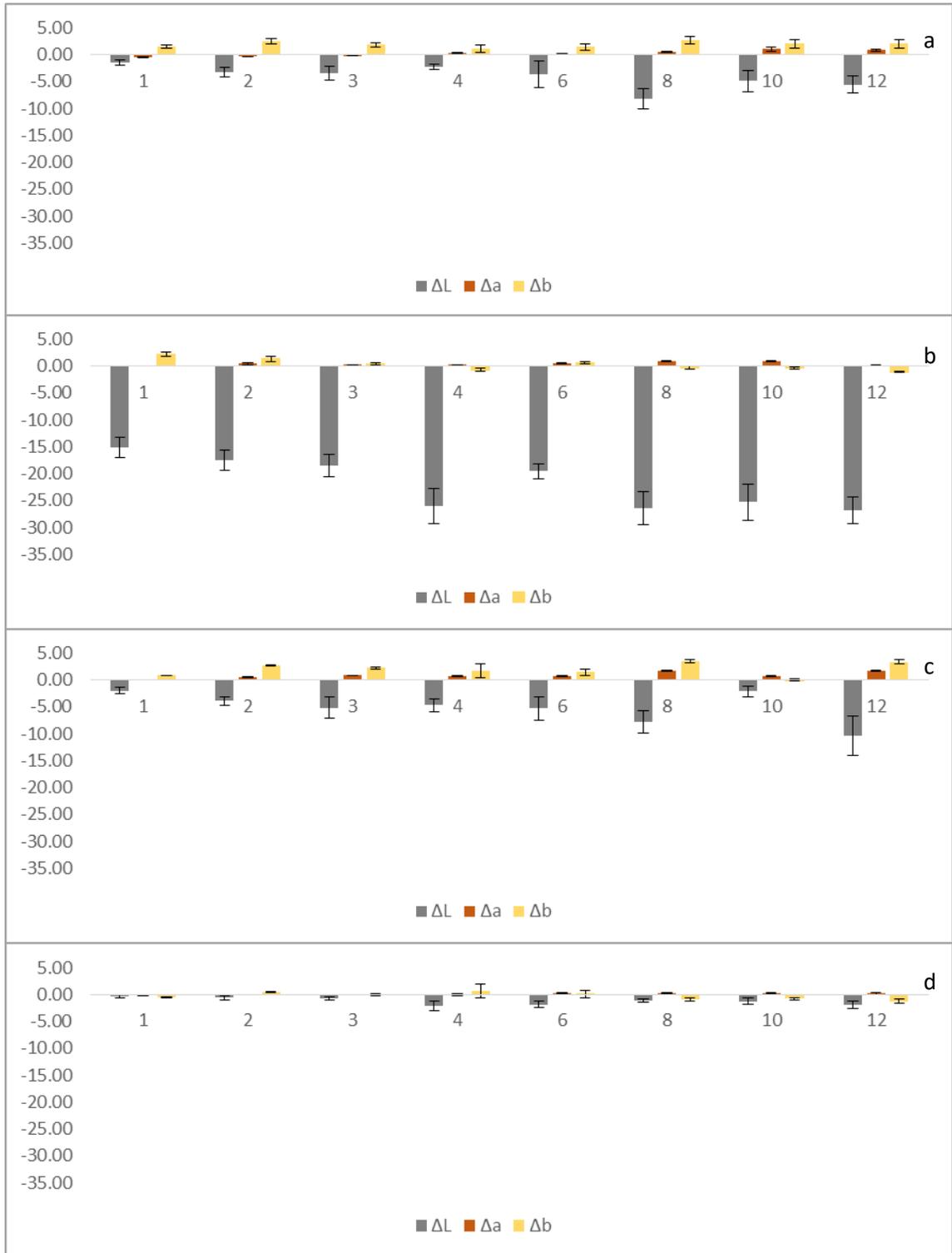
Figure 3.6 a-d- The mean ΔL*a*b* readings for beech wood paper cultivated with inoculums of Aspergillus versicolour *(a),* Cladosporium cladosporiodes *(b),* Penicillium brevicompactum *(C) and the natural biofilm. All were incubated for up to 12 weeks at 20°C, cleaned/sterilised before an average of 5 colorimeter readings calculated. The changes in colour dimensions are represented as ΔL=Lightening/darkening Δa=Red/greening Δb=Yellow/blueing. Error bars represent the calculated standard error.*
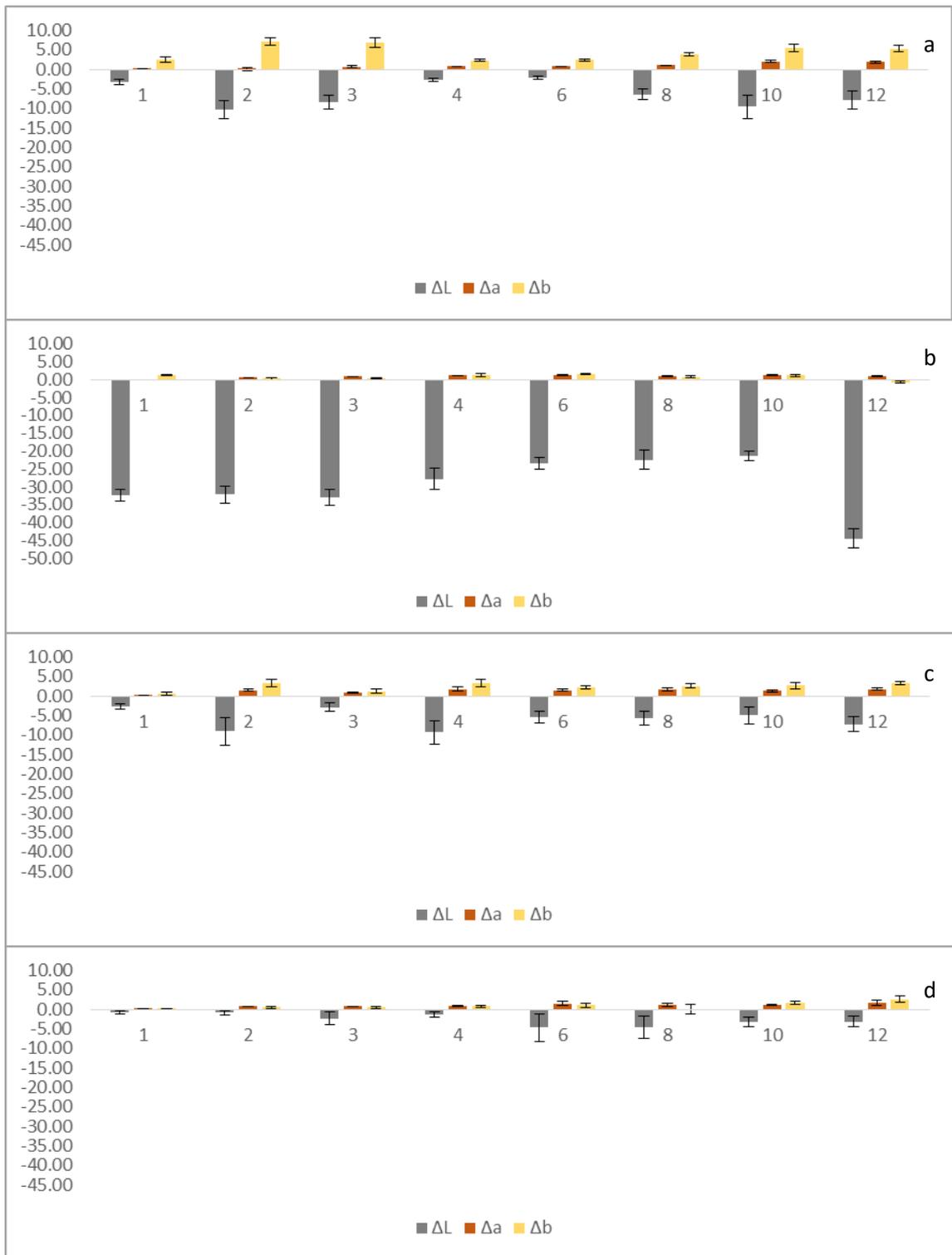
Figure 3.7 a-d- The mean ΔL*a*b* readings for silk cultivated with inoculums of Aspergillus versicolour *(a),* Cladosporium cladosporiodes *(b),* Penicillium brevicompactum *(C) and the natural biofilm. All were incubated for up to 12 weeks at 20℃, cleaned/sterilised before an average of 5 colorimeter readings calculated. The changes in colour dimensions are represented as ΔL=Lightening/darkening Δa=Red/greening Δb=Yellow/blueing. Error bars represent the calculated standard error.*

The colour change of wool inoculated with *Aspergillus* was largely influenced by the lightening and darkening of the sample with the quantity of yellow or blue, for which there was a significant correlation (r=-0.88); the darker the sample, the greater the blue; the lighter the sample, the greater the yellow (Figure 3.8a). Each week there was an increase in the level of red in the textile. This change was positively correlated with the level of yellow in the sample (r=0.78). For wool inoculated with *Cladosporium* there was an increase in the level of red (R^2=0.80) over the trial, after an initial decrease (Figure 3.8b). There was a darkening and increase in blue over all of the weeks of the trial but this had a polynomial trend; a period of increase, decrease and then increase (in line with the ΔE values). The change in darkness and yellowing were closely correlated (r=0.84). The colour change of wool incubated with *Penicillium* (Figure 3.8c) was largely caused by the darkening or yellowing of the wool fibres (negatively correlated, r=-0.68), with a linear increase in red over the trial (R^2=0.70). The change in colour from the natural biofilm was largely dictated by the yellowing of the wool as it was correlated to the overall change in the ΔE value (r=0.82) and followed the same two phases of change Figure 3.8d). There was also an increase in red and a darkening of the wool. The colour changes were dependant on the colonising species and their positions on the fabric, which also accounted for the greater degree of variation between samples. Figure 3.9a illustrates the difference between of individual samples that were cleaned and sterilised after 8 weeks of growth.

The colour change of leather was less than the other proteinaceous materials with only the *Aspergillus* and *Penicillium* showing significant differences. This was primarily due to the formation of isolated colonies on this material which had an effect on the colour of the immediate area, but did not extend to the whole material (Figure 3.9b). This can also be seen in the larger standard error of the colorimeter readings across all of the samples as they were not uniform in their staining. *Aspergillus* caused a general darkening and yellowing of the leather with an increase in red (Figure 3.10a). However, due to different staining patterns from individual colonies, there was not a clear trend and there was then a decrease in red over the latter weeks of the trial. *Penicillium* growth had a similar effect with a general darkening and yellowing over the trial, with the exception of week 4 which had some large colonies form where samples were taken (Figure 3.9b), causing an increase of blue, rather than yellow. The redness of the leather was also affected by colony positioning and both increases and decreases were seen throughout the incubation time (Figure 3.10b).
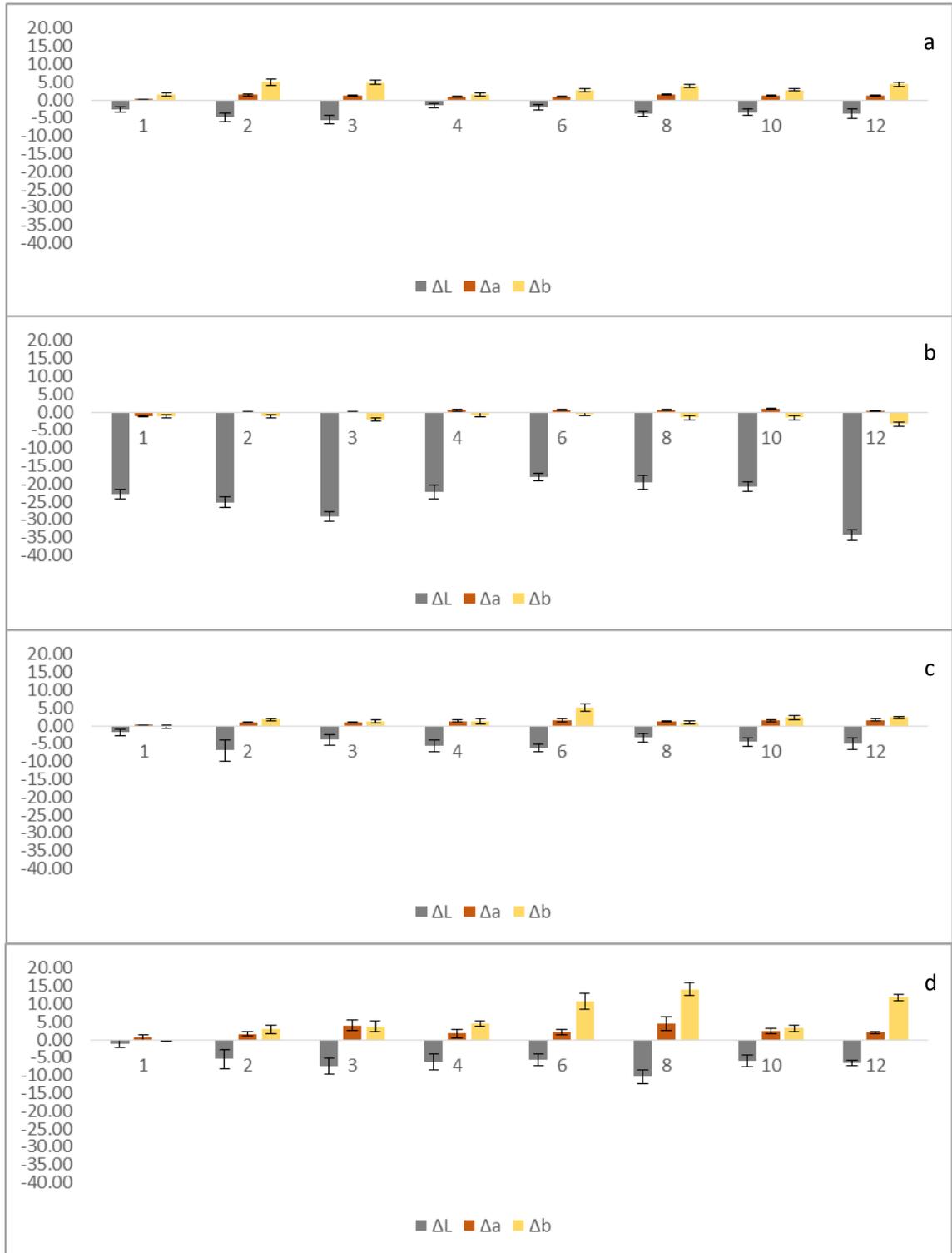
Figure 3.8 a-d- The mean ΔL*a*b* readings for wool cultivated with inoculums of Aspergillus versicolour *(a),* Cladosporium cladosporiodes *(b),* Penicillium brevicompactum *(C) and the natural biofilm. All were incubated for up to 12 weeks at 20°C, cleaned/sterilised before an average of 5 colorimeter readings calculated. The changes in colour dimensions are represented as ΔL=Lightening/darkening Δa=Red/greening Δb=Yellow/blueing. Error bars represent the calculated standard error.*

Figure 3.9 a-b- a) Wool samples incubation with a natural biofilm over 8 weeks at 20°C in high a_w conditions. Samples are shown post vacuum and solvent cleaning. b) Leather samples inoculates with Penicillium brevicompactum *and incubated over 4 weeks at 20°C in high a_w conditions, showing the individual colonies formed during growth. All samples are shown post vacuum and solvent cleaning*
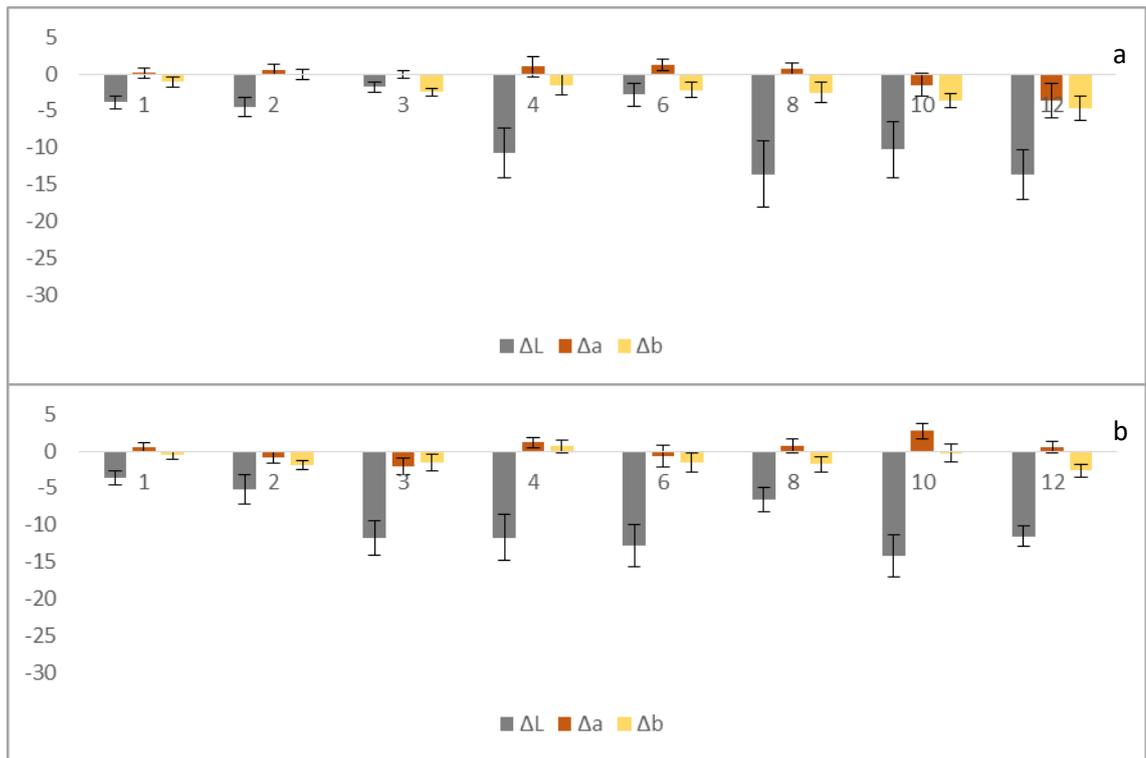
Figure 3.10 a-b- The mean ΔL*a*b* readings for leather cultivated with inoculums of Aspergillus versicolour *(a),* Cladosporium cladosporiodes *(b),* Penicillium brevicompactum *(C) and the natural biofilm. All were incubated for up to 12 weeks at 20°C, cleaned/sterilised before an average of 5 colorimeter readings calculated. The changes in colour dimensions are represented as ΔL=Lightening/darkening Δa=Red/greening Δb=Yellow/blueing. Error bars represent the calculated standard error.*

3.3.2 Confocal laser scanning fluorescence microscopy results

Through the use of confocal laser scanning fluorescence microscopy, it was possible to view the active growth of fungi on the solid substrates, their penetration of materials, reproductive stage and whether they were actively performing endocytosis through the use of the membrane selective dye FM4-64. A summary of each material with the different fungal inoculums follows, with the exception of leather as, due to the density of the material, the laser would not

penetrate. It was not possible to run this investigation with the natural biofilm as germination was too sporadic and species varied over the 12 weeks of incubation.

3.3.2.1 Confocal images of cotton

After 1 week of incubation with Aspergillus versicolor (Figure 3.11) there were fine hyphae visible through the structure of the cotton weave (highlighted in A) and in the orthogonal slices (B & C), it was possible to see that hyphae had already penetrated the cotton fibre and were visible in the irregular shaped lumen.
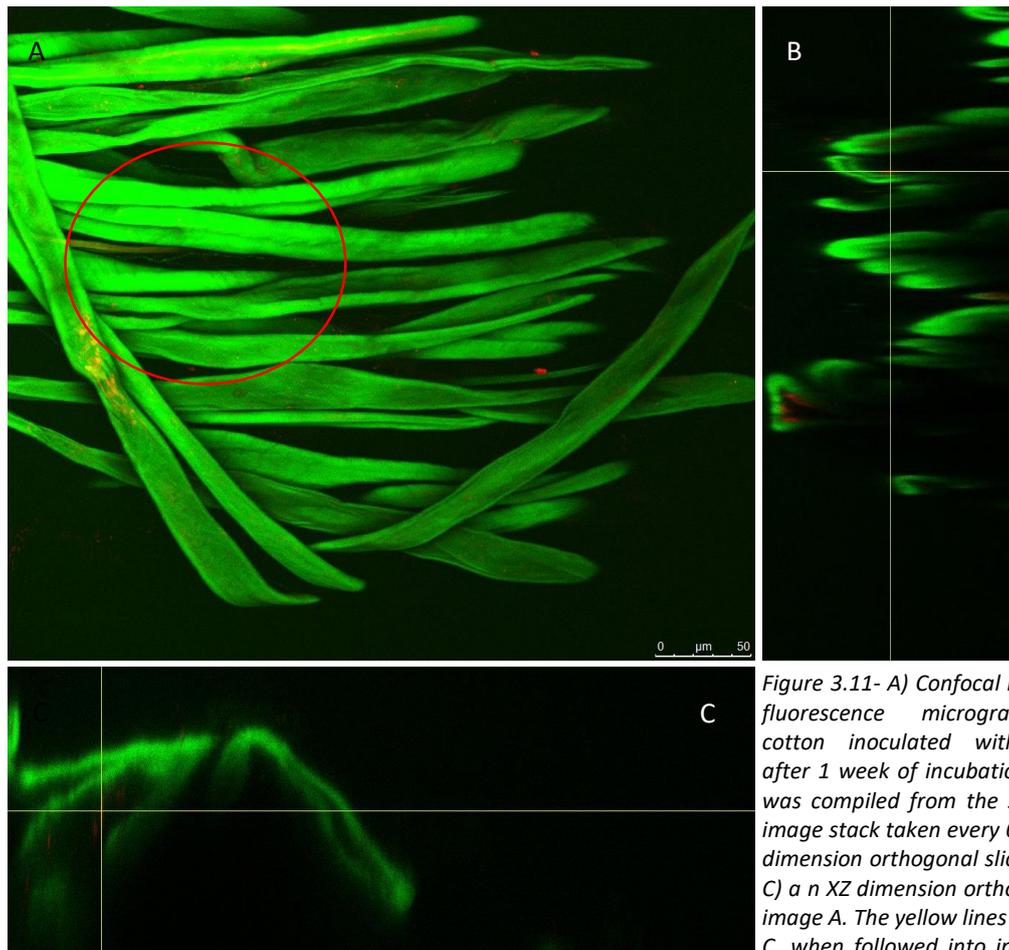
Figure 3.11- A) Confocal laser scanning fluorescence microgram showing cotton inoculated with Aspergillus *after 1 week of incubation. The image was compiled from the sum of a 398 image stack taken every 0.5μm. B) a YZ dimension orthogonal slice of image A. C) a n XZ dimension orthogonal slice of image A. The yellow lines of images B & C, when followed into image A, show the location of the orthogonal slice.*

After four weeks, there were extensive, mature hyphal networks throughout the cotton weave and conidiophores visible above the crown of the weave (Figure 3.12). By the end of the trial there were extensive mature hyphae and evidence of finer, new growth (Figure 3.13). The surface morphology of the fibres had altered, with differing local thicknesses along the length of fibres as well as some pitting and cracks starting to appear.
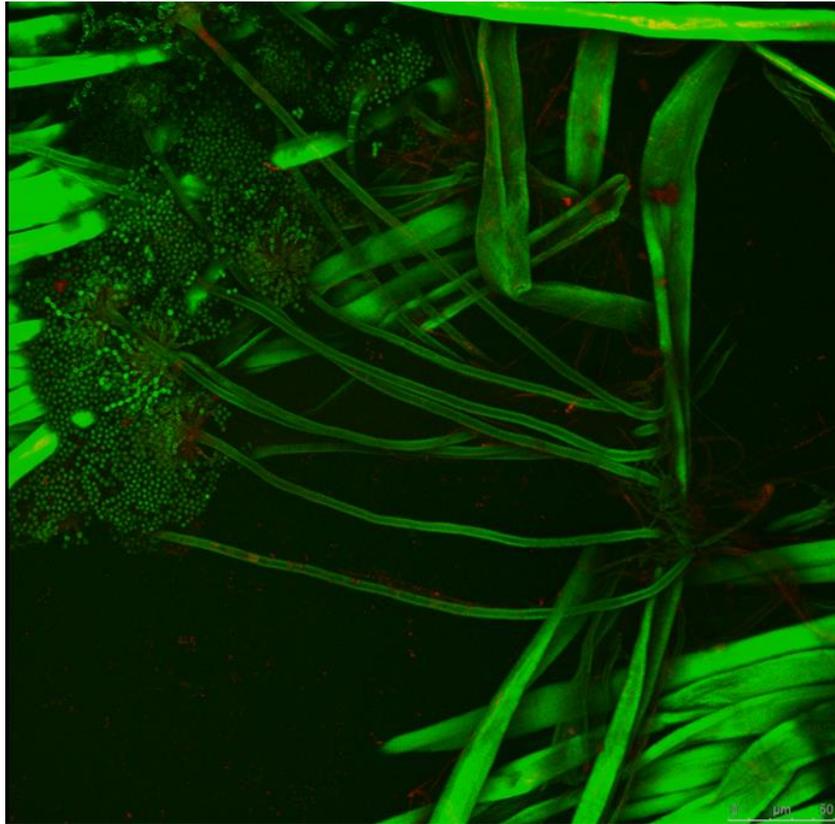
Figure 3.12- 3D projected confocal laser scanning fluorescence microgram showing cotton inoculated with Aspergillus *after 4 weeks of incubation. The image was compiled from the sum of a 140 image stack taken every 0.5µm.*
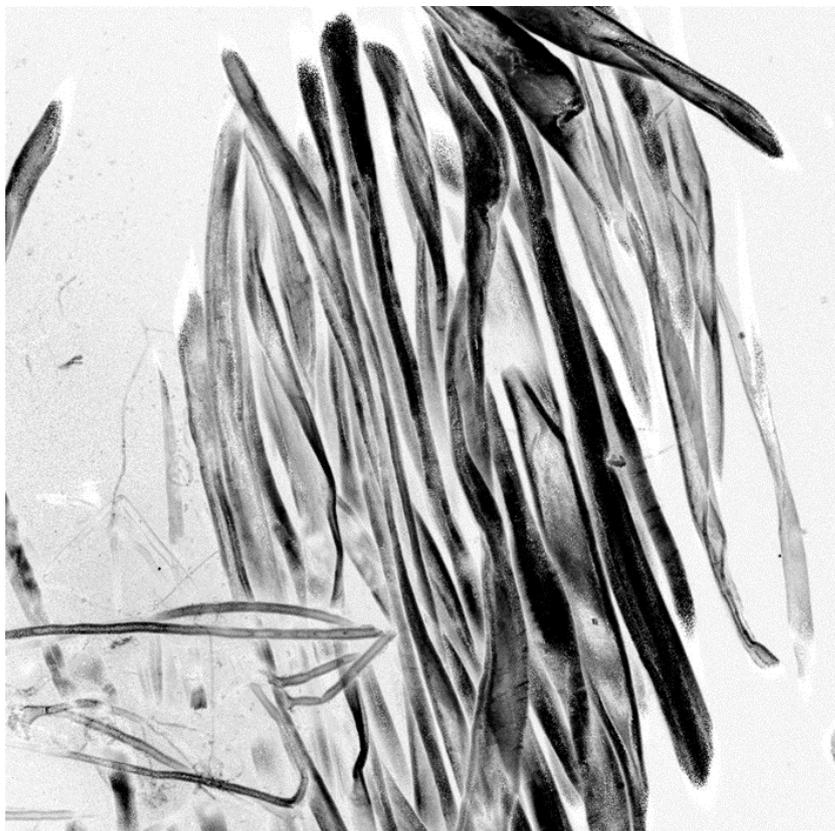
Figure 3.13-Topographical height map created from the confocal laser scanning microgram stack of cotton inoculated with Aspergillus *after 12 weeks of incubation. The image was compiled from the sum of a 142 image stack taken every 0.5µm.*

For *Cladosporium*, during the first few weeks of incubation, growth was slower than for the other species and there was no sign of sporulation until week 3. However the hyphal growth, when visible, was very darkly pigmented and was largely in the lower regions of the weave structure of the cotton. This meant that although the growth could visibly be seen, it was difficult to detect using the fluorescence microscope due to the limited laser penetration through the cotton. Figure 3.14 details the material after 6 weeks of incubation and shows that sporulation has occurred with the reproductive features sitting above the crown of the weave (as highlighted). Even by the end of the trial, the majority of the hyphal growth was not visible as it sat below the crown of the weave, meaning that the laser could not penetrate and give an accurate image.

Figure 3.14- Confocal laser scanning fluorescence microgram showing cotton inoculated with Cladosporium *after 6 weeks of incubation. The image was compiled from the sum of a 353 image stack taken every 0.5µm. Highlighted areas show the* Cladosporium *conidiophores protruding above the structure of the weave, the red FM4-64 dye fluorescence indicates viability of the fungi.*
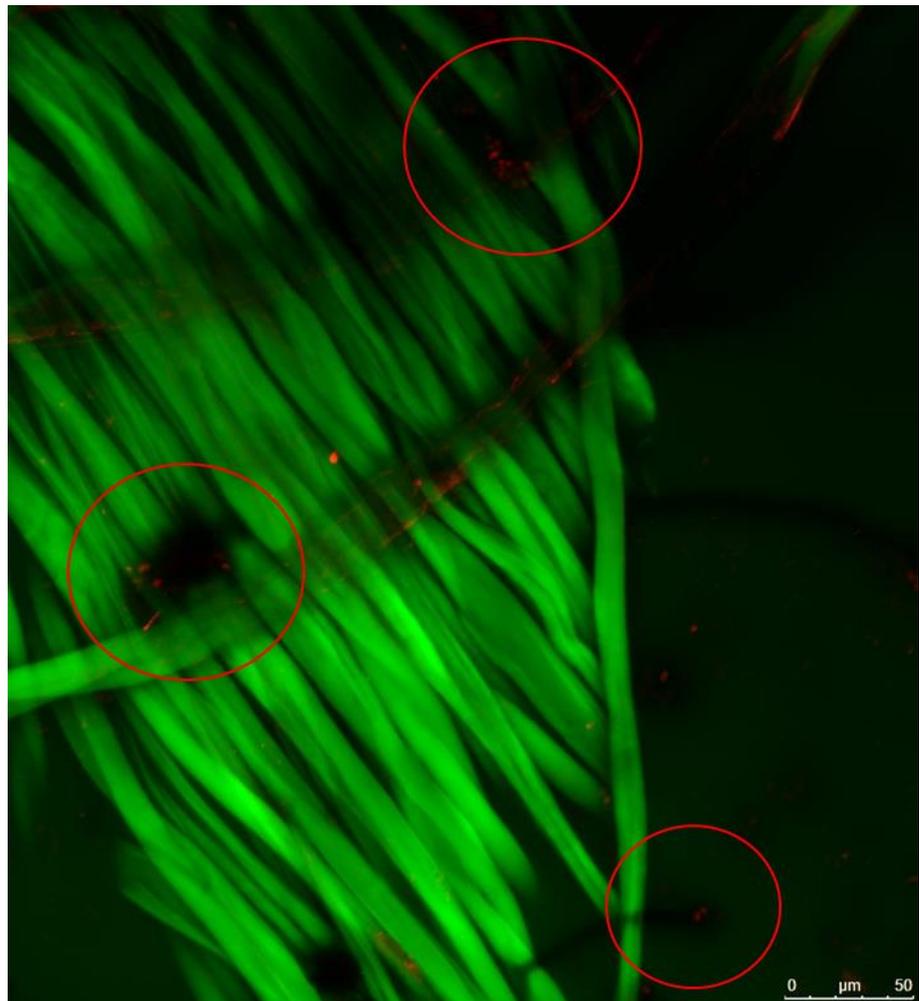
It was however possible to a lot of conidiophores that were still viable, due to the endocytosis dye uptake, showing as red in the highlighted area of Figure 3.15. It is also possible to see that some defibrillation of the cotton had occurred, shown in Figure 3.15A, a local thickness plot of the same image stack. In the fibres around the crown of the weave the macrofibrillar bundle

separation was commonly observed but the fibres that were more tightly grouped within the weave structure were not affected in the same way.
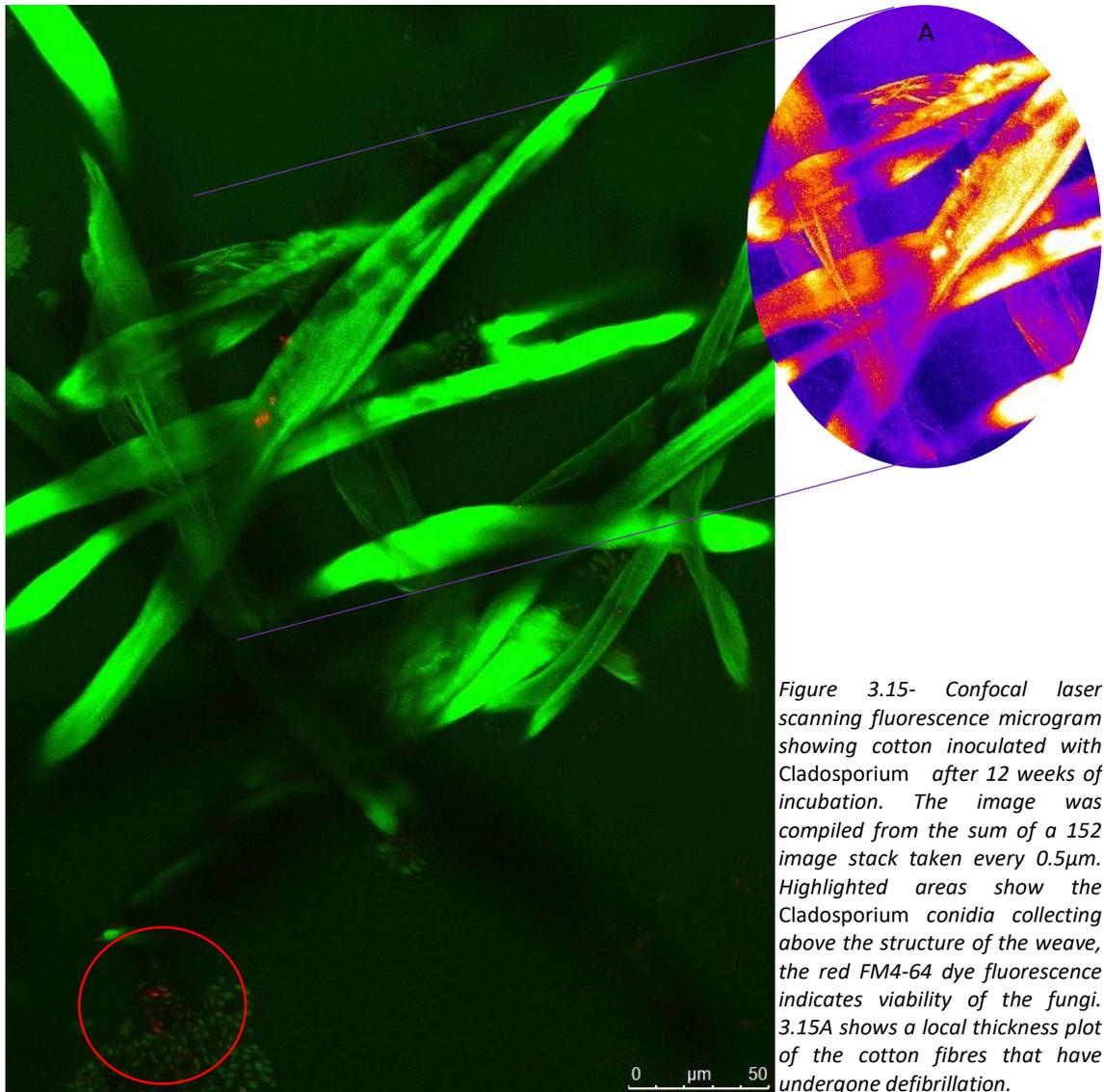
Figure 3.15- Confocal laser scanning fluorescence microgram showing cotton inoculated with Cladosporium *after 12 weeks of incubation. The image was compiled from the sum of a 152 image stack taken every 0.5µm. Highlighted areas show the* Cladosporium *conidia collecting above the structure of the weave, the red FM4-64 dye fluorescence indicates viability of the fungi. 3.15A shows a local thickness plot of the cotton fibres that have undergone defibrillation.*

After one week of *Penicillium* growth there was hyphal interaction within the weave structure of the cotton and immature conidiophores in the fibres above the crown of the weave. After four weeks of growth there was evidence of mature hyphae and conidia production. However, the growth was not as extensive or visible as that of the *Aspergillus*. The morphology of the cotton fibres was visibly altered though with small cracks and pits beginning to appear. Figure 3.16 shows cotton after six weeks of incubation with *Penicillium*. The fibres have continued to change morphologically and there is evidence of the *Penicillium* penetrating through the lumen of the fibre and then growing out through the fissures that have opened in the fibre wall. An example of this can be seen in the area highlighted and expanded with a topographical height

map. The *Penicillium* hyphae is growing out through a crack in the fibre and can clearly be seen to be elevated in the height map; the lighter the feature, the higher in the image stack it is. Further weeks of incubation showed the spread of new hyphae and the further deterioration of the upper fibres in the weave structure.
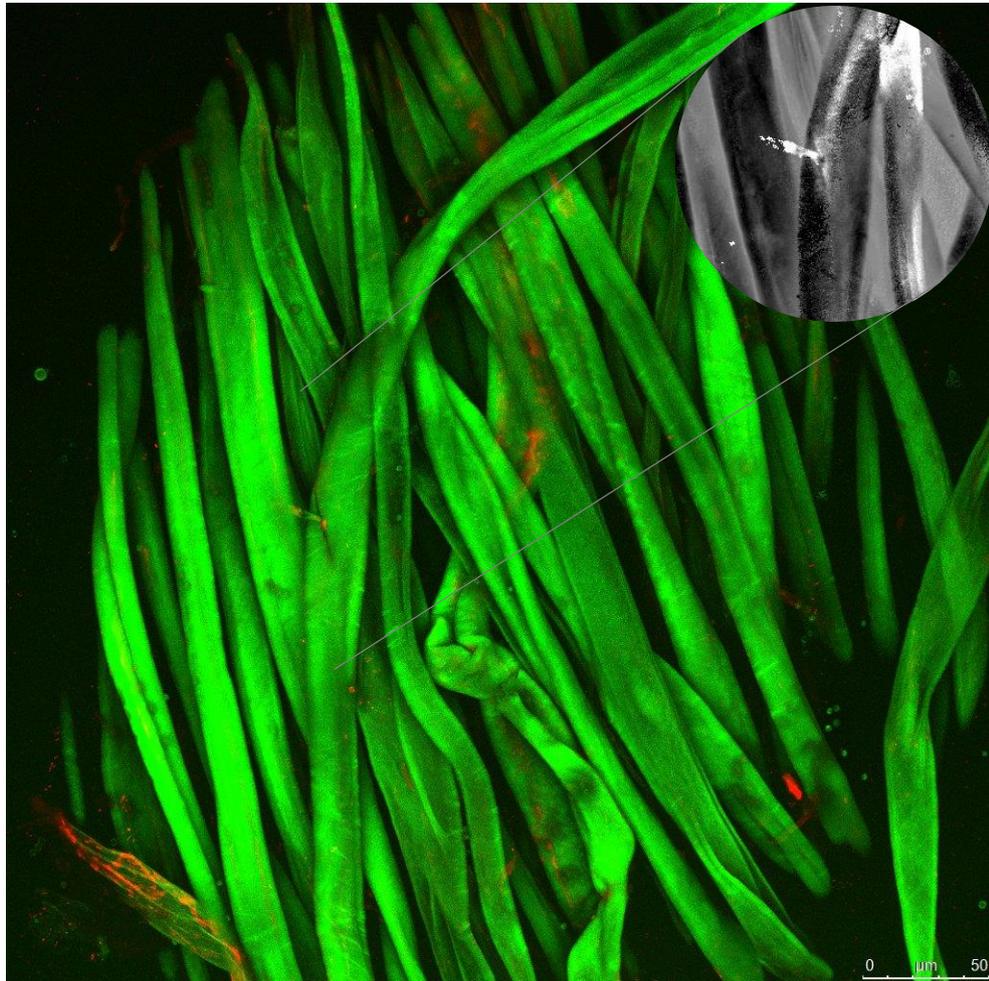
Figure 3.16- Confocal laser scanning fluorescence microgram showing cotton inoculated with Penicillium *after 6 weeks of incubation. The image was compiled from the sum of a 140 image stack taken every 0.5µm. The expanded view shows a topographical height map of the area surrounding a fissure in one of the fibres. The height map shows that the higher a feature is in the stack, the lighter it is.*

3.3.2.2 Confocal images of linen

After the first week of growth with *Aspergillus* there was hyphal growth penetrating through the weave and some small conidiophores above the crown of the fabric weave. After three weeks of growth (Figure 3.17) the conidiophores were larger and the hyphae were interacting with the fibres, some penetrating through to the lumen. After eight weeks of growth there were still small conidiophores visible, but far fewer than the number observed when this species was growing on cotton. There were however signs of fibre damage and morphological changes occurring

(Figure 3.18A). There was some scarring and pitting of the fibre surface, as can be seen in the orthogonal slice (Figure 3.18B) where the wall of the fibre is no longer smooth and fungal debris adhered to the surface. Figure 3.18C is a topographical height map and details the fungal matter on the fibre.
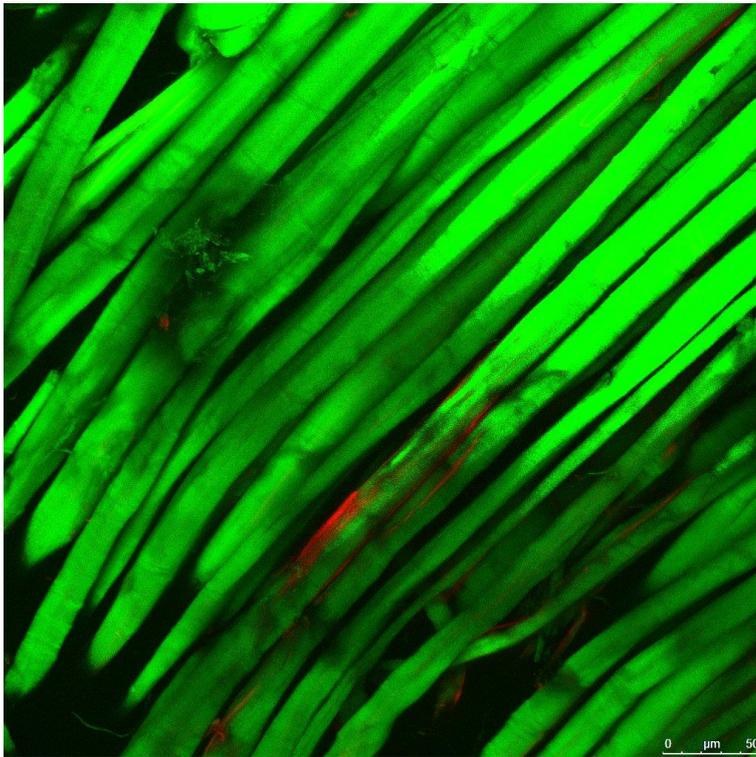
Figure 3.17- Confocal laser scanning fluorescence microgram showing linen inoculated with Aspergillus *after 3 weeks of incubation. The image was compiled from the sum of a 63 image stack taken every 0.5μm*
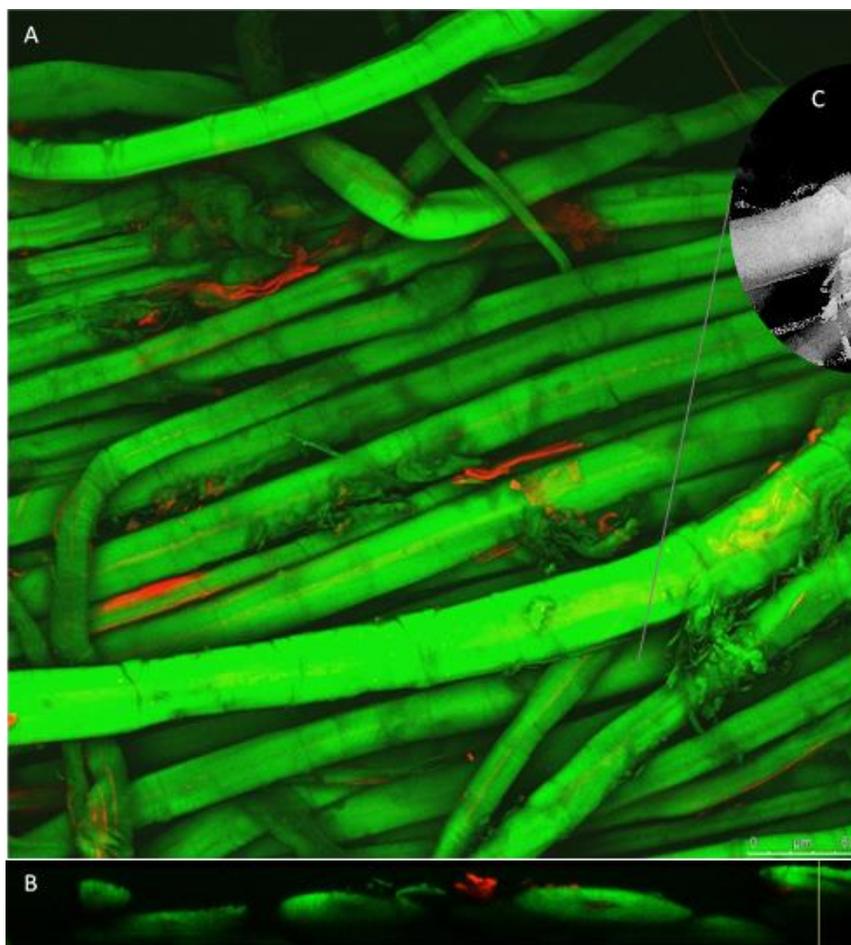
Figure 3.18- Confocal laser scanning fluorescence microgram showing linen inoculated with Aspergillus *after 3 weeks of incubation. The image was compiled from the sum of a 222 image stack taken every 0.5μm. B, details and orthogonal slice and shows that the wall of the linen fibre is no longer as smooth. C, is a topographical height map and shows the pitting of the fibre surface more clearly as the darker features are lower down in the stack and the paler ones higher.*

At the end of the study the fibre damage was still apparent and there were hyphae growing through longitudinal fissures in the fibre walls. At this stage there were no apparent reproductive structures near the surface that could be detected by this imaging technique. Hyphal growth was still extensive though, growing in amongst the fibres of the weave and through their lumens.

After the first few weeks of growth with *Cladosporium*, there was evidence of highly pigmented hyphal growth above the weave structure of the linen and some small conidiophores being produced. By week 3, growth is becoming more integrated within the weave structure of the linen (Figure 3.19), but as with the *Aspergillus*, growth was not as advanced as that seen on the cotton substrate at the same stage.

After six weeks of growth there was still viable growth visible, but it was not extensive. There was some fibre damage recorded although it was also limited (Figure 3.20). This took the form of longitudinal cracks and some defibrillation where there was more intense hyphal growth seen.

Figure 3.19- Confocal laser scanning fluorescence microgram showing linen inoculated with Cladosporium *after 3 weeks of incubation. The image was compiled from the sum of a 180 image stack taken every 0.5μm.*
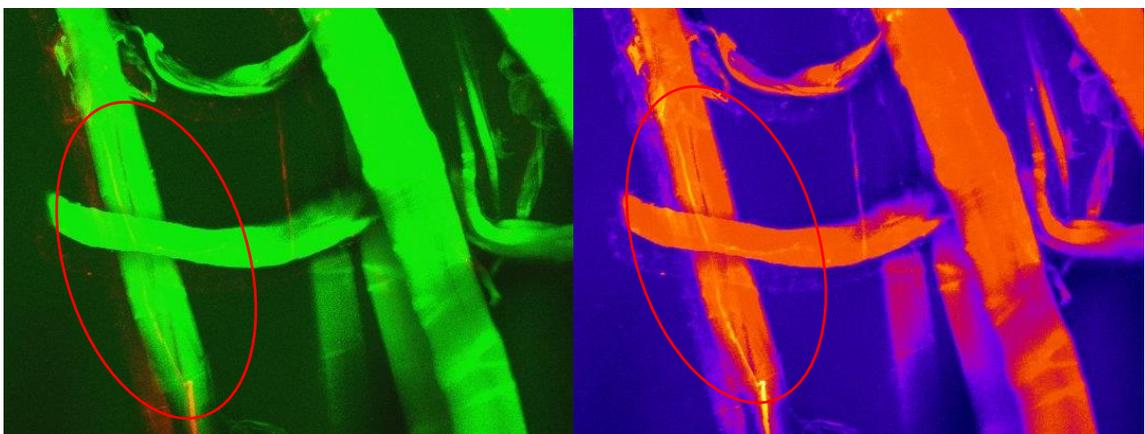
Figure 3.20- Confocal laser scanning fluorescence microgram and local thickness map, showing linen inoculated with Cladosporium *after 6 weeks of incubation. The image was compiled from the sum of a 132 image stack taken every 0.5μm. Highlighted areas show longitudinal fibre cracking.*

After the final weeks of incubation, the fibre damage seen was more extensive, but with less growth visible. Figure 3.21 shows the further cracking of the fibre walls, pitting of the surface and overall change in fibre morphology. These changes were limited to the crown of the weave.
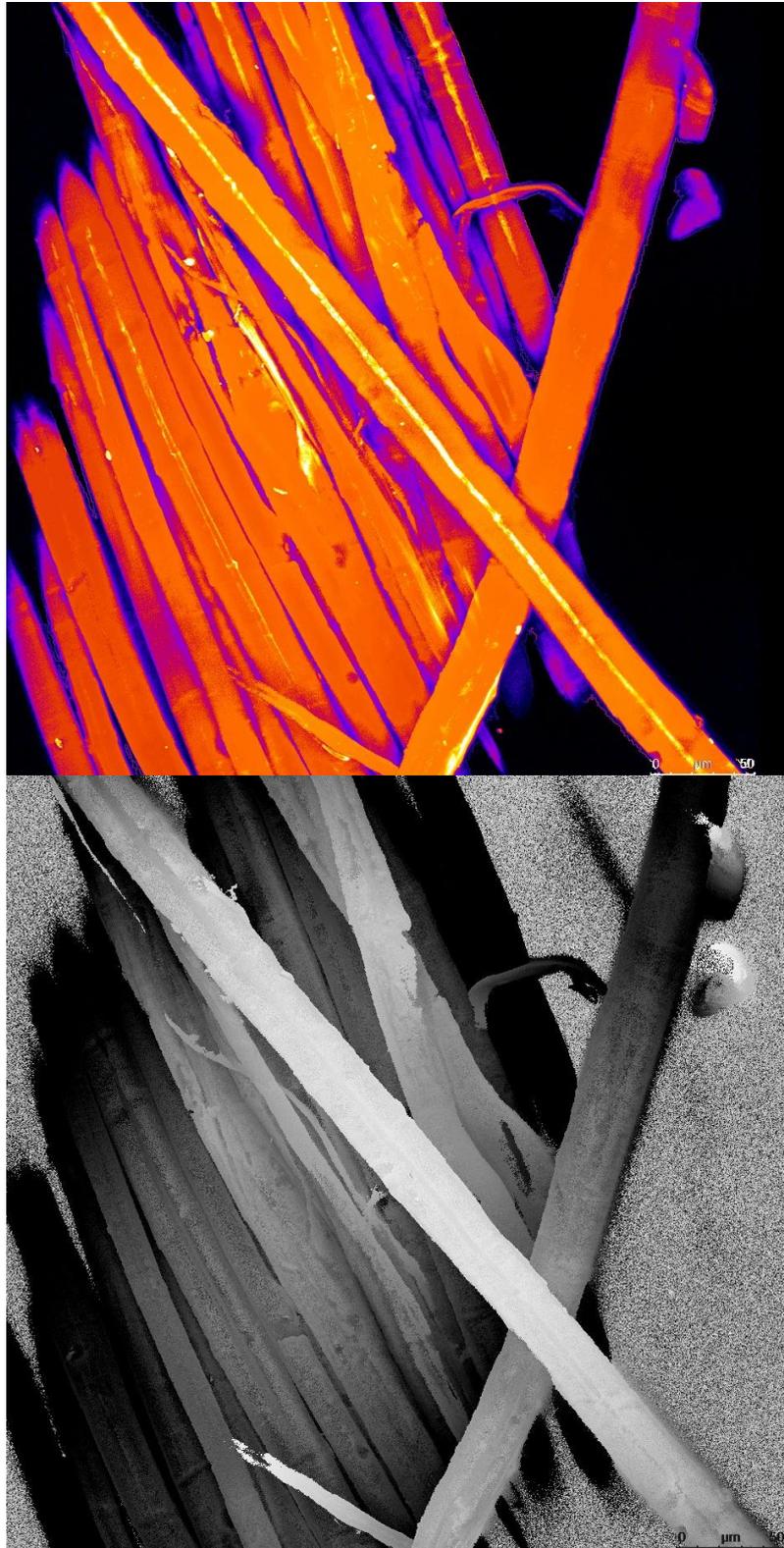
Figure 3.21- Local thickness map (top) and topographical height map (bottom) of linen incubated with Cladosporium *after 12 weeks of growth. The image was compiled from the sum of a 329 image stack taken every 0.5µm.*

After the first week incubating *Penicillium* with linen, there was evidence of extensive hyphal growth on the surface of the weave structure with some penetration between fibres (Figure 3.22).

Figure 3.22- Confocal laser scanning fluorescence microgram showing linen inoculated with Penicillium *after 1 week of incubation. The image was compiled from the sum of a 238 image stack taken every 0.5μm. The highlighted area (B) shows a topographical height map of the area indicated. The paler features are higher in the stack, the darker, lower.*
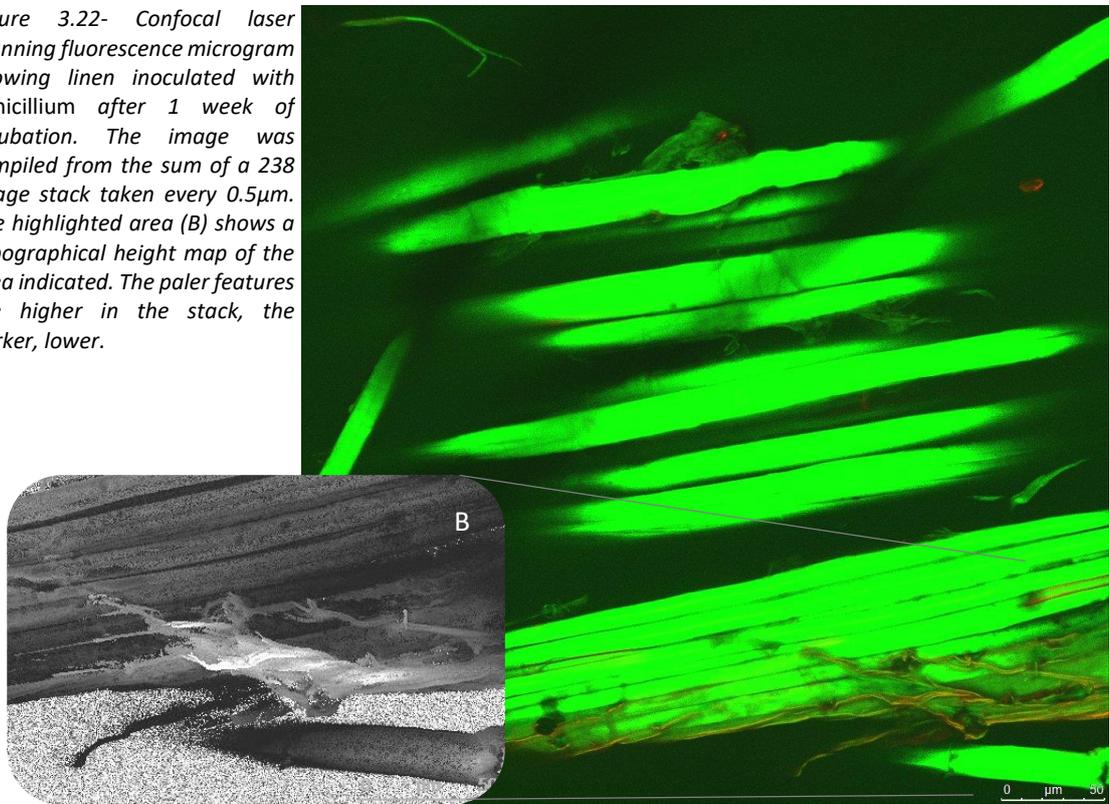
After further incubation, conidiophores could be seen in the loose fibres above the crown of the weave; Figure 3.23 shows an example from week 4. There was also penetration into the weave structure and hyphae detectible within the fibre lumens.
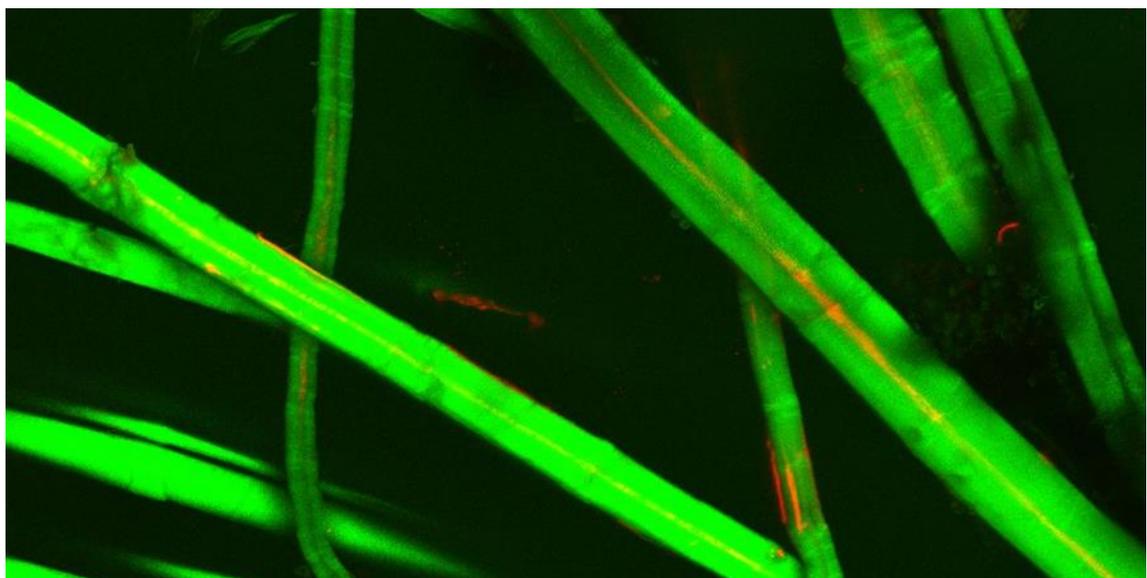
Figure 3.23- Confocal laser scanning fluorescence microgram showing linen inoculated with Penicillium *after 4 weeks of incubation. The image was compiled from the sum of a 168 image stack taken every 0.5μm.*

Towards the end of the experiment, there was still evidence of viable hyphal growth and the surface of the linen fibres exhibited some surface pitting, as can be seen in the local thickness plot of Figure 3.24 where the highlighted parts of the fibre are not as thick as the surrounding area.
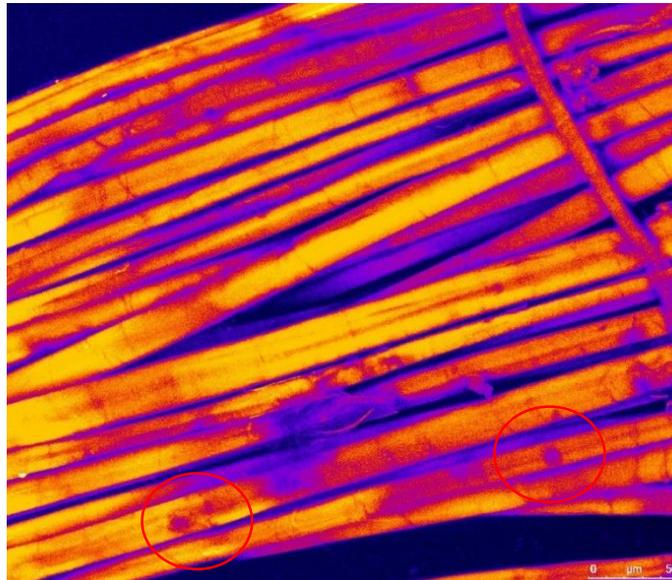
Figure 3.24- Local thickness map of linen incubated with Penicillium *after 12 weeks of growth. The image was compiled from the sum of a 218 image stack taken every 0.5μm.*

3.3.2.3 Confocal images of cotton and linen paper

After one week of *Aspergillus* growth there was evidence of hyphal growth and of sporulation, with conidiophores sitting high above the paper matrix (Figure 3.25). After four weeks of growth, there was further hyphal extension into the paper matrix and conidiophores dispersing conidia amid the paper fibres. There was also evidence of some changes to the surface morphology of the fibres with pitting of the cotton fibres (Figure 3.26).
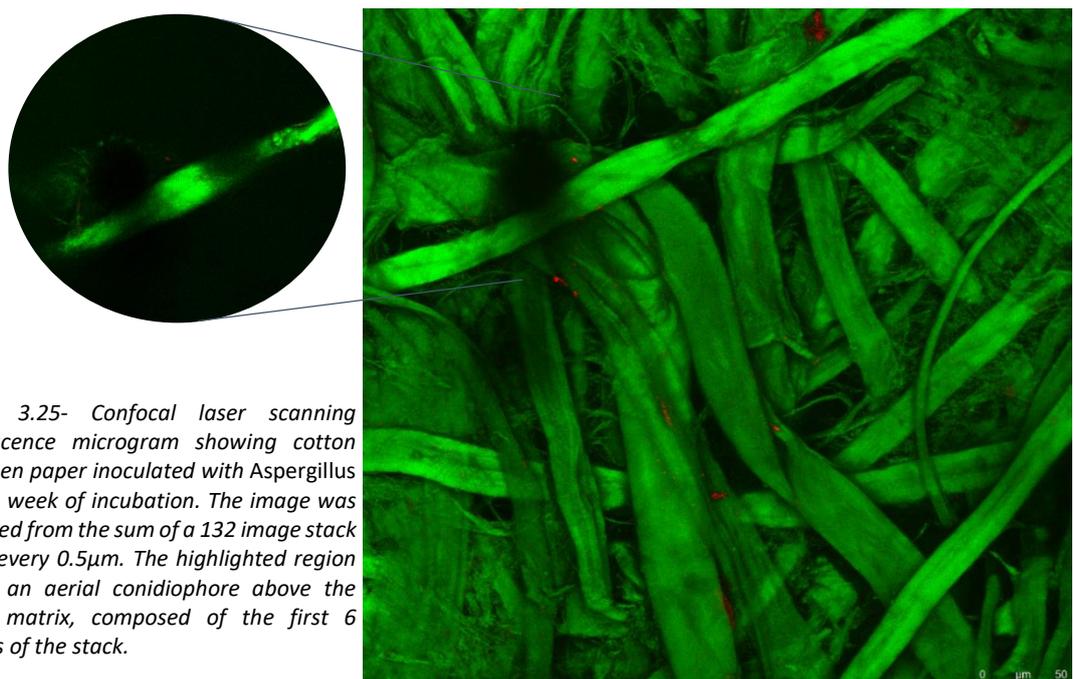
Figure 3.25- Confocal laser scanning fluorescence microgram showing cotton and linen paper inoculated with Aspergillus *after 1 week of incubation. The image was compiled from the sum of a 132 image stack taken every 0.5μm. The highlighted region shows an aerial conidiophore above the paper matrix, composed of the first 6 images of the stack.*
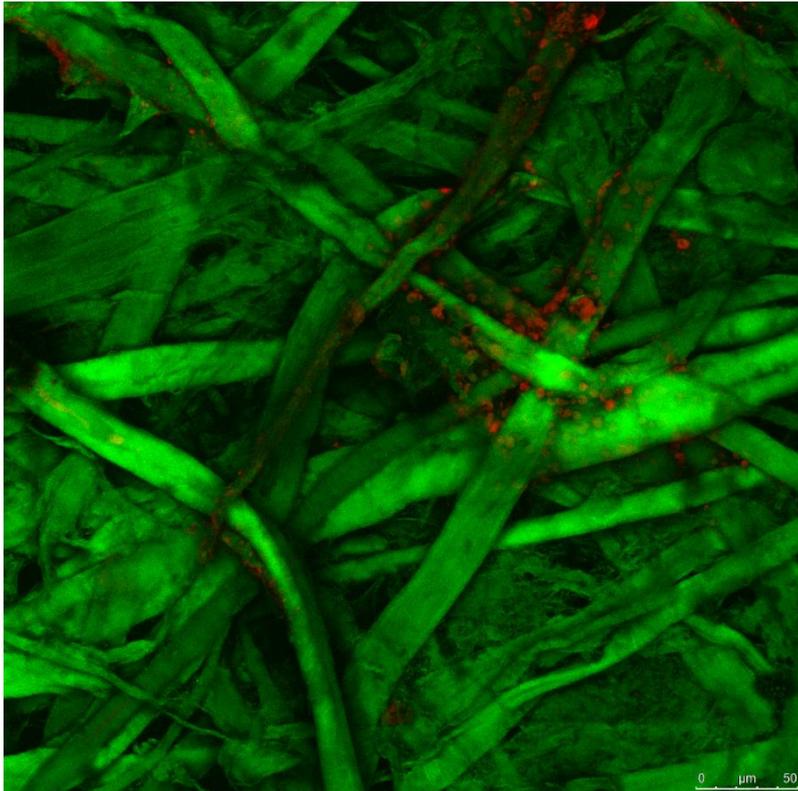
Figure 3.26- Confocal laser scanning fluorescence microgram showing cotton and linen paper inoculated with Aspergillus *after 4 weeks of incubation. The image was compiled from the sum of a 132 image stack taken every 0.5µm.*

As growth progressed, there was further damage to the fibres, with cracking and defibrillation evident and an increasing lack of definition. Figure 3.27 shows the growth after 11 weeks where the loss of fibre definition, defibrillation and longitudinal cracking of the linen fibres can be seen in the highlighted region.
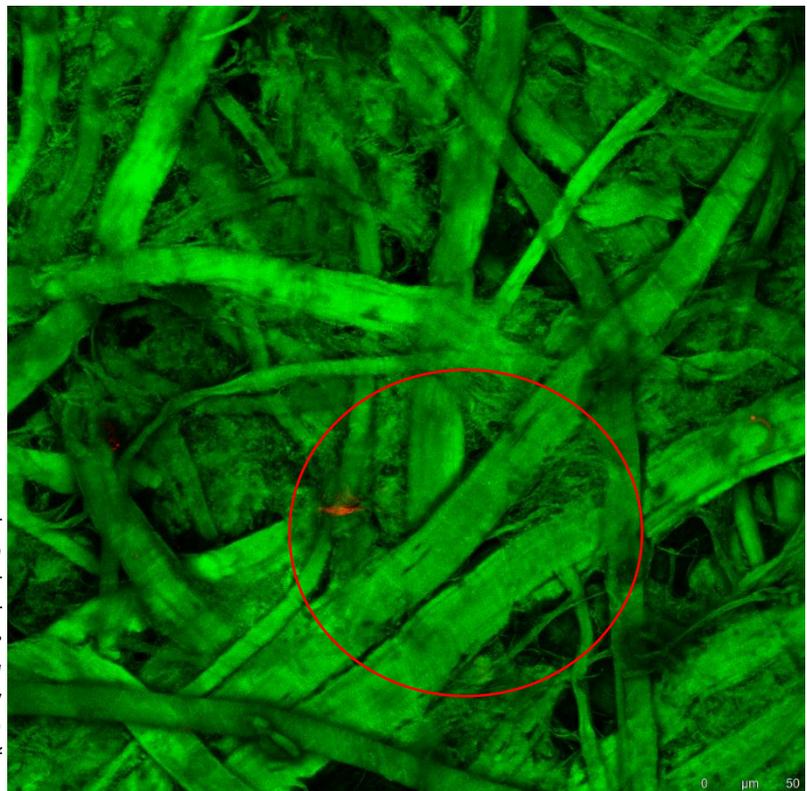
Figure 3.27- Confocal laser scanning fluorescence microgram showing cotton and linen paper inoculated with Aspergillus *after 11 weeks of incubation. The image was compiled from the sum of a 143 image stack taken every 0.5µm. The highlighted region details the longitudinal cracking of linen fibres and loss of definition.*

93

After one week of incubation with *Cladosporium* there was evidence of hyphal growth amid the paper fibres (Figure 3.28), although the hyphae were not yet pigmented, as can be seen after a further three weeks incubation. After this time the hyphae are thicker and darkly pigmented, there was also evidence of aerial conidiophores.
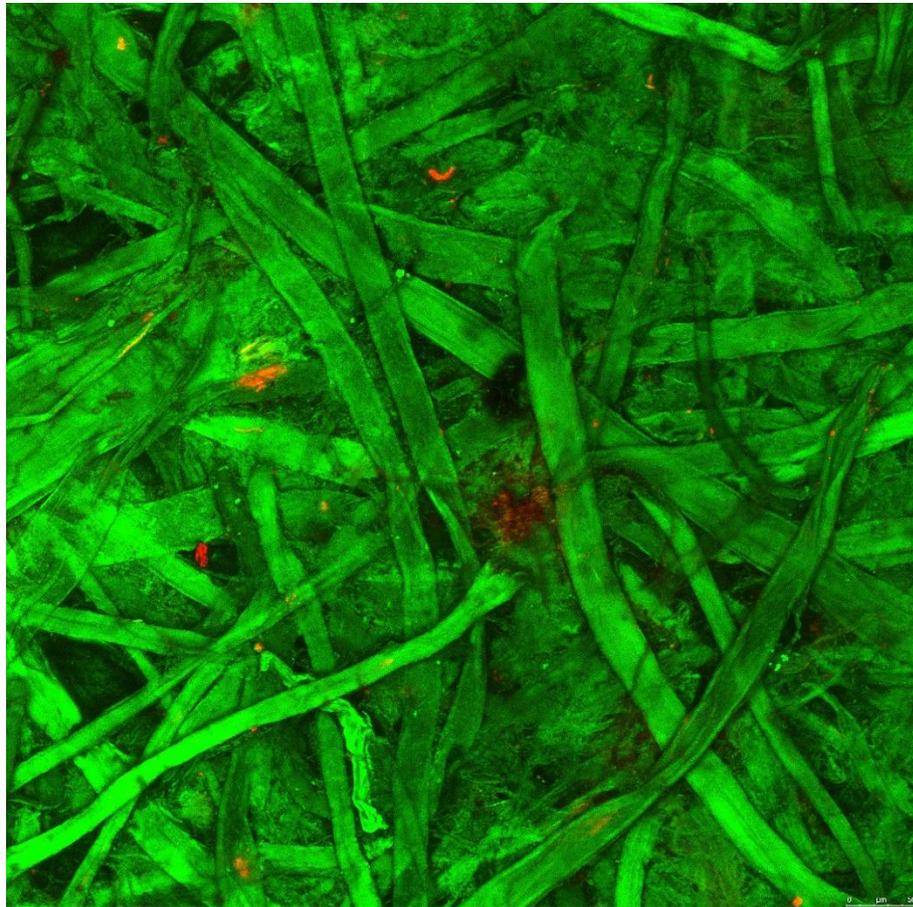
Figure 3.28- Confocal laser scanning fluorescence microgram showing cotton and linen paper inoculated with Cladosporium *after 1 week of incubation. The image was compiled from the sum of a 74 image stack taken every 0.5μm.*

Eight weeks into the incubation and there are fewer fungal features visible, but the morphology of the paper has altered. There was less definition between fibres and some defibrillation occurring (Figure 3.29). At the end of the trial, the cotton and linen fibres in the paper are showing signs of surface cracking, defibrillation and pitting. There was also new fungal growth in evidence, with fine hyphae growing amongst the fibres (Figure 3.30).
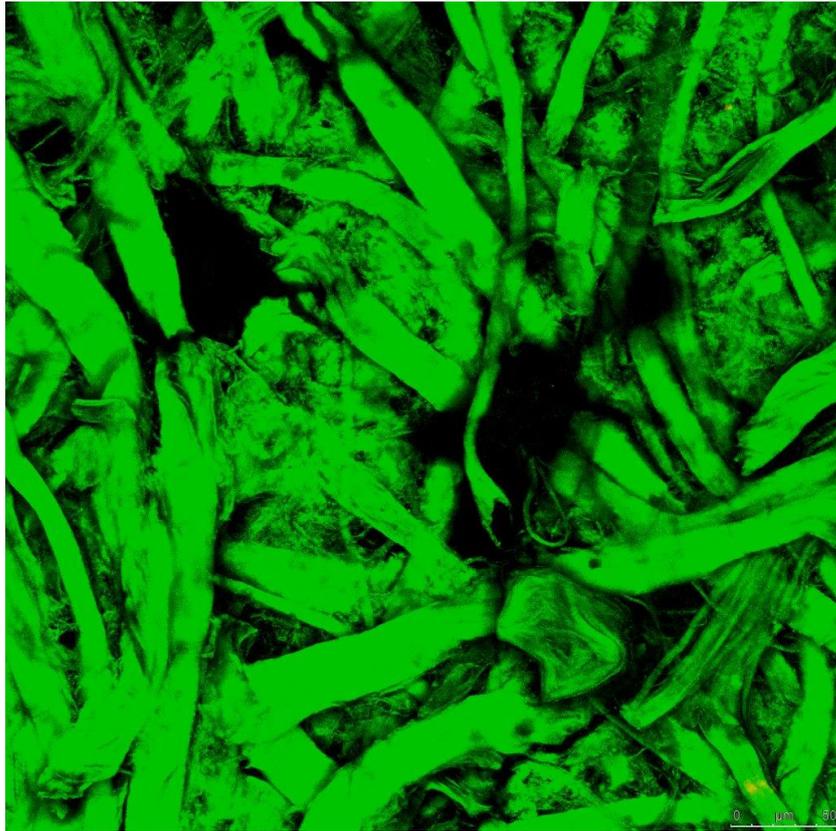
Figure 3.29- Confocal laser scanning fluorescence microgram showing cotton and linen paper inoculated with Cladosporium *after 8 weeks of incubation. The image was compiled from the sum of a 137 image stack taken every 0.5µm.*
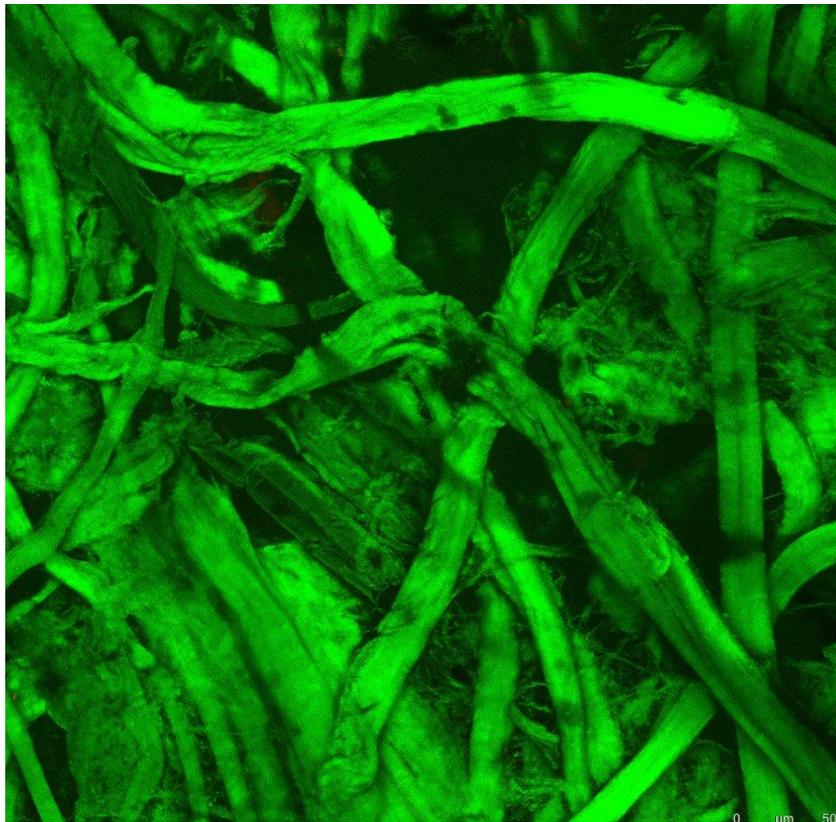
Figure 3.30- Confocal laser scanning fluorescence microgram showing cotton and linen paper inoculated with Cladosporium *after 12 weeks of incubation. The image was compiled from the sum of a 114 image stack taken every 0.5µm.*

After one week of *Penicillium* incubation there was extensive germination seen on the paper in the form of spores with germ tubes and hyphal networks being established in the top layers of the paper matrix. Figure 3.31 shows the germination, young hyphal growth and the coiling of the hyphae around the paper fibres (highlighted).
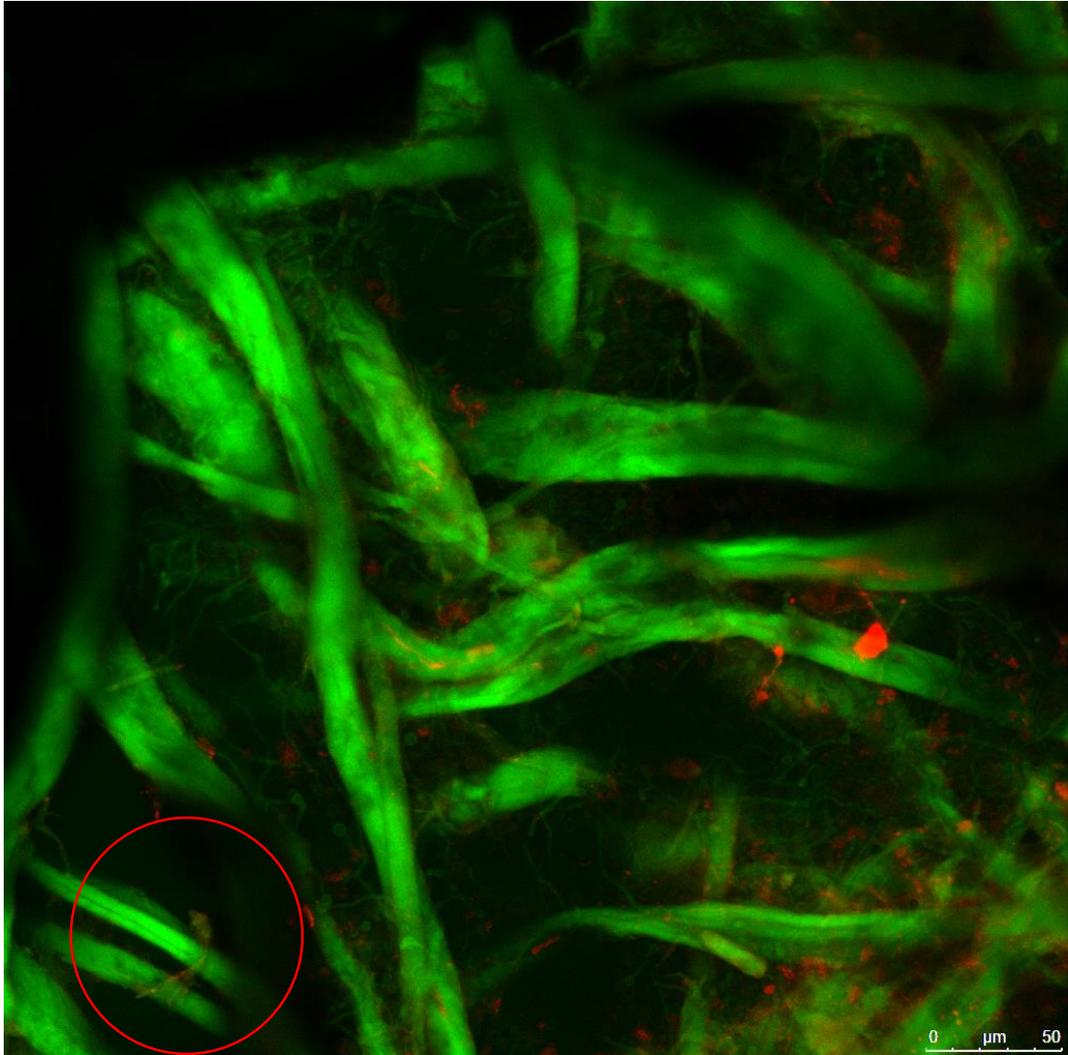
Figure 3.31- Confocal laser scanning fluorescence microgram showing cotton and linen paper inoculated with Penicillium *after 1 week of incubation. The image was compiled from the sum of a 21 image stack taken every 1μm.*

After 4 weeks of growth there were mature hyphae growing within the paper matrix and the morphology of the cotton and linen fibres were changed, with cracks and surface pitting visible. This degradation of fibres was still visible in the week 6 sample; where in Figure 3.32, cracks and surface pitting can clearly be seen in the inverted local thickness map which highlights regions that are further down in the image stack in paler colours.
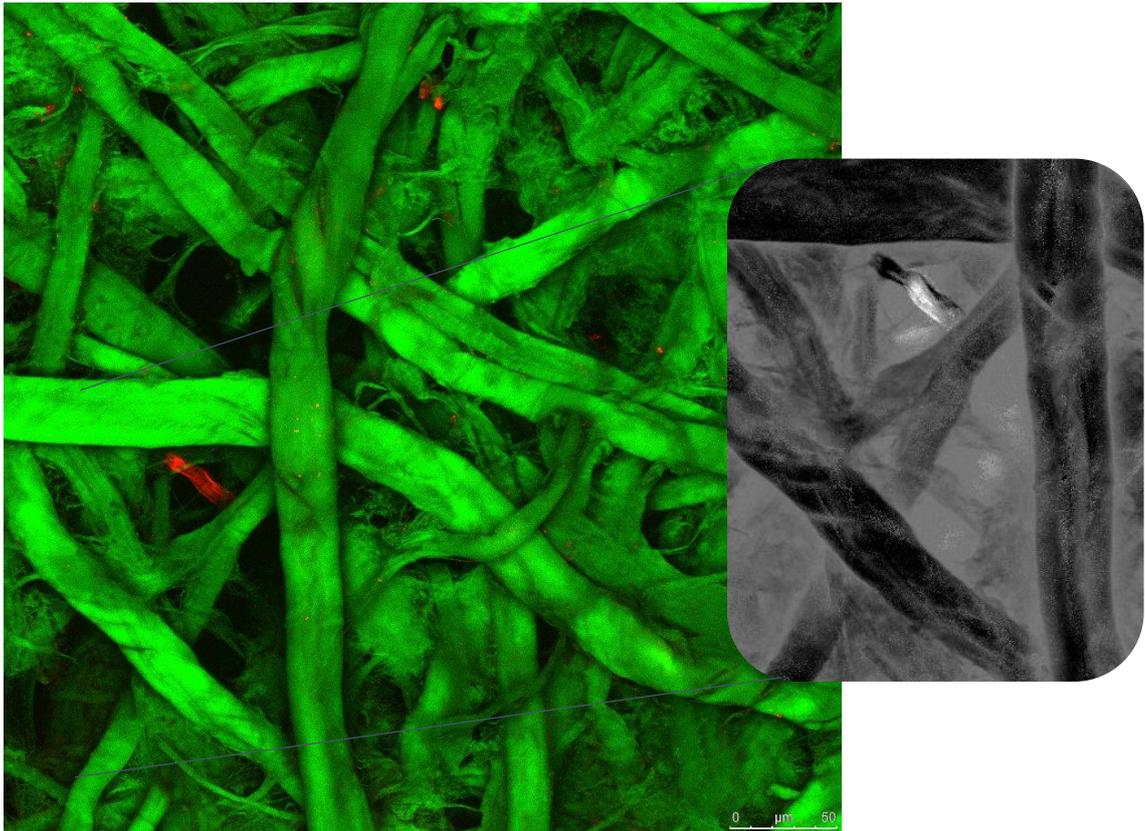
Figure 3.32- Confocal laser scanning fluorescence microgram showing cotton and linen paper inoculated with Penicillium *after 6 weeks of incubation. The image was compiled from the sum of a 112 image stack taken every 0.5μm. The expanded view shows a topographical height map of the fibre morphologies.. The height map shows that the higher a feature is in the stack, the lighter it is.*

Towards the end of the trial, damage to the fibres continued and in week 8, aerial conidiophores and new spore germination could be seen. After 12 weeks of incubation, the paper fibres were less defined, have noticeably altered surface morphologies (cracking, defibrillation and pitting) and are surrounded by hyphal growth. Although, evidence of new growth and reproductive features were not visible.

3.3.2.4 Confocal images of beech wood paper

For the beech wood paper incubated with *Aspergillus*, growth was not established as quickly as with the cotton and linen substrate, only hyphae and not reproductive structures could be seen after 1 week of growth. After three weeks however (Figure 3.33), the fungi had penetrated the matrix of the paper and had produced aerial conidiophores. After 8 weeks of growth there were well established, mature hyphal networks throughout the visible paper matrix. The aerial conidiophores visible had shed their spores, but there was no evidence of further spore production (Figure 3.34). During the latter weeks of incubation, there was evidence of new germination and young hyphal growth within the matric of the paper, in addition to the mature hyphal structures (Figure 3.35).
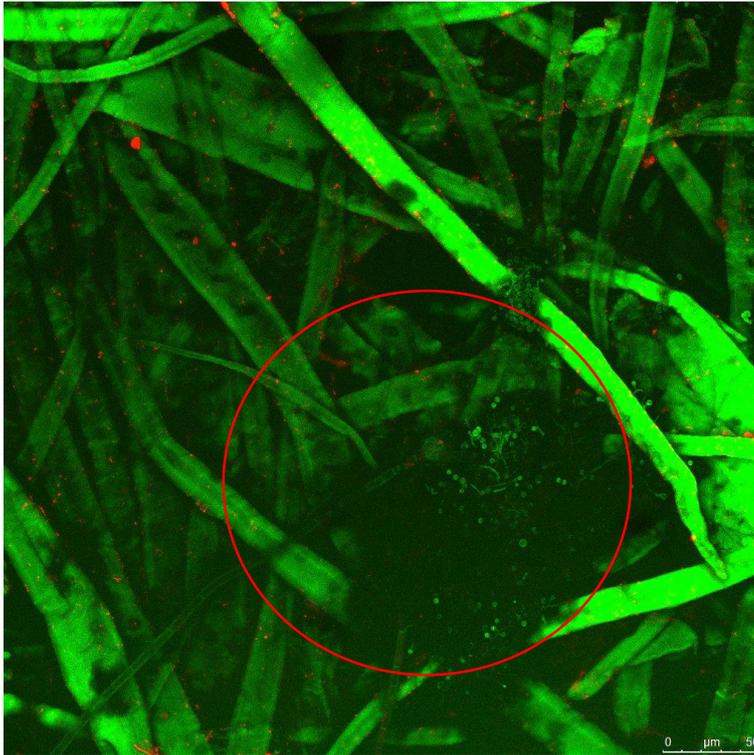
Figure 3.33- Confocal laser scanning fluorescence microgram showing beech wood paper inoculated with Aspergillus *after 3 weeks of incubation. The image was compiled from the sum of a 164 image stack taken every 0.5µm. The highlighted region details the aerial conidiophore and spores.*

Figure 3.34- Confocal laser scanning fluorescence microgram showing beech wood paper inoculated with Aspergillus *after 8 weeks of incubation. The image was compiled from the sum of a 123 image stack taken every 0.5µm.*
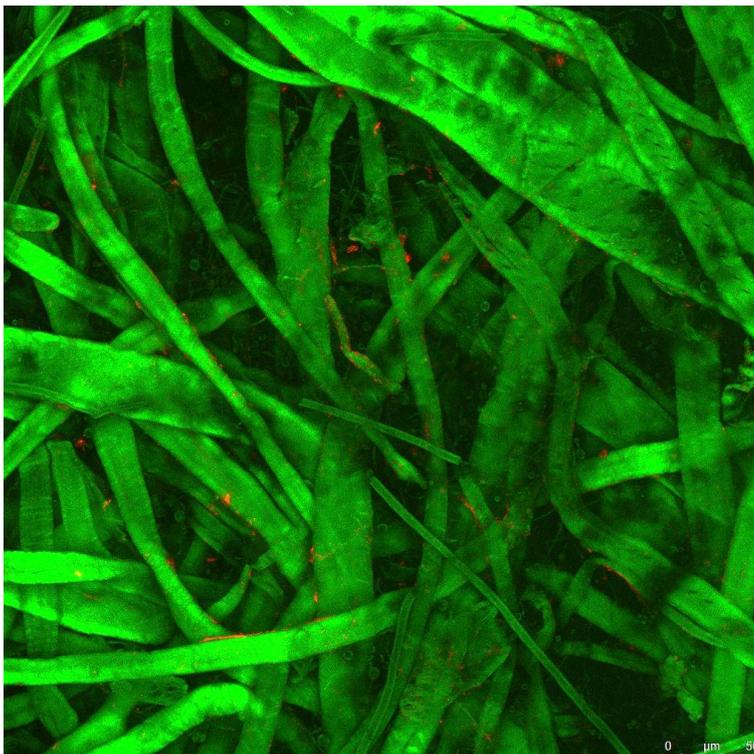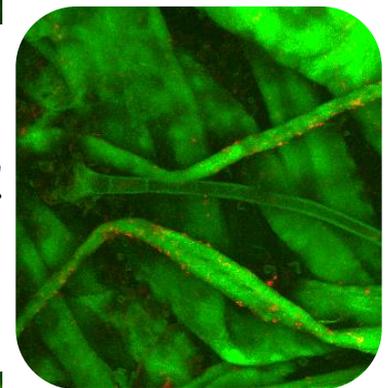
Figure 3.35- Confocal laser scanning fluorescence microgram showing beech wood paper inoculated with Aspergillus *after 11 weeks of incubation. The image was compiled from the sum of a 97 image stack taken every 0.5µm.*

98

After 1 week of growth on beech wood paper, the *Cladosporium* had produced pigmented hyphae over the surface of the paper matrix and there were visible reproductive structures (Figure 3.36). Half way through incubation there was still evidence of viable reproductive structures and extensive hyphae spreading over the surface of the paper (Figure 3.37). The individual fibres of the beech wood were becoming less defined and showing signs of morphological change. After 12 weeks of incubation there were mature pigmented hyphae on the surface of the paper, but no evidence of new growth.
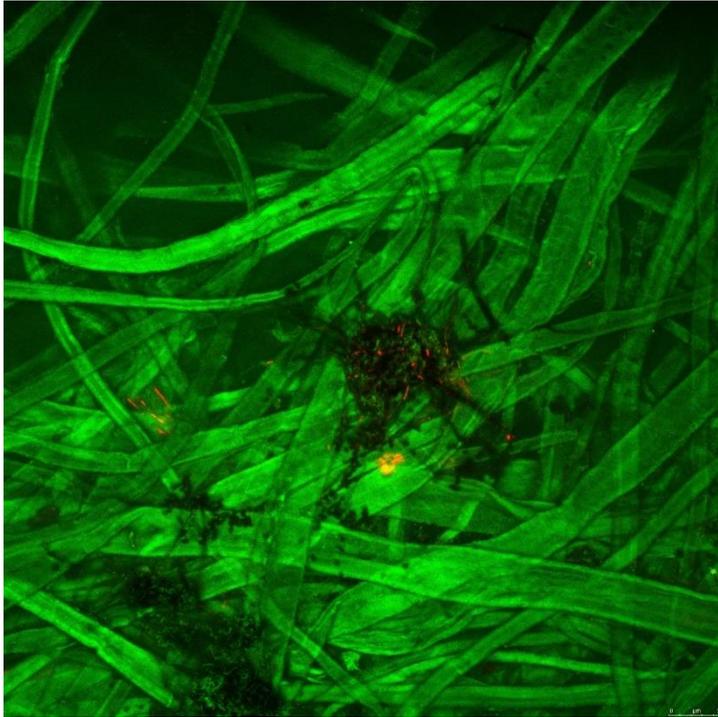
Figure 3.36- Confocal laser scanning fluorescence microgram showing beech wood paper inoculated with Cladosporium *after 1 week of incubation. The image was compiled from the sum of an 83 image stack taken every 0.5µm.*
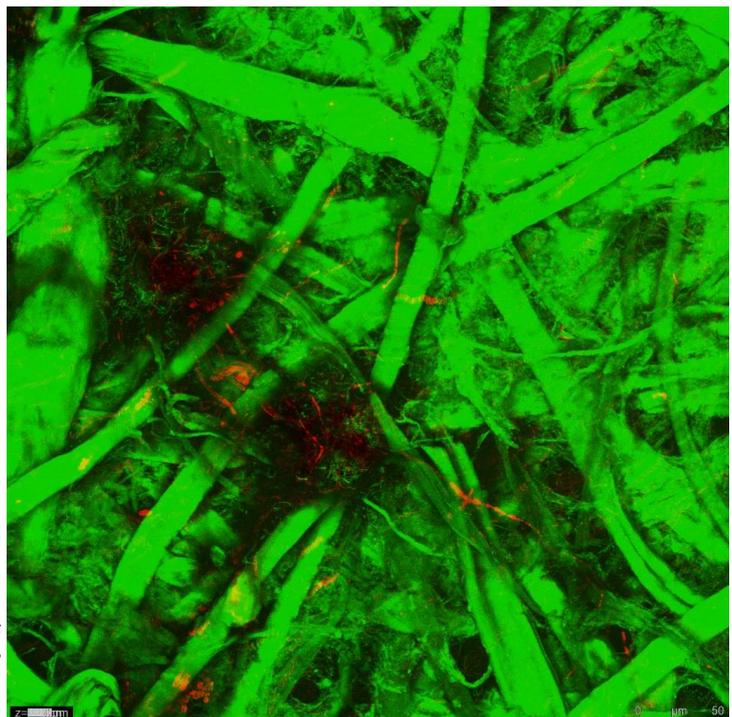
Figure 3.37- Confocal laser scanning fluorescence microgram showing beech wood paper inoculated with Cladosporium after 1 week of incubation. The image was compiled from the sum of an 83 image stack taken every 0.5µm.

The beech wood paper when incubated with *Penicillium* showed germination and hyphal growth after the first week, with the spores becoming trapped amongst the fibres in the top layer of paper (Figure 3.38).
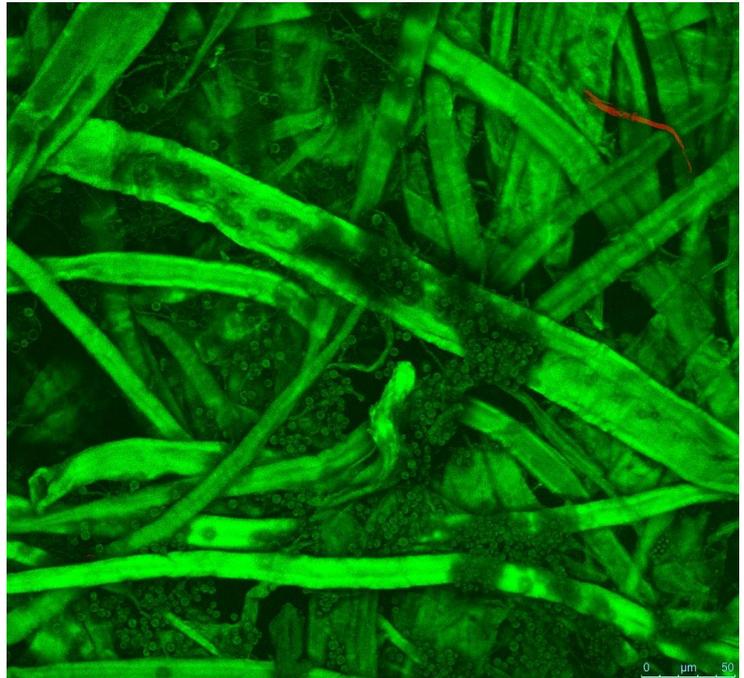
Figure 3.38- Confocal laser scanning fluorescence microgram showing beech wood paper inoculated with Penicillium *after 1 week of incubation. The image was compiled from the sum of a 143 image stack taken every 0.5µm.*

After further growth, a fine hyphal network over the surface of the paper was observed with many un-germinated spores (Figure 3.39). There was little evidence of mature hyphae or aerial conidiophores.
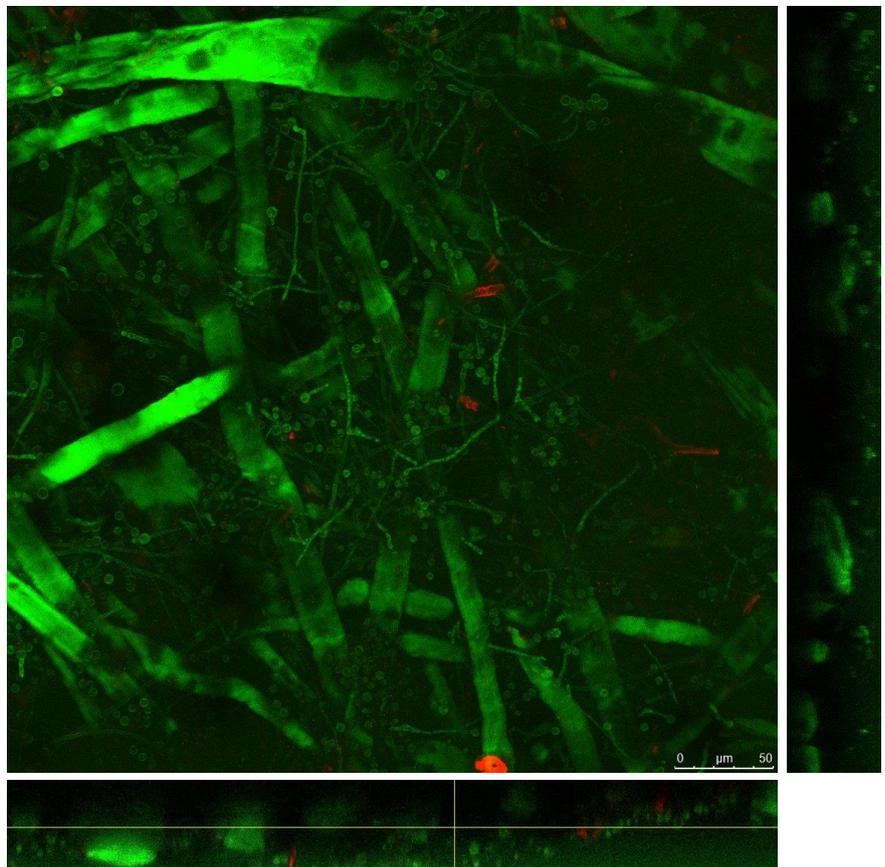
Figure 3.39-Confocal laser scanning fluorescence microgram showing beech wood paper inoculated with Penicillium *after 3 weeks of incubation. The image was compiled from the sum of a 125 image stack taken every 0.5µm.The XZ and YZ orthogonal views show that the spores and hyphal network are predominantly on the surface of the fibre matrix.*

After 8 weeks of growth there were fewer visible spores and more hyphal growth, although the reproductive features seen on other materials were not evident on the beech wood paper. There were however some morphological changes to the fibres, as can be seen in Figure 3.40, with the orthogonal cuts through the stack showing the irregular shape of the once smooth fibres. After 12 weeks of growth, there was again evidence of new spores, germination and hyphal growth; however conidiophores were not found.
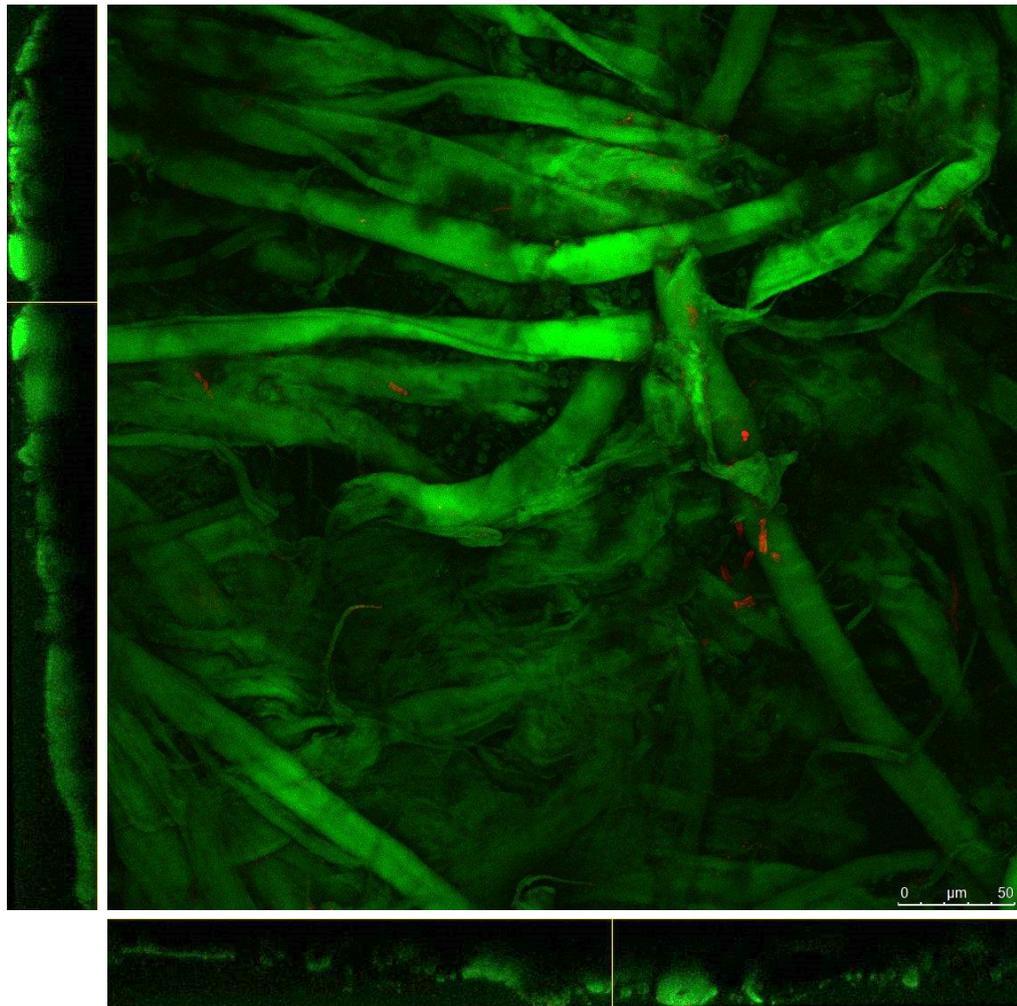
Figure 3.40- Confocal laser scanning fluorescence microgram showing beech wood paper inoculated with Penicillium *after 8 weeks of incubation. The image was compiled from the sum of a 102 image stack taken every 0.5µm.The XZ and YZ orthogonal views show that the fibre morphology has altered with continued incubation.*

3.3.2.5 Confocal images of Pine

Due to the density of the wood samples, the penetration of the confocal laser scanning fluorescence microscopy was limited. However, it was possible to view active growth of the fungi and the interactions with the upper layers of the wood substrates.

After 1 week of incubation with *Aspergillus*, germination, hyphal growth and the production of reproductive structures had occurred (Figure 3.41). The *Aspergillus* could be seen to be growing along the tracheid cell channels and from the orthogonal view, it was possible to see penetration of hyphae through the cell wall.
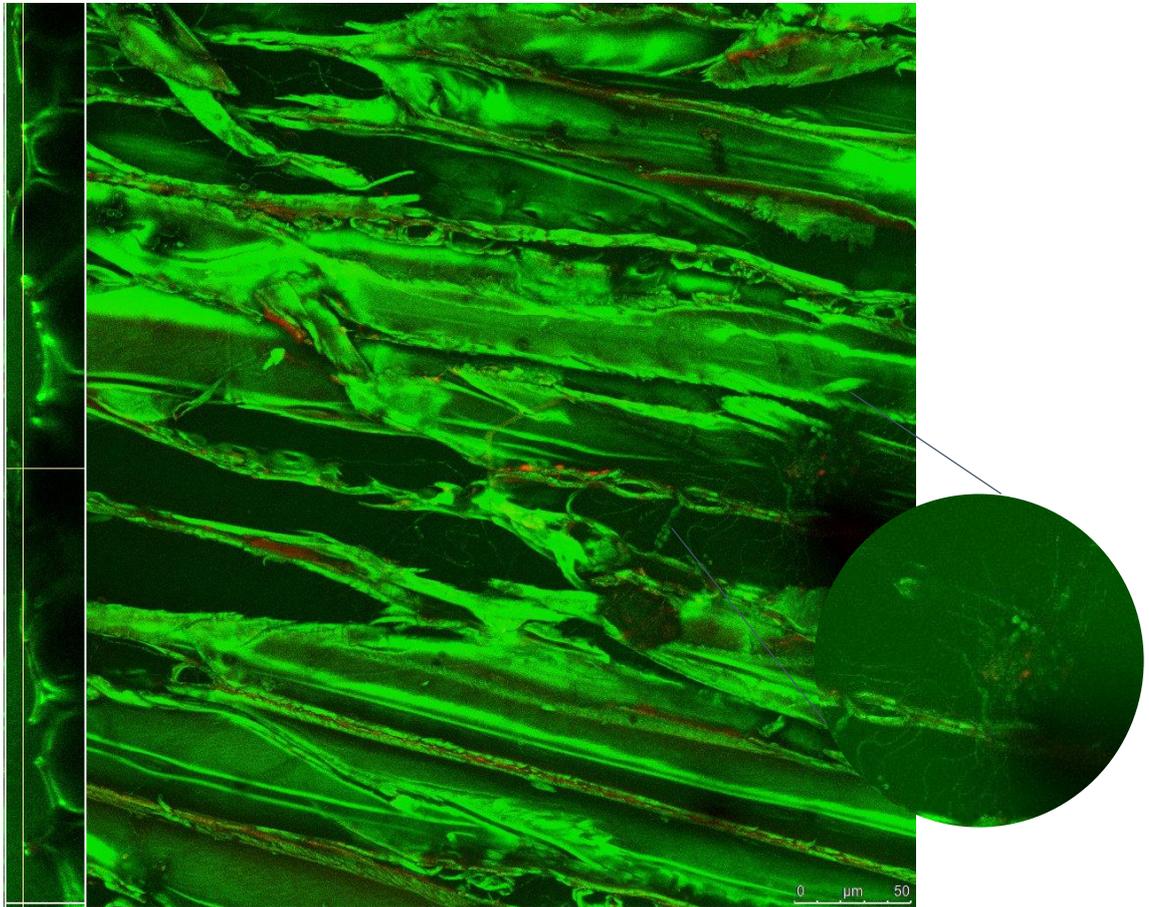
Figure 3.41- Confocal laser scanning fluorescence microgram showing pine inoculated with Aspergillus *after 1 week of incubation. The image was compiled from the sum of a 89 image stack taken every 0.5µm.The YZ orthogonal view shows the tracheid cell walls and the expanded view shows the conidiophore using a stack taken from the first 29 images.*

After 4 weeks, multiple large aerial conidiophores were visible, in addition to an extensive hyphal network through the cells of the pine (Figure 3.42). After 8 weeks of growth there were mature clusters of aerial conidiophores and extensive growth through the cell channels. From Figure 3.43, growth through the middle lamella between the cells can be seen. After the full 12 weeks of incubation, fewer reproductive structures were found, but there were mature hyphae rooted through the tracheid cell walls of the pine and evidence of the fungi still being viable, although growing within the structure of the wood.
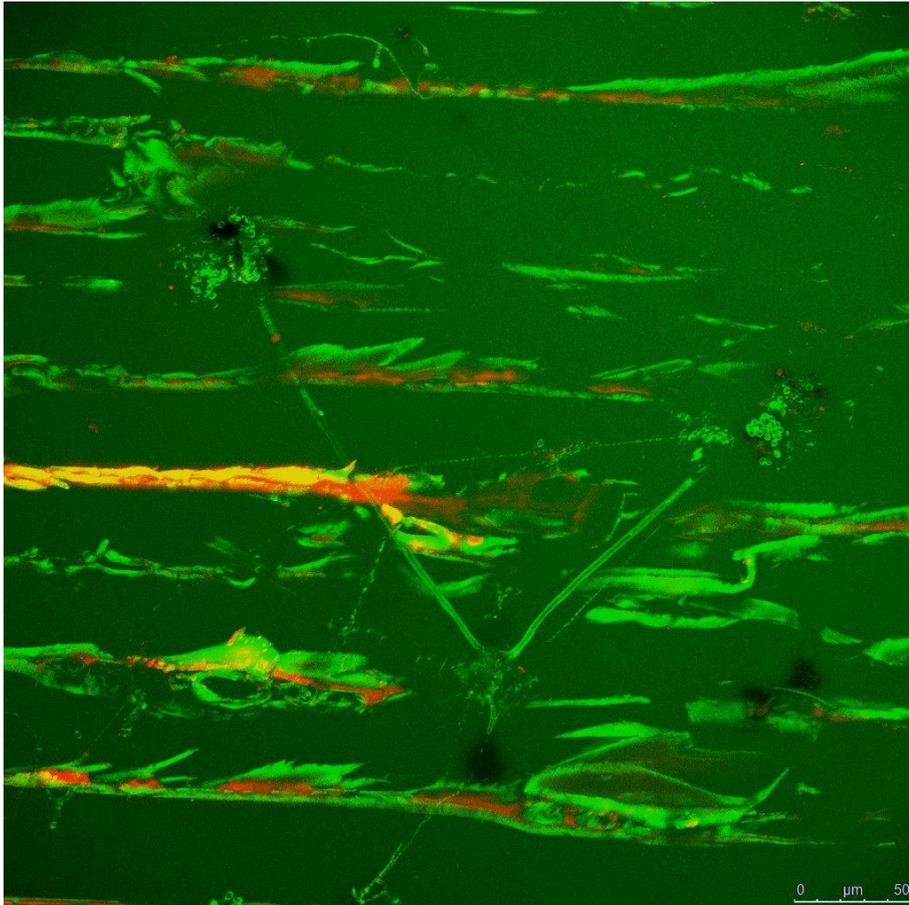
Figure 3.42- Confocal laser scanning fluorescence microgram showing pine inoculated with Aspergillus *after 4 weeks of incubation. The image was compiled from the sum of a 194 image stack taken every 0.5µm.*
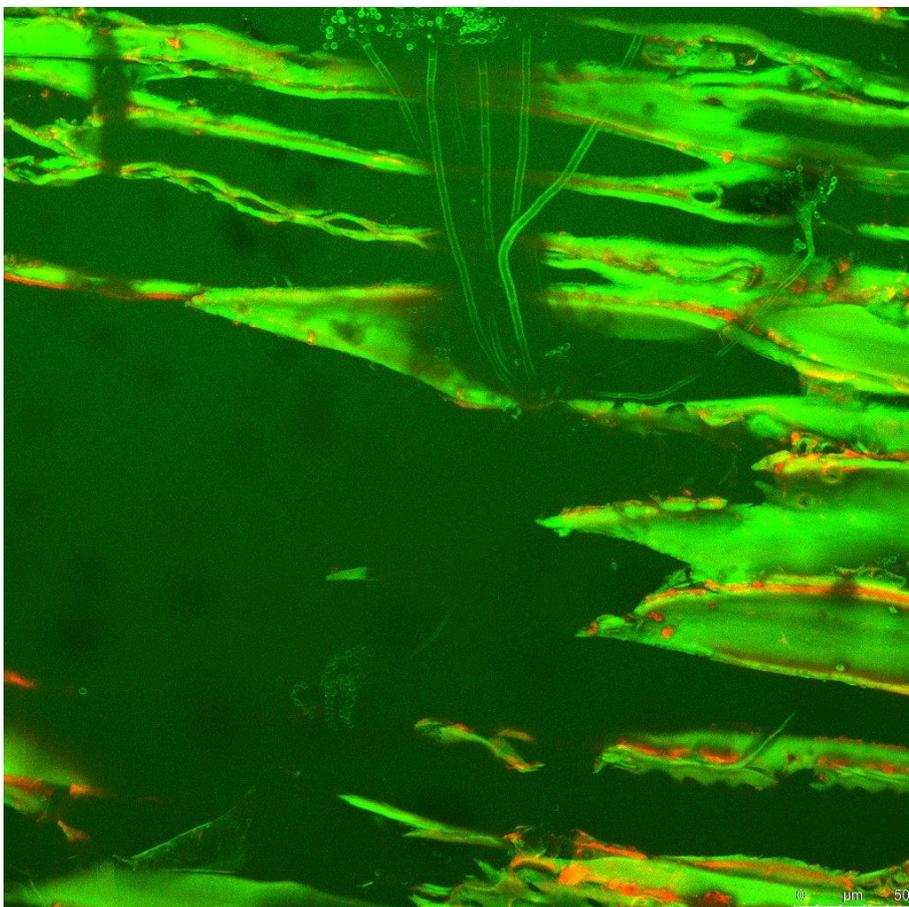
Figure 3.43- Confocal laser scanning fluorescence microgram showing pine inoculated with Aspergillus *after 8 weeks of incubation. The image was compiled from the sum of a 276 image stack taken every 0.5µm.*

After 1 week of growth on pine, the *Cladosporium* had produced pigmented hyphae that spread over the surface of the tracheid cells and finer hyphae that penetrated the middle lamella (Figure 3.44).
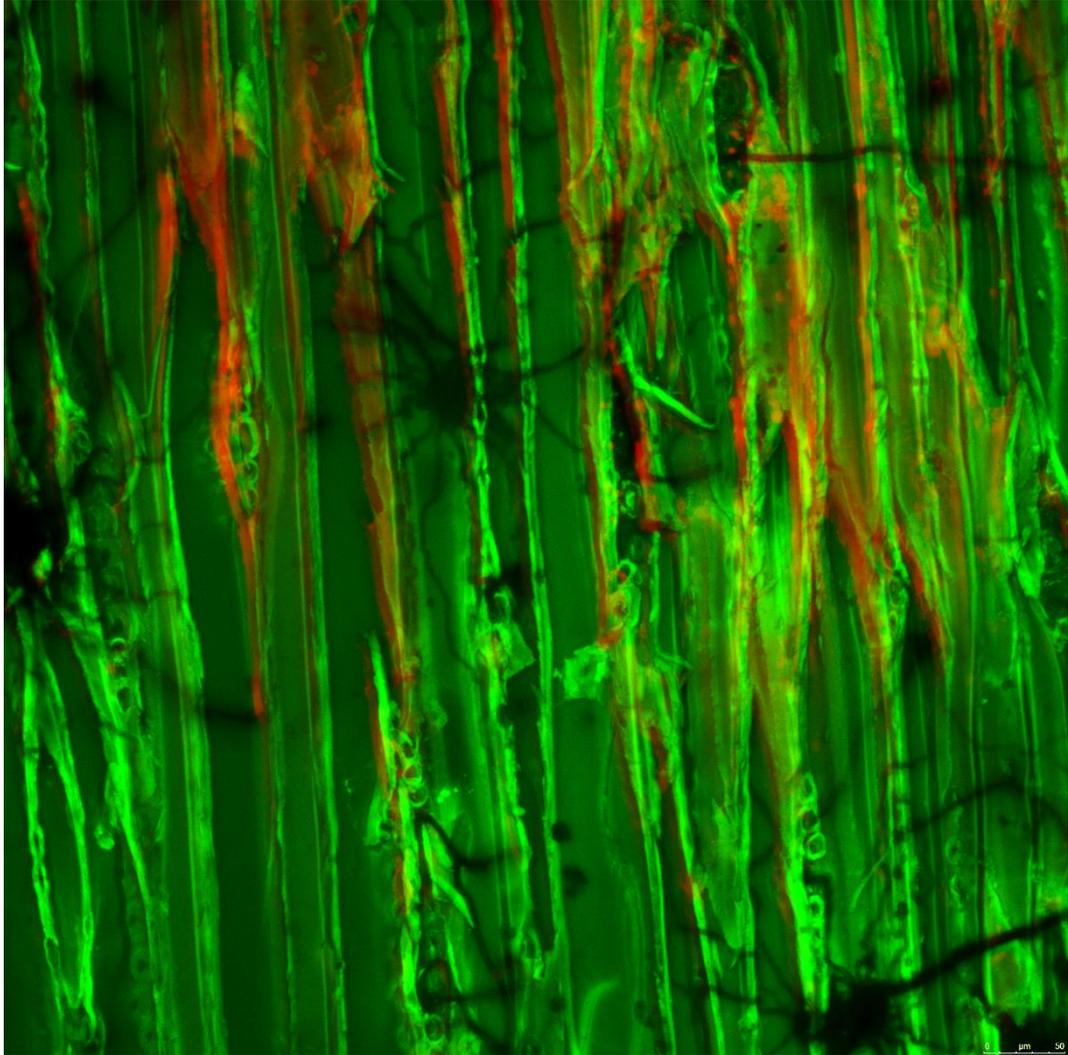
Figure 3.44- Confocal laser scanning fluorescence microgram showing pine inoculated with Cladosporium *after 1 week of incubation. The image was compiled from the sum of a 61 image stack taken every 0.5μm.*

There was little variation in the images taken over the 12 weeks of *Cladosporium* growing on pine. It was not possible to find evidence of conidiophores and after week 6 there was no increase in the visible surface hyphae. Signals from viable hyphae in the middle lamella and some of the tracheid lumens were still present in week 12; indicating that growth was still occurring, although it was likely occurring beyond the range of this imaging technique.

After 1 week of *Penicillium* growth there was evidence of germination and hyphal growth on the upper surfaces of the pine (Figure 3.45).

Figure 3.45- Confocal laser scanning fluorescence micrograph showing pine inoculated with Penicillium *after 1 week of incubation. The image was compiled from the sum of a 90 image stack taken every 0.5µm.*

After 4 weeks of growth there was still evidence of germination and further spore production, although it was not possible to identify conidiophores. These observations continued till week 8 where there were large numbers of spores collected on the fibre surface, but it was still not possible to image one of the conidiophores (Figure 3.46). The hyphae could be seen growing in the lumen of the tracheid cells and there were signals to indicate the growth of hyphae in the middle lamella between some cells.
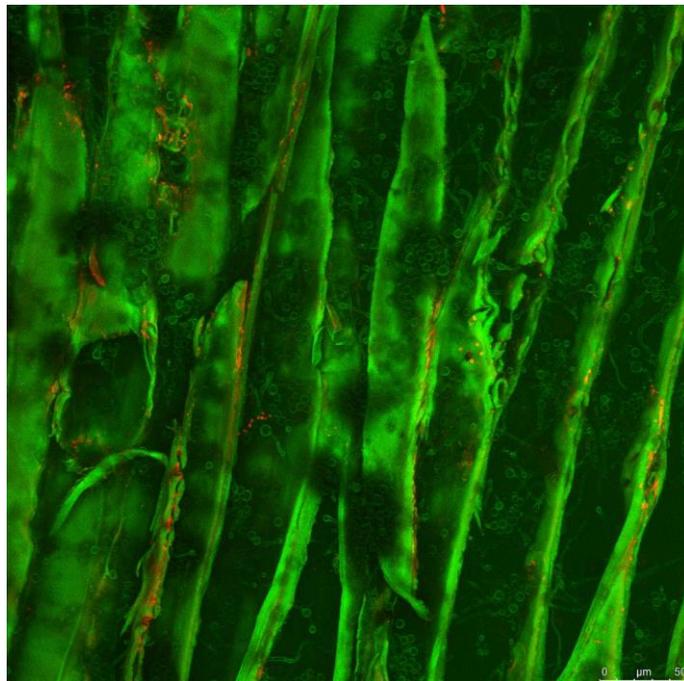
Figure 3.46- Confocal laser scanning fluorescence micrograph showing pine inoculated with Penicillium *after 8 weeks of incubation. The image was compiled from the sum of a 144 image stack taken every 0.5µm.*

After 12 weeks of growth, there were less visible spores and surface hyphal growth, although there was an increase in the FM4-64 signals in the middle lamella (Figure 3.47). This indicated that there was continued growth occurring beyond the scope of the microscope.
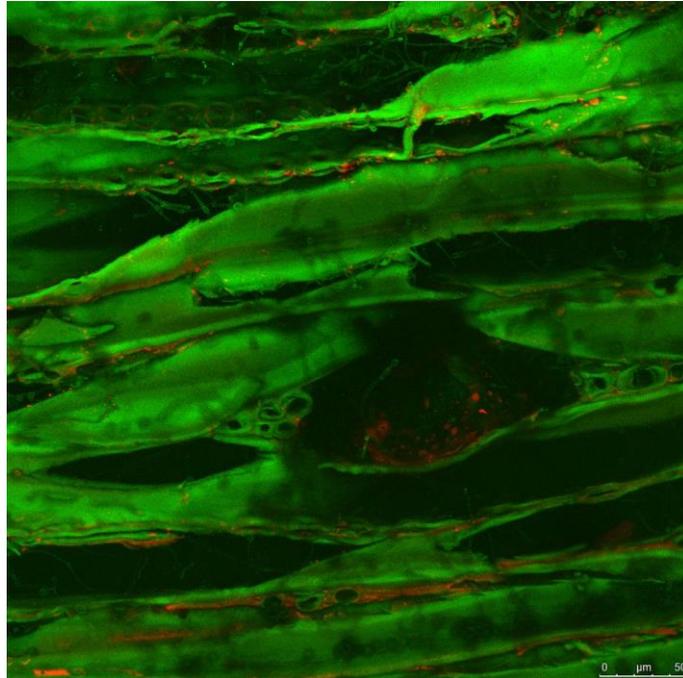
Figure 3.47- Confocal laser scanning fluorescence microgram showing pine inoculated with Penicillium *after 8 weeks of incubation. The image was compiled from the sum of a 144 image stack taken every 0.5µm.*

3.3.2.6 Confocal images of Oak

The growth of *Aspergillus* on oak was far less pronounced than on pine, after 1 week of incubation, there was little evidence of a hyphal network. After further incubation, the *Aspergillus* produced conidiophores and the hyphae could be seen to penetrate the cells in both the longitudinal and radial direction with much of the viable growth occurring in the middle lamella, rather than in the lumen of cells (Figure 3.48). After 8 weeks of growth, the aerial hyphae and conidiophores were further developed and firmly rooted within the cells of the oak (Figure 3.49). However, due to the density of the material, it was not possible to view past one layer of cells in the orthogonal stack.

After the full 12 weeks of growth there was little evidence of new fungal growth within the regions that were visible using this imaging technique. There were however still regions of viable growth detected in the middle lamella.
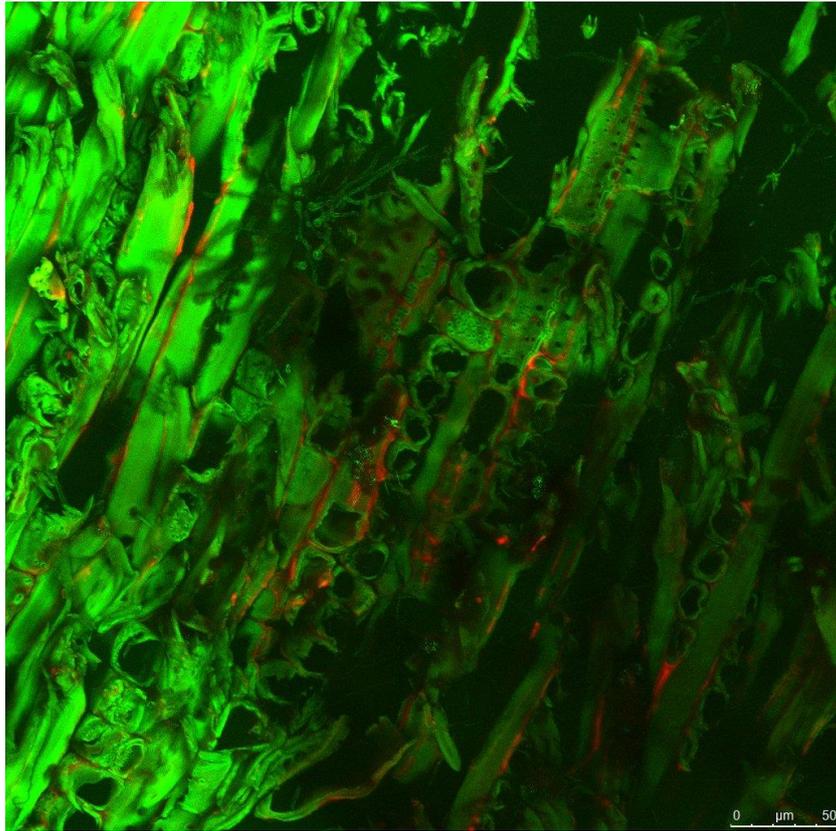
Figure 3.48- Confocal laser scanning fluorescence microgram showing oak inoculated with Aspergillus *after 4 weeks of incubation. The image was compiled from the sum of a 200 image stack taken every 0.5µm.*
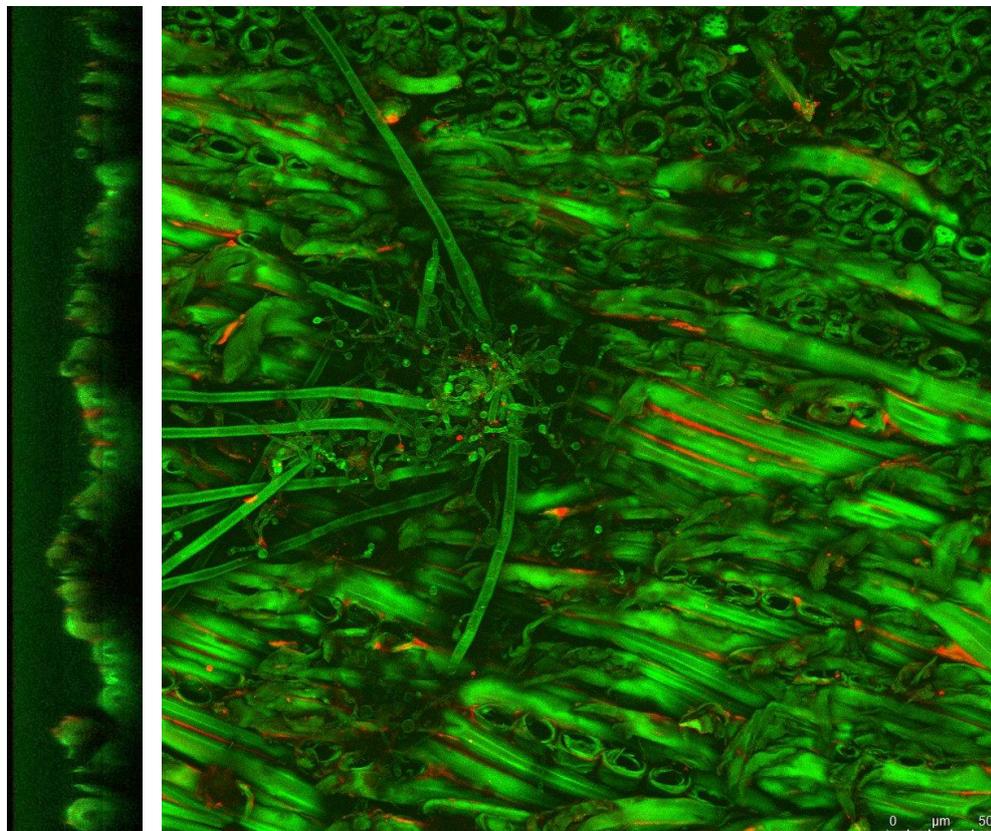
Figure 3.49- Confocal laser scanning fluorescence microgram showing oak inoculated with Aspergillus *after 8 weeks of incubation. The image was compiled from the sum of a 166 image stack taken every 0.5µm. The YZ orthogonal view shows the depth of penetration and viable fungal matter in the middle lamella between cells*

The growth of *Cladosporium* on oak was not visible using the confocal microscope until week 2 and this was only very fine pigmented hyphae on the surface on the wood (Figure 3.50). This continued until week 6 when there was evidence of the fungi penetrating the cellular structure of the oak, with signals in the middle lamella but no longer visible surface hyphae. This continued until the end of the trial (Figure 3.51).

Figure 3.50- Confocal laser scanning fluorescence microgram showing oak inoculated with Cladosporium *after 2 weeks of incubation. The image was compiled from the sum of a 265 image stack taken every 2µm. The highlighted area shows the fine pigmented surface hyphae of* Cladosporium
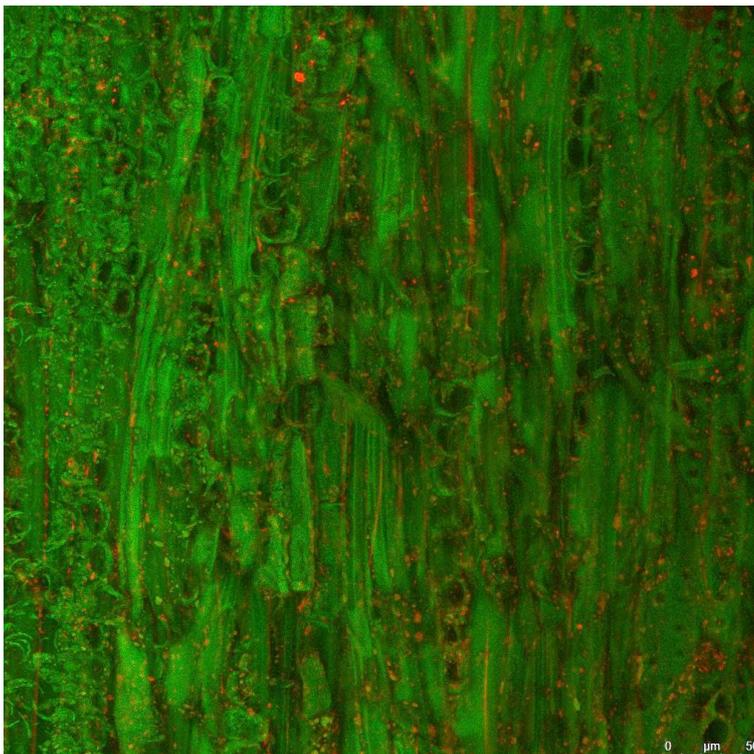
Figure 3.51- Confocal laser scanning fluorescence microgram showing oak inoculated with Cladosporium *after 12 weeks of incubation. The image was compiled from the sum of a 51 image stack taken every 0.5µm.*

For the oak, after 1 week of incubation with *Penicillium* there were also no signs of surface hyphal growth, but there were FM4-64 signals to indicate some minimal and localised growth in the middle lamella. After 2 weeks though, fine hyphae could be seen on some of the higher features of the oak (Figure 3.52).
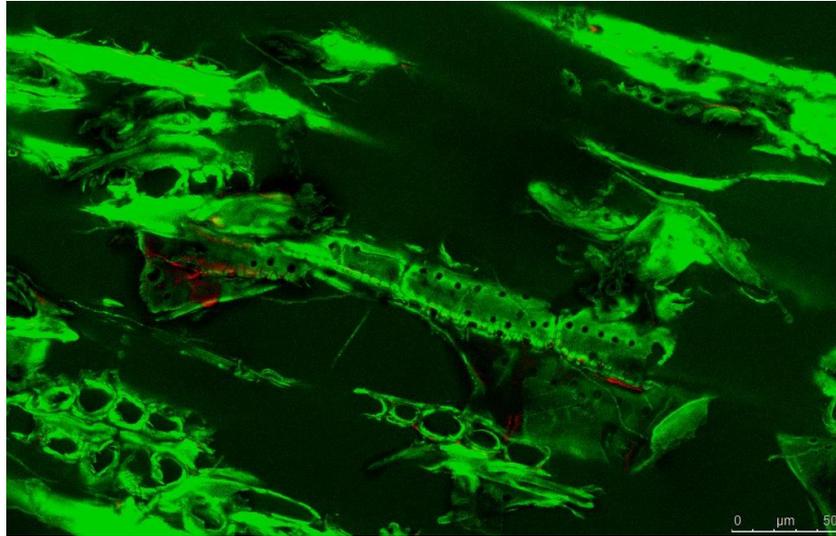
Figure 3.52- Confocal laser scanning fluorescence microgram showing oak inoculated with Penicillium after 2 weeks of incubation. The image was compiled from the sum of a 107 image stack taken every 0.5μm.

As the incubation time increased, the more hyphae became visible on the surface of the oak. There was also evidence to some degradation of the cell walls as pits started to appear (Figure 3.53). By the end of the trial there were many conidiophores protruding through the wood structure to sit on the surface, but the hyphal network was embedded within the cellular network of the oak (Figure 3.54).
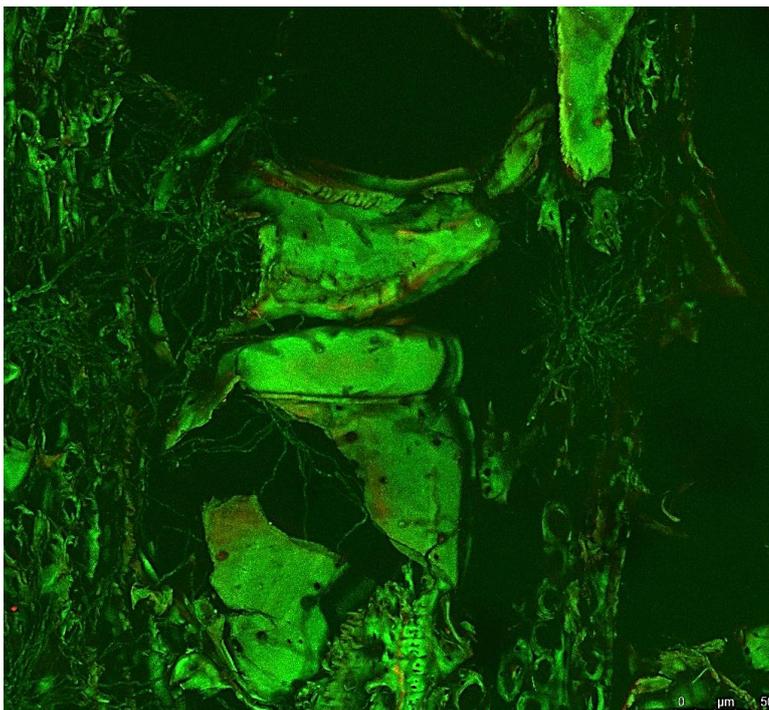
Figure 3.53- Confocal laser scanning fluorescence microgram showing oak inoculated with Penicillium *after 8 weeks of incubation. The image was compiled from the sum of a 131 image stack taken every 0.5μm.*
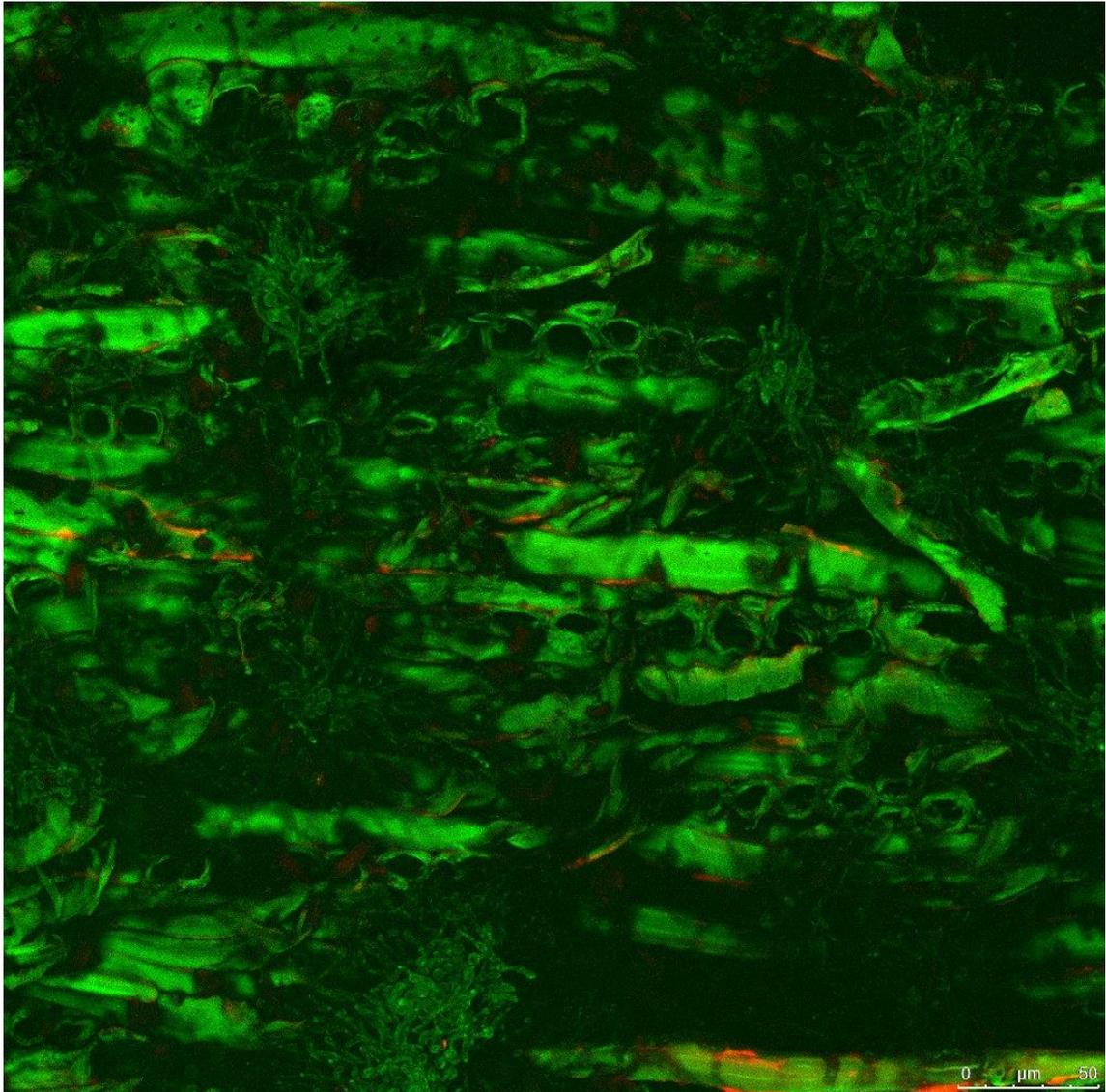
Figure 3.54- Confocal laser scanning fluorescence microgram showing oak inoculated with Penicillium *after 12 weeks of incubation. The image was compiled from the sum of a 166 image stack taken every 0.5µm.*

3.3.2.7 Confocal images of Silk

After one week of growth with *Aspergillus*, it was possible to see that germination and sporulation had occurred on the silk and the hyphae were interacting with the outer structure of the weave, particularly visible at the crown (Figure 3.55). From the composite average of the orthogonal slices, hyphae could be seen growing on the surface of the weave structure, winding around the fibres and penetrating through the crown of the weave. A detail of this (a) is shown from slices 37-60 of the sequence, which represents 23µm. From this it can be seen that fungal hyphae are entwined around and growing between the fibroin filaments and are starting to cause morphological changes. The depth of the features can be seen in Figure 3.56, a

topographical height map computed from the full stack of images. The darkest features are higher in the sample and the palest are deeper into the sample.
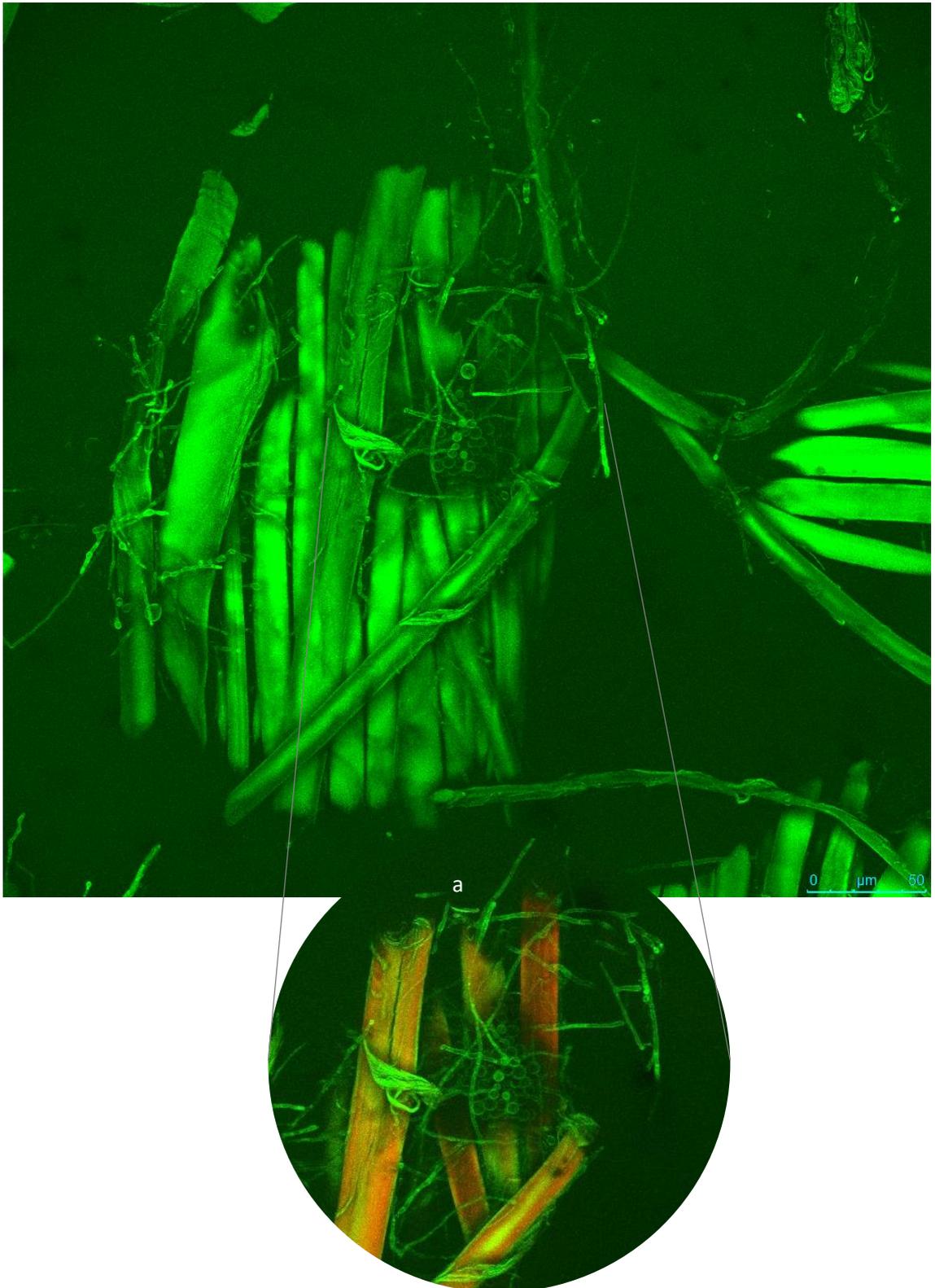
Figure 3.55- Confocal laser scanning fluorescence microgram showing silk inoculated with Aspergillus *after 1 week of incubation at 20°C and high aw. The image was compiled from the sum of a 68 image stack taken every 1μm. 3.55a details a 23μm section of the sample between images 37 and 60 in the orthogonal stack.*

The conidiophore is situated above the crown of the weave, although not very high. As it was not possible to see the aerial hyphae that the conidial structure is attached to, this means that it is below and that the main mycelial network is also below the weave structure and the reproductive structures are able to protrude through the interweave gaps to achieve a height greater than the textile surface.
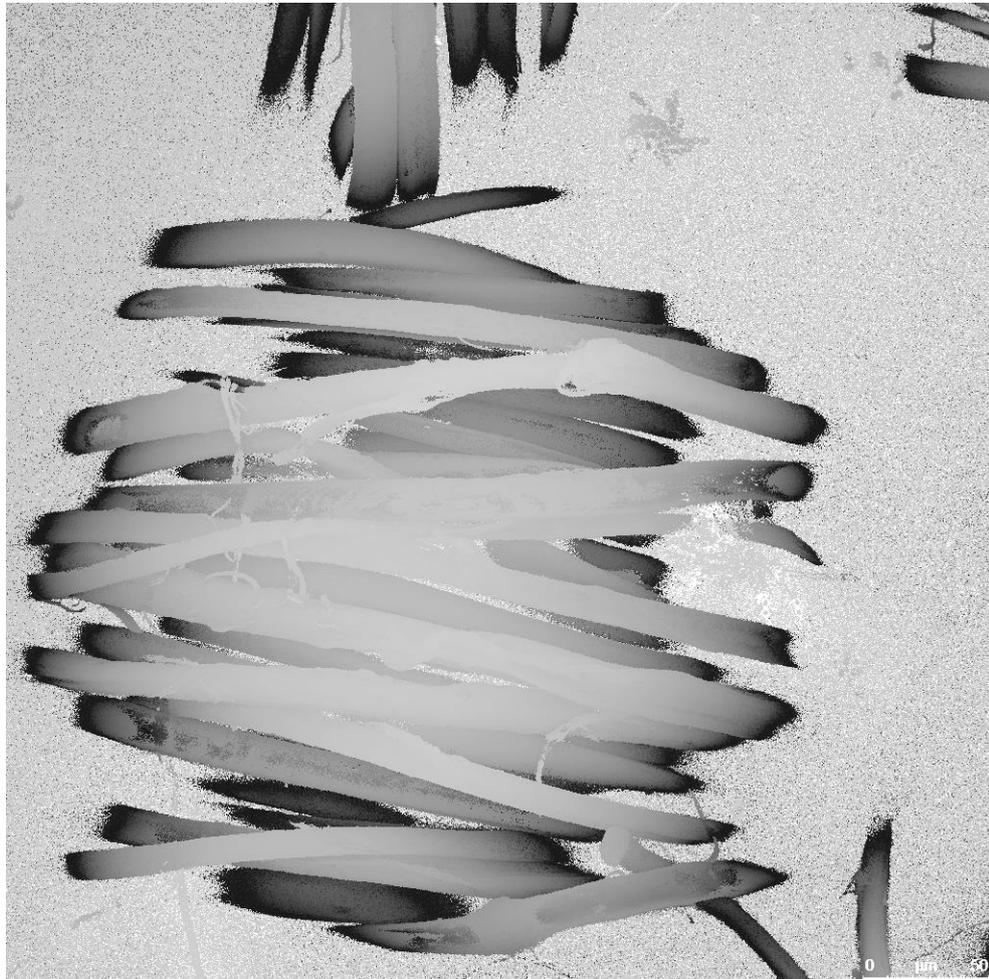
Figure 3.56- Topographical height map created from the 68 image orthogonal stack of Aspergillus versicolor *inoculated silk after one week of incubation at 20°C. Fungal hyphae and reproductive features are visible at various levels of the textile structure with the conidiophores protruding through the inter-weave spaces*

The *Cladosporium* germinated and produced fruiting bodies within the first week of incubation. The hyphae and conidia were so darkly pigmented that although they are visibly twining through the weave structure, they show limited fluorescence (Figure 3.57). Although the conidiophores were aerial and projecting from the weave structure, they were not as elevated as those of the *Aspergillus*.
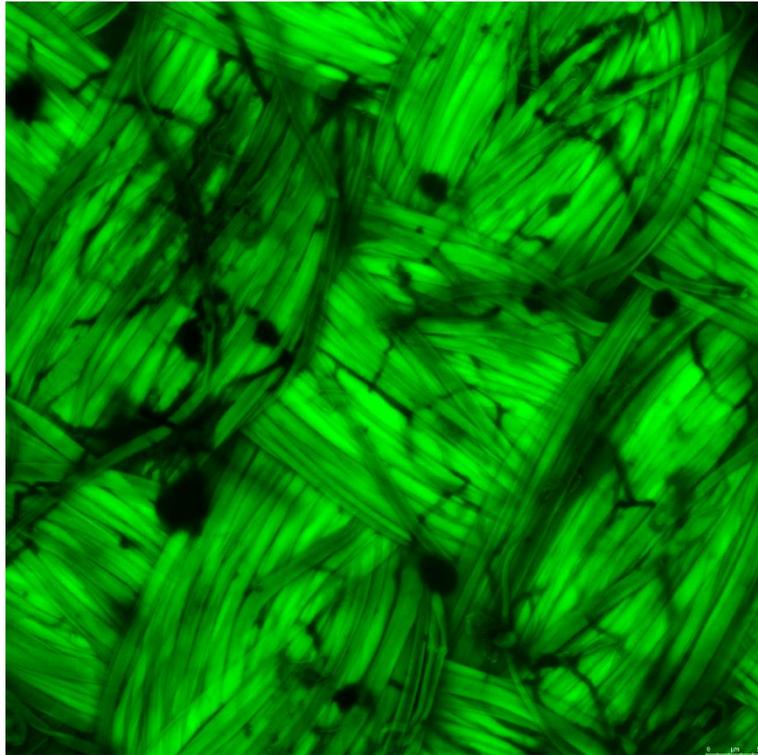
Figure 3.57- Confocal laser scanning fluorescence microgram showing silk inoculated with Cladosporium *after 1 week of incubation at 20°C and high a_w. The image was compiled from the sum of a 63 image stack taken every 1µm. Darkly pigmented hyphae growing through the weave structure and aerial conidiophores can be seen.*

After 12 weeks of incubation, defibrillation of the silk could be seen as the elementary fibrils became visible around the fibres at the crown of the weave which were more exposed (Figure 3.58). In the area that this image was taken, hyphal growth is not evident throughout the depth imaged (78µm). This may be due to the fact that the *Cladosporium* hyphae could be seen to penetrate deeply into the fibre and agar beneath, meaning that growth was deep within the weave structure. There are shadows on the image which indicate aerial hyphae.
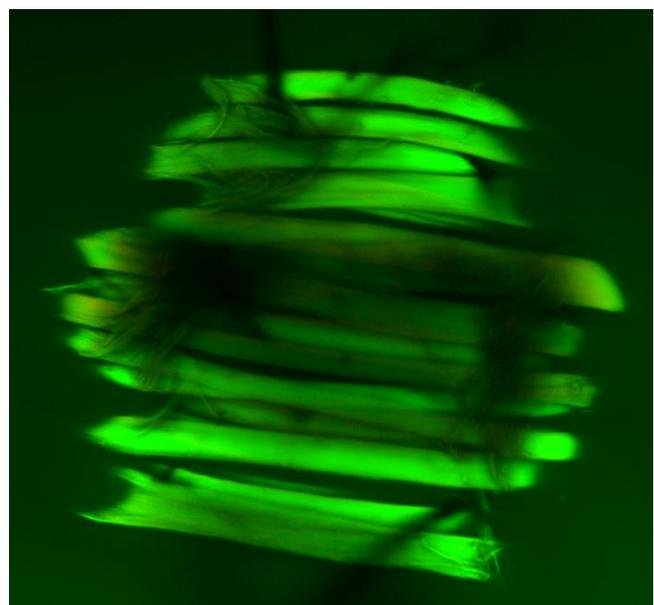
Figure 3.58 - Confocal laser scanning fluorescence microscopy of a weave crown from silk inoculated with Cladosporium *after 12 weeks of incubation at 20°C. This average projection was created from the orthogonal stack of 157 images every 0.5µm.*

Penicillium germinated and was producing fruiting bodies within the first week of incubation on silk (Figure 3.59)
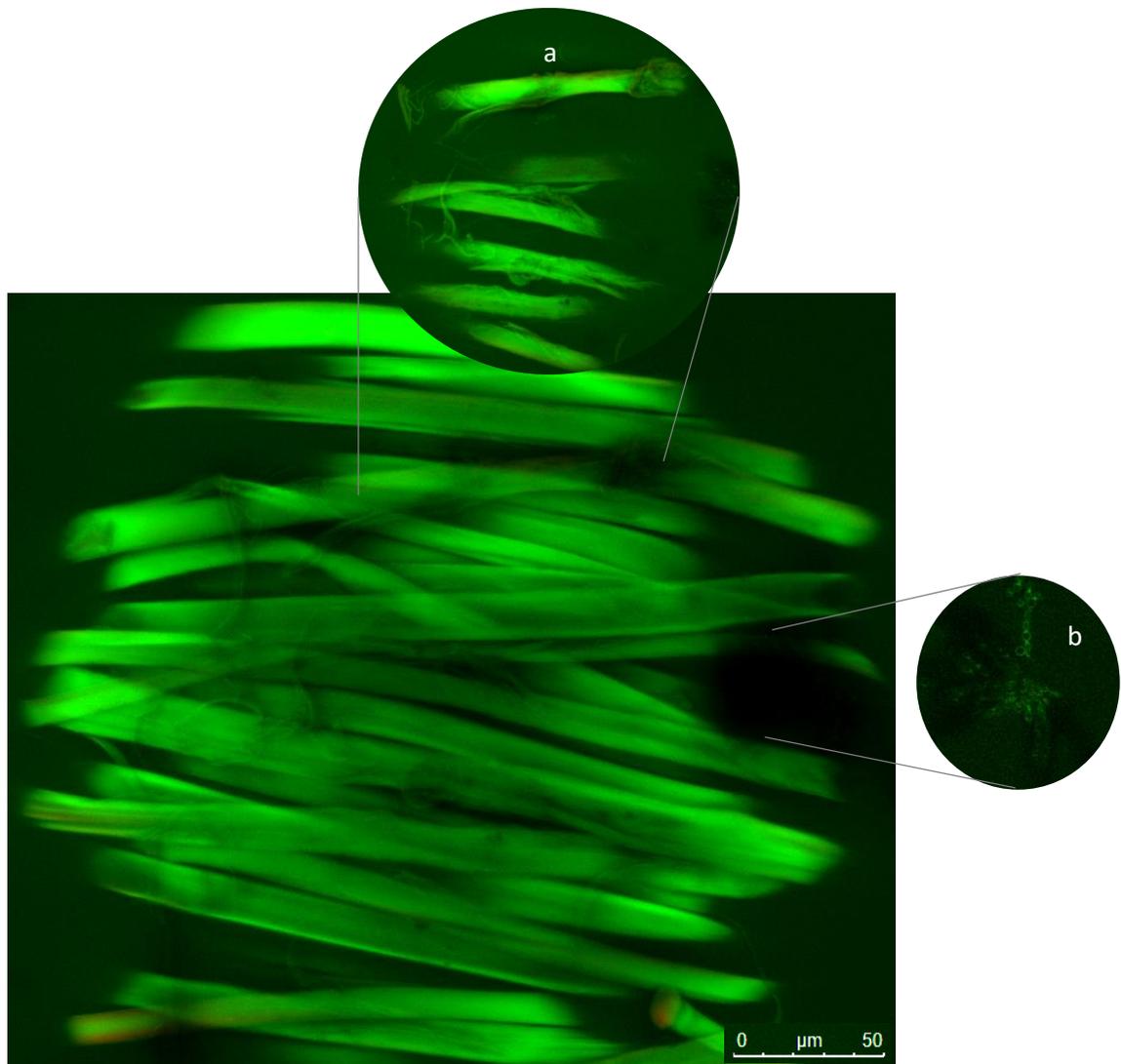
Figure 3.59– Average stack (64 images, 64µm) confocal laser scanning fluorescence microscopy image of plain weave silk one week after inoculation with Penicillium brevicompactum spores and incubation at 20°C. Fungal hyphae are entwined within the weave structure and there are conidiophores protruding through the inter yarn spaces. a) Shows the average composite of the first 10 stack images detailing the spread of hyphae. b) shows the area of image 3 that gives detail of the conidiophore that is causing shadowing over the lower stack images

From the composite average stack of the orthogonal slices, it is possible to see hyphae growing on the surface of the weave structure but also winding around the fibres and penetrating through the crown of the weave. A detail of this (a) is shown from the first 10 slices of the sequence, which represents 10µm. From this it can be seen that fungal hyphae are entwined around and growing between the fibroin filaments and are starting to cause morphological changes to the usually smooth surface.

After 6 weeks of incubation, there are further signs of damage to the fibroin filaments, including loss of fibre, and the overall weave structure is less regular. Figure 3.60 shows a local thickness

map of the silk weave and in the area highlighted, there is hyphal growth and a reduction in fibre thickness. It can also be seen that spores congregate in gaps in the weave structure and that the germination cycle is continuing with new germ tubes visible.
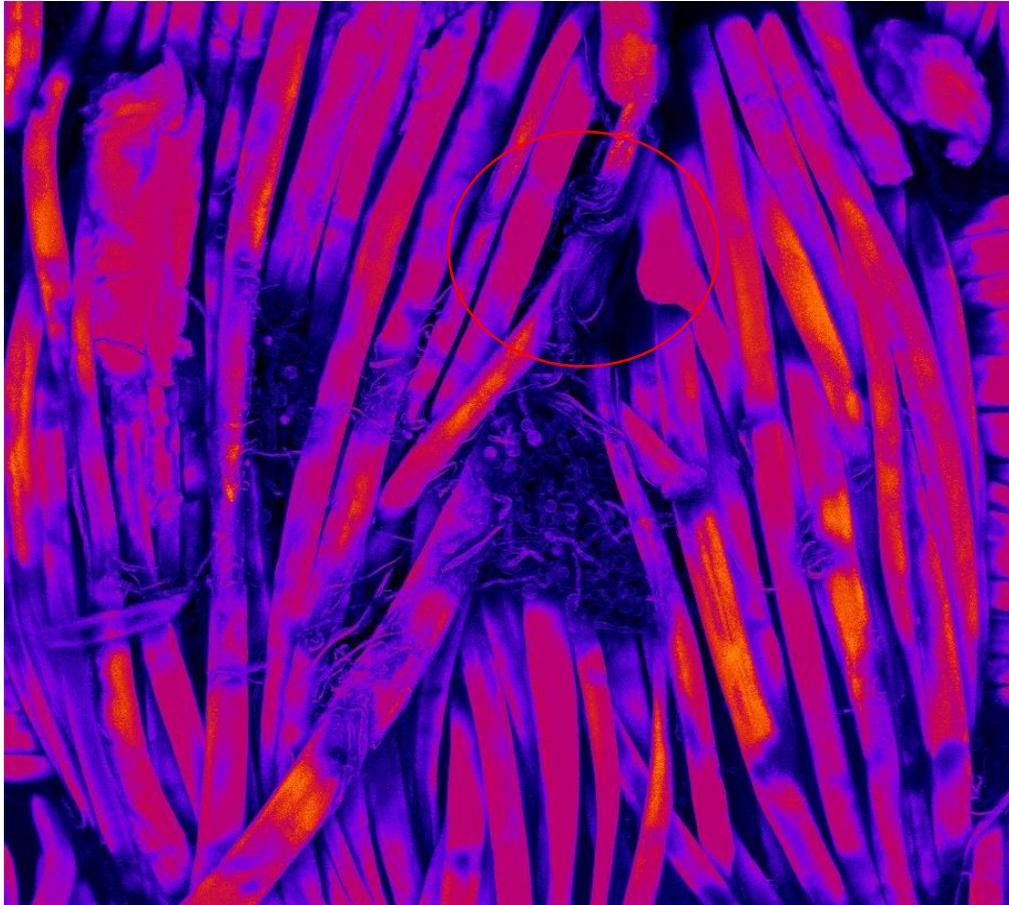
Figure 3.60- Computed local thickness map of silk incubated with Penicillium brevicompactum after six weeks of incubation at 20°C. Image created from a 225 image orthogonal stack with a depth of 0.5μm per scan. A loss in thickness of silk fibroin can be seen along with new germination.

After the full 12 weeks of incubation, pitting could be seen on the surface of most fibres in the crown and with less uniformity to the weave structure. There was also an increase in the uneven thickness of fibres, indicating hyphal penetration and degradation of the fibroin filaments visible on the surface. By this stage, there was less evidence of continued reproduction; fewer spores were found and no germ tubes.

3.3.2.8 Confocal images of Wool

After one week of growth, it was possible to see that germination, hyphal growth and sporulation of the *Aspergillus* had occurred on the wool and the hyphae were interacting with the outer structure of the weave, particularly visible at the crown. After three weeks there was an extensive, but fine branched hyphal network over the surface and the wool was beginning to show signs of cuticle damage and the loss of scales (Figure 3.61).
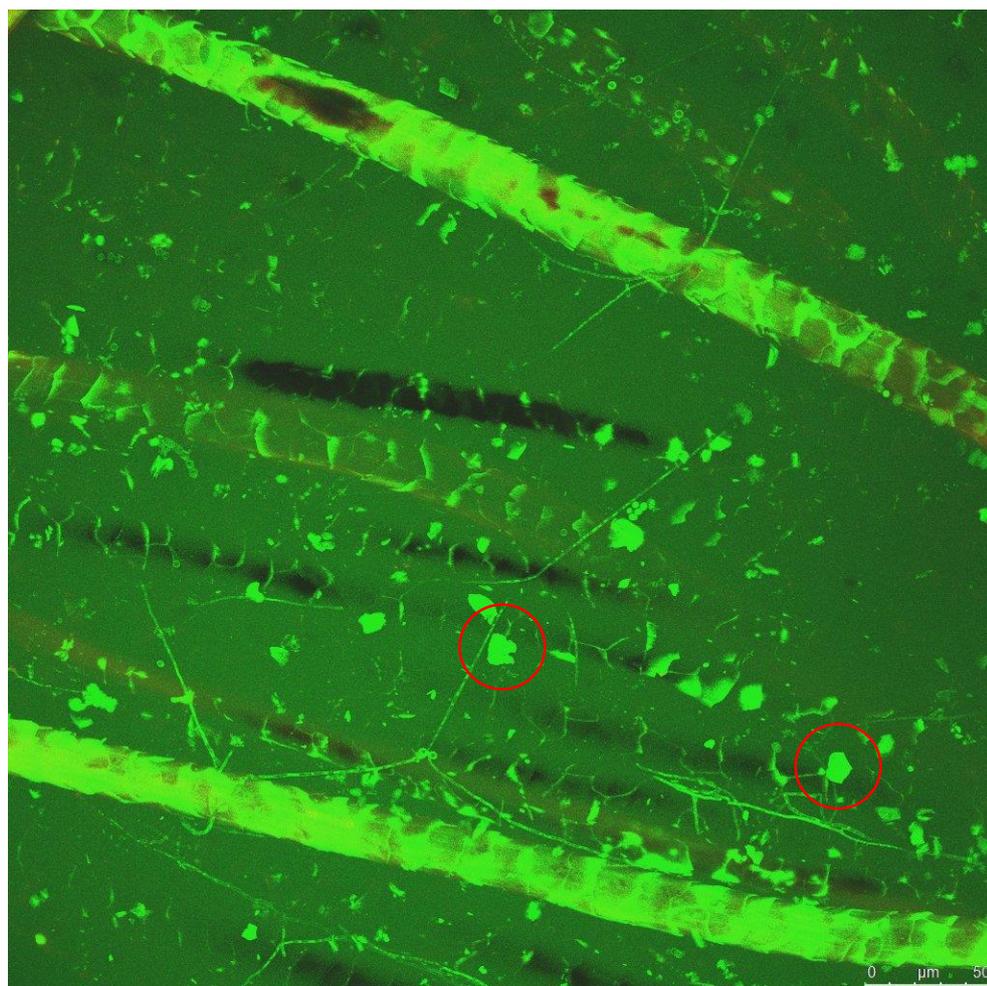
Figure 3.61- Confocal laser scanning fluorescence microgram showing wool inoculated with Aspergillus *after 3 weeks of incubation at 20°C and high a_w. The image was compiled from the sum of a 128 image stack taken every 0.5μm. Highlighted areas detail the independent cuticle scales that have come away from the fibre and are suspended in the mounting media.*

After eight weeks of incubation, there was mature colony growth with large aerial hyphae and reproductive structures as well as intricate mycelium which coiled around and penetrated fibres. There was evidence of damage to the cuticle as the dyes were more readily absorbed and the fibres clearly visible, particularly in the regions of intensive growth. This was supported by a continuing loss of scales, which become more prominent, absorb more dye and are then separated from the fibre; as highlighted in Figure 3.62. The imposed height map of the 64μm

thick stack (Figure 3.62a) shows that the scales are no longer in close connection with the fibre and would soon become independent, as can be seen with the other small fragments of scales.
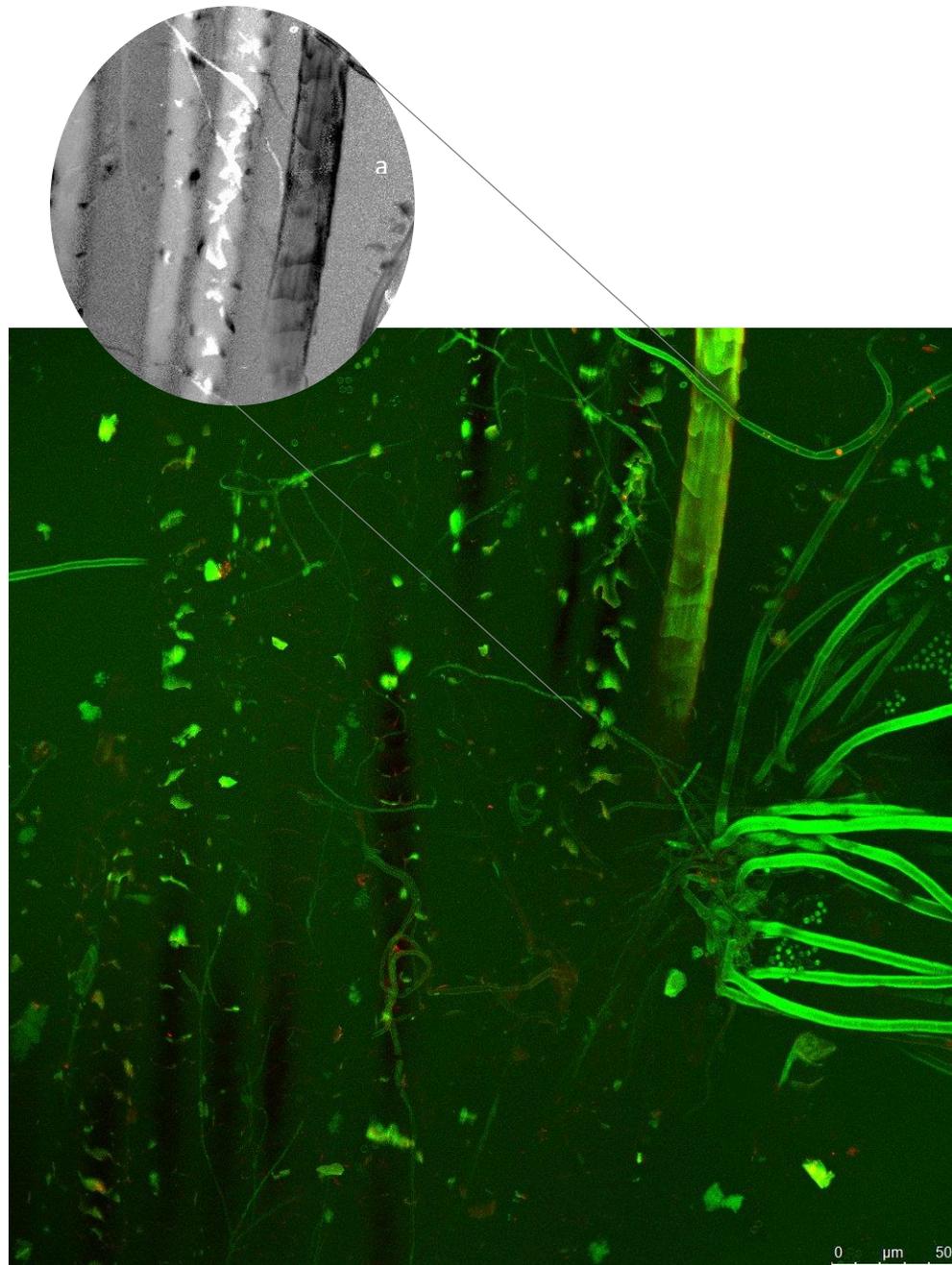

Figure 3.62-Confocal laser scanning fluorescence microgram showing wool inoculated with Aspergillus versicolor after 8 weeks of incubation at 20°C and high a_w. The image was compiled from the sum of a 128 image stack taken every 0.5µm. 3.62a, highlights the height map of the 64µm image with the lighter regions being raised from the surface and are no longer in close association with the main fibre

After twelve weeks of incubation with *Aspergillus*, the wool fibres were more easily penetrated by liquids (greater dye uptake) due to cuticle damage and eventual loss of fibre scales. Extensive hyphal growth can be seen as well as large, mature aerial reproductive structures. Although

these conidia had lost their spores by the time of imaging, the structures were still viable, due to the uptake of FM4-64 (via endocytosis) to create a red signal (Figure 3.63).

*Figure 3.63- Confocal laser scanning fluorescence microgram showing wool inoculated with* Aspergillus *after 12 weeks of incubation at 20°C and high a_w. The image was compiled from the sum of a 125 image stack taken every 0.5µm. Highlighted regions shows the conidial head after spore dispersal with the FM4-64 (red) endocytosis stain confirming viability.*

With wool inoculated with *Cladosporium*, after one week of incubation there was hyphal growth amongst the fibres in the crown of the weave and bridging the inter weave voids. There was also evidence of damage to the cuticle cells, with an increase in their height in comparison to the profile of the fibre. After four weeks of incubation, there was visible aerial hyphae and sporulation of the *Cladosporium*. There was also a swelling of some of the fibres along with a splitting and change in orientation (Figure 3.64 & 3.64a).
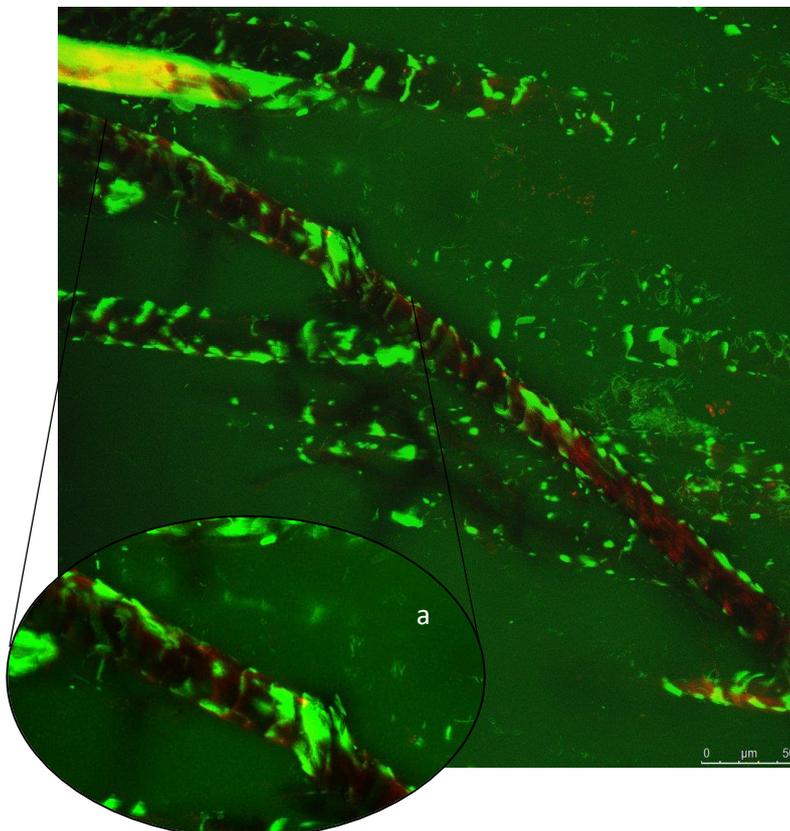
Figure 3.64- Confocal laser scanning fluorescence microgram showing wool inoculated with Cladosporium *after 4 weeks of incubation at 20°C and high a_w. The image was compiled from the sum of a 149 image stack taken every 0.5µm. 3.64a shows a detail of a ruptured fibre where the scales have loosened and the axis is no longer straight.*

118

An increased uptake of the FM4-64 and Eosin Y dyes, indicated further damage to the cuticle, Confirmed by the loosening and release of some of the scales. Towards the latter stages of the trial, growth increased further, with aerial hyphae protruding above the weave and hyphae coiling around fibres and through the weave structure (Figure 3.65). There was clear descaling of the cuticle and swelling in certain areas of the fibres, in the vicinity fungal growth. The hyphae and conidiophores appeared as shadows as transmission of the dye was affected by the darkly pigmented cell walls. There were still viable areas of fungal growth visible, although these were below the crown of the weave.
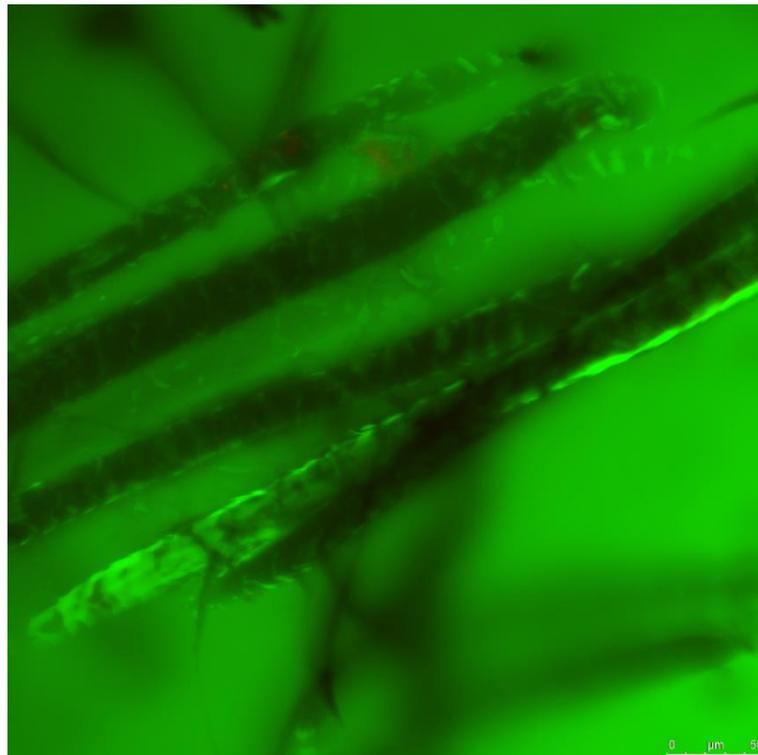

Figure 3.65-Confocal laser scanning fluorescence microgram showing wool inoculated with Cladosporium *after 4 weeks of incubation at 20°C and high a_w. The image was compiled from the sum of a 229 image stack taken every 0.5µm*

For the wool, after one week of incubation with *Penicillium*, some of the conidia had germinated and hyphal growth could clearly be seen throughout the weave structure (Figure 3.66). The conidia in this case seem to have grouped together in the areas below the crown where they could collect in the weave voids and as a result, not all have germinated. After 6 weeks of growth there was visible damage to the cuticle scales, where they had lifted and in some places been released from the fibre (Figure 3.67). Some of the fibres appeared smooth as a result of this, some had changed dimensionally and were able to absorb the fluorescent dyes to a greater degree. Hyphal growth within the spaces of the weave was extensive, but aerial conidiophores limited.
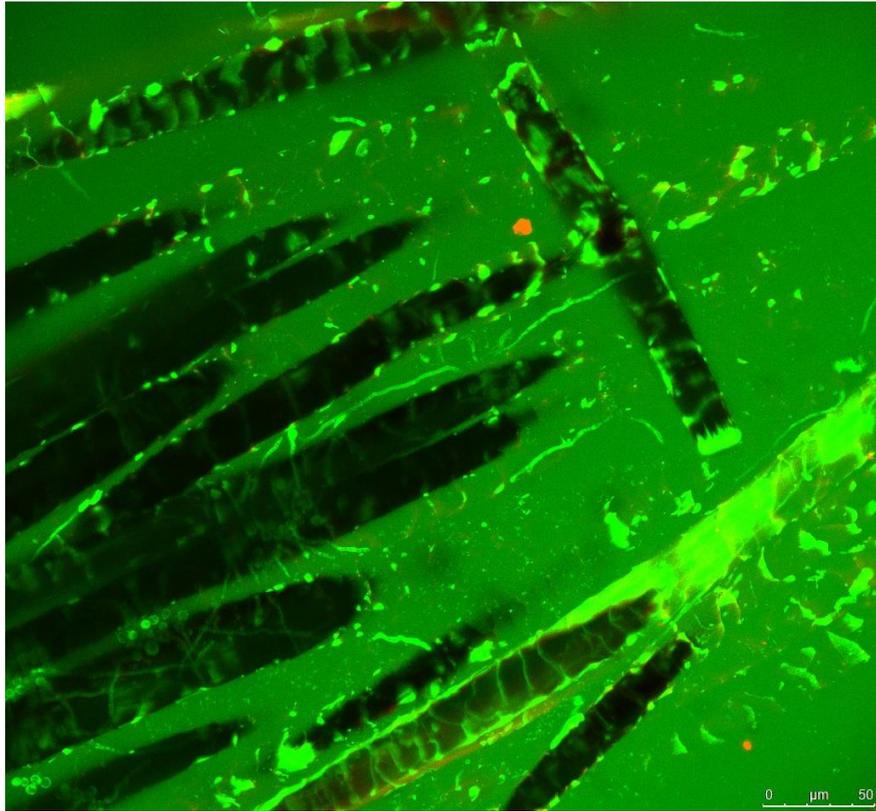
Figure 3.66- Confocal laser scanning fluorescence microgram showing wool inoculated with Penicillium *after 1 week of incubation at 20°C and high a_w. The image was compiled from the sum of a 35 image stack taken every 0.5µm.*

Figure 3.67- Confocal laser scanning fluorescence microgram showing a quadratic topographical height map of wool inoculated with Penicillium *after 6 weeks of incubation at 20°C and high a_w. The image was compiled from the sum of a 158 image stack taken every 0.5µm. The darker features are higher in the stack, showing free cuticle scales and hyphae at different levels of the weave.*

After the full incubation time the surface of many of the wool fibres were smoother with damage to the cuticle (Figure 3.68). Hyphal growth was still observed to be extensive by there were fewer conidia visible and aerial hyphae limited.
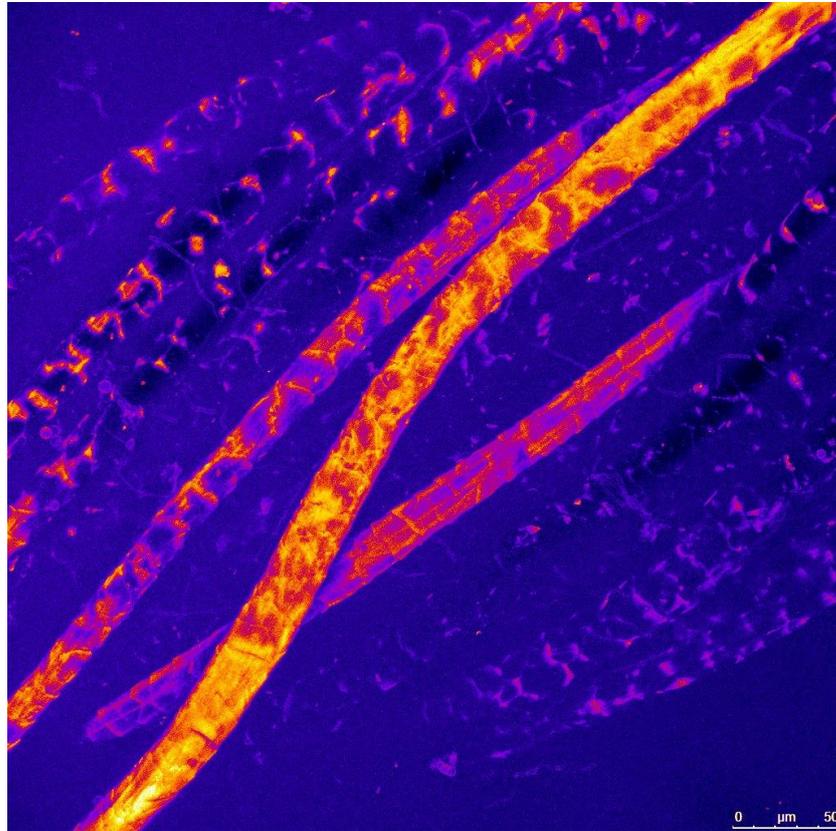
Figure 3.68- Confocal laser scanning fluorescence microgram showing the local thickness of features in wool inoculated with Penicillium *after 12 weeks of incubation at 20°C and high a_w. The image was compiled from the sum of a 134 image stack taken every 0.5µm.*

3.3.2.9 Confocal images of Parchment

Parchment inoculated with Aspergillus showed extensive germination after week of incubation with the greatest density of conidia being held in the follicles of the hide. There were also numerous aerial hyphae with conidiophores (Figure 3.69) which were causing shadowing on the image. After 4 weeks of incubation, deeply rooted aerial hyphae could be seen penetrating through the dermis and collagen fibrils, mostly sited around follicles (Figure 3.70). A fine mycelial network could also be seen over the surface the parchment with some viable detached conidia.

After the fill incubation time, the surface of the parchment was showing signs of pitting but there was less visible surface growth (Figure 3.71). Aerial structures were extensive and shadowed the parchment surface, but viable structures could be seen below the outer dermis and conidia were collected around the follicles.
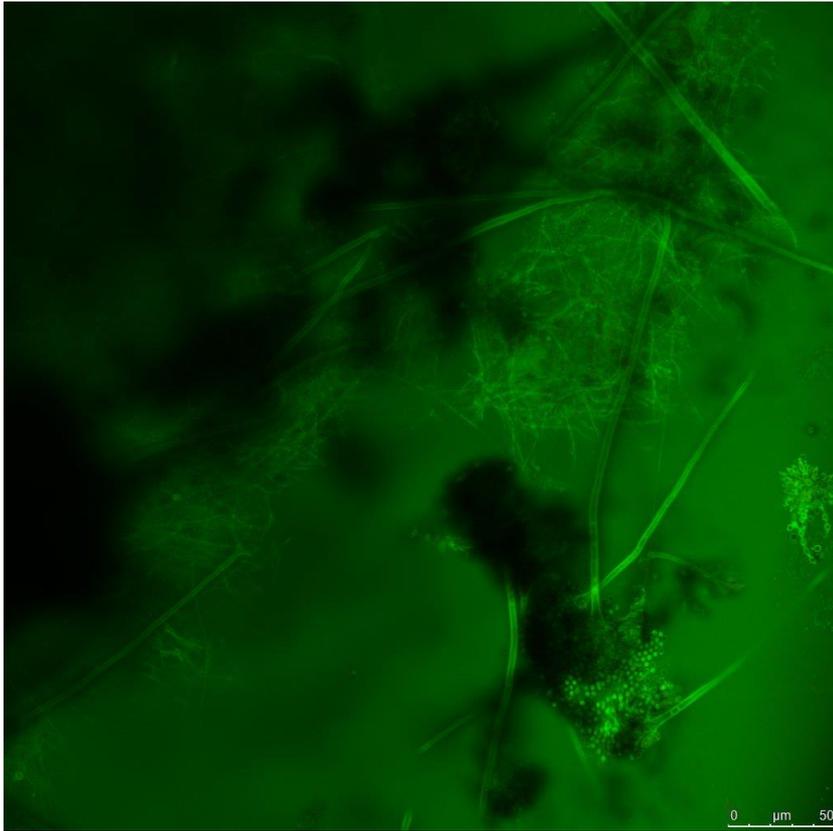
Figure 3.69- Confocal laser scanning fluorescence microgram showing parchment inoculated with Aspergillus *after 1 week of incubation at 20°C and high a_w. The image was compiled from the sum of a 152 image*
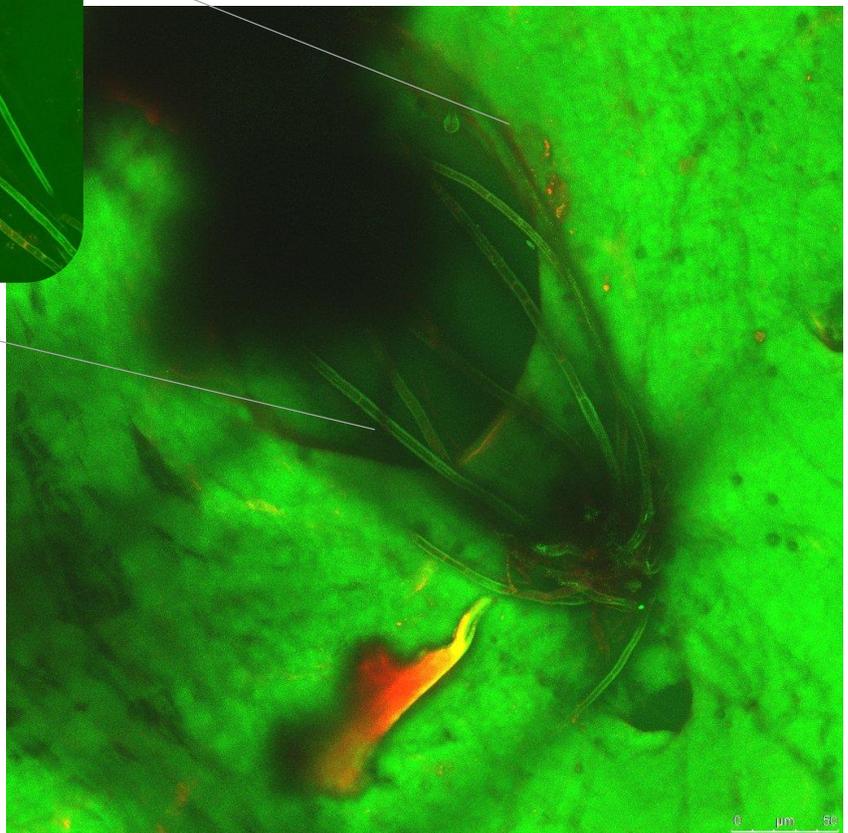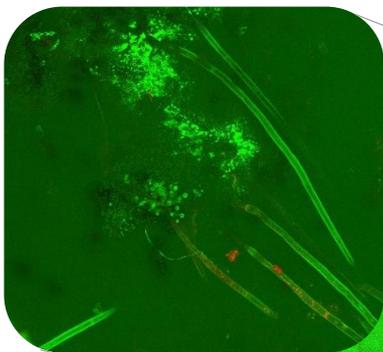
Figure 3.70- Confocal laser scanning fluorescence microgram showing parchment inoculated with Aspergillus *after 4 weeks of incubation at 20°C and high a_w. The image was compiled from the sum of a 195 image stack taken every 0.5µm. Highlighted region shows the top 57 images of the stack where the conidiophores are shading the lower levels of the stack.*
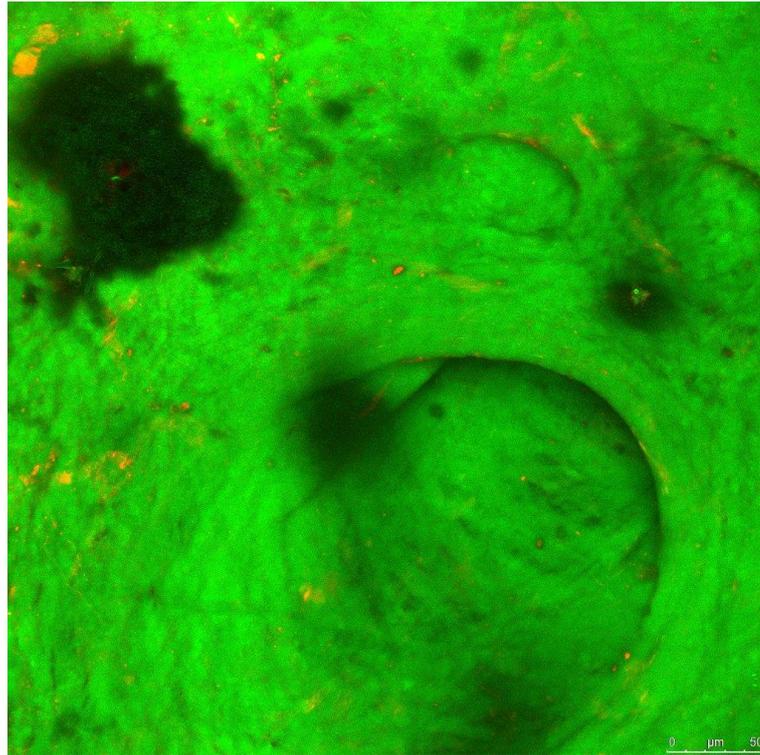
Figure 3.71- Confocal laser scanning fluorescence microgram showing parchment inoculated with Aspergillus *after 12 weeks of incubation at 20°C and high a_w. The image was compiled from the sum of a 171 image stack taken every 0.5µm.*

After 1 week of *Cladosporium* growth on parchment, there was little visible growth on the surface of the hide, although viable spores were collected together in the follicles. Four weeks of incubation and darkly pigmented hyphae could be seen on the surface, but no reproductive structures or viable conidia. Towards the end of the trial, 10 weeks of incubation, viable conidia were again found in follicles but with no evidence of reproductive structures (figure 3.72).
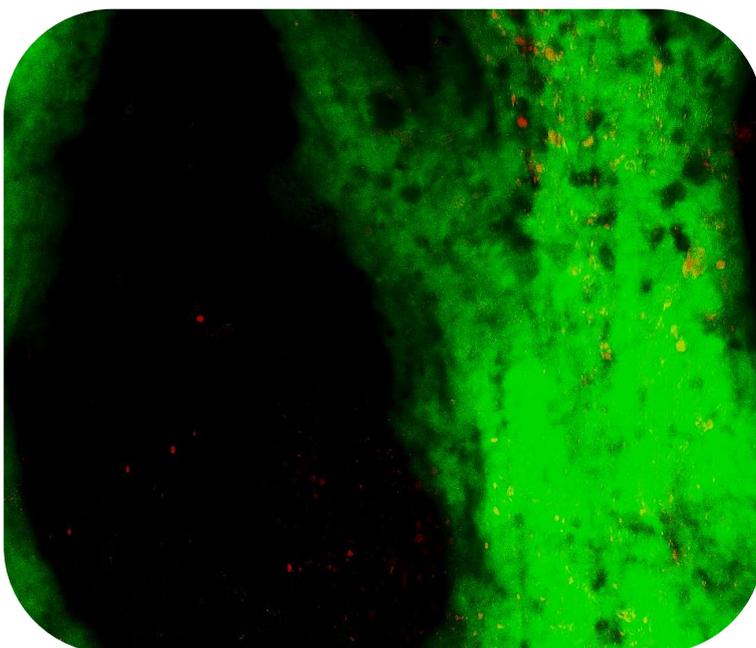

Figure 3.72- Confocal laser scanning fluorescence microgram showing parchment inoculated with Cladosporium *after 10 weeks of incubation at 20°C and high a_w. The image was compiled from the sum of a 251 image stack taken every 0.2µm.*

After 12 weeks of incubation, viable hyphae could be seen on the surface and penetrating through the dermis, but growth was far less established than that of the *Aspergillus* and no reproductive structures were found.

Penicillium when incubated on parchment showed extensive germination after 1 week (3.73) with aerial reproductive structures, as can be seen in the topographical height map of 3.73a. The majority of germination occurred within the follicle structures.
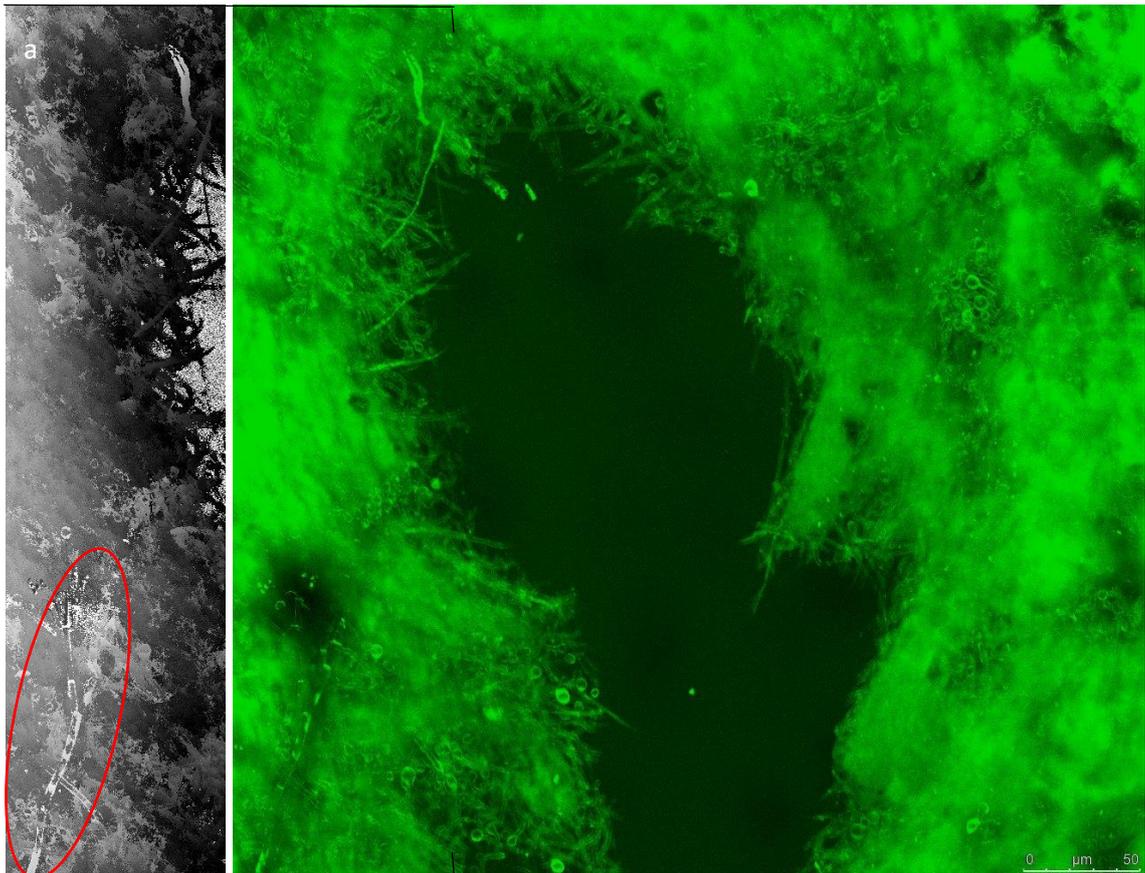
Figure 3.73- Confocal laser scanning fluorescence microgram showing parchment inoculated with Penicillium *after 1 week of incubation at 20°C and high a$_w$. The image was compiled from the sum of a 355 image stack taken every 0.25μm. 3.73a) shows a topographical height map of the left side of the stack with the higher features in the stack as lighter, the lower darker.*

After 6 weeks of incubation there was extensive hyphal growth and mature reproductive structures throughout the layers of the substrate (Figure 3.74). There was also evidence of newly formed germ tubes. Figure 3.74a shows a topographical height map detailing mature conidiophores that are lighter than the surface of the parchment and therefore higher in the image stack. Figure 3.74b shows the collaged fibril structure below the dermis inside a follicle. Even at the base of the follicle, there were hyphae. In some areas hyphae could be seem to have penetrated the dermis and were interacting with the fibrillar layers of the parchment.

After 12 weeks incubation there was evidence of new growth. The surface of the parchment had many conidia that had settled and some of these had produced germ tubes.
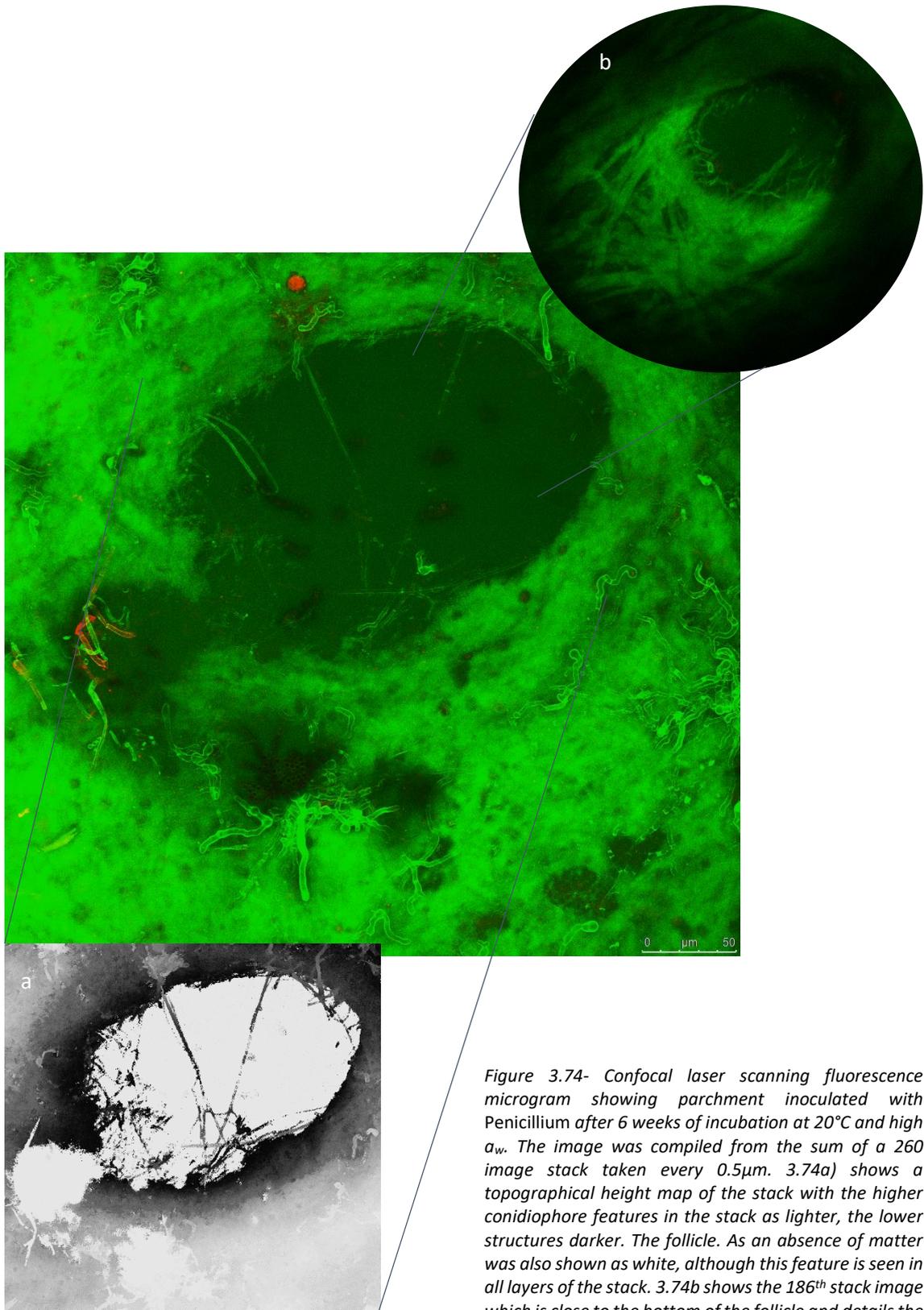
*Figure 3.74- Confocal laser scanning fluorescence microgram showing parchment inoculated with* Penicillium *after 6 weeks of incubation at 20°C and high a_w. The image was compiled from the sum of a 260 image stack taken every 0.5µm. 3.74a) shows a topographical height map of the stack with the higher conidiophore features in the stack as lighter, the lower structures darker. The follicle. As an absence of matter was also shown as white, although this feature is seen in all layers of the stack. 3.74b shows the 186th stack image which is close to the bottom of the follicle and details the hyphal growth at this depth and the collagen structure of the parchment below the dermis.*

3.4 Discussion

From investigations carried out, it can be seen that the growth of fungi on organic substrates can significantly change the physical characteristics of materials. Moreover, the changes can be seen by the naked eye and cause permanent changes to the structure and aesthetic of materials; even after short incubation, if there is an adequate moisture supply.

3.4.1 Spectrodensitometer study

The use of colourimetry enabled the total permanent colour change of materials, along with the dimensional colour change to be determined for each material. This technique was a good quantitative indicator that fungi had caused permanent change, however using a random sample methodology meant that there was a high standard error in readings due to the un-homogenous nature of organic substrates and whether a fungal colony had formed in the vicinity of the reading. The natural biofilm measurements were particularly varied due to the diversity of species found on each of the materials.

3.4.1.1 Total colour change

The total colour change of all materials, represent by the calculated ΔE value, was found to be significant, depending on the fungal inoculum. Colour changes to historic materials colonised by fungi are thought to be caused by metabolic product reactions or the production of pigments (Szostak-Kotowa 2004). It was observed that certain materials are more vulnerable to changes in colour and that the dark pigmentation produced by *Cladosporium cladosporiodes* caused the greatest colour change, as found in other studies (Reis-Menezes et al. 2011). By using colourimetry, colour change could be quantified, although this caused a high degree of variation as changes were greater in the vicinity of specific colonies. It has been noted that the greater the concentration of the inoculum, the greater the colour change of paper (Reis-Menezes et al. 2011). This was difficult to determine in this study due to the nature of dry spore applications. However, where colonies became well established, spread and sporulated on substrates, the larger the colour change observed on all materials. On linen it was found that the colour change caused by *Aspergillus niger* was greater than that of *Penicillium funiculosum* (Abdel-kareem 2010). This study found that the effect of *A. versicolor* was on all cellulosic materials was less than that of *P. brevicompactum,* the difference in result likely due to the dark pigmentation of the *A. niger*.

The only material in which *A. versicolor* than *P. brevicompactum* caused a greater colour change was silk; *Aspergillus sp*. have been noted to cause discoloration of silk and potentially degrade

fibroin, although may also just opportunistically colonise as with *Penicillium sp.* (Seves et al. 1998).

From the total colour change data, it is evident that the proteinaceous materials are more vulnerable to permanent colour change, unless the fungi is *Cladosporium*, when any material is likely to have aesthetically altering stains. Linen was the most resistant to colour change, likely due to having a higher lignin content and being more resistant to fungal degradation (Gutarowska & Michalski 2012; Szostak-Kotowa 2004). This is supported by the fact that the delignified beech wood paper had the most significant colour change of the cellulosic substrates.

3.4.1.2 Natural biofilm cultures

The species found naturally on the organic materials were cultured and identified. Other studies have isolated these genera and then studied their individual effect on materials (Blyskal 2014), however this was beyond the scope of this project. It was also deemed that change produced through mixed culture interactions was more representative of what would be found in a historic house setting and this will be taken into account for all experimental work. Many of the genera found were also collected within the historic property surveys, confirming that the species found on the materials are representative of what might be found in those environments. The high instances of *Aspergillus* and *Penicillium* with the other biofilm genera were also isolated from historic textiles, archives, libraries, wooden objects and painting canvas (Reis-Menezes et al. 2011; Abdel-kareem 2010; Błyskal 2015; Kavkler & Demšar 2012; Kavkler et al. 2015; Sabatini et al. 2018; Borrego et al. 2012; Micheluz et al. 2015). Unusual to this study was the instances of the teleomorphs of *Aspergillus* and *Alternaria* and the yeasts, which are rarely cultured from historic objects (Sterflinger 2010). Teleomorphs of *Penicillium* and *Cladosporium* were also isolated during the survey and from the surface of objects by swabs, indicating that they may be more common in UK heritage environments. *Talaromyces* (*Penicillium* teleomorph) have also been isolated and identified in archives, along with *actinomycetes* (Borrego et al. 2012). Other uncommon cultures found were *Embellisia abundans* and *Neonectria punicea.* Although in the case of *Embellisia*, a close relative of *Alternaria*, it has been isolated in air samples within a library (Micheluz et al. 2015)and was found on the beech wood paper in this study. *Neonectria punicea* has not been isolated from heritage materials and is a plant pathogen, specifically responsible for beech bark disease (Hirooka et al. 2013). As this species was isolated from the leather, it is unlikely that this is a colonising species of the material and was an airborne contaminant. Although, it was isolated from the indoor summer air samples at Claydon, Kenwood and Knole Houses so may be an opportunistic coloniser.

3.4.1.3 Dimensional colour change

The greatest changes observed across the materials was the darkening effect of *Cladosporium* on fibres. This has previously been observed on paper and textiles (Reis-Menezes et al. 2011) and this study confirms the dark pigmentation on all materials, with the exception of the linen. Although change in colour dimensions is not so not well documented, it is possible to determine colour change from published images in some cases. Other studies have found the darkening of papers with *Cladosporium sp*. and yellowing with *Aspergillus sp.* (Reis-Menezes et al. 2011; Pinzari et al. 2006). Research on linen show the same changes in colour dimensions, although they were not statistically significant in the case of the unbleached linen used in this work (Abdel-kareem 2010). The yellowing, reddening and darkening of cellulosic materials seems to be characteristic in the case of *Penicillium* and *Aspergillus* with the darkening effect of *Cladosporium.* As with total colour change, the greatest differences can be seen in the immediate locality of colonies. The ΔE of wool dyed with cochineal on mineral and enriched media showed that fungal species caused a lightening of the fabric (due to a reduction in dye intensity), in addition to staining around colony margins (Błyskal 2015). This effect of decolourisation was seen in the reduction of red colour in the leather samples.

Due to the intense pigment patterns of most fungi, it was not possible to determine background colour change in the material substrate. It could be possible that the yellowing and reddening observed in many materials is due to fibre degradation products, characteristically yellow/brown (Garside & Wyeth 2004a; Millington & Church 1997; Degano et al. 2011). However, as these are typically water soluble, it can be assumed that these were removed during the cleaning with 70% ethanol. Therefore, colour change is likely to be due to permanent pigment damage.

3.4.2 Confocal laser scanning fluorescence microscopy

There have been multiple published works on fungal growth on materials using microscopy, largely scanning electron microscopy (SEM) (Reis-Menezes et al. 2011; Pinzari et al. 2006; Kavkler et al. 2015; Błyskal 2015; Florian & Manning 2000; Naumann et al. 2005). Through these techniques, it has been possible to observe fungi on the surface of materials and penetrating through weave structures and pores in paper (Reis-Menezes et al. 2011). However, SEM and conventional microscopy cannot easily provide material cross sections in multiple planes and the ability to differentiate between live/dead fungal matter and material features. This study has shown that confocal laser scanning fluorescence microscopy can provide valuable information on fungal colonisation over more widely used techniques.

Fungi are said to utilise the cuticle of cellulosic fibres initially, prior to accessing the lumen through the secondary cell wall (Szostak-Kotowa 2004). This was clearly the case in cotton infected with *Aspergillus* as the aerial hyphae could be seen protruding through the cell wall of the fibres. It could also be seen through orthogonal cross sections that the FM4-64 stained fungi were present in the fibre lumens of cotton, linen, wood and paper fibres. Penetration of *Cladosporium* hyphae through pores in paper has been captured through SEM after 7 days incubation. As well as the extensive hyphal growth and pigmentation on and into the fibre structure of the papers, the cellulolytic fungi can also alter the surface texture (Reis-Menezes et al. 2011). This was observed after 8 weeks of incubation for the cotton and linen paper in this study. *Aspergillus* was found to grow and produce conidiophores on paper samples at 75% RH when inoculated with spore containing Sabouraud broth, although localised to the inoculation and smaller differences were noted to occur in linen/hemp fibres than the softwood papers (Pinzari et al. 2006). Although surface changes were found in this study, it took until week 4 of incubation with *Aspergillus* for the cotton and linen paper.

Fungi are reported to decrease the tensile properties of wool through proteolytic damage to the cortical cells (Szostak-Kotowa 2004). Damage to cuticle and penetration to the cortical cell layers could be seen through the FM4-64 fluorescence and in the case of *Aspergillus*, mature aerial hyphae growing through a crack in a fibre. The fungal degradation of silk is not well reported and although *Penicillium* and *Aspergillus* have been isolated from fibres, only *Aspergillus sp*. showed signs of fibroin degradation (Szostak-Kotowa 2004; Seves et al. 1998). Silk deteriorated through soil burial showed surface abrasions to fibres and breaks with a microbial surface covering, although the biofilm was predominantly bacterial (Seves et al. 1998). This study has shown the *Aspergillus*, *Cladosporium* and *Penicillium* are capable of extensive surface growth and penetration into the weave structure of silk, causing surface changes and defibrillation.

This study demonstrated the speed with which fungi can colonise complex substrates and reproduce when moisture is provided. *Aspergillus* in particular showed advanced growth on all materials, embedded within the structure and fibres and producing large aerial structures; a risk for cross contamination of objects if growth were to occur within a collection.

4. Chemical changes cause by fungal growth on organic materials

This chapter aims to assess the growth capabilities of common ascomycete fungi on organic materials and determine chemical changes that can be observed as a result. The following methods were intended to evaluate potential methods of depolymerisation, namely substrate specific enzyme production and the volatile/non-volatile organic compounds released during growth. The deterioration potential of the fungi were then applied to solid substrates and significant changes to the polymer substrates investigated through attenuated total reflectance Fourier transform infrared spectroscopy ATR-FTIR. This work will inform the assessment of fungal outbreaks on historic objects and may influence health and safety precautions and prioritisation of treatment in a heritage environment.

4.1 Introduction

In order to decompose complex polymers for simple nutritional carbon, nitrogen and other trace elements, fungi must be able to produce a range of depolymerase enzymes to diffuse into the environment surrounding the growing hyphal tips and catalyse the degradation of the substrate. There are typically a complex of enzymes acting together and there may be a need for more to be produced in order to digest specific materials. In addition to the exo-enzymes, there are membrane bound ones that represent the final stages of depolymerisation into the smallest absorbable components (Deacon 2006). During growth and substrate exploitation, fungi can also produce a wide range of secondary metabolic products in the form of pigments, antibiotics, organic acids, volatile organic compounds and mycotoxins. The production of these metabolites varies, depending on the nutrient availability, environmental conditions (pH, temperature) and water availability, as well as depending on the species of fungi and their interactions with other micro-organisms in the locality (Pasanen et al. 1997; Korpi et al. 2009) These compounds can have serious implications within a heritage context even after the growth of the fungi has ceased due to the acid/alkali catalysed decomposition of already weakened substrate, the potentially permanent visual distortion of objects through pigment staining and the production of dangerous volatile organic compounds and mycotoxins (Korpi et al. 2009; Szostak-Kotowa 2004; Sterflinger 2010).

The fungi to be tested will be grown on synthetic media designed to contain key components of heritage materials. The cellulosic materials will be largely analysed using plate assays to determine the enzyme production of each species on the (Pointing 1999; Hankin & Anagnostakis 1975). Enzyme activity will be assessed by colony and area of activity measurements with digital callipers and the creation of a relative enzyme activity index (Bradner, Gillings, et al. 1999). The plate assays will represent the capabilities of fungi to degrade various levels of the complex polymer and other constituents of the plant based fibres; cellulose, cellobiose, hemicellulose, pectin and lignin. These represents the major components of cellulosic fibres (Timar-Balazsy & Eastop 2007; Garside & Wyeth 2003). The specific endo1, 4-β-glucanase activity, responsible for long chain cellulose scission (Deacon 2006), was assessed using the extracellular supernatant method and measured spectrophotometrically.

Liquid protein solutions to represent the key proteins found within heritage collections; collagen, keratin and fibroin (Florian 2007b) will also be created for plate assays and extracellular supernatant analysis. Coomassie Blue (in the form of Bio-Rad Bradford reagent for supernatant analysis) will be used due to its binging to protein, but not small proteolytic products that would be released during enzyme digestion (Buroker-kilgore & Wang 1993).

The proteinaceous synthetic substrates were created from the materials used for the growth studies, with the fibres digested following the protocols of Aluigi *et al.* and Yamada *et al.* for wool and silk respectively (Aluigi et al. 2007; Yamada et al. 2001). Although the methods of protein extraction using cyanide based compounds (potassium cyanide for wool, lithium thiocyanate for silk) have been found to be the most effective for structural preservation (Goddard & Michaelis 1935; Hallett & Howell 2005), this was discounted due to health and safety concerns. Gelatin was used as a representative model for collagen (Florian 2007b).

The analysis of fungal metabolites using high performance liquid chromatography with mass spectrometry (HPLC-MS) has been used for distinguishing mycotoxins and substances harmful to human health (Haleem Khan & Mohan Karuppayil 2012; Korpi et al. 2009). This technique has also been utilised for the analysis of historic and archaeological textiles and their degradation products (Degano et al. 2011; France 2004). Through the separation of samples (HPLC) and subsequent ionisation (MS), samples can be separated according to retention time and then quantified and identified from the ion mass to charge ratio. During this work, a high-throughput, crude and non-destructive method for metabolite analysis is proposed and data analysis performed using the online metabolomics platform XC-MS (Smith et al. 2006; Tautenhahn et al. 2007) with specific peak analysis conducted using MZmine2 (Pluskal et al. 2010; Katajamaa et al. 2006).

There are numerous methods that have been employed to assess the chemical changes that occur to organic materials, much of the research relating to paper and textiles. FTIR, Ramen spectroscopy, HPLC, XFR, NMR and spectrodensitometry have all been used in order to determine the condition of cellulose and its crystalline structure (Zhao et al. 2007; Abdel-kareem & Morsy 2004; Park et al. 2009; Oh, Dong, et al. 2005; Kavkler & Demšar 2011; Menart et al. 2011).

ATR-FTIR has been employed widely for characterising chemical differences (Garside & Wyeth 2003; Zotti et al. 2008; Kavkler, Gunde-Cimerman, et al. 2011; Kavkler et al. 2015). This method uses infrared radiation to excite molecular vibrations within the chemical species of a material which will give a characteristic absorbance spectra (Garside & Wyeth 2006). The sample is pressed onto a crystal window and the IR beam, reflected through the crystal, produces an evanescent wave which probes the sample to a depth of a few micrometres (Richardson 2009; Garside & Wyeth 2006). One of the advantages over conventional FTIR is that materials can be measured whole, with minimal preparation and non-destructively so further analysis of samples is possible. The method is also highly reproducible. Other studies have successfully used this technique to monitor changes in materials due to fungal growth and to measure changes in the crystalline structure (Kavkler et al. 2015; Zotti et al. 2011). The functional groups represented by specific wavenumbers will then be identified from literature references (Garside & Wyeth 2003; Kavkler, Gunde-Cimerman, et al. 2011; Kavkler et al. 2015; Lammers et al. 2009; Colom et al. 2003; Proniewicz et al. 2001).

Although crystallinity can be far more accurately investigated using NMR, XRD and polarised ATR-FTIR (Oh, Dong, et al. 2005; Zhao et al. 2007; Garside & Wyeth 2006; Garside & Wyeth 2007), these methods are beyond the scope of this project. It has been demonstrated that crystallinity indices can be calculated from ATR-FTIR spectra using the peak height intensities of characterised functional groups (Oh, Dong, et al. 2005; Oh, Yoo, et al. 2005; Akerholm et al. 2004; Garside & Wyeth 2004b). This methodology was used in a study of biodegraded textiles (Kavkler, Gunde-Cimerman, et al. 2011).

4.2 Methods

The selection and preparation of organic substrates and inoculation techniques can be found in chapter 3.2. Due to limitations in the material available, it was not possible to use the natural biofilm to analyse the metabolic products or FTIR spectra of pine, oak and parchment.

4.2.1 Synthetic enzyme assays

The production of extracellular enzymes by the target species was assessed in relation to the cellulosic and proteinaceous fibre components that would be at risk in a heritage environment. Plate assays and extracellular supernatant analysis were conducted in order to screen for enzyme production and quantification of activity.

Prior to any assays, the target species (*P. brevicompactum, A, versicolor* & *C. cladosporiodes*) were sub-cultured and incubated for 10 days on basal minimal media (Pointing 1999). For the cellulosic assays, this consisted of 5g/l^{-1} ammonium tartrate, 1g/l^{-1} potassium phosphate, 0.5g/l^{-1} magnesium sulphate, 0.1g/l^{-1} yeast extract and 0.001g/l^{-1} calcium chloride in deionised water, supplemented with 0.4% w/v glucose and set with 1.6% w/v purified agar. The lignin assay was 1g/l^{-1} potassium phosphate, 0.5 g/l^{-1} ammonium tartrate, 0.5g/l^{-1} magnesium sulphate, 0.01g/l^{-1} calcium chloride, 0.01g/l^{-1} yeast extract, 0.001g/l^{-1} copper sulphate, 0.001g/l^{-1} iron (III) sulphate and 0.001g/l^{-1} manganese sulfate in deionised water, supplemented with 0.4% w/v glucose and set with 1.6% w/v purified agar. Protein assay cultures were grown on 5g/l^{-1} yeast extract, 1g/l^{-1} ammonium phosphate, 1g/l^{-1} potassium chloride and 0.5g/l^{-1} magnesium sulphate in deionised water, supplemented with 0.4% w/v glucose and set with 1.6% w/v purified agar. All media (plate and liquid culture) was sterilised by autoclave and transferred aseptically to growth vessels prior to inoculation.

Cellulosic substrates and the gelatin were all sourced in powdered form, the fibroin and keratin were generated from the woven fabrics used in other experimental stages using the following protocols. The keratin was obtained using the suphitolysis reaction (Aluigi et al. 2007). Solvent extraction and cleaning with petroleum ether was not used in this case as the wool was treated during the weaving process. The fabric was washed in distilled water and dried before cutting into sections of no more than 3 warps by wefts. This was left in ambient conditions for 24 hours prior to weighing 5g to add to a 100ml solution of 8M urea and 0.5M m-bisulphite adjusted to pH 6.5 with sodium hydroxide. This was shaken at 65°C for 2 hours until a thick liquid was produced. This was dialysed against distilled water in cellulose Visking dialysis tube (1200-1400 molecular weight cut off) for 3 days under ambient conditions. The resulting milky solution was filtered and stored at -20°C and left to equilibrate for 24 hour prior to use. Fibroin was collected using the Ajisawa method (Yamada et al. 2001). Silk was washed in deionised water, dried and then cut into pieces no more than 5 warps by wefts. This was then weighed and added to 15 times w/v Ajisawa reagent (CaCl$_2$/ethanol/water, 11/92/144 in weight) to the amount of silk.

This was stirred at 75°C until a clear liquid was formed. This was then dialysed and stored using the same method as for keratin.

4.2.1.1 Plate assays

Plate assays for specific target substrates were prepared in triplicate and inoculates with 8mm fungal cores extracted from the outer boarders of the colony, after incubation on minimal media. All inoculation was conducted within a class II laminar flow hood with inverted plates to reduce the spread of any dry spores and create clear colony and enzyme activity margins. Plates were then sealed with Parafilm and incubated at 20°C for up to 1 week, taking care to ensure that movement/spore disturbance was kept to a minimum. All incubation, unless otherwise stated, was conducted at 20°C to represent the average annual indoor temperature of properties (extreme outliers removed).

Pectin plate assays were prepared using a liquid growth culture well test developed with hydrochloric acid, a positive result being a clear halo around the outside of the wells (Souza et al. 2003). The growth media containing 0.09% dipotassium phosphate, 0.1% ammonium sulphate, 0.01% magnesium sulphate, 0.1% yeast extract and 0.5% citric pectin. Flasks with 50ml of media were inoculated with approximately 10^4 (determined by haemocytometer) spores from the minimal media growth plate after rinsing with saline solution (0.9% NaCl, 0.01% Tween 80 in deionised water). Flasks were shaken at 100rpm, 20°C for 7 days. Post incubation, the culture was centrifuged and the liquid supernatant used to determine pectinase production. Plates were created with 1% pectin and 1.8% bacteriological agar buffered with sodium acetate (0.1M) to pH5. This agar was poured to a depth of 4mm and once set, 5 equidistant wells were created aseptically using a 5mm borer. The growth supernatant (100µl) was placed into the well and the plates sealed and incubated for 2 days at 37°C before zones of activity were assessed.

The Lignin plate assay used the same basal medium as previously detailed with a 20% glucose solution sterilised separately and 1ml of this introduced for every 100ml of media made. Petri dishes were filled to a depth of 5mm ad once set, inoculated with the target fungi. Plates were incubated for 7 days at 20°C prior to cutting 5mm diameter wells around the colony boarder. Wells were filled with 0.1% w/v ABTS (for laccase activity) and 0.1% w/v ABTS with 0.5% hydrogen peroxide (for lignin peroxidase activity) with 1 well serving as a control, filled with ethanol. Activity was assessed after 30 minutes by colour development.

The hemicellulose plate assay was conducted using a xylan derived from birch and the target fungi were grown on cellulose basal minimal media. The assay growth media is that of the celluloase minimal media with glucose substituted for 4% w/v xylan. Post sterilisation the plates

were poured aseptically whilst agitating to ensure a homogeneous distribution of the xylan. Plates were then inoculated with the target fungi and incubated for 7 days at 20°C. The plates were then flooded with iodine and left to develop for 5 minutes, before the stain was poured off. After de-staining with deionised water, a positive result for endoxylanase and β-xylosidase would be a pale yellow halo extending from the colony boarder with the rest of the agar, containing un-degraded xylan, being a dark blue/purple colour.

Long chain cellulose degradation was screened in the form of carboxymethyl cellulose (CMC) assays for 1,4-βendoglucanase and β-glucosidase. Short chain cellobiose cleavage was assessed using esculin (6,7-dihydroxycoumarin 6-glucoside) containing plates to determine β-glucosidase and cellobiohydrolase activity. Fungi were inoculated from cellulose minimal media plates.

The CMC plates are prepared by substituting the glucose for 2% w/v CMC in the cellulose basal minimal media. The powdered CMC was added to the liquid media slowly whilst stirring and over gentle heat to produce a homogenous solution. Plates were subsequently inoculated with the test fungi and incubated for 7 days at 20°C. After this time the plates were flooded with 2% w/v congo red and developed for 15minutes before being rinsed with deionised water. The plates were then de-stained using 1M sodium chloride for 15 minutes. Enzyme activity was measured as a pale halo around the colony boarder with the un-degraded CMC remaining a deep red colour. The cellobiose plates were prepared as for the cellulose basal minimal media but substituting the glucose with 0.5% w/v esculin along with a 2% w/v ferric sulphate solution in deionised water. Post sterilisation, 1ml ferric sulphate should be aseptically added for each 100ml of media prepared and plates poured to 5mm. In addition to plates inoculated with the target fungi, clear control plates should also be incubated to monitor any colour development. Plates were measured every 2 days over 14 days and the regions of activity (a dark red/black halo where β-glucosidase has been produced) and colony diameter were recorded using digital callipers. The coloured product is produced when the glucose and a coumarin product, formed by depolymerisation, react with the iron sulphate.

The three protein assays were prepared in the same way with either collagen (gelatin), fibroin or keratin added in as the protein substrate. The media was prepared using the protein basal minimal media with 1% w/v or v/v of target protein added pre sterilisation for the gelatin and post for the keratin and fibroin solutions, along with 0.1% Coomassie blue dye. The prepared plates were inoculated and incubated for 14 days at 20°C with measurements taken every 2 days. The area of enzyme activity was considered to be where the Coomassie blue dye was removed.

4.2.1.2 Extracellular enzyme supernatant analysis

The cellulose degradation potential of the target fungi was assessed using a liquid culture method to analyse the supernatant for the micromoles of glucose released per minute and converting this to a specific activity (Duncan et al. 2008; Duncan et al. 2006). Cellulose minimal media cultures were flooded and the collected spores rinsed with saline (0.9% sodium chloride, 0.01% Tween 80 in deionised water). The following reactions were repeated in triplicate for each of the 3 target fungi. The spore suspensions were then diluted to approximately 10^5 with distilled water and added to 50ml of a liquid media containing 1% ball milled cellulose, 1.5% soya bean flour, 1.5% dipotassium phosphate, 0.5% ammonium sulphate, 0.006% calcium chloride, 0.006% magnesium sulphate and 0.02% Tween 80 in a 250ml flask. This culture was shaken for 7 days at 20°C, 150rpm. The resulting suspension was centrifuged (4000rpm for 10 minutes) to separate the liquid supernatant, which was removed. A substrate solution of 1% hydroxyethyl cellulose in 0.05M citrate buffer (0.05M citric acid and 0.05M sodium citrate) at pH4.8 was prepared, 480µl of which was added to 320µl of the growth supernatant. This was incubated for 10 minutes at 50°C, the optimal temperature for enzyme activity (Duncan et al. 2008). The reaction was stopped with 1.2ml of 1% dinitrosalicylic acid, 1.6% sodium hydroxide and 30% Rochelle salts in deionised water (the salts were added slowly with continuous stirring and the solution filtered before use) and incubated at 100°C for 5 minutes. A control was also prepared in which the supernatant was added at the stop stage (100°C for 5 minutes). The absorbance of the samples was measured spectrophotometrically at 540nm, along with a standard curve created with serial dilutions of glucose. The total protein content of the supernatant was measured at 595nm using the Bradford assay and a bovine serum albumen (BSA) standard. The micromoles of glucose released per minute were calculated using the glucose standard absorbance with the polynomial fit function in Excel. The protein content was calculated in the same way and the specific enzyme activity was expressed as micromoles of glucose per minute divided by the supernatant protein content.

The proteolytic activity analysis was developed from colorimetric assays for measuring protease activity (Buroker-kilgore & Wang 1993). The growth media was prepared using 50ml of the protein basal minimal media, without the agar, placed in 250ml flasks. Cells were harvested, rinsed and added as previously described, prior to incubation for 7 days at 20°C and 150rpm. The growth supernatant was centrifuged to remove cell debris and 2% target protein was added to 500µl prior to incubation for 30 minutes at 25°C and then stored on ice. The reaction was made up to 1000µl with deionised water and 100µl added to 100µl of Bio-Rad Bradford reagent with 50µl of water. After mixing, the colour was developed for 10 minutes before reading the

absorbance spectrophotometrically at 595nm. Controls were created where the protein was added at the post incubation stage. Reactions were performed in triplicate and expressed at micrograms of protein per millilitre, calculated from a BSA standard curve. Protease activity was recorded as the percentage difference in protein content between the control and reaction sample.

4.2.2 High performance liquid chromatography with mass spectrometry

The necessary post growth sterilisation and cleaning of the organic materials afforded the opportunity to create non-invasive, crude solvent extracts that could be used for metabolite analysis. HPLC-MS was used to separate the isolated compounds and produce total ion chromatograms for quantification. All solvents used were HPLC/analytical grade. The ethanol extracts generated during sterilisation were sealed and stored at 4°C until required.

Vacuum evaporation (3 hours at 30°C) was used to drive off the ethanol and the resulting products were re-suspended in 1ml of methanol by vortex. These stock solutions were filtered and stored at -20°C. For each run, Agilent screw top vials with septum lids for auto-sampling were used with 300µl of sample. HPLC was performed using an Agilent 1100 series fitted with an Ace®3µm Phenyl 100 x 2.1 mm semi-micro column. This was flushed and cleaned prior to each use with methanol and the injector system cleaned with deionised water between each sample. A flow rate of 0.2ml/min of 55% methanol and 45% water was used for the mobile phase. The Mass Spectrometer used was a Bruker Daltonics Esquire 3000, ESI-Ion Trap running in positive ion detection between 50-1500 m/z over a 40 minute retention time. Between each sample run, a short negative ion programme was run with methanol to clean the system. Both machines were operated using the Bruker Daltonics Esquire 5 programmes (MS) including Agilent Chemstation A.08.03 (HPLC) and Bruker DataAnalysis 3 (chromatogram and spectral analysis). The Bruker .YEP output files were converted to .MZXML format using MSConvert (ProteoWizard 3.0.9490). This enabled chromatogram analysis to be performed using XC-MS 3.5.1 (https://www.xcmsonline.scripps.edu) with multi-group settings and multivariate statistical analysis. Tentative feature matching was performed with pathway analysis. Specific peaks were also interrogated using MZmine 2.23 which also allowed for spectral manipulation and approximate analyte identity searches through online database catalogues. Controls of raw materials were prepared and novel metabolic compounds were considered to be peaks which were not detected within control chromatograms. Statistical significance of multivariate analysis was set to *p=0.05* to detect influential compounds produced by fungi on each material. Novel

compounds and their tentative matches were compared to published literature and the Reaxys database (https://www.reaxys.com) for identity confirmation.

4.2.3 ATR-FTIR

Samples were measured using a Bruker ALPHA Platinum ATR with single reflection diamond crystal. A scan range between 4000-400cm-1 was used with a resolution of 4cm-1. An accumulated average of 32 scans was used (Garside & Wyeth 2003). The samples were prepared so that they could be measured in the same orientation and position as the spectrodensitometer measurements. The samples were positioned centrally over the crystal window ensuring that the growth surface was faced down. The first reading was taken 5mm from the top of the sample and the subsequent two readings were taken 5mm further down the sample in the warp direction (top to bottom in the case of the paper, leather, parchment and wood). Background calibration was conducted between each set of strips from different fungal conditions and the crystal surface cleaned with 80% isopropyl alcohol. The position of the mallet was checked and adjusted prior to the each set of different materials to ensure that an even pressure was applied to each sample set. All readings were taken under ambient conditions but the relative humidity and temperature of the lab was recorded in case of anomalies. Any peak changes in the region of 2400-2300cm^{-1} were discounted from analysis as this region corresponds to carbon dioxide which can be influenced by the surroundings.

The recorded spectra were base line corrected in the Bruker OPUS spectroscopy software with the spectral averaging and peak height analysis conducted in GRAMS/AI. Statistical analysis was performed using The Unscrambler X and IBM SPSS statistics. Specifically, standard normal variate and principle components analysis were performed in order to normalise and reduce the data, identify sources of variation and make analysis of regions of change more achievable (Hori & Sugiyama 2003). The inoculated strips were treated as the population and the spectral peak height intensities recorded between 4000-400cm^{-1} were taken to be the characteristic variables in this case. The data was mean square centred and the number of principle components calculated was determined from initial scree plots of the data.

Crystallinity indices were also calculated using the characterised bands that are assigned to crystalline and amorphous regions of cellulosic materials. The wavenumbers chosen for the study of cellulosic materials were 1370cm^{-1}/2900cm^{-1} and 1430cm-1/897cm^{-1} (Kavkler, Gunde-Cimerman, et al. 2011; Garside & Wyeth 2004b) and 1505cm^{-1}/1375cm^{-1} for lignin (Fackler et al. 2007). Fibroin was represented by the ratio between the β and α protein conformation 1615/1655cm^{-1} (M. A. Koperska et al. 2015).

4.3 Results

The results of the potential chemical changes caused by fungal growth on organic materials, determined by synthetic enzyme assay, high performance liquid chromatography with mass spectrometry (HPLC-MS) and attenuated total reflectance Fourier transform infrared (ATR-FTIR) spectroscopy investigations, are recorded below and organised by technique, then material.

4.3.1 Synthetic enzyme assays

Plate and liquid media assays were conducted using different substrates, in order to determine the degradative capability of *A. versicolor*, *C. cladosporiodes* and *P. brevicompactum*. The relative enzyme activity was determined from the ratio of the mean colony and decolourised agar diameter and the specific endoglucanase activity.

4.3.1.1 Cellulosic substrate plate assays

A cellulose substrate, carboxymethyl cellulose (CMC) was used to indicate long chain depolymerisation, with the area of activity indicated by an area of agar remaining unstained by Congo Red. Figure 4.1 shows the activity of the fungi on this media after 6 days of incubation, staining and decolourisation. *Penicillium* showed the greatest enzyme activity, followed by *Aspergillus* and then the *Cladosporium*. However, in terms of colony size, the *Aspergillus*, had greater activity as the mean colony diameter was 43% less than that of the *Penicillium*. All of the fungi had a relative enzyme activity lower than 1.
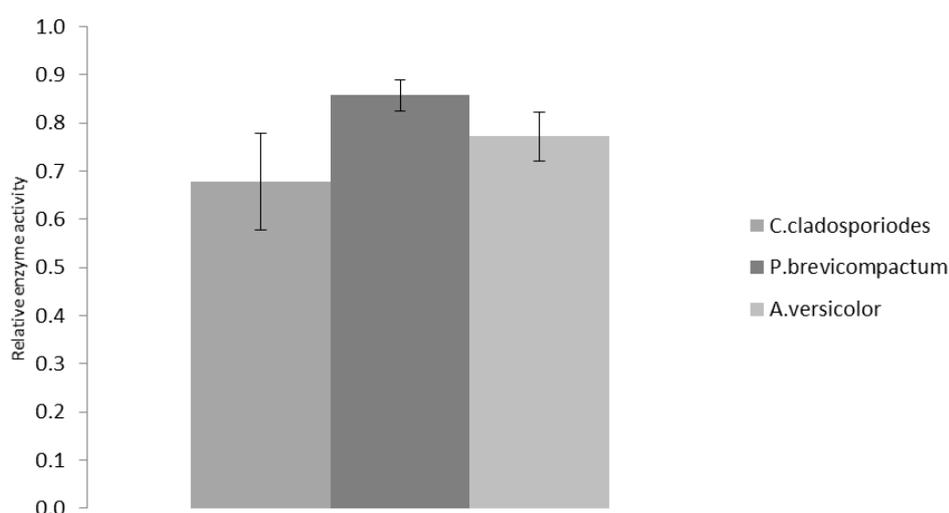
Figure 4.1- The mean relative enzyme activities of C. cladosporiodes*, P. brevicompactum and* A. versicolor *grown on a CMC agar medium for 6 days at 20°C. The level of activity was determined through a Congo Red stain post incubation. Error bars: SD*

The ability of the fungi to degrade shorter chain cellulose substrates was determined using an esculin assay, to look at the β-glucosidase production of fungi. As glucoside is hydrolysed, a coumarin product is released, creating a dark brown/ black halo in the area of hydrolytic activity (Figure 4.2A). Over the 10 days of incubation the diameter of the coumarin was measured until the outer perimeter of the Petri dish was reached by one of the *Penicillium* colonies. All of the fungal species showed a higher level of activity on the shorter polymer structure of the cellobiose (Figure 4.3) than on the longer chain cellulose (CMC) assay with a relative enzyme activity index greater than 1 after only 2 days of incubation.
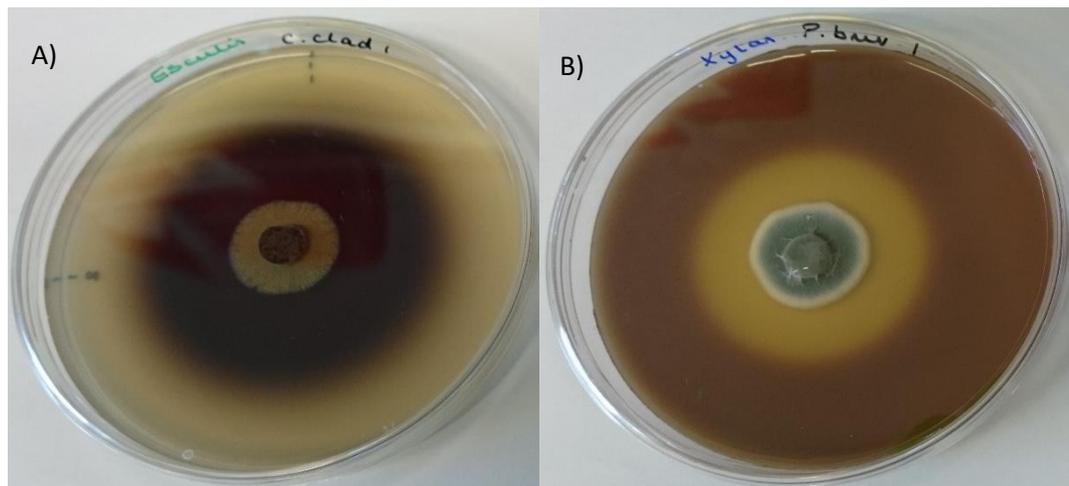
Figure 4.3- A) Cladosporium *enzyme assay plate showing the potential hydrolytic activity of the species on a short chain cellulose (cellobiose) substrate. As the esculin substrate in the agar is degraded, a coumarin product is released, leaving a dark stain to the agar where hydrolysis had occurred. B)* Penicillium *enzyme assay plate showing the potential hydrolytic activity on a hemicellulose (xylan) substrate. Areas of hydrolytic degradation around the colony boarder are not stained by iodine.*
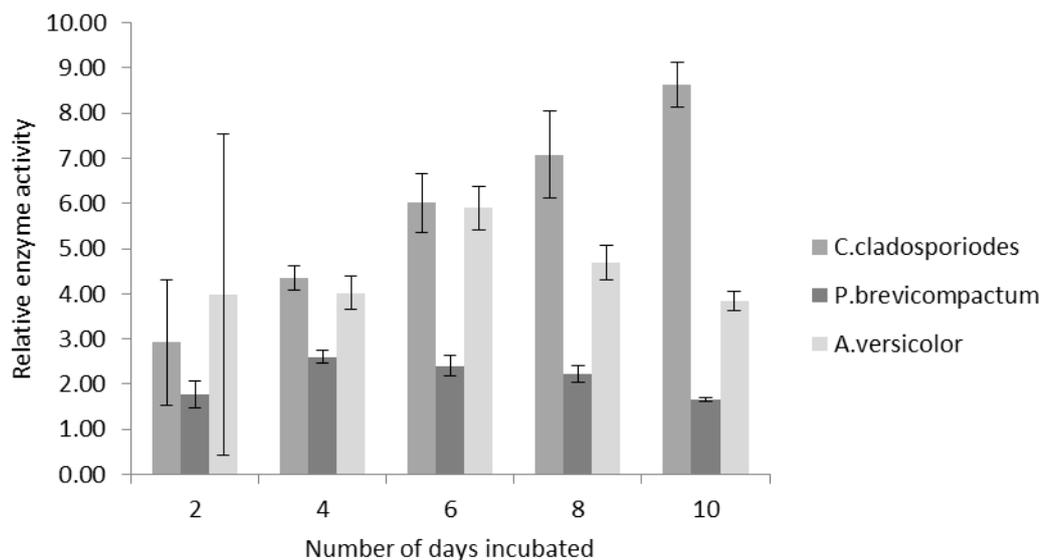
Figure 4.2- The mean relative enzyme activities of C. cladosporiodes, P. brevicompactum *and* A. versicolor *grown on an esculin agar medium for 6 days at 20°C. The level of activity was determined through the agar being naturally stained with a coumarin product as the result of esculin hydrolytic degradation. Error bars: SD*

Over the 10 days, *Cladosporium* showed the greatest capacity to hydrolyse short chain cellulose like molecules. The *Aspergillus* showed the greatest initial activity which increased until peak activity was recorded on day 6 and a decrease recorded thereafter. The *Penicillium* showed the lowest activity, although this was still higher than the CMC assay, with activity peaking after 4 days of incubation. The high standard deviation seen during the first 2 days incubation was due to the uneven growth rates of the repeat core plugs, but this effect was lessened over time.

The capacity to utilise another constituent of cellulosic fibres, hemicellulose, was assessed using a solid media assay with a xylan substrate. The fungal plugs were incubated for 6 days on the xylan plates, prior to staining with iodine and de-staining. The area of enzyme activity was then measured as the halo of agar around the colony perimeter, not stained by the iodine (Figure 4.2B). *Aspergillus* had the greatest capacity to utilise hemicellulose (Figure 4.4), with repeat cultures showing similar levels of activity. The *Penicillium* had a relative enzyme activity over 2 in all cases and although colonies remained small, the area of activity expanded far beyond the colony margins (Figure 4.2B). *Cladosporium* showed the least consistent enzyme activity on a hemicellulose substrate.
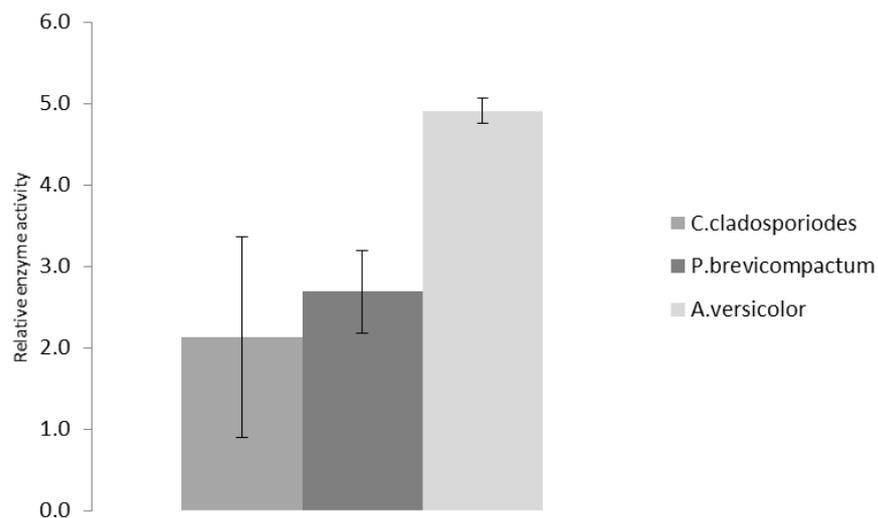
Figure 4.4- The mean relative enzyme activities of C. cladosporiodes*,* P. brevicompactum *and* A. versicolor *grown on a xylan agar medium for 6 days at 20°C. The level of activity was determined through an iodine stain post incubation. Error bars: SD*

Assays to assess the degradation potential of the fungi on a lignin and pectin substrate were performed using liquid substrate cultures and well plate tests and a solid media plate in the case of lignin. Over the 7 day incubation, none of the fungal cultures produced enough enzymes in the supernatant as to be effectively measured by the well tests. Despite the lack of recordable enzyme activity, the fungi all grew in the broths and the dry weight of the colonies increased approximately 300% for the *Aspergillus* and *Penicillium* and 200% for *Cladosporium* with a lignin

substrate. The dry weight biomass of the pectin cultures was less, but there was still an increase in weight of between 6% (*Penicillium*) and 19% (*Aspergillus*). Lignin substrate plate assays also did not record any enzyme activity either, but the growth of the colonies could be more closely observed. The hyphae were very fine and widely spaced, rather than the typical dense lawns. There was also no evidence of sporulation, even after two weeks of incubation.

4.3.1.2 Cellulosic substrate extracellular enzyme supernatant assay

A liquid media assay was performed to quantify the change in cellulose levels spectrophotometrically. Figure 4.5 shows that in a liquid ball-milled cellulose culture (not limited by water availability, surface area, colony diameter and toxic metabolic products) the fungi are able to exhibit high levels of specific endoglucanase activity; expressed as the amount of glucose (µM) produced per minute per ml in relation to the weight of soluble protein in the supernatant. *A. versicolor* had a higher rate of specific endoglucanase activity meaning a greater ability to scission long chain cellulose when not inhibited by the growth restrictions of a cellulose media plate. The *P. brevicompactum* showed a only 0.1 difference in activity from the cellulose plate assay but the *C. cladosporiodes* activity increased, however repeats still showed higher variability than the other species.
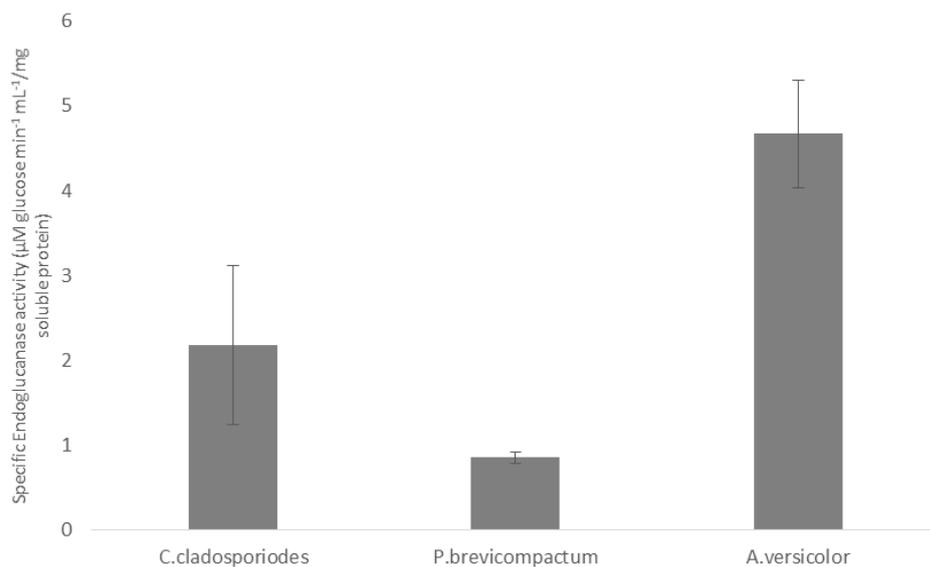
Figure 4.5- The mean specific endoglucanase activity of Cladosporium, Penicillium *and* Aspergillus *as expressed by the amount of glucose (µM) per minute/soluble protein (mg). Error bars: SD*

4.3.1.3 Proteinaceous substrate plate assays

Plate assays were conducted, using digested silk and wool suspensions and gelatin as nutritional sources, stained with Coomassie Blue in order to determine the specific protease production capabilities. The relative enzyme activity was determined by the same method described in 4.3.1.1. Figure 4.6 shows one of the silk and *Aspergillus* assay plates before and after illumination to visualise the decolourised zone.
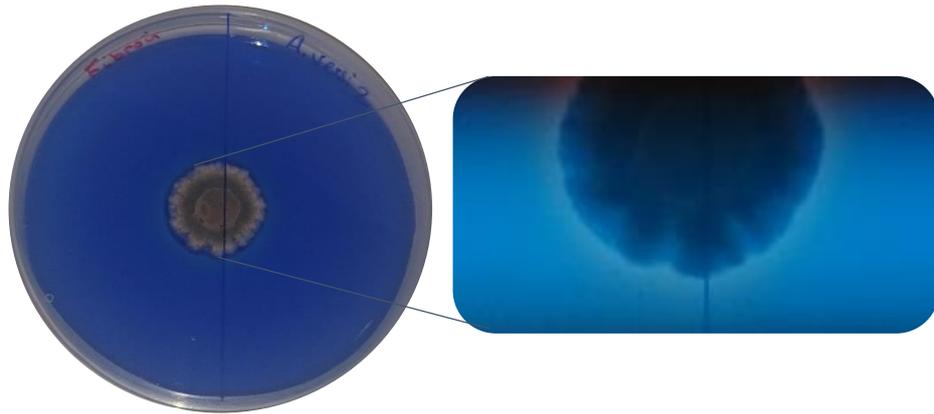
Figure 4.6- Silk assay plate stained with Coomassie Blue for the detection of enzyme activity. The colony of Aspergillus versicolour *is shown before and after illumination, for the visualisation of the zone of decolourisation. The relative enzyme activity of plates was determined from the ration of the colony diameter and halo of activity after incubation at 20°C*

The activity of each species is recorded in Figure 4.7. All species show a lower relative enzyme activity than seen for the cellulosic substrates and a greater degree of variability between samples. The *Aspergillus versicolor* showed the greatest digestion of protein, despite having the
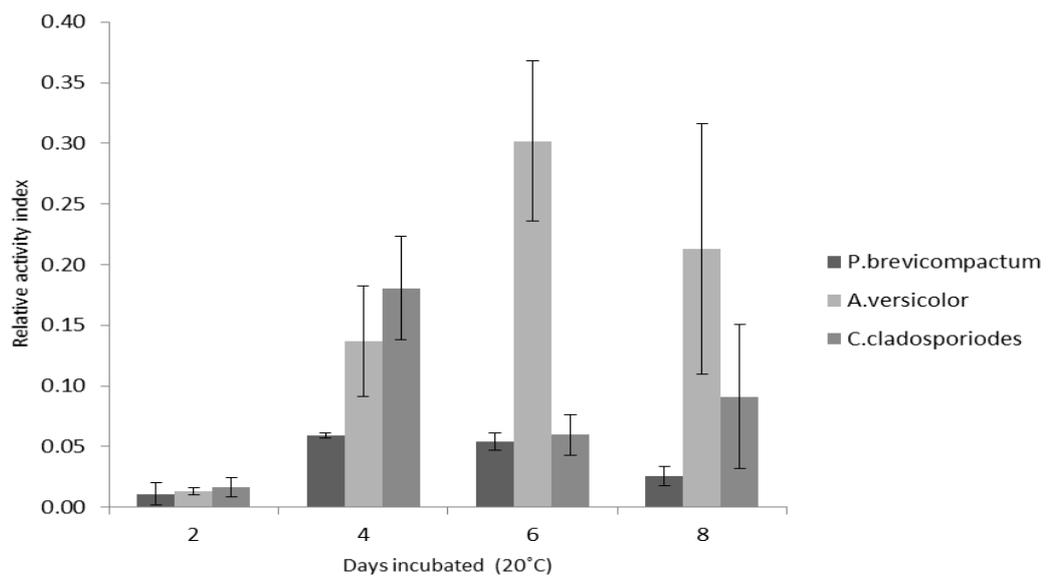
Figure 4.7- The mean relative enzyme activities of C. cladosporiodes, P. brevicompactum and A. versicolor grown on silk agar medium with Coomassie blue. Error bars: SD

smallest mean colony diameter (19mm). *Cladosporium* did not depolymerise protein as effectively as *Aspergillus*, but had a larger mean colony diameter, 45mm. The *Penicillium* showed very little enzyme activity, however had the largest colony growth with an average final diameter of 48mm.

The relative enzyme activity of the fungi on solid keratin media is lower than that of silk (Figure 4.8). *Cladosporium* and *Aspergillus* again show a greater degree of activity than *Penicillium,* but the *Aspergillus* is again showing the larges zone of activity around the smallest colonies (22mm compared to 40 & 42mm). There was also a great degree of variation between the repeat plates, as can be seen by the standard deviation bars in.
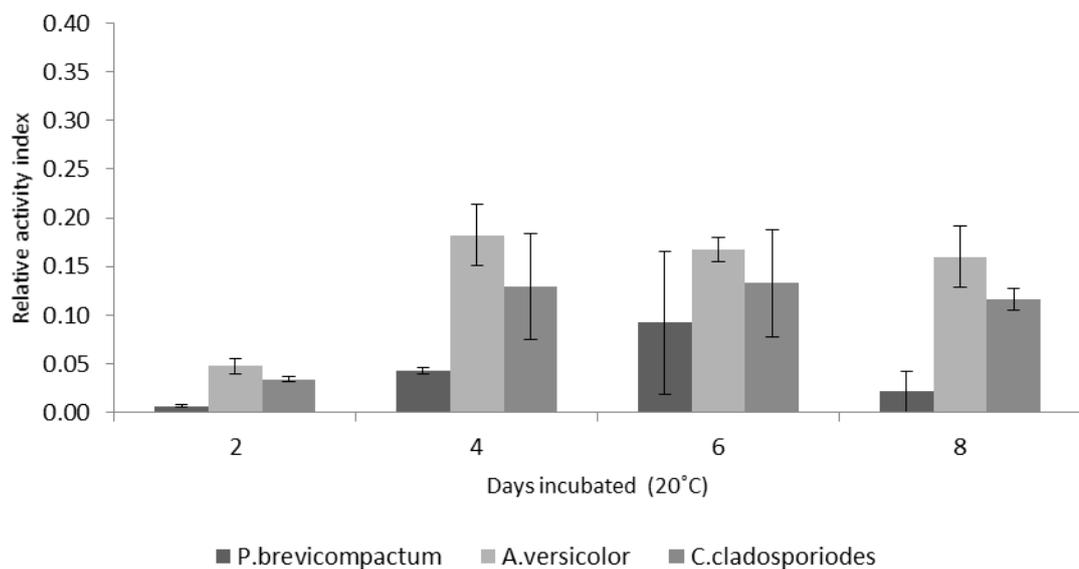
Figure 4.8- The mean relative enzyme activities of C. cladosporiodes, P. brevicompactum *and* A. versicolor *grown on keratin agar medium with Coomassie blue. Error bars: SD*

Figure 4.9 demonstrates the activity of fungi on a digested collagen substrate (gelatine). The relative enzyme activity of all fungi is again far lower than that of the cellulose assays. The *Cladosporium* was better able to grow and use this substrate with less variation between cultures although the mean colony diameter was lower than the other protein substrates at 36mm. The *Aspergillus* cultures were again smaller than the other two species, but were more irregular in shape and larger than those previously observed on silk and wool plates (30mm). On the gelatine plate, *Penicillium* had the largest colonies seen on any of the proteinaceous assays with a mean diameter of 60mm but with a mean enzyme activity of 0.08.
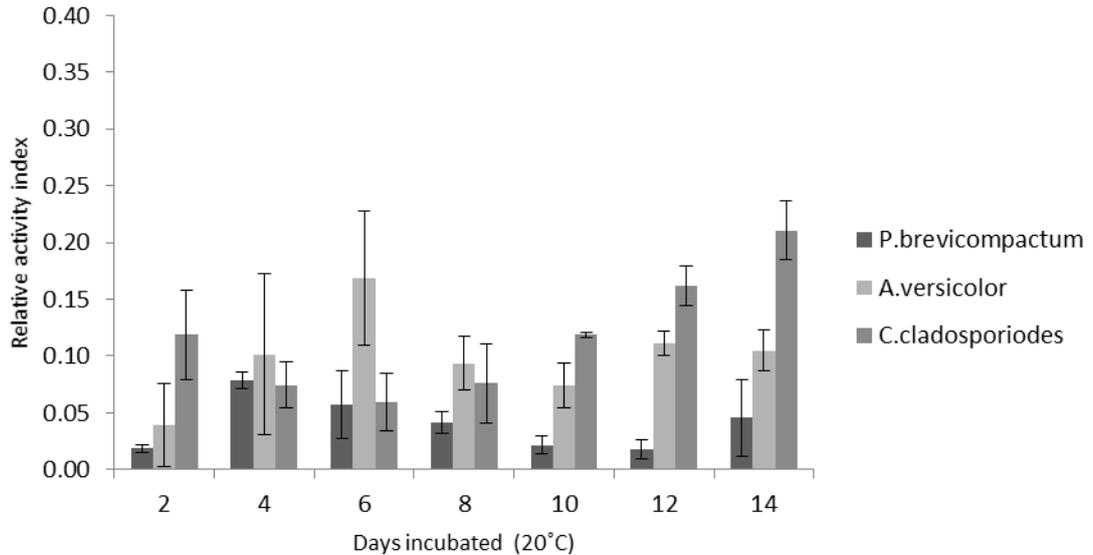
Figure 4.9- The mean relative enzyme activities of C. cladosporiodes, P. brevicompactum *and* A. versicolor *grown on gelatine agar medium with Coomassie blue. Error bars: SD*

4.3.1.4 Proteinaceous substrate extracellular enzyme supernatant assay

Liquid media assays were performed to quantify the change in protein levels spectrophotometrically. Figure 4.10 shows that in liquid culture, not limited by water availability, surface area and colony diameter, the fungi are able to reduce the protein content of silk.
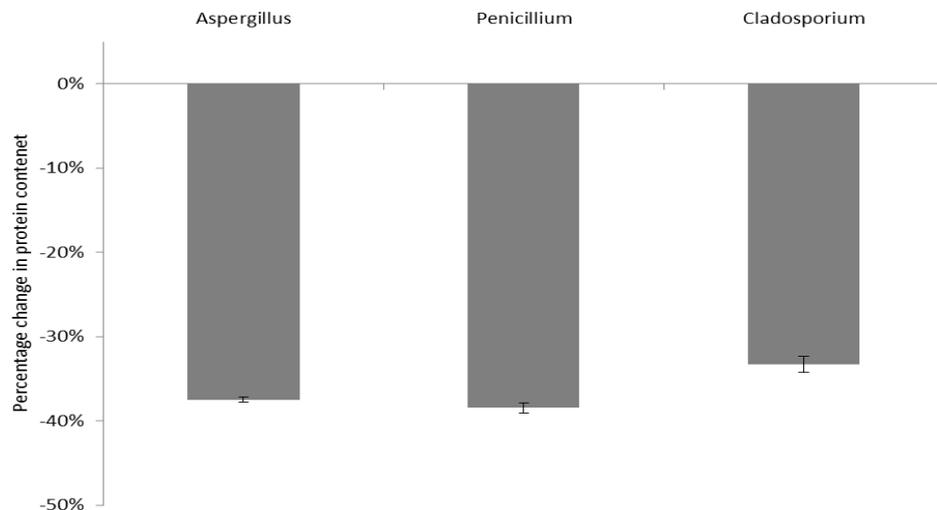
Figure 4.10- The change in silk protein content of a liquid shaken broth culture incoluated with Aspergillus, Penicillium *and* Cladosporium *spore suspensions, prior to incubation at 20°C for 7 days. The protein content was determined by spectrophotomety at 595nm, using the Bradford assay. Error bars: SD*

The assay is sensitive to large chain protein structures, rather than short peptide features, so the result can be viewed as a measure of depolymerisation of the fibroin protein. The closely related *Penicillium* and *Aspergillus* were able to hydrolyse 38% and 37% of the protein

respectively with *Cladosporium* clearing 33%. Fibroin was by far the most easily accessible protein for all three species. The fungi were also able to reduce the protein content of wool, but there is minimal difference between the species ability to depolymerise the keratin protein (Figure 4.11). All three species showed a reduction in protein content in the order of 10% over the 7 days of incubation.
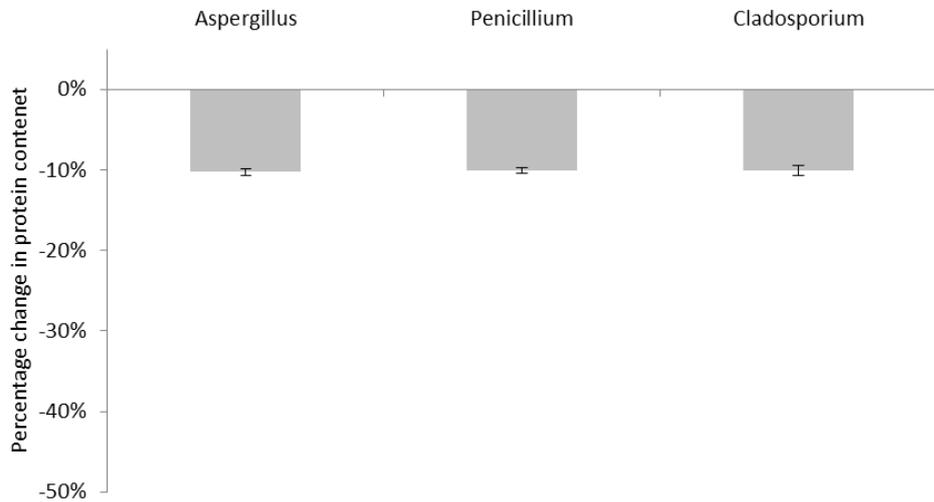
Figure 4.11- The change in wool protein content of a liquid shaken broth culture incoluated with Aspergillus, Penicillium *and* Cladosporium *spore suspensions, prior to incubation at 20°C for 7 days. The protein content was determined by spectrophotomety at 595nm, using the Bradford assay. Error bars: SD*

The protein content of the collagen substrate plate (gelatine) was reduced by 46% by *Penicillium*, the greatest change observed by any of the fungi on proteinaceous plates (Figure 4.12). The *Aspergillus* biomass increased in the liquid gelatine media, but had a minimal effect on the protein content. The *Cladosporium* had a mean protein reduction of 10%, but there was a high degree of variation between repeats.
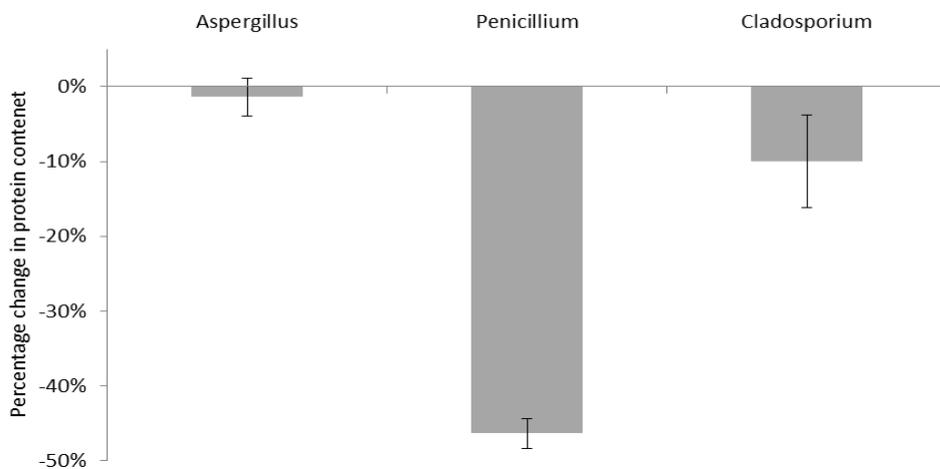
Figure 4.12- The change in gelatine protein content of a liquid shaken broth culture incoluated with Aspergillus, Penicillium *and* Cladosporium *spore suspensions, prior to incubation at 20°C for 7 days. The protein content was determined by spectrophotomety at 595nm, using the Bradford assay. Error bars: SD*

4.3.2 HLPC-MS

In addition to assessing the enzyme capabilities of the fungal species, the secondary metabolic products from incubation on the material were also monitored using crude solvent extraction and HPLC-MS. The resulting chromatograms were high throughput analysed using XC-MS and the significant compounds identified using METLIN. For the purposes of this study only the general chemical taxonomy and classifications of pigments, aromatics and toxins for the ten most significant compounds will be reported. Mass spectra and tables of significant compounds can be found in Appendices-Chapter 4.

4.3.2.1 Metabolic products of fungi on cotton

Figure 4.13 shows the number of significant compounds (*p=0.01*) detected in the extracts from cotton incubated with fungi. Over the 12 weeks of incubation the natural biofilm produced the greatest number of significant compounds, followed by the *Cladosporium*, *Penicillium* and then the *Aspergillus*. Chromatograms and
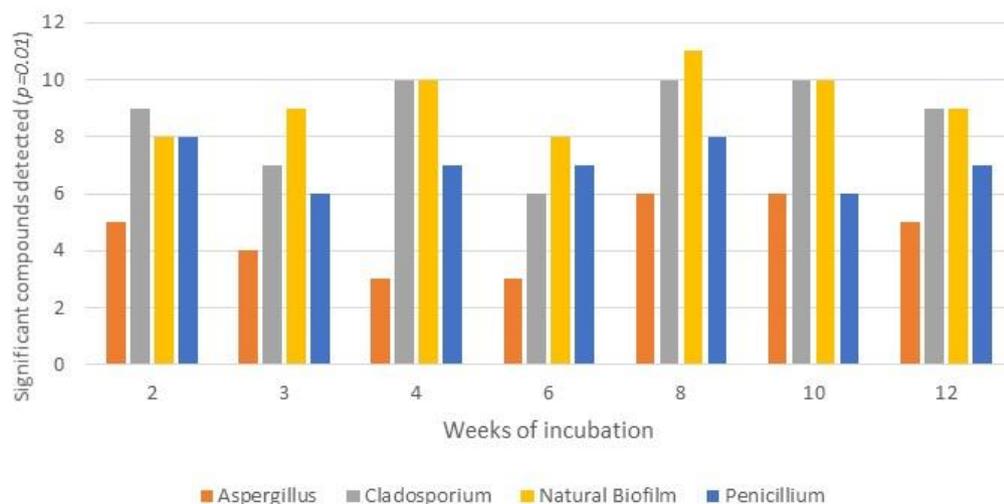
Figure 4.13- The number of significant (p=0.01) features detected from high throughput analysis of HPLC-MS spectra by XC-MS. Spectra were produced from solvent extraction of inoculated woven cotton after timed incubation at 20°C with Aspergillus*,* Cladosporium*,* Penicillium *and the natural biofilm found on the cotton.*

The *Aspergillus*, with the fewest number of different compounds, produced some of the most volatile with: a flavonoid (pigment), two organoheterocyclic compounds (a triazine & an azaspirodecane derivative), an organonitrogen compound, aminoglycoside (presumed toxic) and a benzoic acid ester. The *Cladosporium* produced similarly volatile compounds with further organic acid derivatives and lipid like molecules. The ten compounds recorded were: an alkanolamine, an oligosaccharide, a triazine (presumed toxic), a benzene substitute/derivative, a carboxylic acid derivative, an oligopeptide, a glycoside, fatty acyls and a tetraterpene.

147

The natural biofilm again produced more lipid based and acidic compounds. The significant eleven detected included: a glycerophospholipid, fatty acid ester, a fatty acyl, an oxepane, oligopeptides, oligosaccharide, a thioester, an anthocyanidin (pigment), a triterpene saponin (aromatic) and an azonaphthalene (pigment). The *Penicillium*, similar to the *Aspergillus* produced fewer, but more potentially volatile compounds. Of the eight significant ones recorded, there was: a galloyl ester, an indole/derivative (aromatic), a flavone/flavonol (pigment), a prenol lipid, a pyrazine (aromatic), a phenol ether, an oligosaccharide (presumed toxic) and a sterol.

4.3.2.2 The metabolic products of fungi on linen

Figure 4.14 shows the number of significant compounds (*p=0.01*) detected that were not found in the control linen extract. Over the 12 weeks of incubation the *Penicillium* and *Cladosporium* produced the most compounds, followed by the *Aspergillus* and then the natural biofilm.
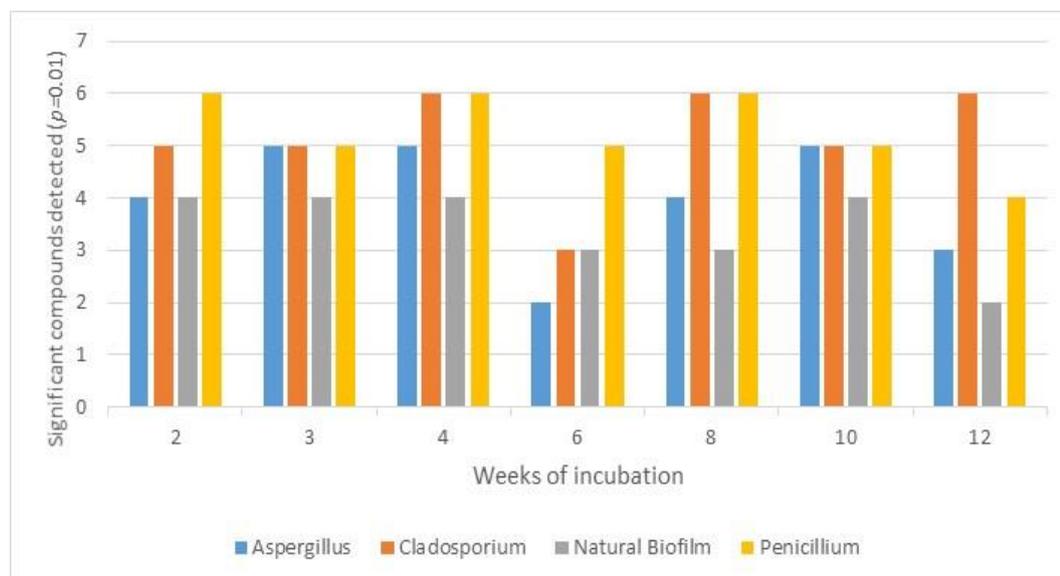
Figure 4.14- The number of significant (p=0.01) features detected from high throughput analysis of HPLC-MS spectra by XC-MS. Spectra were produced from solvent extraction of inoculated woven linen after timed incubation at 20°C with Aspergillus*,* Cladosporium*,* Penicillium *and the natural biofilm found on the linen.*

The *Aspergillus* samples only produced 5 significant compounds over the incubation time and that were not present in the control linen. These included some potential toxins and an aromatic compound: a quinoline/derivative, a phosphosphingolipid, a benzoic acid ester, a sterol and an oligopeptide. The *Cladosporium* only produced 6 significant compounds when grown on the linen. These included more pigmented and aromatic compounds than the *Aspergillus*, such as: a benzoic acid ester, a flavone/flavonol, a pyrimidine nucleoside, a hexose, an anthocyanidin and a benzene/substituted derivative. It is possible that the hexose is a product of carbohydrate metabolism. The natural biofilm produced the least compounds, but one of these is thought to

be a product of carbohydrate metabolism. The four significant compounds were: an aminoglycoside, an azine/derivative, a cyclic amide and a tannin. The *Penicillium* produced six compounds and also contained potential products from carbohydrate metabolism: two benzene substituted/derivatives, an aminoglycoside, an oligopeptide, a fatty amide and a cardenolide glycoside/derivative.

4.3.2.3 The metabolic products of fungi on cotton and linen paper

Figure 4.15 shows the number of significant compounds (*p=0.01*) detected that were in the cotton and linen paper extract. Over the 12 weeks of incubation the *Cladosporium* produced the most compounds, followed by the natural biofilm, *Penicillium* and then the *Aspergillus.*
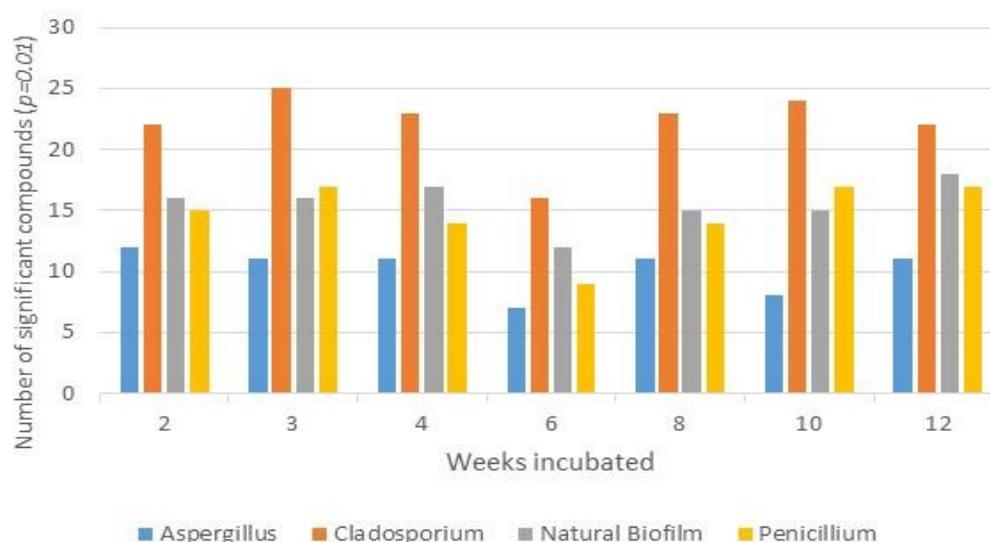
Figure 4.15- The number of significant (p=0.01) features detected from high throughput analysis of HPLC-MS spectra by XC-MS. Spectra were produced from solvent extraction of inoculated cotton and linen paper after timed incubation at 20°C with Aspergillus*,* Cladosporium*,* Penicillium *and the natural biofilm found on the paper.*

The *Aspergillus* samples produced 12 significant compounds over the incubation time and that were not present in the control cotton and linen paper. These included some aromatic compounds and a pigment. The ten most abundant products were found to contain: benzene substituted derivatives, an anthocyanidin, an oligopeptide, glycerophospholipids, a quinoline derivative and a glycerolipid. The *Cladosporium* produced 25 significant compounds in the fungal solvent extracts. The ten most abundant included: an oligopeptide, a benzimidazole, a flavonoid, a terpene glycoside, benzene substituted derivatives, a fatty acyl, an amino acid derivative, an amine and a Glycerolipid derivative. There was one pigment and aromatic compound found among these, meaning that the *Cladosporium* products are potentially less volatile than the *Aspergillus*. The natural biofilm extract was found to have 18 significant compounds not found in the control. The ten most concentrated products included pigments and a potential toxin:

anthocyanidins, oligopeptides, an amino acid/peptide analogue, a fatty acyl glycoside, a glycerophospholipid derivative, an oligosaccharide (thought to be toxic) and a benzene substituted derivative. The *Penicillium* extracts produced 17 significant compounds not found in the control and included pigments and two potential toxins; a biphenyl derivative and steroidal glycoside. The other compounds included: fatty Acyls, a long chain fatty alcohol, a steroidal glycoside, anthocyanidins, an alkane, a carboxylic acid ester and an aromatic hydrocarbon.

4.3.2.4 The metabolic products of fungi on beech wood paper

Figure 4.16 shows the number of significant compounds (*p=0.01*) detected that were not found in the control beech wood paper extract. Over the 12 weeks of incubation the *Aspergillus* produced the most compounds, followed by the natural biofilm, *Cladosporium* and then the *Penicillium.*
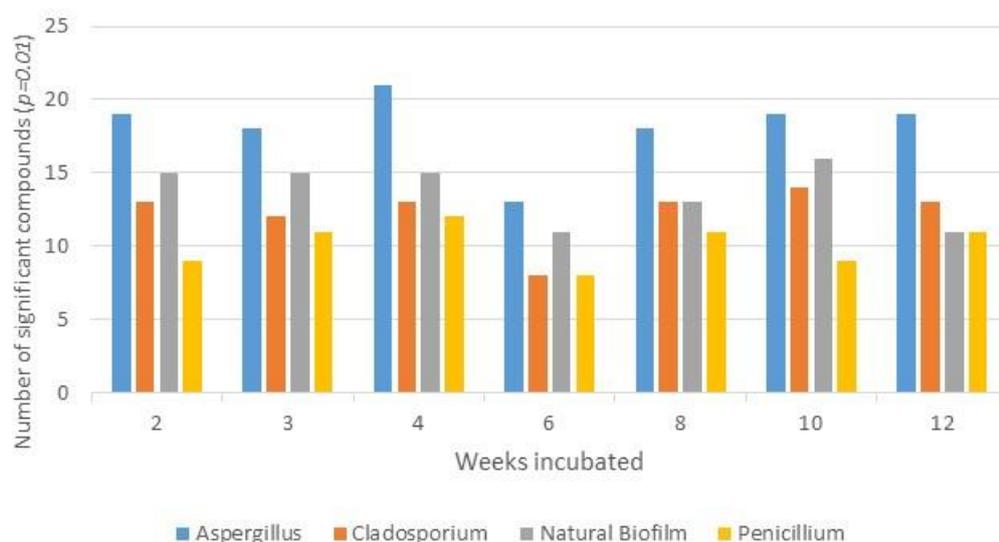
Figure 4.16- The number of significant (p=0.01) features detected from high throughput analysis of HPLC-MS spectra by XC-MS. Spectra were produced from solvent extraction of inoculated beech wood paper after timed incubation at 20°C with Aspergillus*,* Cladosporium*,* Penicillium *and the natural biofilm found on the paper.*

The *Aspergillus* extract contained 21 compounds that were not present in the control sample, including a potential toxin in the form of a quinazoline. The other ten most abundant compounds included: a fatty acid ester, a triradylglycerol, glycerophospholipids, a purine derivative, a substituted pyrrole, an oligopeptide and a cycloalkane. The *Cladosporium* was found to have 14 compounds, the ten most abundant including: glycerophospholipids, an alcohol/polyol, a carboxylic acid ester (aromatic) and other derivative (pigment), a glycosyl compound, a fatty amide, an acetamide, a fatty acid amide and a coumarin derivative (pigment).The natural biofilm produced 16 compounds that were not found in the control, the ten most concentrated of which included 4 difference aromatic, 3 pigmented and one potentially toxic compounds. These were: a carbonyl, a quinazoline (toxin), a benzene substituted derivative, a flavonoid, a naphthalene,

an anthracene, a fatty acid ester, a peptoid-peptide hydrid, a pyrimidine nucleotide sugar and a glycerophospholipid. The *Penicillium* only produced 12 compounds that were not in the control, but these were again volatile, with 3 aromatic, one pigmented and one potentially toxic compounds. Those compounds were: a phosphoric acid ester, a quinoline derivative (toxin), a naphthalene sulfonic acid/derivative, an organoheterocyclic compound, a phosphosphingolipid, a peptoid-peptide hydrid, an indole/derivative, a piperazine/derivative, an acetamide and a fatty acid ester.

4.3.2.5 The metabolic products of fungi on pine

Figure 4.17 shows the number of significant compounds (*p=0.01*) detected in the pine extract. Over the 12 weeks of incubation the *Penicillium* produced the most compounds, followed by the *Cladosporium* and then the *Aspergillus.*
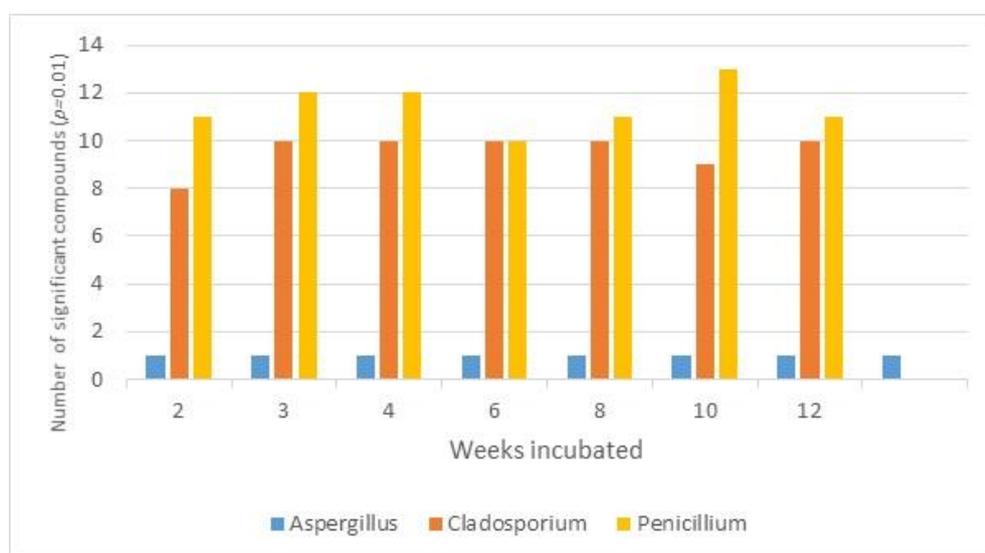
Figure 4.17- The number of significant (p=0.01) features detected from high throughput analysis of HPLC-MS spectra by XC-MS. Spectra were produced from solvent extraction of pine after timed incubation at 20°C with Aspergillus, Cladosporium *and* Penicillium*.*

Over the course of incubation, only one compound, an acyl Coenzyme A, was found in the *Aspergillus* and pine extract that was not present in the control sample. The *Cladosporium* was more volatile, producing 10 compounds that weren't in the control, including a pigment and some aromatic substances, although these were not observed in every week; the lipid based compounds were not found in week 2 and the glycerophospholipid was not detected in week 10. The compounds isolated were: oligopeptides, a cyclic nucleotide, an organoheterocyclic compound, a benzofuran, a glycerophospholipid, an oligosaccharide, a chalcone/dihydrochalcone, a biflavonoid/polyflavonoid and a triacylglycerol. The *Penicillium* produced a total of 13 compounds over the 12 weeks of incubation, with a potentially toxic terpenoid and a pigment. The 10 most abundant included: oligopeptides, an oligolactosamine,

a fatty acid ester, a benzene/substituted derivative, a carbohydrate/conjugate (not detected until week 3), a glycerophosphoserine, a dicarboxylic acid ester, a terpenoid and a xanthene.

4.3.2.6 The metabolic products of fungi on oak

Figure 4.18 shows the number of significant compounds ($p=0.01$) detected that were not found in the control oak extract. Over the 12 weeks of incubation the *Penicillium* produced the most compounds, followed by the *Aspergillus* and then the *Cladosporium.*
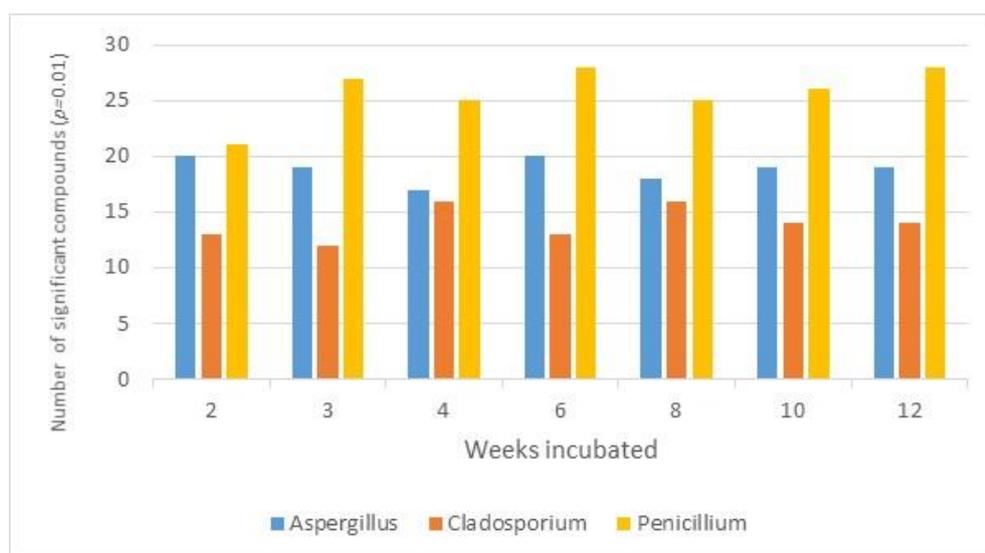
Figure 4.18- The number of significant (p=0.01) features detected from high throuput analysis of HPLC-MS spectra by XC-MS. Spectra were produced from solvent extraction of oak after timed incubation at 20°C with Aspergillus, Cladosporium *and* Penicillium.

The *Aspergillus* produced 21 compounds that were not detected in the control oak sample. Of the 10 most abundant, many were lipid based. The compounds found included: an oligopeptides, a cyclic peptide, diterpenoids, glycerophospholipids, a purine nucleotide and a triterpenoid. The *Cladosporium* produced the least compounds with only 16 that were not also found in the control, although these did include a potentially toxic monosaccharide derivative (Demethyllactenocin). The ten most prevalent compounds in descending order were: a monosaccharide derivative, a diterpenoid, a phenolic glycoside, a Cucurbitacin glycoside, a glycerophospholipid, oligopeptides, a naphthalene, a fatty acyl and a triradylglycerol. The *Penicillium* produced 29 novel compounds with the 10 most concentrated including: glycerophospholipids, oligopeptides, a benzothiazole, a pyrazole, an alkyl-phenylketone, a diacylglycerol, an isoquinoline/derivative and a piperidine.

4.3.2.7 The metabolic products of fungi on silk

Figure 4.19 shows the number of significant compounds (*p=0.01*) detected that were not found in the control silk extract. *Penicillium* produced the most compounds over the 12 weeks of incubation, followed by the *Cladosporium*, then the natural biofilm and lastly the *Aspergillus*.
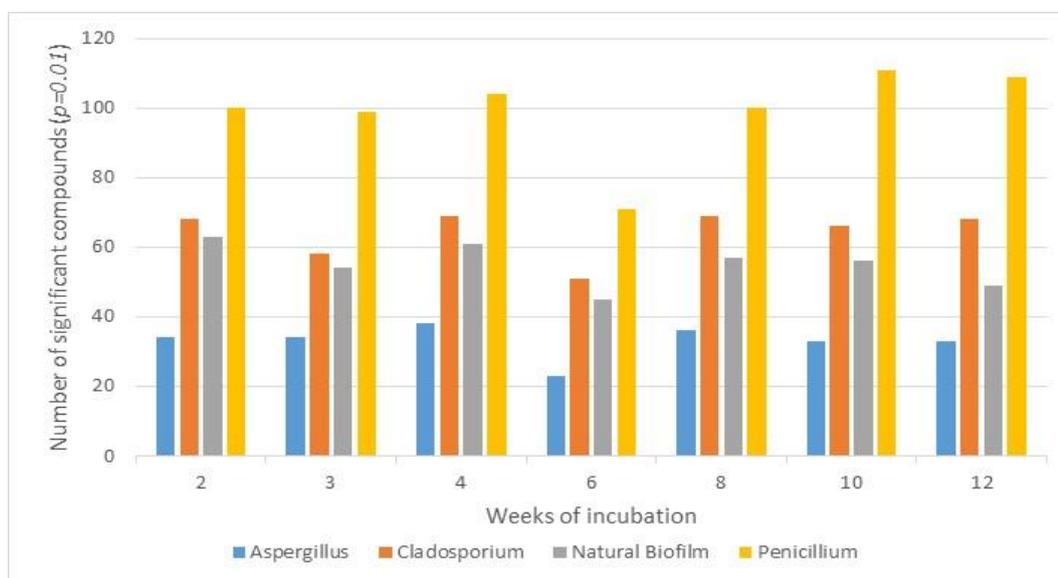
Figure 4.19- The number of significant (p=0.01) features detected from high throughput analysis of HPLC-MS spectra by XC-MS. Spectra were produced from solvent extraction of inoculated woven silk after timed incubation at 20°C with Aspergillus, Cladosporium, Penicillium *and the natural biofilm found on the silk.*

Over the incubation period, there were varying levels of compounds detected, although in a cases, there was a reduced number seen in the week 6 sample; this was not however a significant variation over the sample range (*p*=0.42). The *Aspergillus* extract was found to contain the greatest number of high intensity compounds (16 compounds with a chromatogram intensity of over 10,000), despite producing the lowest total number of significant compounds. The ten with the greatest concentration included: an aromatic protein derivative, lipid sterol, cyclic peptide, amino acid & nucleoside derivatives, benzenenoids (including a sesquiterpene), oligopeptides and a diacylglcerol. The *Cladosporium* compounds included: an alkane, fatty acid derivative & amide, amino acid derivatives, a glycophospholipid, a pyran based mycotoxin and a triterpene saponin. Compounds in lower concentrations included a number of pigments, lipid like molecules and a carboxylic acid derivative. The most concentrated natural biofilm extracts were: an aromatic protein derivative, a phenylpropanoid/polyketide, a carboxylic acid derivative, a pyran based mycotoxin and a triterpene saponin, a pyridine derivative, lipid like molecules and a benzenoid pigment. The most intense *Penicillium* peaks included: oligopeptides, a flavonol (pigment), protein derivatives, an acyclic alkanes, fatty acids, a coumarin (pigment) and a saccharolipid.

4.3.2.8 The metabolic products of fungi on wool

Figure 4.20 shows the number of significant compounds (*p=0.01*) detected that were not found in the control extract. There were far fewer compounds detected from the wool than silk, however ratio of products was found, with *Penicillium* having the most then *Cladosporium*, the natural biofilm and *Aspergillus*.
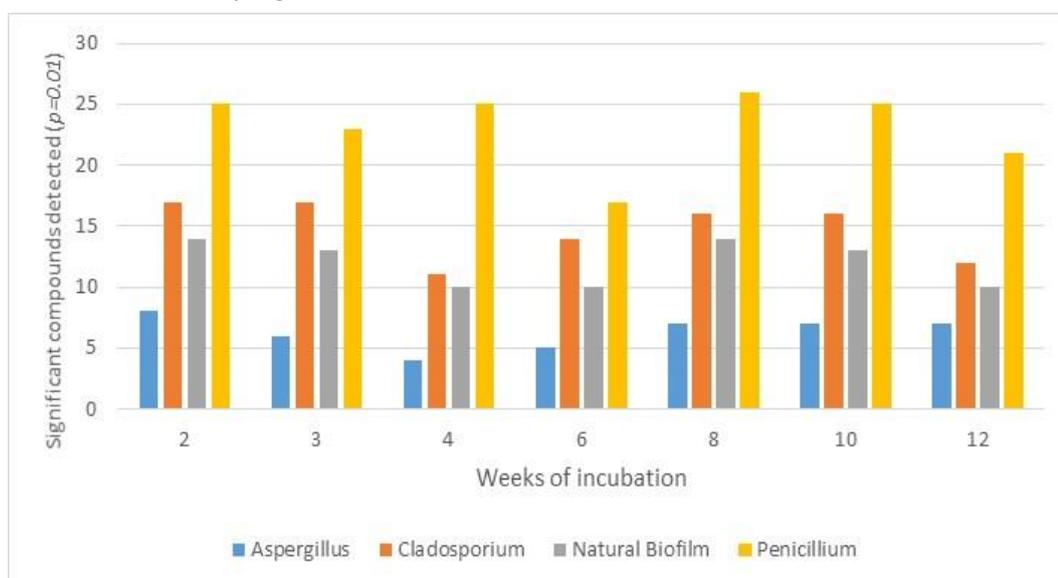
Figure 4.20- The number of significant (p=0.01) features detected from high throughput analysis of HPLC-MS spectra by XC-MS. Spectra were produced from solvent extraction of inoculated woven wool after timed incubation at 20°C with Aspergillus, Cladosporium, Penicillium *and the natural biofilm found on the wool.*

The *Aspergillus* extract was found to contain the lowest total number of significant compounds. The eight found were: lipid like molecules, amino acid derivatives, a flavonol (pigment), a fatty acid, an acridine and a naphthalene sulfonic acid derivative. The *Cladosporium*, produced more products relating to protein degradation and those containing sulphur. There was also a greater diversity in the compounds detected. The ten with the greatest intensities were: a protein derivative, an aromatic amine, an isothiocyanate, amino acid derivatives, a heterocyclic amine, a cinnamic acid derivative, a substituted aniline, an acyl amine, cyclic dispeptide and an oligopeptide. The natural biofilm produced more volatile, potentially toxic and pigmented compounds than the other fungi. These included: a polyamine, lipid like molecules, a carboximidic acid derivative, a phenylpropane, naphthalene sulfonic acid derivative, amino acid derivatives & polypeptides, a fatty acid ester and a diphenylether. This increase in volatile compounds may be due to the different species colonising the material, however this does not affect their ability to utilise the wool as are still protein derived compounds. The *Penicillium* produced the most significant compounds over the 12 weeks, including an antimicrobial. The ten most concentrated were: oligopeptides, an organoheterocyclic compound, an

oligolactosamine, protein derivatives, flavonoids, a triradylglycerol and a penicillanic acid ester. Despite showing the lowest enzyme activity on solid plate media, the *Penicillium* was still able to produce derived protein compounds.

4.3.2.9 The metabolic products of fungi on leather

Figure 4.21 shows the number of significant compounds (*p=0.01*) detected that were not found in the control extract. There were no significant compounds detected for the *Penicillium* on
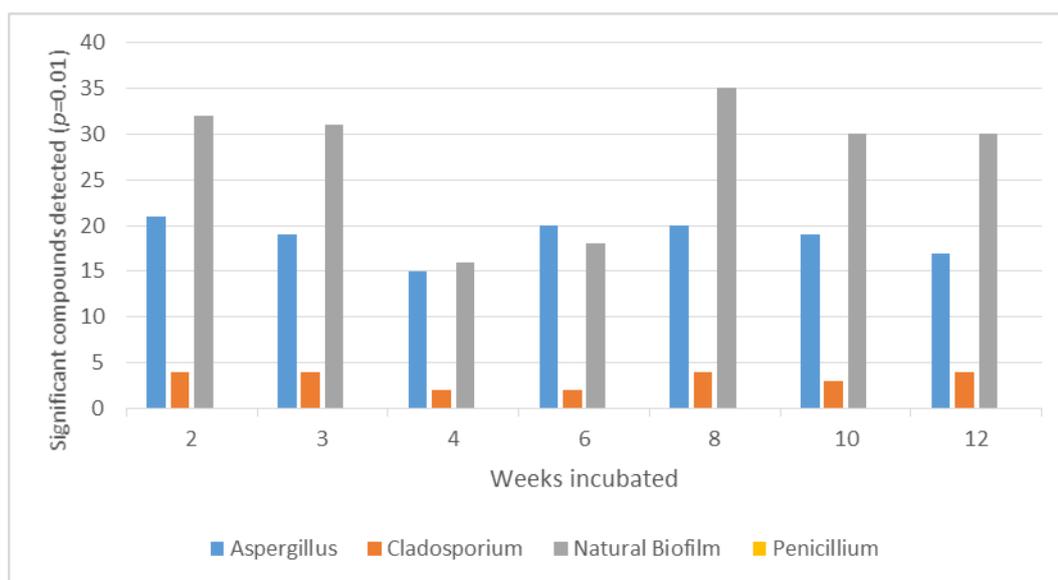
Figure 4.21- The number of significant (p=0.01) features detected from high throughput analysis of HPLC-MS spectra by XC-MS. Spectra were produced from solvent extraction of inoculated leather after timed incubation at 20°C with Aspergillus, Cladosporium, Penicillium *and the natural biofilm found on the leather.*

leather with the natural biofilm having the most, then *Aspergillus* and the *Cladosporium*.

The most concentrated compounds found in the *Aspergillus* extract were: a steroidal saponin, an oligopeptide, a long-chain fatty acyl CoA, a fatty acyl CoA, an anthraquinone (pigment), a naphthalene derivative (aromatic), a benzene derivative, a phenothiazine (toxin), an anthracene (toxin) and a benzoic acid derivative. The *Cladosporium* extract only contained 4 significant compounds: a benzamide (aromatic), a naphthalene sulfonate (pigment), an anthocyanidin (pigment) and a triterpenoid (aromatic). The most concentrated compounds from the natural biofilm extract were: benzene/substituted derivatives, a naphthalene sulfonate (pigment), oligopeptides, a fatty acid ester, a steroid derivative, a glycerophosphoglycerol and a quinolone/derivative (aromatic).

4.3.3 The metabolic products of fungi on parchment

Figure 4.22 shows the number of significant compounds (*p=0.01*) detected from parchment that were not found in the control extract. *Aspergillus* produced the most compounds with the *Cladosporium* and *Penicillium* both producing 8.
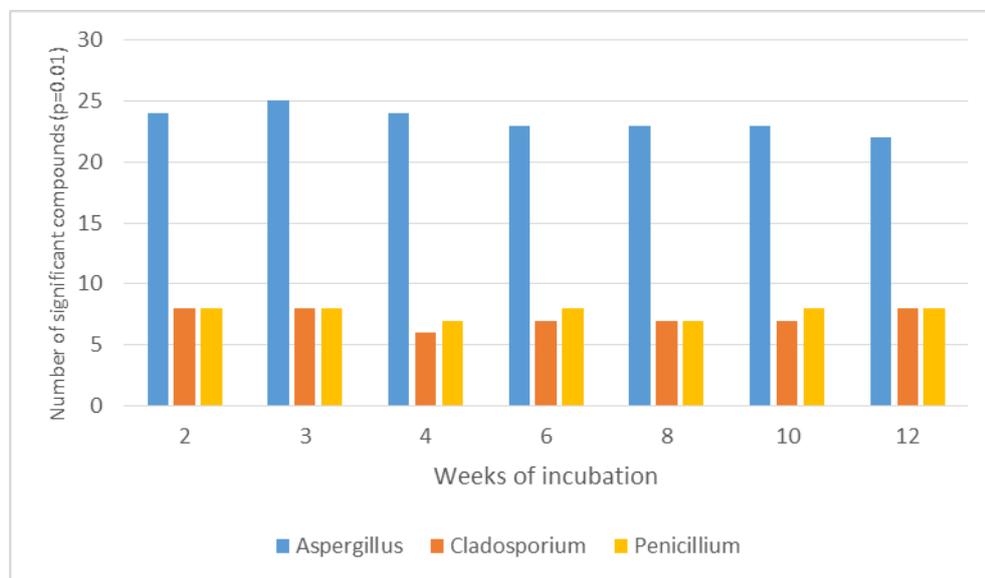
Figure 4.22- The number of significant (p=0.01) features detected from high throughput analysis of HPLC-MS spectra by XC-MS. Spectra were produced from solvent extraction of inoculated parchment after timed incubation at 20°C with Aspergillus*,* Cladosporium & Penicillium.

The compounds with the highest concentration from the *Aspergillus* extract were: an oxygenated hydrocarbon, an anthocyanidin (pigment), a triazine (aromatic), a benzofuran (aromatic), oligopeptides, an aromatic organonitrogen compound, a heteroaromatic compound and an alkanolamine. The *Cladosporium* extract contained: a volatile amine, an acetamide, a 5'-deoxy-5'-thionucleoside, a tryptamine/derivative, a triazine, a flavone/flavonol (pigment), a ceramide phosphoinositol and an oligopeptide. The *Penicillium* compounds were: flavone/flavonols (pigment), a bipyridine/oligopyridine, an oligolactosamine, and organic acid ester, a purine ribonucleoside triphosphate, an oligopeptide and a cyclic depsipeptide.

4.3.4 ATR-FTIR

Chemical changes substrates were analysed using ATR-FTIR to determine vibrational differenced in chemical species on the surface of materials. Spectra were produced from an average of 32 scans between 4000-400cm^{-1} and at a resolution of 4cm^{-1} in absorbance mode. This mode was selected as according to Beer's Law, the peak intensity of each band is directly proportional to the concentration of the absorbing chemical species. The tests were performed under ambient conditions with pressure adjustment before each reading. Baseline corrections were performed using 64 baseline points and a straight line rubber band method. Spectra were normalised with

standard normal variate (SNV), prior to principal components analysis (PCA). The loadings of the PCA scores were used to highlight significant regions of change and the features were assigned from published sources (Garside & Wyeth 2006; Garside & Wyeth 2003; Garside & Wyeth 2004b; Vilaplana et al. 2015; Nilsson et al. 2010; Luo et al. 2012; Kavkler, Šmit, et al. 2011; Kavkler & Demšar 2012; Kavkler et al. 2015; Mohebby 2005; Fackler et al. 2007; Millington & Church 1997; Wojciechowska et al. 2002; Wojciechowska et al. 2004; Wojciechowska et al. 1999; Larsen et al. 2005; Bicchieri et al. 2011; Odlyha et al. 2009; Falcão & Araújo 2014; Puică et al. 2006; Tondi et al. 2015; Pandey & Pitman 2003; Naumann et al. 2005; Coates 2000).

4.1.1.1 ATR-FTIR of cotton

Figure 4.23 details the PCA scores for cotton. There is a clear overlap of the *Aspergillus*, *Cladosporium* and control scores. The *Penicillium* shows a greater diversity in the PC-1 scores along the x-axis, particularly during the earlier weeks of incubation. The natural biofilm scores are tightly clustered together but show a greater positive PC-1 score and a lower PC-2 score than the control fabric. This indicates that the natural biofilm and *Penicillium* have caused the most significant change to the chemical structure of cotton. Average spectra for all materials and fungal conditions can be found in Appendices-Chapter 4.
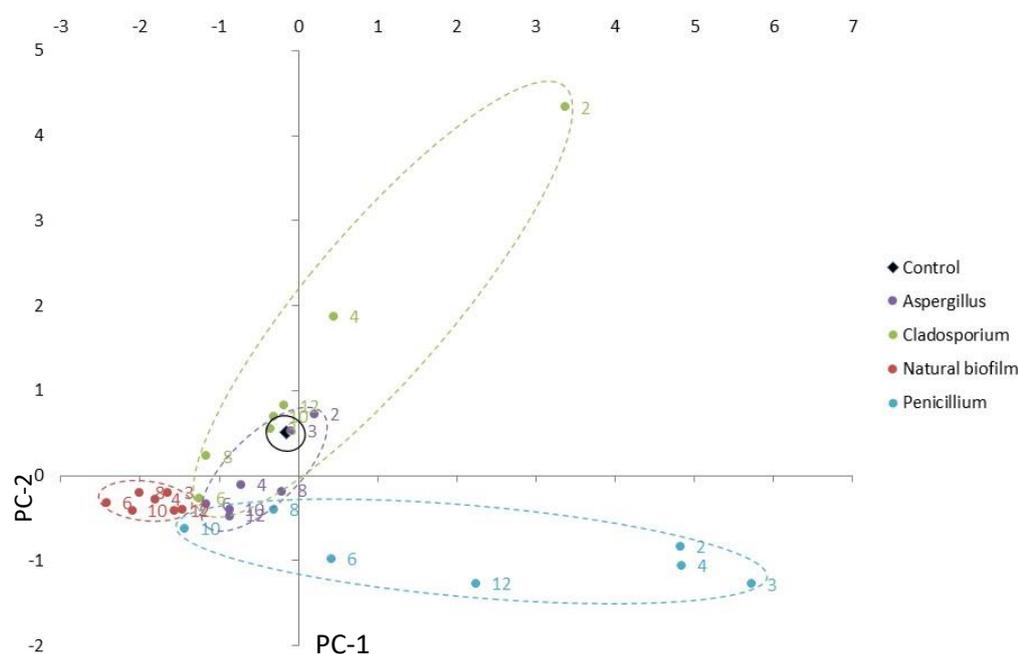
Figure 4.23- Mean PCA (PC-1 x axis & PC-2 y axis) scores for cotton incubated with Aspergillus, Cladosporium, Penicillium *and the natural biofilm over 12 weeks at 20°C. Scores were calculated from the baseline corrected ATR-FTIR spectra formed from an average of 32 scans, between 4000-400cm^{-1}, at a resolution of 4cm^{-1}after SNV normalisation*

The significant regions of change in cotton after fungal growth can be seen in Table 4.1. *Aspergillus* caused a linear reduction in the C-H and C-H$_2$ peak height intensities over the 12 week incubation, after an initial increase. There was an increase in peaks associated with

carbonyls, the greatest change occurring over the first 3 weeks of growth and increased vibration in the adsorbed water, C-C ring breathing, C-OH stretching of primary alcohols and C-H wagging in plane. *Cladosporium* caused similar changes to the cotton, although they were less linear in nature. The *Penicillium* caused both increase and decrease in the C-H peak height over the incubation but a decrease in the C-H$_2$ peak. There was again and increase in the peaks associated with carbonyls with an increase to base widths and wavenumber.

Table 4.1- The assigned ATR-FTIR peaks for cotton which exhibited significant change after incubation with A. versicolor, C. cladosporiodes, P. brevicompactum *and the natural biofilm for 12 weeks. Spectra were produced from an average of 32 scans between 4000-400cm^{-1} and at a resolution of 4cm^{-1} in absorbance mode. Data was baseline corrected, normalised (SNV) and the PCA loadings used to determine significant change in features.*
+ *denotes increase, - denotes decrease and a combination indicates differences during the 12 weeks*

	Wavenumber (cm^{-1})	Assignment	Peak height	Peak base	Peak position
Aspergillus versicolor	2930-9210	C-H stretching	+ -	+	+
	2860-2840	C-H$_2$ stretching	+ -	-	
	1750-1720	C=O stretching of carbonyls	+	+	+ -
	1635	adsorbed water	+	-	+
	1155	C-C ring breathing (asymmetric stretching)	+		
	1025	C-OH stretching primary alcohols	+		
	980	C-H wagging in-plane	+		
Cladosporium cladosporiodes	2930-9210	C-H stretching	- +	+	+
	2860-2840	C-H$_2$ stretching	+ -	+	+
	1750-1720	C=O stretching of carbonyls	+	+	+
	1635	adsorbed water	+		+
	1155	C-C ring breathing (asymmetric stretching)	+		
	1025	C-OH stretching primary alcohols	+		
	980	C-H wagging in-plane	+ -		
Penicillium brevicompactum	2930-9210	C-H stretching	- + -	+	+
	2860-2840	C-H$_2$ stretching	-		+
	1750-1720	C=O stretching of carbonyls	+	+	+
	1635	adsorbed water	+	-	+
	1155	C-C ring breathing (asymmetric stretching)	+		-
	1025	C-OH stretching primary alcohols	+		+
	980	C-H wagging in-plane	+		
Natural biofilm	2930-9210	C-H stretching	+		
	2860-2840	C-H$_2$ stretching	-	-	
	1750-1720	C=O stretching of carbonyls	+	+	+ -
	1635	adsorbed water	+	-	+
	1155	C-C ring breathing (asymmetric stretching)	+		
	1025	C-OH stretching primary alcohols	+		
	980	C-H wagging in-plane	+		

The adsorbed water peak showed the greatest difference to the other two fungal conditions with an increase in intensity, but a decrease in base width and a shift to higher wavenumbers. There were intensity increases for the other significant features, with a shift to lower wavenumber for the C-C ring breathing vibration and higher for the C-OH stretching of primary alcohols. The natural biofilm showed similar trends with an increase in C-H and a decrease in C-H_2 stretching. Changes to the carbonyl region were the lower than those of the inoculated fungi but still showed an increase in peak height, a decrease in base width and a shift towards higher wavenumbers. There were intensity increases for the other significant features.

In order to interrogate the structural changes that may have occurred in the cellulose conformation, crystallinity indices were calculated for the total crystallinity (TCI) from the peak height intensities of 1372/2900cm^{-1}; representing changes in the cellulose I & II of the cotton. A lateral order index (LOI) was also calculated using the intensities of the peaks at 1430/897cm^{-1}; representing the cellulose I conformation. *Aspergillus, Cladosporium* and *Penicillium* showed a trend towards an increase in crystallinity over the incubation period with a decrease in cellulose I. This indicates that the reduction in cellulose I is due to a conformational change in the cellulose and a shift from cellulose I towards the more ordered and crystalline cellulose II. The same trend was seen for the natural biofilm, although the changes in TCI and LOI were smaller.

4.1.1.2 ATR-FTIR of linen

Figure 4.24 is of the PCA scores for linen under all of the incubation conditions. The scores for the linen have far more overlap and little distinction between the groups than the ones observed for cotton. *Aspergillus* scores do not overlap with the control, but there is little movement, with the earlier incubation weeks moving more on the PC-1 axis. The *Cladosporium* has a broad range of scores with the greatest deviation from the control occurring in the week 10 samples. The *Penicillium* also has widespread scores, meaning that there are spectral changes, although they are not uniform and are in the dimensions of PC-1 and PC-2. The natural biofilm shows the least change in scores, compared to the control, and they predominantly shift along the PC-2 axis.

The significant regions of change for each fungal incubation condition can be seen in Table 4.2. In linen the broad based band centred around 3300cm^{-1} is attributed to O-H stretching vibrations and can be influenced by the hydrogen bonding of cellulose. There are two peaks visible, the higher wavenumber being linked to intra-molecular hydrogen bonding and the lower wavenumber one to the inter-molecular bonds. The change in peak height vibrations for linen were related to the intra-molecular bonds between 3340-3310cm^{-1}. There was no significant change in this region for *Aspergillus*, but was for *Cladosporium, Penicillium* and the natural

biofilm, indicating that there were changes in the intra-molecular bonds between the cellulose chains which help to determine the secondary structure.
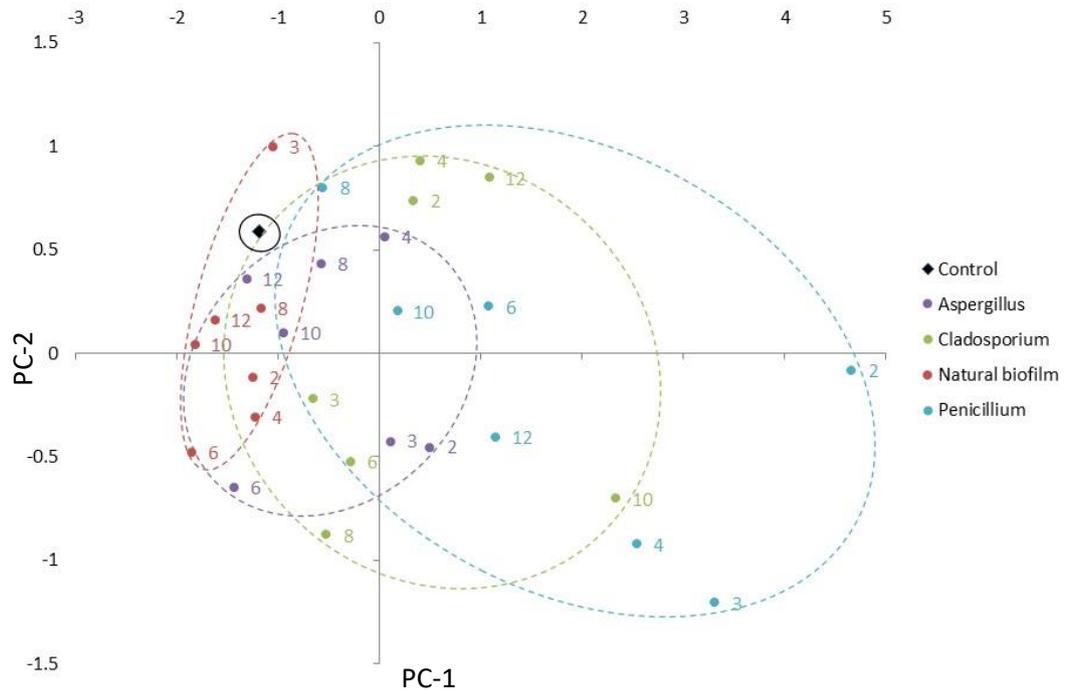
Figure 4.24- Mean PCA (PC-1 x axis & PC-2 y axis) scores for linen incubated with Aspergillus, Cladosporium, Penicillium *and the natural biofilm over 12 weeks at 20°C. Scores were calculated from the baseline corrected ATR-FTIR spectra formed from an average of 32 scans, between 4000-400cm^{-1}, at a resolution of 4cm^{-1}after SNV normalisation*

The region 2935-2900cm^{-1} is related to C-H stretching, *Aspergillus* did not show a significant change in this region but again, *Cladosporium, Penicillium* and natural biofilm caused an increase in peak height intensity and a shift to higher wavenumbers. A similar result is observed for the C-H$_2$ symmetrical stretching found at 2860-2845cm^{-1}, although peak shifts with didn't occur. The adsorbed water peak at 1635cm^{-1} showed and increase with *Aspergillus*, *Cladosporium* and *Penicillium,* and to a lesser extent the natural biofilm, with a broadening of the peak base. Other regions highlighted by the PCA were the C-OH stretch vibrations of secondary alcohols (1095-1060cm^{-1}) and C-H in-plane wagging (970-920 cm^{-1}). There was no significant change recorded with the *Aspergillus* and natural biofilm, but *Cladosporium* caused a peak height increase in both these regions and *Penicillium* in the C-H wagging.

The TCI and LOI were also calculated to determine changes in the cellulose crystallinity of linen. *Aspergillus, Penicillium* and the natural biofilm growth did not show any significant change in either index, indicating that there was little change to the structure or conformation of cellulose in the linen. *Cladosporium* caused an increase in the TCI and a decrease in the LOI, indicating that there was a small increase in the cellulose I content of the linen meaning that there have been some changes in the more crystalline cellulose II content.

Table 4.2-The assigned ATR-FTIR peaks for linen which exhibited significant change after incubation with A. versicolor, C. cladosporiodes, P. brevicompactum *and the natural biofilm for 12 weeks. Spectra were produced from an average of 32 scans between 4000-400cm^{-1} and at a resolution of 4cm^{-1} in absorbance mode. Data was baseline corrected, normalised (SNV) and the PCA loadings used to determine significant change in features.*
+ denotes increase, - denotes decrease and a combination indicates differences during the 12 weeks

	Wavenumber (cm^{-1})	Assignment	Peak height	Peak base	Peak position
Aspergillus versicolor	3340-3310	O-H stretching			
	2935-2900	C-H stretching			
	2860-2845	C-H$_2$ stretching			
	1635	adsorbed water	+	+	
	1095-1060	C-OH stretching secondary alcohols			
	970-920	C-H wagging in-plane			
Cladosporium cladosporiodes	3340-3310	O-H stretching	+ - +		
	2935-2900	C-H stretching	+	+	+
	2860-2845	C-H$_2$ stretching	+		
	1635	adsorbed water	+	+	
	1095-1060	C-OH stretching secondary alcohols	+		
	970-920	C-H wagging in-plane	+		
Penicillium brevicompactum	3340-3310	O-H stretching	+		
	2935-2900	C-H stretching	+		+
	2860-2845	C-H$_2$ stretching	+		
	1635	adsorbed water	+	+	
	1095-1060	C-OH stretching secondary alcohols			
	970-920	C-H wagging in-plane	- + -		
Natural biofilm	3340-3310	O-H stretching	+		
	2935-2900	C-H stretching	+		
	2860-2845	C-H$_2$ stretching	+		
	1635	adsorbed water	+	+	
	1095-1060	C-OH stretching secondary alcohols			
	970-920	C-H wagging in-plane			

4.1.1.3 ATR-FTIR of cotton and linen paper

Figure 4.25 is of the PCA scores for cotton and linen paper under all of the incubation conditions. The scores for the fungi on cotton and linen paper largely overlap, but they are distinct from the control and groupings are clearer for the *Aspergillus* and *Cladosporium*, showing greater deviation along the PC-1 axis. The *Penicillium* has the widest distribution of scores, with those of weeks 2-4 and week 12 being higher on the PC-1 axis and lower on the PC-2. The natural biofilm is the most distinctive category, with deviation along the PC-2 axis from the control. There is a tight cluster of scores until week 12, where the PC-2 score is far greater that the other incubation times.
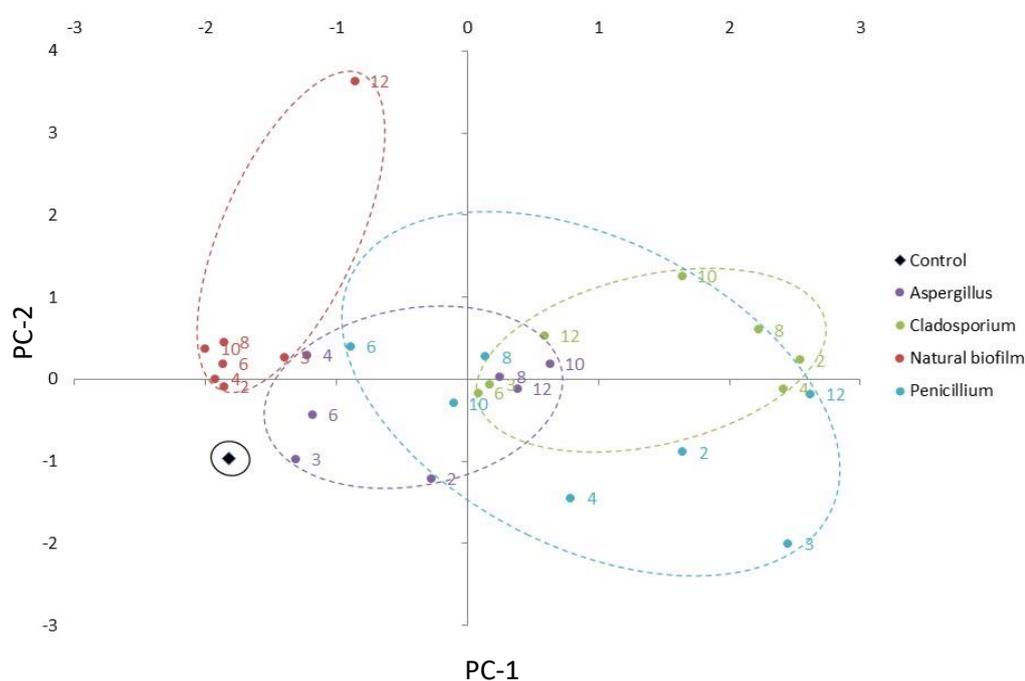
Figure 4.25- Mean PCA (PC-1 x axis & PC-2 y axis) scores for cotton and linen paper incubated with Aspergillus, Cladosporium, Penicillium *and the natural biofilm over 12 weeks at 20°C. Scores were calculated from the baseline corrected ATR-FTIR spectra formed from an average of 32 scans, between 4000-400cm^{-1}, at a resolution of 4cm^{-1}after SNV normalisation*

The significant regions of change for each fungal incubation condition can be seen in Table 4.3. The broad based band that is centred around 3300cm^{-1} is attributed to O-H stretching vibrations and can be influenced by the hydrogen bonding of cellulose. There are two peaks visible, the higher wavenumber being linked to intra-molecular hydrogen bonding and the lower wavenumber one to the inter-molecular bonds. Change in peak height vibrations for cotton and linen paper could be seen over all of the peaks in this region. After incubation with *Aspergillus, Cladosporium, Penicillium* and the natural biofilm there was a significant change to both main peaks. This indicates that there have been changes in the inter/intra-molecular bonds between

the cellulose chains which help to determine the secondary structure. The region at 2935-2900cm^{-1} is related to C-H stretching and after incubation with *Aspergillus, Cladosporium, Penicillium* and natural biofilm there was a significant increase in the vibrational intensity. The *Penicillium* and natural biofilm also caused a broadening of the peak base and a shift to a higher wavenumbers. A similar change was also seen for the C-H$_2$ symmetrical stretching vibration found at 2860-2845cm^{-1} but with *Cladosporium, Penicillium* and the biofilm causing a small change to the peak base width. Although not highlighted by the PCA, there are significant changes in the peak at 1744cm^{-1} for all fungal conditions. This peak can be attributed to carbonyl groups associated with the degradation of cellulose. The adsorbed water peak at 1635cm^{-1} showed a linear increase with *Aspergillus* and the natural biofilm over the incubation period, indicating that the longer cotton and linen paper is incubated under these conditions, the greater the adsorbed water of the fibres post drying. *Cladosporium* and *Penicillium* caused an increase in the adsorbed water content, although the effect over the incubation period was varied. The region of 1326-1301cm^{-1} is attributed to CH wagging deformation. For the paper incubated with *Aspergillus, Cladosporium, Penicillium* and natural biofilm there is a significant increase in the peak centred at 1315 cm^{-1}. For the biofilm, this increase had a linear relationship with the number of weeks the sample was incubated for. Other regions highlighted by the PCA were the C-OH stretch vibrations of secondary and primary alcohols (1081-1032cm^{-1}) and C-H in-plane wagging (970-920cm^{-1}). Both of these regions showed significant peak height intensity increases and an increase in peak base width after incubation with *Aspergillus, Cladosporium, Penicillium* and natural biofilm with the latter two having the greatest effect.

The TCI and LOI were also calculated to determine changes in the cellulose crystallinity of cotton and linen paper. *Aspergillus* caused a small decrease in the total crystallinity over the incubation period, with an increase in the lateral order index. This indicates that there may have been a shift towards a more disordered conformation but overall there was little change in the crystallinity of the cellulose polymer. No trends were apparent in the crystallinity indices of cotton and linen paper after incubation with *Cladosporium*, indicating that this species does not discernibly alter the conformation of the cellulose structure. After incubation with *Penicillium* and the natural biofilm there is a trend towards a slight increase in the TCI and the LOI of the paper samples. This indicates that the slight increase in crystallinity is not due to cellulose conformational changes, but a reduction of the amorphous regions of the cellulose.

Table 4.3- The assigned ATR-FTIR peaks for cotton and linen paper which exhibited significant change after incubation with A. versicolor, C. cladosporiodes, P. brevicompactum *and the natural biofilm for 12 weeks. Spectra were produced from an average of 32 scans between 4000-400cm⁻¹ and at a resolution of 4cm⁻¹ in absorbance mode. Data was baseline corrected, normalised (SNV) and the PCA loadings used to determine significant change in features.*
+ denotes increase, - denotes decrease and a combination indicates differences during the 12 weeks

	Wavenumber (cm⁻¹)	Assignment	Peak height	Peak base	Peak position
Aspergillus versicolor	3340-3310	O-H stretching	+ - +	+	
	2935-2900	C-H stretching	+	+	+
	2860-2845	C-H$_2$ stretching	+		
	1750-1720	C=O stretching of carbonyls	+		
	1635	adsorbed water	+	+	
	1326-1301	C-H wagging deformation	+ -		-
	1081-1032	C-OH stretching primary & secondary alcohols	+	+	
	970-920	C-H wagging in-plane	+	+	
Cladosporium cladosporiodes	3340-3310	O-H stretching	+ -	+	
	2935-2900	C-H stretching	+	+	
	2860-2845	C-H$_2$ stretching	+	+	
	1750-1720	C=O stretching of carbonyls	+	+	
	1635	adsorbed water	+	+	
	1326-1301	C-H wagging deformation	+ - +		
	1081-1032	C-OH stretching primary & secondary alcohols	+		
	970-920	C-H wagging in-plane	+	+	-
Penicillium brevicompactum	3340-3310	O-H stretching	+ -		
	2935-2900	C-H stretching	+	+	+
	2860-2845	C-H$_2$ stretching	+		+
	1750-1720	C=O stretching of carbonyls	+	+	
	1635	adsorbed water	+	+	
	1326-1301	C-H wagging deformation	+		
	1081-1032	C-OH stretching primary & secondary alcohols	+		
	970-920	C-H wagging in-plane	+		
Natural biofilm	3340-3310	O-H stretching	+	+	
	2935-2900	C-H stretching	+ -	+	+
	2860-2845	C-H$_2$ stretching	+ -	+	
	1750-1720	C=O stretching of carbonyls	+	+	+ -
	1635	adsorbed water	+	+	
	1326-1301	C-H wagging deformation	+		
	1081-1032	C-OH stretching primary & secondary alcohols	+	+	
	970-920	C-H wagging in-plane	+	+	

4.1.1.4 ATR-FTIR of beech wood paper

Figure 4.26 is of the PCA scores for beech wood paper under all of the incubation conditions. The scores for the *Penicillium* and *Cladosporium* on beech wood paper largely overlap but there is a broad spread of the scores. Groupings are clearer for the *Aspergillus* and the natural biofilm;

although these are in close association with the control, meaning that there has been less change in the chemical structure of the paper for these conditions. The significant regions of change for each fungal incubation condition can be seen in Table 4.4.

The broad based band that is centred around 3300cm^{-1} is attributed to O-H stretching vibrations
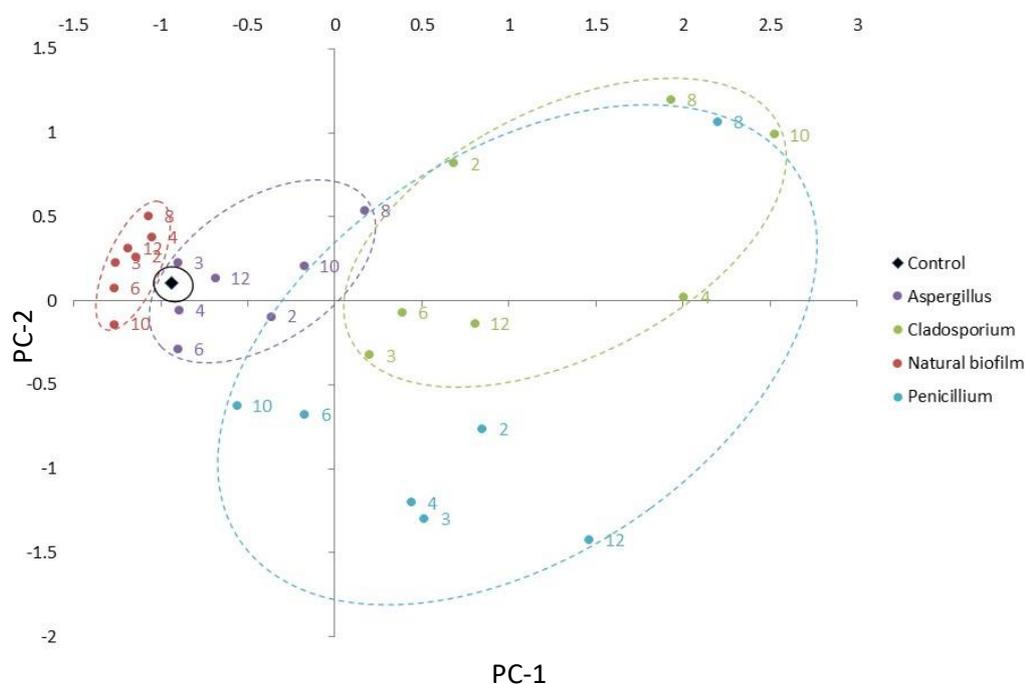
Figure 4.26- Mean PCA (PC-1 x axis & PC-2 y axis) scores for beech wood paper incubated with Aspergillus, Cladosporium, Penicillium *and the natural biofilm over 12 weeks at 20°C. Scores were calculated from the baseline corrected ATR-FTIR spectra formed from an average of 32 scans, between 4000-400cm^{-1}, at a resolution of 4cm^{-1}after SNV normalisation*

and can be influenced by the hydrogen bonding of cellulose. There are two peaks visible, the higher wavenumber being linked to intra-molecular hydrogen bonding and the lower wavenumber one to the inter-molecular bonds. After incubation with *Aspergillus, Cladosporium* and the natural biofilm there were significant changes to both peaks, indicating changes in the inter and intra-molecular bonds between the cellulose chains which help to determine the secondary structure. The paper incubated with *Penicillium* did not show any significant changes to these peaks. The region at 2935-2900cm^{-1} is related to C-H stretching and after incubation with *Aspergillus, Cladosporium* and natural biofilm there was an increase in the vibrational intensity but no significant change with the *Penicillium*. The C-H$_2$ symmetrical stretching vibration found at 2860-2845cm^{-1}also showed a similar increase in addition to the *Penicillium*. The peak at 1635cm^{-1} is related to adsorbed water in the paper. After incubation with *Aspergillus, Cladosporium* and *Penicillium* there was a significant increase in the intensity of the adsorbed water vibration over the 12 weeks of incubation and a broadening of the peak base. However the natural biofilm incubation reduced the height and base width of this peak.

Table 4.4- The assigned ATR-FTIR peaks for beech wood paper which exhibited significant change after incubation with A. versicolor, C. cladosporiodes, P. brevicompactum and the natural biofilm for 12 weeks. Spectra were produced from an average of 32 scans between 4000-400cm^{-1} and at a resolution of 4cm^{-1} in absorbance mode. Data was baseline corrected, normalised (SNV) and the PCA loadings used to determine significant change in features.
+ denotes increase, - denotes decrease and a combination indicates differences during the 12 weeks

	Wavenumber (cm^{-1})	Assignment	Peak height	Peak base	Peak position
Aspergillus versicolor	3340-3310	O-H stretching	+ -	+ -	
	2935-2900	C-H stretching	+	+	+
	2860-2845	C-H$_2$ stretching	+		
	1635	adsorbed water	+	+	
	1326-1301	C-H wagging deformation	+		
	1150-1140	C-C ring breathing & C-O-C stretching	+		
	1081-1032	C-OH stretching primary & secondary alcohols	+		
	970-920	C-H wagging in-plane	+		
Cladosporium cladosporiodes	3340-3310	O-H stretching	+ -	+ -	
	2935-2900	C-H stretching	+	+	
	2860-2845	C-H$_2$ stretching	+	+	
	1635	adsorbed water	+	+	
	1326-1301	C-H wagging deformation			
	1150-1140	C-C ring breathing & C-O-C stretching	+ - +		
	1081-1032	C-OH stretching primary & secondary alcohols	+		
	970-920	C-H wagging in-plane	+		
Penicillium brevicompactum	3340-3310	O-H stretching			
	2935-2900	C-H stretching			
	2860-2845	C-H$_2$ stretching	+		
	1635	adsorbed water	+	+	
	1326-1301	C-H wagging deformation			
	1150-1140	C-C ring breathing & C-O-C stretching			
	1081-1032	C-OH stretching primary & secondary alcohols	+		
	970-920	C-H wagging in-plane			
Natural biofilm	3340-3310	O-H stretching	+	+	
	2935-2900	C-H stretching	+	+	
	2860-2845	C-H$_2$ stretching	+		
	1635	adsorbed water	-	-	
	1326-1301	C-H wagging deformation	+		
	1150-1140	C-C ring breathing & C-O-C stretching	+		
	1081-1032	C-OH stretching primary & secondary alcohols	+	+	
	970-920	C-H wagging in-plane	+		

The region of 1326-1301cm^{-1} is attributed to C-H wagging deformation. For the beech wood paper incubated with *Aspergillus* and the natural biofilm there was an increase in the peak centred at 1315 cm^{-1}, *Cladosporium* and *Penicillium* caused no significant change. The region of 1150-1140cm^{-1} has been attributed to the area between the C-C ring breathing and C-O-C

stretching vibrations of the cellulose ring and glycosidic bond. After incubation with *Aspergillus, Cladosporium* and the natural biofilm the beech wood paper showed a significant increase in the vibrational intensities of these species; indicating that change occurred within the polymer backbone. *Penicillium* did not have a significant effect. Other regions highlighted by the PCA were the C-OH stretch vibrations of secondary and primary alcohols (1081-1032cm^{-1}) and C-H in-plane wagging (970-920cm^{-1}). Both of these regions showed significant peak height intensity increases after incubation with *Aspergillus, Cladosporium* and the natural biofilm but only the C-OH stretch vibrations of secondary and primary alcohols with *Penicillium*.

For the beech wood paper with *Aspergillus* and *Penicillium*, there is a trend for the increase in total crystallinity and a decrease in the lateral order index. This indicates that there was a shift toward a more crystalline and ordered form of cellulose, although this was unlikely due to a conformational change. The natural biofilm caused an increase in the TCI and a decrease in LOI. This may mean that there are conformational changes to the cellulose with a shift from the less ordered, native cellulose I to the more crystalline cellulose II. For *Cladosporium*, there were no appreciable changes to the crystallinity indices.

4.1.1.5 ATR-FTIR of pine

Figure 4.27 is of the PCA scores for pine under all of the incubation conditions. All of the fungal PCA scores have deviated from the control higher along the PC-2 axis. There is also variation in the scores in both directions of the PC-1 axis, although this varies between each sample group. There is some overlap between the *Cladosporium* and *Penicillium* and to a lesser extent the *Penicillium* and *Aspergillus* scores. This indicated a similar spectral changes for these samples. The significant regions of change for each fungal incubation condition can be seen in Table 4.5.

The broad based band that is centred around 3300cm^{-1} is attributed to O-H stretching vibrations and can be influenced by the hydrogen bonding of cellulose. There are two peaks visible, the higher wavenumber being linked to intra-molecular hydrogen bonding and the lower wavenumber one to the inter-molecular bonds. After incubation with the fungi, there was no significant change either peak. This indicates that there has been minimal change to the inter and intra-molecular bonds between the cellulose chains which help to determine the secondary structure. The region at 2935-2900cm^{-1} is related to C-H stretching and after incubation with *Aspergillus, Cladosporium* and *Penicillium* there was a significant increase in the vibrational

intensity. The same change was also seen for the C-H$_2$ symmetrical stretching vibration found at 2860-2845cm^{-1}
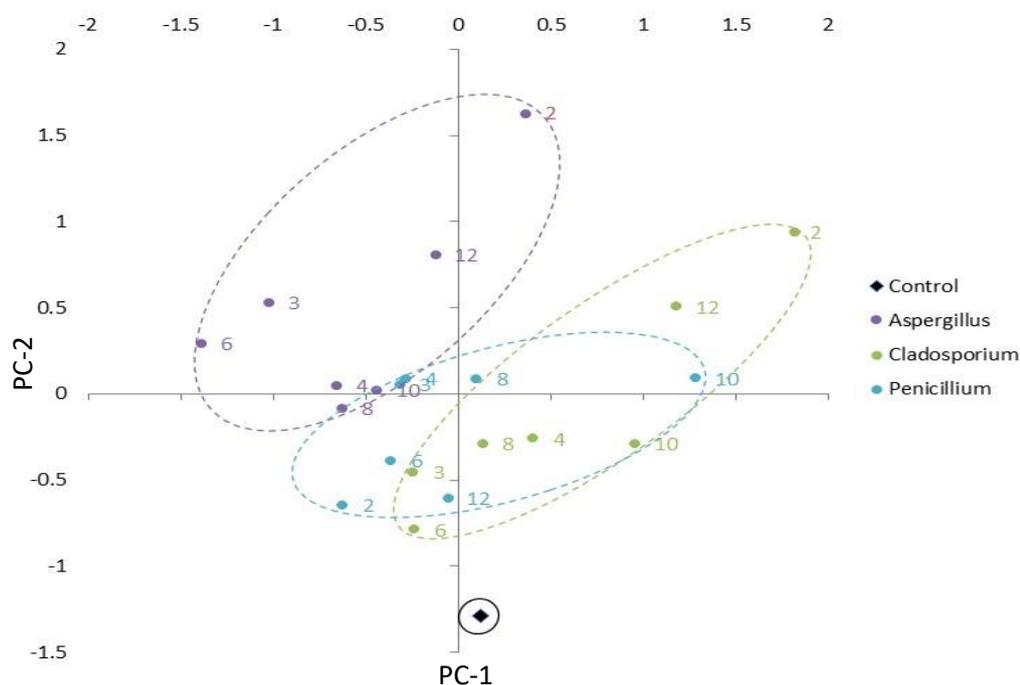
Figure 4.27- Mean PCA (PC-1 x axis & PC-2 y axis) scores for pine incubated with Aspergillus, Cladosporium & Penicillium *over 12 weeks at 20°C. Scores were calculated from the baseline corrected ATR-FTIR spectra formed from an average of 32 scans, between 4000-400cm^{-1}, at a resolution of 4cm^{-1}after SNV normalisation*

Aspergillus and *Cladosporium* significantly changed the region associated with carbonyl C=O vibrational stretching 1746-1705cm^{-1}. In wood the 1735 cm^{-1} peak of pectin and the 1738 cm^{-1} peak of xylan are discernible and showed significant changes after incubation. *Penicillium* growth reduced the peak height intensities in this region. Other peaks in the region can be attributed to carbonyl groups associated with the degradation of cellulose. The peak at 1635cm^{-1} is related to adsorbed water in pine. After incubation with *Aspergillus, Cladosporium* and *Penicillium* there was a significant increase in the intensity of the vibration with a peak shift toward higher wavenumbers with the *Aspergillus*.

The peak in the region of 1580-1540cm^{-1} is attributed to C=C stretching of the aromatic ring in lignin. For the pine incubated with *Aspergillus* and *Penicillium* there is a significant reduction in the peak centred at 1565 cm^{-1}, with the exception of the week 8 samples. *Cladosporium* caused a reduction in the peak at 1560 cm^{-1}. At 1510-1505cm^{-1} the peak is associated with the C=O stretching of the aromatic ring in lignin. Here there was no significant change with any of the fungi. Other regions highlighted by the PCA were the C-OH stretch vibrations of secondary alcohols 1087-1067cm^{-1} and C-H in-plane wagging 1015-966 cm^{-1}, both of which showed significant vibrational increases with *Aspergillus*, but not with *Cladosporium* and *Penicillium*.

Table 4.5- The assigned ATR-FTIR peaks for pine which exhibited significant change after incubation with A. versicolor, C. cladosporiodes *&* P. brevicompactum *for 12 weeks. Spectra were produced from an average of 32 scans between 4000-400cm^{-1} and at a resolution of 4cm^{-1} in absorbance mode. Data was baseline corrected, normalised (SNV) and the PCA loadings used to determine significant change in features.*
+ denotes increase, - denotes decrease and a combination indicates differences during the 12 weeks

	Wavenumber (cm^{-1})	Assignment	Peak height	Peak base	Peak position
Aspergillus versicolor	3340-3310	O-H stretching			
	2935-2900	C-H stretching	+	+	
	2860-2845	C-H$_2$ stretching	+	+	
	1746-1705	C=O stretching	+ -		
	1635	adsorbed water	+		+
	1580-1540	C=C aromatic ring stretching	- + -		
	1510-1505	C=O aromatic ring stretching			
	1087-1067	C-OH stretching of secondary alcohols	+ - +		
	1015-966	C-H wagging in-plane	+ - +		
Cladosporium cladosporiodes	3340-3310	O-H stretching			
	2935-2900	C-H stretching	+		
	2860-2845	C-H$_2$ stretching	+		
	1746-1705	C=O stretching	+ -	+	
	1635	adsorbed water	+		
	1580-1540	C=C aromatic ring stretching	-		
	1510-1505	C=O aromatic ring stretching			
	1087-1067	C-OH stretching of secondary alcohols			
	1015-966	C-H wagging in-plane			
Penicillium brevicompactum	3340-3310	O-H stretching			
	2935-2900	C-H stretching	+		
	2860-2845	C-H$_2$ stretching	+		
	1746-1705	C=O stretching	-		
	1635	adsorbed water	+		
	1580-1540	C=C aromatic ring stretching	- + -		
	1510-1505	C=O aromatic ring stretching			
	1087-1067	C-OH stretching of secondary alcohols			
	1015-966	C-H wagging in-plane			

Crystallinity indices were calculated for the total crystallinity (TCI) from the peak height intensities of 1372/2900cm^{-1}; representing changes in the cellulose I & II of the pine. A lateral order index (LOI) was also calculated using the intensities of the peaks at 1430/897cm^{-1}; representing the cellulose I conformation. A ratio to investigate the lignin content of the wood was also performed between the lignin peak at 1505cm^{-1} and one of the peaks assigned to carbohydrate content at 1375cm^{-1}. There was a decrease in total crystallinity and increase in lateral order with all fungal inoculums. This indicates that there may be a slight shift towards a more disordered conformation, from cellulose II to cellulose I. The lignin content of the pine was found to decrease after incubation with *Aspergillus, Cladosporium* and *Penicillium*.

4.1.1.6 ATR-FTIR of oak

Figure 4.28 is of the PCA scores for pine under all of the incubation conditions. There is a large deviation in the scores for the oak incubated with fungi, indicating that there have been significant differences in the spectra, in comparison to the untreated oak. The *Cladosporium* and *Penicillium* scores almost fully overlap. This is also the case for the *Aspergillus*, with the exceptions of the scores from weeks 3, 6 and 8, which deviate along the PC-1 axis. The significant regions of change for each fungal incubation condition can be seen in Table 4.6.
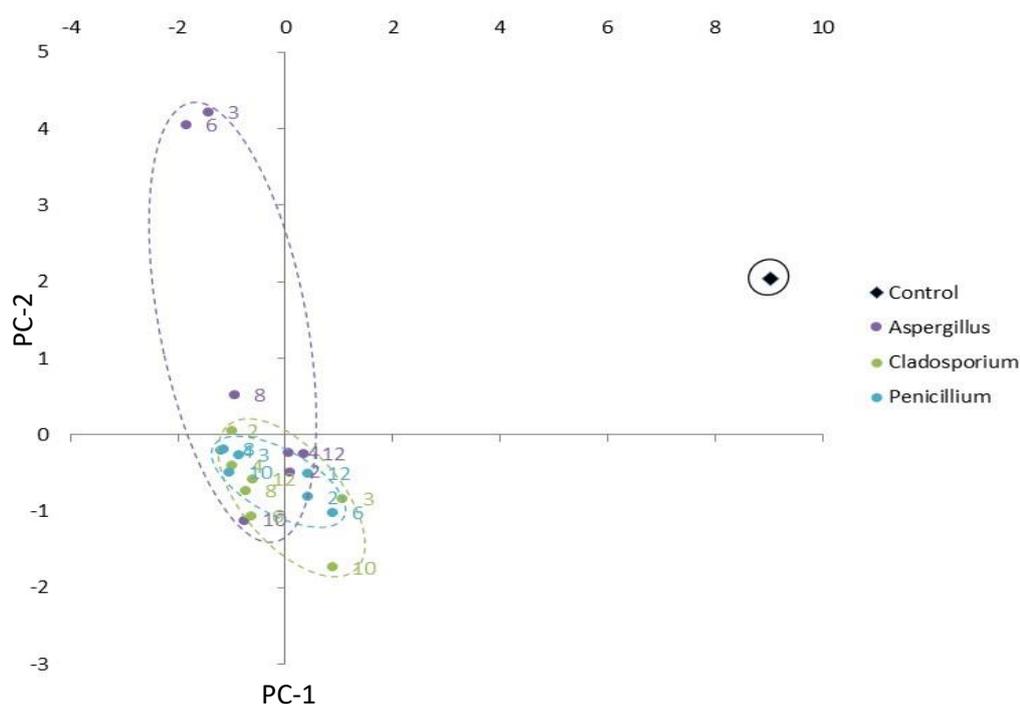
Figure 4.28- Mean PCA (PC-1 x axis & PC-2 y axis) scores for oak incubated with Aspergillus, Cladosporium & Penicillium *over 12 weeks at 20°C. Scores were calculated from the baseline corrected ATR-FTIR spectra formed from an average of 32 scans, between 4000-400cm^{-1}, at a resolution of 4cm^{-1}after SNV normalisation*

The broad based band that is centred around 3300cm^{-1} is attributed to O-H stretching vibrations and can be influenced by the hydrogen bonding of cellulose. After incubation with *Aspergillus, Cladosporium* and *Penicillium*, there was a significant difference to both main peaks indicating that there have been changes in the inter and intra-molecular bonds between the cellulose chains which help to determine the secondary structure.

The region at 2935-2900cm^{-1} is related to C-H stretching and after incubation with all fungal inoculums, there was a significant decrease in the vibrational intensity and peak base width. The same change was also seen for the C-H$_2$ symmetrical stretching vibration found at 2860-2845cm^{-1}. There are significant changes in the region associated with carbonyl C=O vibrational stretching 1738-1714cm^{-1}. In wood the 1735 cm^{-1} peak of pectin and the 1738 cm^{-1} peak of xylan are visible

and show significant decrease after incubation with *Aspergillus* and *Cladosporium*. The *Penicillium* did not cause any significant change, although the peak heights in this region were also reduced. The peak at 1635cm^{-1} is related to adsorbed water in the oak. After incubation with *Aspergillus* and *Cladosporium* there was a significant increase in the intensity of the vibration. The *Penicillium* initially caused a decrease in the peak height intensity, but then during the latter half of the trial, the intensity of the adsorbed water peak increased. The peak in the region of 1246-1226cm^{-1} is attributed to C-OH out of plane deformation. For all fungal conditions, there is a significant linear increase in the peak centred at 1235 cm^{-1}. Other regions highlighted by the PCA were the C-OH stretch vibrations of secondary alcohols 1085-1065cm^{-1} and CH in-plane wagging 970-920 cm^{-1}. Both of these regions showed significant linear increases after incubation with *Aspergillus, Cladosporium* and *Penicillium*.

Table 4.6- The assigned ATR-FTIR peaks for oak which exhibited significant change after incubation with A. versicolor, C. cladosporiodes *&* P. brevicompactum *for 12 weeks. Spectra were produced from an average of 32 scans between 4000-400cm^{-1} and at a resolution of 4cm^{-1} in absorbance mode. Data was baseline corrected, normalised (SNV) and the PCA loadings used to determine significant change in features.*
+ denotes increase, - denotes decrease and a combination indicates differences during the 12 weeks

	Wavenumber (cm^{-1})	Assignment	Peak height	Peak base	Peak position
Aspergillus versicolor	3340-3310	O-H stretching	+ - +		
	2935-2900	C-H stretching	-	-	
	2860-2845	C-H$_2$ stretching	-	-	
	1746-1705	C=O stretching	-	-	
	1635	adsorbed water	+	+	+
	1246-1226	C-OH out of plane deformation	+	+	
	1085-1065	C-OH stretching of secondary alcohols	+	+	
	970-920	C-H wagging in-plane	+		
Cladosporium cladosporiodes	3340-3310	O-H stretching	+ -		
	2935-2900	C-H stretching	-	-	
	2860-2845	C-H$_2$ stretching	-	-	
	1746-1705	C=O stretching	-		+
	1635	adsorbed water	+	+	+
	1246-1226	C-OH out of plane deformation	+	+	
	1085-1065	C-OH stretching of secondary alcohols	+	+	
	970-920	C-H wagging in-plane	+	+	
Penicillium brevicompactum	3340-3310	O-H stretching	+ - +		
	2935-2900	C-H stretching	-	-	
	2860-2845	C-H$_2$ stretching	-	-	
	1746-1705	C=O stretching			
	1635	adsorbed water	- +		
	1246-1226	C-OH out of plane deformation	+		
	1085-1065	C-OH stretching of secondary alcohols	+		
	970-920	C-H wagging in-plane	+		

There is a trend for the increase of the total cellulose index over the period of incubation with all fungal inoculums, but a decrease in the lateral order. This indicates that there was a shift toward increasingly crystalline cellulose, although this was unlikely due to a conformational change. The lignin content changed over the weeks of incubation with *Aspergillus*, although no trends were evident. With *Cladosporium* and *Penicillium*, the lignin content of oak was reduced.

4.1.1.7 ATR-FTIR of silk

Figure 4.29 details the PCA scores for silk under all of the incubation conditions. There is a clear overlap with the control and the compact natural biofilm sample groupings, which does not occur in any of the other inoculated fungal species. This indicates that the natural biofilm spectra exhibits the least change. The *Aspergillus*, *Penicillium* and *Cladosporium* samples all overlap, but with the two week incubations and weeks 8 (*Penicillium*) and 12 (*Cladosporium*) having scores furthest away from that of the control; indicating that some of the greatest spectral changes occurred after only 2 weeks.
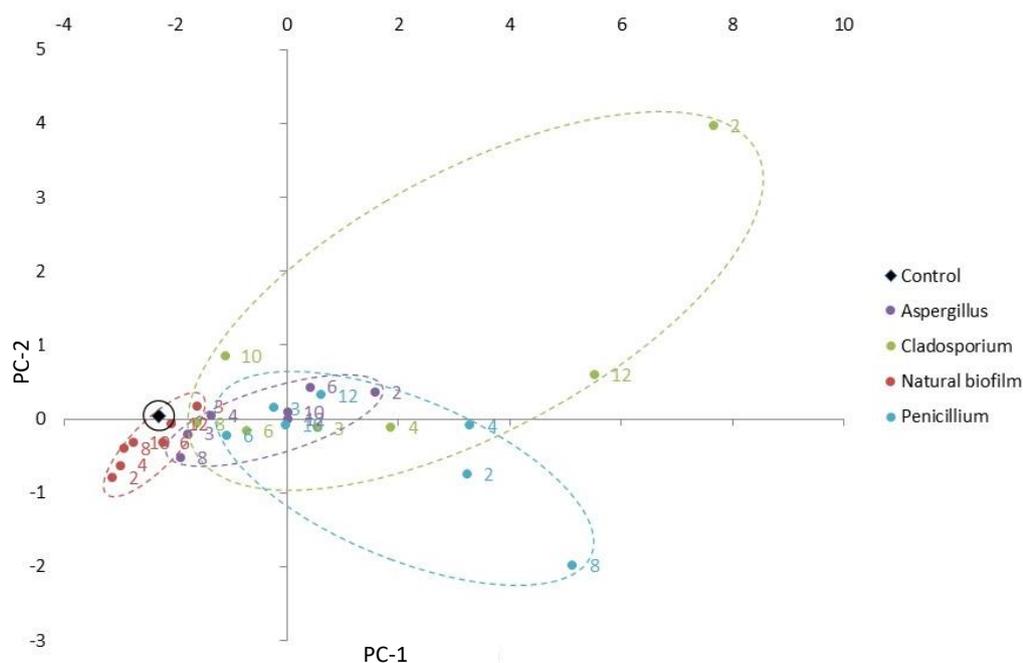
*Figure 4.29- Mean PCA (PC-1 x axis & PC-2 y axis) scores for silk incubated with* Aspergillus, Cladosporium, Penicillium *and the natural biofilm over 12 weeks at 20°C. Scores were calculated from the baseline corrected ATR-FTIR spectra formed from an average of 32 scans, between 4000-400cm^{-1}, at a resolution of 4cm^{-1}after SNV normalisation*

The significant regions of change for each fungal incubation condition can be seen in Table 4.7. The amide bonds of the protein polymer are represented by three characteristic amide peaks. Amide I (1700-1580cm^{-1}) is attributed to C=O stretching, C-N stretching and C-H-N in-plane bending vibrations. This region is associated with structural conformation changes in the polymer backbone. Amide II (1580-1470cm^{-1}) is attributed to N-H in-plane bending, C-N

stretching and C=O in plane bending. Amide III (1300-1200cm^{-1}) is attributed to N-H bending and C-N stretching vibrations. This region is associated with the peptide side chain functional groups.

Table 4.7- The assigned ATR-FTIR peaks for silk which exhibited significant change after incubation with A. versicolor, C. cladosporiodes, P. brevicompactum *and the natural biofilm for 12 weeks. Spectra were produced from an average of 32 scans between 4000-400cm^{-1} and at a resolution of 4cm^{-1} in absorbance mode. Data was baseline corrected, normalised (SNV) and the PCA loadings used to determine significant change in features.*
+ denotes increase, - denotes decrease and a combination indicates differences during the 12 weeks

	Wavenumber (cm^{-1})	Assignment	Peak height	Peak base	Peak position
Aspergillus versicolor	1605-1579	Amide I- C=O stretching, C-N stretching & C-H-N in-plane bending	+ - +		
	1526-1477	Amide II- N-H in-plane bending, C-N stretching & C=O in plane bending	+ - +		
	1151-1116	Primary & secondary aliphatic amine C-N stretching	+ - +		
	1100-973	C-N & C-C skeletal stretching	+	+	
	685-406	S-S stretching	+ - +		
Cladosporium cladosporiodes	1605-1579	Amide I- C=O stretching, C-N stretching & C-H-N in-plane bending	-		
	1526-1477	Amide II- N-H in-plane bending, C-N stretching & C=O in plane bending	-		
	1151-1116	Primary & secondary aliphatic amine C-N stretching	+ -		
	1100-973	C-N & C-C skeletal stretching	+	+	
	685-406	S-S stretching	+ -		
Penicillium brevicompactum	1605-1579	Amide I- C=O stretching, C-N stretching & C-H-N in-plane bending	- + - +		
	1526-1477	Amide II- N-H in-plane bending, C-N stretching & C=O in plane bending	- + - +		
	1151-1116	Primary & secondary aliphatic amine C-N stretching	+		-
	1100-973	C-N & C-C skeletal stretching	+	+	
	685-406	S-S stretching	+ - +		
Natural biofilm	1605-1579	Amide I- C=O stretching, C-N stretching & C-H-N in-plane bending	+		+
	1526-1477	Amide II- N-H in-plane bending, C-N stretching & C=O in plane bending	+		-
	1151-1116	Primary & secondary aliphatic amine C-N stretching	+	+	
	1100-973	C-N & C-C skeletal stretching	+ -		
	685-406	S-S stretching	+ - +		-

After incubation with *Aspergillus*, the amide I peak of silk showed an increase in vibration intensity, with the exceptions of week 6 and 10. Changes in this region indicate conformational changes to the polymer backbone. If the anomalous weeks (6 & 10) are excluded, there is a significant linear trend to the increase in intensity (*p*= 0.02). Increased peak height in this region is indicative of hydrolysis. *Cladosporium* incubation cause a reduction in the peak intensity of amide I. *Penicillium* causes both increase and decrease in the peak height of amide I during incubation. The natural biofilm caused an increase in the amide I & II peak heights. The amide II

peak also showed significant change with *Aspergillus*, although to a lesser extent than the amide I. The *Cladosporium* again reduced the vibrational intensity of the peak with *Penicillium* again increasing and decreasing intensity. Changes to the amide III peak were not significant after incubation with *Aspergillus* and *Penicillium* but *Cladosporium* reduced the peak height.

Although not indicated as significant by the PCA analysis, changes to the carbonyl region 1775-1700 cm^{-1} were observed with intense peaks at 1746 cm^{-1} & 1732cm^{-1} with *Aspergillus*, 1744 cm^{-1} & 1726 cm^{-1} with *Cladosporium* and lower intensity peaks throughout the region, also observed with *Penicillium* and the natural biofilm. Carbonyl peaks can be indicative of degradative processed, particularly oxidation. There were also spectral changes in the regions relating to aliphatic amines (1260-920cm^{-1}) assigned to primary and secondary aliphatic amine C-N stretching; indicating that depolymerisation may have occurred with *Penicillium*, the biofilm and to a lesser extent *Aspergillus*. *Cladosporium* caused a decrease in the vibrations in this region. The changes in the spectra between 685-400cm^{-1} were indicated by the PCA as being significant. This region is attributes to disulphide (S-S) features that can be indicative of changes in the tertiary structure of proteins through side chain functional groups. However for silk incubated with *Aspergillus, Penicillium* and the natural biofilm significant change was not recorded. With the exception of an increase in the second week samples, *Cladosporium* reduced peak heights in this region.

Potential conformational changes in the silk were interrogated calculating a crystallinity index of the theoretical maximum of the fibroin β-pleated sheet (1615cm^{-1}) and the random coil (1655cm^{-1}). The I_β/I_α index indicated a decrease in crystallinity over the incubation period with *Aspergillus, Cladosporium* and *Penicillium*. There was no clear trend in the I_β/I_α index of the natural biofilm with both increases and decreased in vibration observed during incubation.

4.1.1.8 ATR-FTIR of wool

Figure 4.30 details the PCA scores for wool under all of the incubation conditions. There is no overlap between the mean PCA scores of the wool incubated with fungi and the control, indicating that there are distinct changes in the spectra after incubation has occurred. There are overlaps between the scores of *Aspergillus* and the natural biofilm and then the three fungal inoculums which have a broad spread and are highly influenced by the results of the week 2 samples. The natural biofilm has more closely related results, although the week 2 sample still has a higher score on the PC-2 axis.
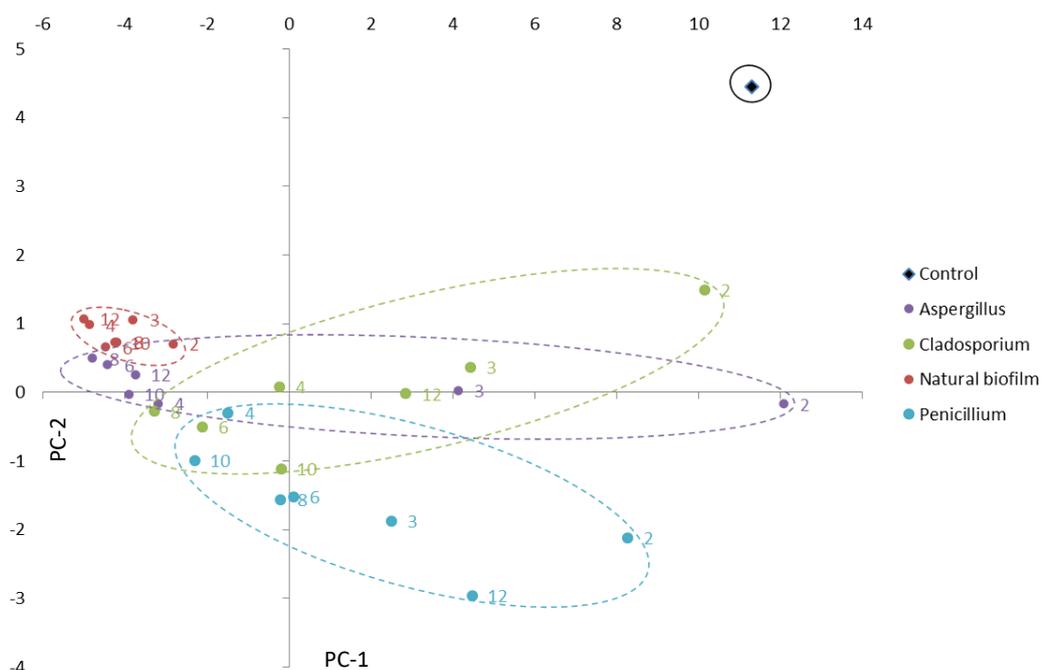
Figure 4.30- Mean PCA (PC-1 x axis & PC-2 y axis) scores for wool incubated with Aspergillus, Cladosporium, Penicillium *and the natural biofilm over 12 weeks at 20°C. Scores were calculated from the baseline corrected ATR-FTIR spectra formed from an average of 32 scans, between 4000-400cm^{-1}, at a resolution of 4cm^{-1}after SNV normalisation*

The significant regions of change for each fungal incubation condition can be seen in Table 4.8. The C-H stretching vibration (2942-2897cm^{-1}) show an increase in vibration after 2 weeks incubation with *Aspergillus*, but a decrease after further time. The same can be seen for the spectra of *Cladosporium* inoculated wool, with a shift in the peak centre toward higher wavenumbers. The wool incubated with *Penicillium* showed a decrease in vibrational intensity for the peaks in this region over all sample weeks and shifted the peak centre. The natural biofilm also reduced the vibrational intensity of peaks in this region. *Aspergillus* also caused an initial increase, then decrease in the C-H$_2$ region at 2862-2844cm^{-1}. The *Cladosporium* inoculated wool had increased peak height intensities for weeks 2 and 3 before a decrease occurred and the peak centre shifted towards higher wavenumbers. The *Penicillium* and natural biofilm showed a similar result, with a reduction in the peak height intensities of all sample weeks. There are visible changes in the wool spectral region 1770-1700cm^{-1}, attributed to free carbonyl groups. Wool incubated with *Aspergillus* showed a reduction in the native peaks after 4 weeks of incubation, after an initial increase and shift in the peak centre to higher wavenumbers and the separation of the native peaks at 1738 cm^{-1} and 1734cm^{-1}, with a greater reduction in vibrational intensity of the latter. Wool incubated with *Cladosporium* showed similar spectral changes. *Penicillium* inoculated wool showed a reduction in the peak heights of this region but again separated the peaks at 1738 cm^{-1} and 1734cm^{-1}, a reduction in the peak height of 1734cm$^{-1,}$ and

175

shifted the centres to higher wavenumbers. The natural biofilm inoculated wool also showed a reduction in the peak heights of this region, but the peak separation was not so pronounced and there were no positional shifts. The amide bonds of the protein polymer are represented by three characteristic amide peaks. Amide I (1700-1580cm^{-1}) is attributed to C=O stretching, C-N stretching and C-H-N in-plane bending vibrations. This region is associated with structural conformation changes in the polymer backbone. Amide II (1580-1470cm^{-1}) is attributed to N-H in-plane bending, C-N stretching and C=O in plane bending. Amide III (1300-1200cm^{-1}) is attributed to N-H bending and C-N stretching vibrations. This region is associated with the peptide side chain functional groups. Changes to the secondary structure of wool are indicated by the height and position of amide I indicating helical change and amide II representing β- sheet conformation. All of the growth conditions for wool caused an increase in the intensity of the amide I and amide II peaks, with a shift of the amide II towards higher wavenumbers. The amide III peak was reduced by all incubation conditions, with a reduction in the peak centre position. Other spectral regions of wool that were notably affected by the fungi were those associated with the di-sulphide bridges formed between cysteine functional groups; cysteine monoxide (1077cm^{-1}), cysteic acid (1040cm^{-1}) and the *S*-sulphocysteine residue (S-SO$_3^-$), an acidic product of cysteine reduction appears in the region of 1022cm^{-1}. *Aspergillus* and *Cladosporium* incubations reduced the peak height intensity of all of these regions after 3 weeks with a reduction in the peak base width and a reduction in peak definition, although the *Aspergillus* caused the greater change. The *Penicillium* caused a decrease in the peak height of the cysteine monoxide (1077cm^{-1}) with a shift towards lower wavenumbers. The cysteic acid peak (1040cm^{-1}) shifted towards lower wavenumbers and the intensity was increased for the first 3 weeks and the week 12 samples, the other incubation times caused a decrease in peak height intensity. The *S*-sulphocysteine residue peak shifted towards higher wavenumbers and had an increased peak height for the week 2 and 12 samples but a reduction in intensity was seen for the rest of the incubation period. The natural biofilm reduced the peak height intensities and definition for all of the peaks in this region.

Table 4.8-The assigned ATR-FTIR peaks for wool which exhibited significant change after incubation with A. versicolor, C. cladosporiodes, P. brevicompactum *and the natural biofilm for 12 weeks. Spectra were produced from an average of 32 scans between 4000-400cm^{-1} and at a resolution of 4cm^{-1} in absorbance mode. Data was baseline corrected, normalised (SNV) and the PCA loadings used to determine significant change in features.*
+ denotes increase, - denotes decrease and a combination indicates differences during the 12 weeks

	Wavenumber (cm^{-1})	Assignment	Peak height	Peak base	Peak position
Aspergillus versicolor	2942-2897	C-H stretching	+ -		
	2862-2844	C-H$_2$ stretching	+ -		
	1754-1738	C=O stretching of carbonyls	+ -	-	+
	1677-1590	Amide I- C=O stretching, C-N stretching & C-H-N in-plane bending	+		
	1580-1477	Amide II- N-H in-plane bending, C-N stretching & C=O in plane bending	+		-
	1273-1218	Amide III- 1260–1300 α-helix, 1240–1250 disordered structure, 1230–1240 β-pleated sheet	-		-
	1102-1000	S-O stretching resulting from cysteine	+ -	-	
Cladosporium cladosporiodes	2942-2897	C-H stretching	+ -		+
	2862-2844	C-H$_2$ stretching	+ -		+
	1754-1738	C=O stretching of carbonyls	+ -	-	+
	1677-1590	Amide I- C=O stretching, C-N stretching & C-H-N in-plane bending	+		
	1580-1477	Amide II- N-H in-plane bending, C-N stretching & C=O in plane bending	+		
	1273-1218	Amide III- 1260–1300 α-helix, 1240–1250 disordered structure, 1230–1240 β-pleated sheet	-		-
	1102-1000	S-O stretching resulting from cysteine	+ -	-	
Penicillium brevicompactum	2942-2897	C-H stretching	-		+
	2862-2844	C-H$_2$ stretching	-		
	1754-1738	C=O stretching of carbonyls	-		+
	1677-1590	Amide I- C=O stretching, C-N stretching & C-H-N in-plane bending	+		
	1580-1477	Amide II- N-H in-plane bending, C-N stretching & C=O in plane bending	+		
	1273-1218	Amide III- 1260–1300 α-helix, 1240–1250 disordered structure, 1230–1240 β-pleated sheet	-		-
	1102-1000	S-O stretching resulting from cysteine	+ -		- +
Natural biofilm	2942-2897	C-H stretching	-		
	2862-2844	C-H$_2$ stretching	-		
	1754-1738	C=O stretching of carbonyls	-	+	+
	1677-1590	Amide I- C=O stretching, C-N stretching & C-H-N in-plane bending	+	+	
	1580-1477	Amide II- N-H in-plane bending, C-N stretching & C=O in plane bending	+		
	1273-1218	Amide III- 1260–1300 α-helix, 1240–1250 disordered structure, 1230–1240 β-pleated sheet	-		-
	1102-1000	S-O stretching resulting from cysteine	-		

4.1.1.9 ATR-FTIR of leather

Figure 4.31 details the PCA scores for leather under all of the incubation conditions. There is an overlap between the natural biofilm and Aspergillus samples with the control, specifically the samples of week 6 for each and week 8 for the biofilm. This indicates that these conditions have had little effect on the spectra of leather. The biofilm samples show the greatest variation on the PC-2 axis and are clustered within 5 along the PC-1 axis. The scores of the other fungal conditions are more widely spread, with the Penicillium scores showing the greatest variation over the incubation time and only overlapping with the Aspergillus and Cladosporium in the week 8 and 10 samples respectively.
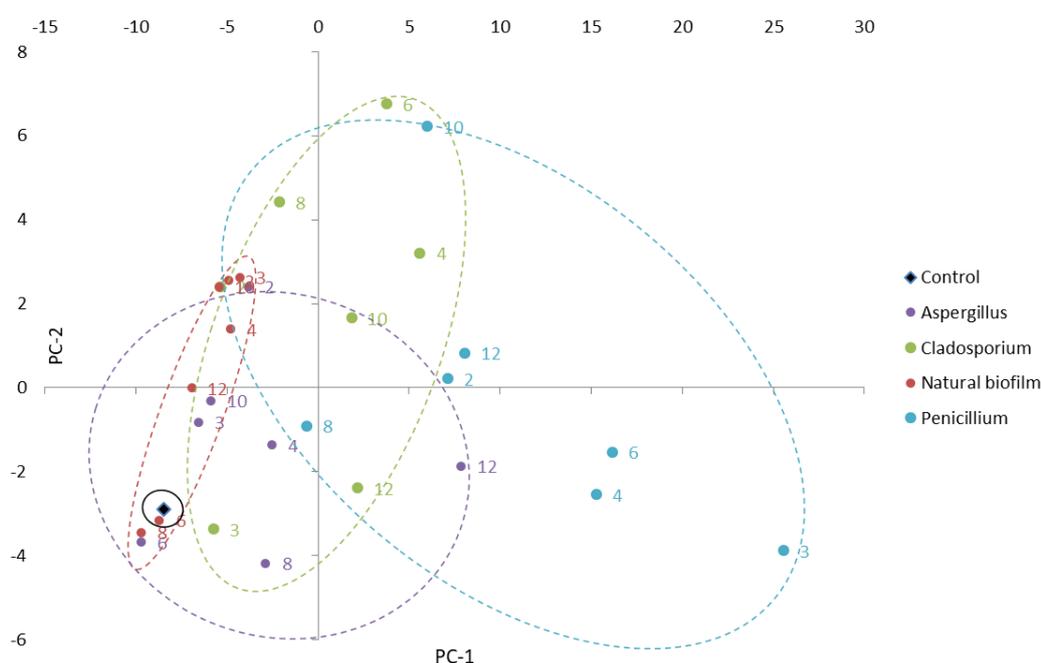
*Figure 4.31- Mean PCA (PC-1 x axis & PC-2 y axis) scores for leather incubated with* Aspergillus, Cladosporium, Penicillium *and the natural biofilm over 12 weeks at 20°C. Scores were calculated from the baseline corrected ATR-FTIR spectra formed from an average of 32 scans, between 4000-400cm^{-1}, at a resolution of 4cm^{-1}after SNV normalisation*

The significant regions of change for each fungal incubation condition can be seen in Table 4.9. Although not significant, the O-H stretch of tanning compounds in leather found at 3700-3600cm^{-1} was found to decrease over the incubation time with *Aspergillus*, *Cladosporium* and *Penicillium*. The C-H stretching vibration (2958-2889cm^{-1}) show a decrease with *Aspergillus* in all weeks (except 4 and 8) with a shift toward higher wavenumbers. *Cladosporium* also caused a decrease in intensity and peak shift but with the exception of samples in week 10. The *Penicillium* caused a vibrational decrease but no peak shift, with the exception of the leather in week 10. *Aspergillus*, *Cladosporium* and *Penicillium* incubation had the same effect on the C-H$_2$ region at 2870-2842cm^{-1}. The natural biofilm did not cause and significant change in these regions.

Table 4.9- The assigned ATR-FTIR peaks for leather which exhibited significant change after incubation with A. versicolor, C. cladosporiodes, P. brevicompactum and the natural biofilm for 12 weeks. Spectra were produced from an average of 32 scans between 4000-400cm^{-1} and at a resolution of 4cm^{-1} in absorbance mode. Data was baseline corrected, normalised (SNV) and the PCA loadings used to determine significant change in features.
+ denotes increase, - denotes decrease and a combination indicates differences during the 12 weeks

	Wavenumber (cm^{-1})	Assignment	Peak height	Peak base	Peak position
Aspergillus versicolor	2958-2889	C-H stretching	- + -		+
	2870-2842	C-H$_2$ stretching	- + -		+
	1675-1590	Amide I- C=O stretching, C-N stretching & C-H-N in-plane bending	- + -		
	1569-1536	Amide II- N-H in-plane bending, C-N stretching & C=O in plane bending	- + -		
	1465-1436	C-H$_3$ in-plane bending	- + -		
	1153-1134	Amide III- 1260–1300 α-helix, 1240–1250 disordered structure, 1230–1240 β-pleated sheet	- + - +		-
	1100-959	C-O-C, C-O, C-H and C-N stretching (s)/ bending (b) in primary/secondary alcohols (s), alkenes (b) and aliphatic amines (s)	+		-
	916-910	O-H out of plane bending of carboxylic acids	+ -		
	561-518	Torsional N-H oscillation (525cm^{-1})	+ - + -		
	479-414	N-H wagging in-plane	+ -		
Cladosporium cladosporiodes	2958-2889	C-H stretching	- + -		+
	2870-2842	C-H$_2$ stretching	- + -		+
	1675-1590	Amide I- C=O stretching, C-N stretching & C-H-N in-plane bending	-		
	1569-1536	Amide II- N-H in-plane bending, C-N stretching & C=O in plane bending	-		
	1465-1436	C-H$_3$ in-plane bending	-		
	1153-1134	Amide III- 1260–1300 α-helix, 1240–1250 disordered structure, 1230–1240 β-pleated sheet	- + -		-
	1100-959	C-O-C, C-O, C-H and C-N stretching (s)/ bending (b) in primary/secondary alcohols (s), alkenes (b) and aliphatic amines (s)	+ - + -		-
	916-910	O-H bending of carboxylic acids	+ - + -		
	561-518	Torsional N-H oscillation (525cm^{-1})	+ - + -		
	479-414	N-H wagging in-plane	+ -		
Penicillium brevicompactum	2958-2889	C-H stretching	- + -		
	2870-2842	C-H$_2$ stretching	- + -		
	1675-1590	Amide I- C=O stretching, C-N stretching & C-H-N in-plane bending	-		
	1569-1536	Amide II- N-H in-plane bending, C-N stretching & C=O in plane bending	-		
	1465-1436	C-H$_3$ in-plane bending	-		
	1153-1134	Amide III- 1260–1300 α-helix, 1240–1250 disordered structure, 1230–1240 β-pleated sheet	- + -		- -
	1100-959	C-O-C, C-O, C-H and C-N stretching (s)/ bending (b) in primary/secondary alcohols (s), alkenes (b) and aliphatic amines (s)	+ -	+	- +
	916-910	O-H bending of carboxylic acids	- + -		+
	561-518	Torsional N-H oscillation (525cm^{-1})	- + -		-
	479-414	N-H wagging in-plane	- + -		-

	2958-2889	C-H stretching		
	2870-2842	C-H$_2$ stretching		
	1675-1590	Amide I- C=O stretching, C-N stretching & C-H-N in-plane bending	- +	
	1569-1536	Amide II- N-H in-plane bending, C-N stretching & C=O in plane bending	- +	
	1465-1436	C-H$_3$ in-plane bending	- +	
Natural biofilm	1153-1134	Amide III- 1260–1300 α-helix, 1240–1250 disordered structure, 1230–1240 β-pleated sheet		
	1100-959	C-O-C, C-O, C-H and C-N stretching (s)/ bending (b) in primary/secondary alcohols (s), alkenes (b) and aliphatic amines (s)	+	-
	916-910	O-H bending of carboxylic acids	+	
	561-518	Torsional N-H oscillation (525cm^{-1})	+	
	479-414	N-H wagging in-plane	+	

The amide I peak (1675-1590cm^{-1}) intensity of the leather was reduced in all but the week 6 samples after incubation with *Aspergillus* with the week 12 having the greatest reduction. The *Cladosporium* caused little change after a 2 week incubation with leather, but then reduced the intensity of the amide I. Incubation with *Penicillium* caused a reduction in the amide I with a Greater reduction in the peak at 1650cm^{-1} than the one at 1630cm^{-1}. The natural biofilm reduced the vibrational intensities in this regions for the first 3 weeks of incubation, but there was then an increase in the peak heights. The amide II region of leather incubated with fungi showed the same changes as the amide I range. The asymmetrical peak at 1452cm^{-1} is attributed to C-H$_3$ in-plane bending. Again, *Aspergillus* caused a reduction in vibration for all but the week 6 leather, *Cladosporium* and *Penicillium* caused a reduction in all weeks and the natural biofilm samples showed a decrease in peak height for the first 3 weeks before longer incubation caused an increase. The amide III region of the leather was significantly changed after incubation with *Aspergillus* with both rises and falls in peak height intensity and a shift towards lower wavenumbers for the peak centred at 1160cm^{-1}, the greatest shift occurring in the week 12 samples. *Cladosporium* incubation saw little change in the week 3 samples, but a reduction in the peak height and a shift towards lower wavenumbers for other incubation weeks. The *Penicillium* caused the largest position change in the peak at 1160cm^{-1} and a vibrational increase for weeks 3-6, with the other weeks causing a decrease in intensity. The natural biofilm did not alter the peak position and the changes in peak height intensity were not significant.

The peaks in the region of 1100-959cm^{-1} are attributed to C-O-C, C-O, C-H and C-N stretching in primary/secondary alcohols and aliphatic amines and bending in alkenes. For leather specifically the tannin peak in the region of 1030cm^{-1} and the stretching of C-O-C of the ester and C-O of the carboxylic indicate chemical change. Incubation with *Aspergillus* and natural biofilm caused an

increase in the peak height intensities and a shift towards lower wavenumbers. The leather incubated with *Cladosporium* showed both increase and decrease to peak heights throughout the trial and changes to peak positions. Incubation with *Penicillium* caused the greatest change in this region with an increase in peak heights until week 12, when a decrease was seen. The broad peak centred at 1097cm^{-1} shifted towards lower wavenumbers and lost definition, whilst the double peak at 1034cm^{-1} and 1012cm^{-1} showed a positional shift and a loss in definition with the height difference in the peaks reduced, indicating changes to tannin. The position of the peak centred at 916cm^{-1}, attributed to O-H bending, increased for the first 3 weeks of incubation with *Aspergillus*, but was reduced in the weeks after. The *Cladosporium* showed an increase in intensity for the week 2 and 8 samples but a reduction for all other samples. The peak moved towards higher wavenumbers and was reduced in intensity for all but the week 10 leather samples after incubation with *Penicillium*. The natural biofilm caused an increase or no change in intensity for all of the incubation weeks of leather. For the region of 561-518cm^{-1} there was an increase in vibrational intensity for the first 3 weeks and the samples from week 6 when incubated with *Aspergillus*. There was a reduction in intensity for the other leather samples. For *Cladosporium* inoculation, the leather showed increased peak intensities for the week 2 and 8 samples but a reduction for the others. The leather inoculated with *Penicillium* showed a decrease in peak height intensity for all week except the samples in weeks 8 and 10 and with a shift towards lower wavenumbers. The natural biofilm caused an increase in the peak height for all samples. The N-H wagging in-plane region (479-414cm^{-1}) showed an initial increase in vibrational intensity with *Aspergillus* and *Cladosporium* until weeks 4-6, where there was minimal change and then a decrease in intensity seen for the remaining weeks of incubation. The *Penicillium* caused a reduction in the peak height intensity for all weeks except the samples removed after 10 weeks and there was a shift towards lower wavenumbers. The natural biofilm samples showed an increase in intensity for all weeks of the trial.

The amide I peak heights (1660/1630cm^{-1}) were used to determine whether degeneration of the collagen triple helix had occurred. A change of 0-5% indicates undamaged, 5-12% slightly damaged, 12-20% considerably damaged for this ratio in parchment. Changes of 0-5% were found for *Aspergillus* inoculated leather until week 12 when there was a reduction of 8%. *Cladosporium* inoculated leather showed reductions of 6-7% in weeks 4, 6, 10 and 12 but 0-5% change in other weeks. The *Penicillium* inoculated leather showed the greatest change in this ratio with reductions of 4-17% recorded over the incubation time, the greatest change seen in the week 3 samples. The natural biofilm did not show any changes of over 5%.

An increase to the height of the amide I band is indicative of hydrolysis of protein polymer as an increase in O-H vibrations at 1650cm^{-1}. The ratio of the peak height of the amide I and II can therefore highlight if hydrolysis had occurred. For the leather incubated with *Aspergillus* there was an increase in peak height ratio over all sample weeks, compared to the reference leather. The greatest increases were seen in the week 2 (17%) and week 12 (14%) samples. The *Cladosporium* inoculated leather also showed an increase in peak height ratio with the week 12 samples ratio increasing by 15%. The leather with *Penicillium* showed the greatest change in the peak height ratio with increases of 10-79% and the greatest change occurring in the week 3 samples. The natural biofilm caused a reduction in the peak height ratio until week 6 when the maximum increase (3%) was recorded.

The distance between the amide I and amide II peaks is indicative of collagen denaturation due to shifts in the amide II peak towards lower wavenumbers when there is reduction of the collagen helix to the more disordered gelatin. Changes of 6cm^{-1} and greater are deemed significant. None of the fungal incubation conditions caused a significant change in the peak distance indicating that collagen denaturation has not occurred.

4.3.4.1 ATR-FTIR of parchment

Figure 4.32 details the PCA scores for parchment under all of the incubation conditions. There is no overlap between the control parchment and the samples inoculated with fungi, indicating that there have been significant spectral changes.
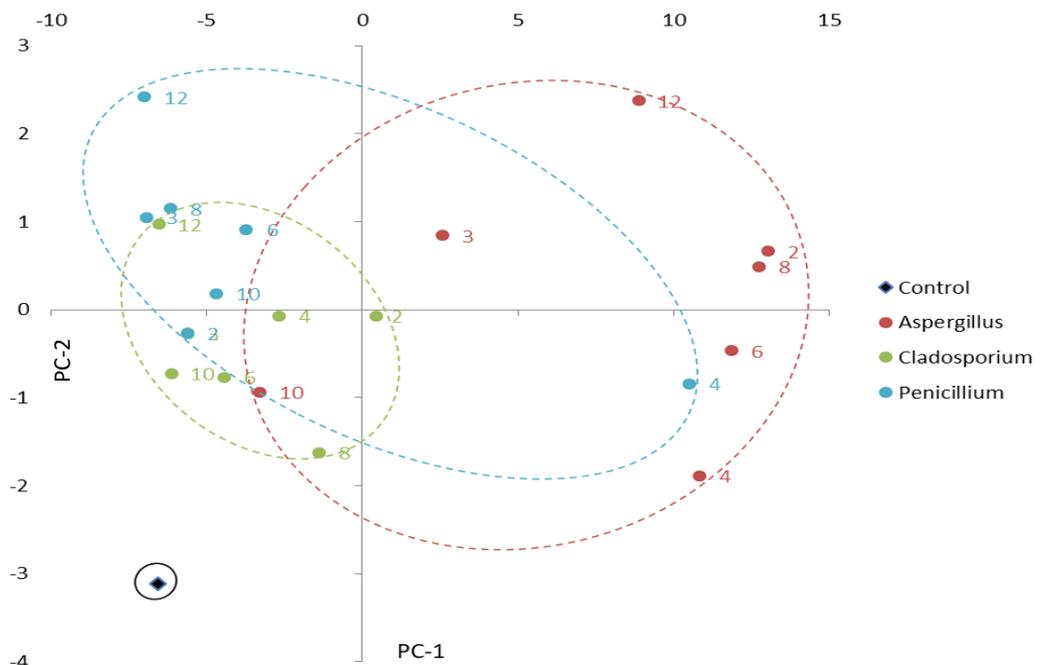

Figure 4.32-Mean PCA (PC-1 x axis & PC-2 y axis) scores for parchment incubated with Aspergillus, Cladosporium & Penicillium *biofilm over 12 weeks at 20°C. Scores were calculated from the baseline corrected ATR-FTIR spectra formed from an average of 32 scans, between 4000-400cm^{-1}, at a resolution of 4cm^{-1}after SNV normalisation*

All of the fungi have overlapping scores with the *Aspergillus* and *Penicillium* being the most widely spread and the *Aspergillus* the greatest difference in score to the control parchment. The significant regions of change for each fungal incubation condition can be seen in Table 4.10.

Table 4.10- The assigned ATR-FTIR peaks for parchment which exhibited significant change after incubation with A. versicolor, C. cladosporiodes, *and* P. brevicompactum *for 12 weeks. Spectra were produced from an average of 32 scans between 4000-400cm^{-1} and at a resolution of 4cm^{-1} in absorbance mode. Data was baseline corrected, normalised (SNV) and the PCA loadings used to determine significant change in features.*
+ denotes increase, - denotes decrease and a combination indicates differences during the 12 weeks

	Wavenumber (cm^{-1})	Assignment	Peak height	Peak base
Aspergillus versicolor	2923-2911	C-H stretching	+	
	2850-2848	C-H$_2$ stretching	+	
	1652-1612	Amide I- C=O stretching, C-N stretching & C-H-N in-plane bending	- + -	
	1581-1512	Amide II- N-H in-plane bending, C-N stretching & C=O in plane bending	- +	
	1112-983	C-O-C, C-O, C-H and C-N stretching (s)/ bending (b) in primary/secondary alcohols (s), alkenes (b) and aliphatic amines (s)	+	+
	655-443	N-H torsional oscillation/wagging in-plane	- + -	
Cladosporium cladosporiodes	2923-2911	C-H stretching	+ - +	
	2850-2848	C-H$_2$ stretching	+ - +	
	1652-1612	Amide I- C=O stretching, C-N stretching & C-H-N in-plane bending	+	+
	1581-1512	Amide II- N-H in-plane bending, C-N stretching & C=O in plane bending	+	+
	1112-983	C-O-C, C-O, C-H and C-N stretching (s)/ bending (b) in primary/secondary alcohols (s), alkenes (b) and aliphatic amines (s)	+	+
	655-443	N-H torsional oscillation/wagging in-plane	- + -	
Penicillium brevicompactum	2923-2911	C-H stretching	+ - + - +	
	2850-2848	C-H$_2$ stretching	+ - +	
	1652-1612	Amide I- C=O stretching, C-N stretching & C-H-N in-plane bending	- +	
	1581-1512	Amide II- N-H in-plane bending, C-N stretching & C=O in plane bending	- +	
	1112-983	C-O-C, C-O, C-H and C-N stretching (s)/ bending (b) in primary/secondary alcohols (s), alkenes (b) and aliphatic amines (s)	+	+
	655-443	N-H torsional oscillation/wagging in-plane	- + -	

The C-H stretching vibrations (2923-2911cm^{-1}) show an increase with *Aspergillus* in all weeks with the samples of week 12 showing the greatest change. *Cladosporium* inoculation caused an increase in intensity for all weeks except 4 and 6, where a reduction was recorded. The *Penicillium* caused a vibrational increase in the parchment for all sample weeks except 3, 6 and 8. The greatest change was observed in the week 12 parchment. *Aspergillus* and *Cladosporium* incubation had the same effect on the C-H$_2$ peak at 2850-2848 cm^{-1}. *Penicillium* only caused a

vibrational increase in weeks 2, 10 and 12 in this region. The amide I region of parchment was reduced in vibrational intensity after incubation with *Aspergillus*, with the exception of the week 10 samples, where an increase in intensity was recorded. The *Cladosporium* caused an increase to the peak height over all incubation weeks with a broadening of the peak base. The *Penicillium* showed an initial decrease in the amide I peak heights but after 8 weeks of incubation there was a linear increase in intensity observed for the remaining samples. The amide II region was changed in a similar way after *Aspergillus* growth with an additional increase in peak height of the week 12 samples. The parchment incubated with the *Cladosporium* and *Penicillium* showed the same pattern of peak intensity change for the amide I and II bands. The peaks in the region of 1112-983cm^{-1} are attributed to C-O-C, C-O, C-H and C-N stretching in primary/secondary alcohols and aliphatic amines and bending in alkenes. Parchment incubated with *Aspergillus, Cladosporium* and *Penicillium* growth all caused an increase in vibrational intensity for all peaks with a broadening of the peak bases. The region 655-443cm^{-1} is attributed to N-H torsional oscillation and wagging in-plane. After incubation with *Aspergillus* and *Penicillium* the peaks in this region showed a decrease in vibrational intensity, with the exception of the week 4 parchment samples that had increased intensity. *Cladosporium* showed more variation throughout the trial with in initial decrease, until weeks 8 and 10 where the samples had increased vibrational intensity. The week 12 samples however decreased in intensity.

The amide I peak heights (1660/1630cm^{-1}) were used to determine whether degeneration of the collagen triple helix had occurred. A change of 0-5% indicates undamaged, 5-12% slightly damaged, 12-20% considerably damaged for this ratio in parchment. For all of the fungal conditions, no change above 3% was observed in the peak height ratio, indicating that there has been no degeneration to the collagen triple helix.

An increase to the height of the amide I band is indicative of hydrolysis of protein polymer as an increase in O-H vibrations at 1650cm^{-1}. The ratio of the peak height of the amide I and II can therefore highlight if hydrolysis had occurred. There were both increases and decreases in the amide peak height ratio of parchment after incubation with *Aspergillus*. The week 6 samples showed the greatest increase (3%) and the week 12 the greatest decrease (6%). There was an increase in the peak height ratio after incubation with *Cladosporium* (<2%) until weeks 10 and 12 where 1% and 2% decreases were recorded. The *Penicillium* caused an increase in the peak height ratio of parchment (<4%) until the week 12 samples where a 5% decrease occurred.

The distance between the amide I and amide II peaks is indicative of collagen denaturation due to shifts in the amide II peak towards lower wavenumbers when there is reduction of the collagen helix to the more disordered gelatin. Changes of 6cm^{-1} and greater are deemed

significant. For all fungal incubation conditions, there were no significant changes to the distance between the amide peaks.

4.4 Discussion

From experimental work on organic substrates and the potential of *A. versicolor, C. cladosporiodes* & *P. brevicompactum*, it has been shown that these fungi have the capabilities to produce hydrolytic enzymes and metabolic products that alter the chemical structure of the materials.

4.4.1 Synthetic enzyme assays

Plate based enzyme assays are a fast and qualitative way to determine whether fungal cultures secrete the enzymes necessary to degrade particular substrates and will give a positive or negative result. One of the limitations of these qualitative assays is that there is little scope for comparison to other studies due to different methodologies nutrient sources being employed (Pointing 1999). However, for the *A. versicolor, C. Cladospiriodes* and *P. brevicompactum* isolated from heritage buildings, a positive or negative result for enzyme production is a useful screening technique. This approach has also been used for screening the enzyme production of fungi isolated from historic structures and environments in the Antarctic (Duncan et al. 2008; Duncan et al. 2006; Bradner, Gillings, et al. 1999; Bradner, Sidhu, et al. 1999). The results of this work have shown that airborne fungi, commonly isolated from the air of historic buildings demonstrated the ability to degrade cellulose on a CMC media, *P. brevicompactum* being the most effective of the three tested. However, the activity is deemed to be low as the relative enzyme activity is lower than 1 for all three fungi, the level used in other works as significant enzyme activity during screening (Duncan et al. 2008; Bradner, Gillings, et al. 1999). Enzymes that degrade other components of cellulosic fibres were secreted in greater quantities by the fungi with the relative enzyme activity of fungi on shorter chain cellulose was between 1.8 and 8.2 with *Cladosporium* clearing the largest area of the media, understandable as it is a plant degrading genus (Bensch et al. 2005). Hemicellulases were also effectively secreted by the fungi with *Aspergillus* having the greatest activity. Bradner (1999) found that hemicellulases and proteases were most effectively secreted by a broad range of fungi at different temperatures including *Penicillium*, *Alternaria* and *Trichoderma* species (Bradner, Gillings, et al. 1999). As these species can adapt to secrete enzymes at lower temperatures, monitoring fungal activity in unheated historic houses during the winter should be recommended.

For the proteinaceous plate assays, it seems that the larger the colony growth, the lower the relative enzyme activity. This could indicate that fungi that are not able to digest the substrate effectively have an increased rate of growth to search for a source of nutrients. Contrary to the findings of other studies, proteolytic activity of the tested strains was low (Bradner, Gillings, et al. 1999). This may be due to the complex protein structures of fibroin, keratin and collagen used in the media for this study whereas skim milk powder was used by Bradner (1999). It has been reported that fibroin is largely resistant to fungal degradation, with the possible exception of *Aspergillus sp*. (Szostak-Kotowa 2004; Seves et al. 1998). This would support the *Aspergillus* having the highest relative enzyme activity on the fibroin substrate, although with minimal enzyme secretion. A previous review indicated that fungi are capable of degrading wool, with *Aspergillus* and *Penicillium* noted among the genera (Szostak-Kotowa 2004), although enzyme secretion was low in the case of this study. *Cladosporium* was not mentioned among the genera capable of degrading wool, although Kavkler (2012) has since found that *Cladosporium* caused the greatest damage to wool fibres (Kavkler & Demšar 2012).

The liquid media assays with specific enzyme activity calculated give a quantitative result for enzyme secretion into a liquid media (Duncan et al. 2008; Duncan et al. 2006; Bradner, Sidhu, et al. 1999). The fungi all showed endo-1,4-βglucanase activity, indicating the ability to randomly scission and depolymerise cellulose chains; although the activity levels were lower than those exhibited by certain niche fungi (Duncan et al. 2008; Duncan et al. 2006). This supports the idea that the airborne fungi in historic houses are not specifically adapted to be there, but if they are deposited on object surfaces and conditions are right, they can opportunistically colonise cellulosic materials and degrade them. The specific protein assays also indicated a higher rate of activity than the palate assays and the by quantifying the protein content of the media (Buroker-kilgore & Wang 1993) before and after growth, the percentage change could be calculated. Contrary to the plate assays, this showed that the fungi are capable of reducing the long chain protein content of silk, wool and collagen containing materials when there are not constrained by plate growth. This supports the findings of the confocal microscopy study (Chapter 3) which showed evidence of degradation on all protein fibres.

4.4.2 HPLC-MS

The non-destructive, crude extraction of whole materials after incubation with fungi has enabled the comparison of metabolic and degradation products from samples that were then used in further analysis. Gas chromatography- mass spectrometry has been used extensively to look at fungal volatile organic compounds (Xiao et al. 2014; Müller et al. 2013; Iamanaka et al. 2014;

Matysik et al. 2009; Polizzi et al. 2012; Wihlborg et al. 2008) and solid phase micro extraction was trialled for use in this study. Unfortunately, the RH in the headspace above agar and inoculated whole materials did not produce reliable results with large siloxane peaks, presumed to be from the septa of the auto sample vials. So that the same growth conditions could be used for the samples, solvent extraction and HPLC-MS was used instead (Luciana et al. 2014; Pose et al. 2010; Giorni et al. 2014; Giorni et al. 2008).

4.4.2.1 Cotton

The solvent extracts of cotton gave evidence of pigments, aromatic and toxic compounds, along with polymer degradation products in the form of oligosaccharides, oligopeptides, and glycosides (Szostak-Kotowa 2004; Valaskova & Baldrian 2006; Goodell 2003). *Aspergillus versicolor* and *Penicillium brevicompactum* have been found to produce toxic compounds (Nielsen & Fog Nielsen 2003; Nielsen et al. 1998). The pigments, found in extracts, two in the natural biofilm and one in the *Penicillium* and *Aspergillus*, indicate that the fungal staining of cotton could be reduced by solvent cleaning for these species. There were also large quantities of fatty acid and lipid derived compounds, which have been linked to the microbial load in house dust (Saraf et al. 1997) and are produced during the primary metabolism of fungi (Korpi et al. 2009). Lipids are produced and stored during fungal growth and can account for up to 35% of fungal dry biomass (Dey et al. 2011). Dey et al. (2011) also found that lipid production increased under conditions of nutrient stress for *Alternaria*, indicating that the nutritional profile of cotton was not sufficient for the natural biofilm, which produced the greatest number of lipid derived compounds. Other work has shown fungal lipid content in paper and highlighted the potential for further degradation of the material by lipid auto-oxidation (Florian & Manning 2000). The presence of carbonyl and carboxyl (organic acid/ester) compounds in relation to cellulosic materials are indicative of depolymerisation (Menart et al. 2011; Manso & Carvalho 2009; Garside & Wyeth 2003; Garside & Wyeth 2004b; Bicchieri et al. 2002), which has also been observed in other fungal degradation studies (Kavkler et al. 2015; Kavkler, Gunde-Cimerman, et al. 2011). The continued presence of these compounds in historic materials could lead to further degradative processes occurring, such as acid catalysed hydrolysis (Menart et al. 2011; Manso & Carvalho 2009).

4.4.2.2 Linen

Fewer significant compounds were found in the linen extracts than on the cotton. The presence of glycosides and a hexose in the extracts of *Cladosporium*, *Penicillium* and the natural biofilm indicate that there has been some depolymerisation of the linen (Szostak-Kotowa 2004),

however, this is greatly reduced in comparison to the degradation products of cotton and there are no carbonyl/carboxyl compounds to indicate degradation (Garside & Wyeth 2006; Kavkler, Gunde-Cimerman, et al. 2011). There are also a number of benzene derived compounds, commonly found in indoor environments with fungal growth (Korpi et al. 2009). There are still a number of lipid derivatives, indicative of primary metabolism (Korpi et al. 2009), although are produced as an outcome of nutrient stress (Dey et al. 2011). The cellulose content of linen is lower and the content of lignin and pectin higher than that of cotton (Garside & Wyeth 2006), with the fungal inoculums unable to utilise the latter two (4.3.1.1); indicating that the fungi are not able to digest this substrate effectively. This may indicate why the linen extracts have an increased number of aromatic and benzene derived compounds, likely formed through secondary metabolic pathways and due to nutritional stress (Korpi et al. 2009).

4.4.2.3 Cotton and linen paper

The incubation of fungi on cotton and linen paper produced fewer degradation products then those of cotton alone, but more aromatic, pigments and potential toxins. Cotton and linen paper had some of the lower total colour changes recorded, even after *Cladosporium* (Table 3.2). As pigmented compounds were found in all of the extracts, this indicated that there is potential for reducing fungal staining through aqueous cleaning. There were also a number of lipid like compounds including fatty acyls, alcohols acyl CoAs and glycerolipids. This may indicate nutrient stress in the fungi (Dey et al. 2011) and cause future degradation through lipid auto-oxidation (Florian & Manning 2000). CoAs are also a precursor to many volatile compounds and atmospheric reactions can also occur post fungal growth (Korpi et al. 2009). Potential nutrient stress and volatiles produced through secondary metabolism was also observed for the linen extracts (4.4.2.3). The cotton and linen paper extracts also has a number of benzene along with quinoline, napthol and terpene derived compounds, indicating a similar production of aromatic volatiles to those of the linen.

4.4.2.4 Beech wood paper

There were few degradation products (simple sugars/peptides) that could be attributed to depolymerisation in the beech wood paper extracts, however the presence of carbonyl and carboxylate compounds indicate that depolymerisation had occurred (Bogaard & Whitmore 2002; Menart et al. 2011; Manso & Carvalho 2009; Bicchieri et al. 2002). The organic acids/esters that were produced by the fungi could cause further degradation of the paper through acid catalysed hydrolysis (Menart et al. 2011). There were again pigment compounds found in all of the paper extracts, indicating that some fungal staining could be removed through aqueous

treatment, however, the total colour change of the beech wood paper was still greater than that of the cotton and linen composition (Table 3.2). Similarly to the cotton and linen paper, there were compounds to indicate nutrient stress and secondary metabolism in the fungi, such as benzene, quinoline, napthol based compounds and the production of glycero and phospho lipids; all of which can have implications for the future stability of paper (Menart et al. 2011; Florian & Manning 2000; Florian 2007a).

4.4.2.5 Pine

There was only one significant compound found in the extract of pine after *Aspergillus* incubation, a coenzyme A which could be used for the production of secondary metabolites. This, plus the lack of other significant products indicates nutrient stress (Korpi et al. 2009). The *Penicillium* and *Cladosporium* showed a greater range of compounds including degradation products associated with depolymerisation (oligosaccharides, oligopeptides, oligolactosamines & a carbohydrate/conjugate) (Szostak-Kotowa 2004). There were also carboxylic products associated with cellulose chain scission (Manso & Carvalho 2009). The fatty acid, triacylglycerol and glycerophospholipid compounds may again be an indication of nutrient stress (Dey et al. 2011), particularly as the fungal inoculums do not show specific ligninase activity (4.3.1.1). Although it was not possible to determine the total colour change of the pine after incubation, the presence of pigments in the extracts of *Cladosporium* and *Penicillium* indicate that aqueous cleaning would remove some staining caused by fungal growth.

4.4.2.6 Oak

There were more significant compounds produced from fungal incubation on oak, than pine. These included aromatic, lipid like and potentially toxic compounds. No pigments were found in the ten most concentrated compounds, indicating that colour change as a result of fungal pigments on oak are less likely to be removed through aqueous cleaning. Some compounds that could be associated with depolymerisation were found, including oligopeptides, a monosaccharide derivative and glycosides. However, there were again a number of lipid like compounds that could be indicative of nutrient stress (Dey et al. 2011) as a result of not being able to utilise lignin and pectin and a limited capacity to use cellulose in the oak (4.3.1.1). There were also a higher proportion of terpene, benzene, isoquinoline and naphthalene compounds in oak (than pine), indicative of secondary metabolism, rather than the enzyme based primary (Korpi et al. 2009).

4.4.2.7 Silk

As *Aspergillus* has one of the greatest enzyme capabilities in silk protein media, the protein derived products are likely to be as a result of hydrolytic activity (Szostak-Kotowa 2004; Seves et al. 1998). *Penicillium* also produced a number of protein derived compounds, indicating that there was some hydrolytic activity, although not as much as the *Aspergillus*, supported by the slightly lower specific enzyme activity observed. There were however far more pigmented and aromatic compounds detected and a number of organic acids and alcohols. There were fewer protein derived compounds in the natural biofilm extract but there is a distinct overlap with the *Cladosporium*, including the lipid like molecules and the mycotoxin detected; likely due to the *Cladosporium* and *Alternaria* species isolated from the silk.

4.4.2.8 Wool

The enzyme capabilities of the fungal inoculums indicate that they have a low ability to digest wool. However, a number protein derivatives were found for all growth conditions that were likely a result of hydrolysis (Szostak-Kotowa 2004; Gutarowska & Michalski 2012). The sulphur containing compounds may be as a result of degradation to the sulphur rich cysteine of wool (Szostak-Kotowa 2004; Kavkler & Demšar 2012; Gutarowska & Michalski 2012). The presence of fatty acid amides/esters and other lipid derivatives that weren't found in the control are also evidence of fungal degradation of the wool fibres as a reduction in these compounds is indicated in aged wool fibres (Odlyha et al. 2007). There were also a number of potentially toxic compounds produced by the *Penicillium* and natural biofilm, which may also have been *Penicillium* derived as the genus has been reported to produce them (Fog Nielsen & Smedsgaard 2003; O'Brien et al. 2006; Fog Nielsen 2003; Fog Nielsen 2002).

4.4.2.9 Leather

The *Penicillium* and *Cladosporium*, despite biomass increase over the incubation time, appear to have failed to thrive, as the *Penicillium* produced no significant compounds in the extract and the *Cladosporium* four. These compounds were aromatic and pigmented, indicating nutrient stress (Korpi et al. 2009). Although the presence of the pigments indicated that cleaning of the leather aqueously would improve the appearance after *Cladosporium* growth, which caused the greatest colour change in the leather. The *Penicillium* caused the second greatest change in the colour of the leather after incubation, however a lack of pigmented products found in the extract indicates that those changes would be permanent. The *Aspergillus* and natural biofilm produced more compounds, including oligopeptides associated with protein depolymerisation (Gutarowska & Michalski 2012). There were a number of lipid like compounds that may have

been generated through deterioration of the leather (Orlita 2004; Kowalik 1980), or as a result of prolonged growth and nutrient stress (Dey et al. 2011), with the CoA compounds found in the *Aspergillus* indicative of the further volatile production (Korpi et al. 2009). There were also a number of aromatic and potentially toxic compounds identified, derived from benzene, naphthalene, anthracene, terpenes and quinoline, all of which were likely produced through secondary metabolic pathways and are a sign of nutrient stress (Korpi et al. 2009).

4.4.2.10 Parchment

Fungal growth on parchment saw all fungi more capable of depolymerisation of the substrate with oligopeptides, oligolactosamine, a purine ribonucleoside triphosphate and other amine/amide/peptide derived compounds found in significant concentrations. There were also no lipid like compounds detected and fewer aromatic ones, indicating that the fungi are using primary metabolism of the protein substrate (Korpi et al. 2009). There were also a number of pigmented compounds found, particularly in the Penicillium extracts. Although the total colour change of parchment could not be recorded, these results indicate that discolouration could be reduced through aqueous cleaning.

4.4.3 ATR-FTIR

The technique of ATR-FTIR has been used to look at spectral changes in materials caused by degradation through time, physical and chemical processes (Falcão & Araújo 2014; Puică et al. 2006; Cardamone 2010; Wojciechowska et al. 2002; Badea et al. 2008; Dolgin et al. 2012; Odlyha et al. 2007; Odlyha et al. 2009; Erra et al. 1997; Oh, Dong, et al. 2005; Derrick 1991; Carr & Lewis 1993; Oh, Yoo, et al. 2005) and the degradation caused through fungal colonisation (Naumann et al. 2005; Zotti et al. 2008; Kavkler, Šmit, et al. 2011; Pandey & Pitman 2003; Kavkler, Gunde-Cimerman, et al. 2011). The use of PCA to group changes in materials has also been used (Sebestyén et al. 2015; Watanabe et al. 2006; van der Werf et al. 2017; Luo et al. 2012; Hori & Sugiyama 2003). This work showed that it was possible to identify spectral differences on different materials and group them according to PCA scores.

Due to the drying of samples prior to ATR-FTIR measurements taking place (Koperska et al. 2014), it can be assumed that changes to the adsorbed water in the materials are due to fungal changes in this region. In some materials (linen, the papers and oak), this could be attributed to the changes in hydrogen bonds of the inter/intra-molecular bonds of the secondary structure (O-H stretching 3340-3310cm^{-1}). For other materials, this may be due to changes on the degree of wetting in fibres, likely due to secondary metabolic products like lipids, fatty acids, glycerol and derivatives (section 4.3.2) and also remains of fungal growth not removed by cleaning. This

may explain the reduction in adsorbed water in some beech wood paper and oak samples, both found to contain a significant concentration of glycerophospholipids in the solvent extraction. The oak extract also contained a diacylglycerol which can increase surface wetting and may explain the variation in bound water in samples over the incubation.

4.4.3.1 Cotton

Changes in the C-H and C-H$_2$ vibrations of cotton can be representative of the organic content of a cellulosic material (Garside & Wyeth 2003), indicating that all of the fungi tested reduced the vibrations of organic content of cotton over a 12 week incubation. This has also been found in other studies and was linked with the presence of carbonyl products (Kavkler et al. 2015). The reduced vibrations may also be accounted for by an increase in hydrogen bonding (Garside & Wyeth 2004a). The increase of carbonyl peaks have been observed in other fungal deterioration studies of cotton and linen textiles (Kavkler et al. 2015; Kavkler, Gunde-Cimerman, et al. 2011) and are referenced in literature (Menart et al. 2011; Manso & Carvalho 2009; Garside & Wyeth 2003; Garside & Wyeth 2004b). The results of this study indicate that degradation of the polymer backbone of cotton occurred under all fungal incubation conditions. All of the changes in the spectra of cotton indicate that the fungal inoculums and natural biofilm have to potential to cause depolymerisation of cellulose. The crystallinity indices calculated from the spectra indicate that all of the fungi cause a reduction in the total crystallinity of cotton with a decrease in the cellulose I conformation, and an increase in the less ordered cellulose II. An decrease in total crystallinity with increase in cellulose II conformation has also been noted for the bio deterioration of hemp and that the changes were greater than those observed in environmentally aged fibres, however significant changes to the crystallinity of cotton were not observed (Kavkler, Šmit, et al. 2011). Thermally degraded linen has also been shown to have a decrease in crystallinity through the 1372/2900cm^{-1} index (Garside & Wyeth 2004b), indicating that the results observed do indicate that incubation with fungi has caused degradation to cotton and altered the crystal structure of cellulose. The greater effect of the fungal inoculums, rather than the natural biofilm, in degrading cellulose can be seen in the PCA scores.

4.4.3.2 Linen

The minimal deviation in PCA scores from those of the control indicate that there has been minimal change to the structure of linen, as can be seen in the crystallinity indices, supporting the resistance of linen to chemical degradation (Garside & Wyeth 2004a). Only *Cladosporium* appeared to change the crystallinity by a reduction in the cellulose I content of the linen, as could be expected due to its utilisation of plant matter (Bensch et al. 2005). *Aspergillus*

incubation did not produced any significant spectral changes, apart from the adsorbed water region, indicating that structural and conformational changes did not occur. The most change occurred in regions associated with C-H and C-H$_2$ vibrations and as there was an increase observed for the free O-H region with the *Penicillium* and natural biofilm (in some cases the *Cladosporium*), it is likely that there have been changes to the inter/intra molecular hydrogen bonds of the linen.

4.4.3.3 Cotton and linen paper

The PCA scores of cotton and linen paper indicate that there have been significant vibrational changes in the paper after incubation and there are no treatment groups overlapping with the control samples. Changes in the O-H, C-H and C-H$_2$ regions were also observed in the linen samples and the C-H/C-H$_2$ for cotton. As there was an increase in the C-H/C-H$_2$ stretching after incubation with the fungal inoculums, and changes to the O-H, this indicates that there have been reductions in the hydrogen bonds of the inter and intra molecular regions of fibres. The increase in peak heights in the 1750-1720cm^{-1} region indicate an increase in carbonyl compounds as a result of depolymerisation of the paper fibres (Manso & Carvalho 2009; Menart et al. 2011) and was observed after all incubation conditions. This has also been found in studying foxing on paper (Bicchieri et al. 2002). The *Aspergillus*, *Penicillium* and natural biofilm seem to have altered the crystallinity of the paper. The *Aspergillus* through conformational changes (cellulose I to II) and the others through utilisation of the amorphous regions of the paper (Garside & Wyeth 2004b).

4.4.3.4 Beech wood paper

The PCA scores show that the *Aspergillus* and natural biofilm caused the least variation in spectra, compared to the control paper. Although the *Penicillium* caused significant change in the fewer regions. As with the cotton and linen paper, the beech wood shows changes in the O-H, C-H and C-H$_2$ regions, with the addition of C-C ring breathing & C-O-C stretching and C-OH stretching in primary & secondary alcohols. This indicates that there was a decrease in hydrogen bonds in the C-H species allowing further vibration; this is supported by the increased C-C ring breathing & C-O-C stretching of the polymer backbone. An increase in high wavenumber O-H, C-H and C-O-C species vibration has been observed in other fungal decay work (Mohebby 2005), but found peak height reductions in other regions. Basidiomycete degradation of beech wood also saw an increase in C-O-C stretching, although noted decreased peak height intensities of C-H species (Fackler et al. 2007). This is likely due to a loss in carbohydrate through wood rot, whereas the fungi trialled during this study do not have the enzymatic capabilities for that level

of degradation to the cellulose polymer (4.3.1.1). Fackler et al. also observed an increase in the carbonyl region, attributed to degradative processes (Fackler et al. 2007). The crystallinity of beech wood paper may have been affected by the fungi with the *Aspergillus*, *Penicillium* and natural biofilm showing an increase in total crystallinity. This may be due to shifts in hydrogen bonding and deterioration of the amorphous regions of the paper, thereby producing carbonyl products.

4.4.3.5 Pine

The *Aspergillus* incubated pine showed a significant difference in more regions of the spectra than the other fungi, despite the lack of degradation products and the signs of nutrient stress reported in the LC-MS extracts (4.4.2.5). Increases were seen in the intensity of the higher wavenumber C-H and C-H$_2$ regions, although there were no significant changes to the free O-H peaks for the fungi, indicating that the change might not be related to hydrogen bonding. The C=C and C=O stretching of lignin have been shown to reduce after irradiation (Colom et al. 2003) and longer incubation fungi was shown to reduce these. This is supported by a reduction in the lignin ratio calculated from spectra (Fackler et al. 2007). The effect of irradiation was also shown to be sporadic over the sample period for box and aspen wood, and there was also an increase in the C=O stretching of 1740cm^{-1} after fungal growth in this study, indicating degradation products (Colom et al. 2003). There were both increases and decreases to the carbonyl peaks for pine incubated with fungi during this study. This is attributed to an increase in degradation products and the decrease in hemicellulose intensity, indicating that it has been hydrolysed by the fungi (Pandey & Pitman 2003). There was a decrease in total crystallinity and increase in lateral order with all fungal inoculums. This indicates that there may be a slight shift towards a more disordered conformation, from cellulose II to cellulose I.

4.4.3.6 Oak

No changes in the main lignin regions of the oak spectra were significant (with the exception of an increase to C-O stretching, 1246-1226cm^{-1}), confirming the low enzyme activity of *Aspergillus*, *Cladosporium* and *Penicillium* on a lignin substrate. A reduction in the C-H and C-H$_2$ vibrations of wood was found, along with peak height reductions in the carbonyl region. The vibrations in the carbohydrate region of beech wood were found to reduce after incubation with fungi (Pandey & Pitman 2003; Fackler et al. 2007), although the higher wavenumber vibrations increased in one study, along with changes in the free O-H region (Mohebby 2005). The C=O vibrations of xylan are situated at 1738-1734cm^{-1} (Pandey & Pitman 2003), which were reduced after fungal incubation, indicating that the fungi were able to utilise the hemicellulose content of the wood.

This confirms their ability to hydrolyse these polymers, as seen in the plate assay (4.3.1.1). This indicates that the fungi in this study were not capable of depolymerising the wood cellulose polymer (no reduction in C-H vibration and no carbonyl compounds), but may have caused changes in the inter/intra molecular hydrogen bonding (increase in C-H species vibration and changes in O-H intensity). They were however capable of degrading the hemicellulose content of oak, which is higher in hardwoods (Pandey & Pitman 2003). Pandey & Pitman also observed an increase to the C-O stretching of lignin after fungal growth, attributed to changes in xylan which also displays C-O vibrations in the region (Pandey & Pitman 2003).

4.4.3.7 Silk

Other studies into the degradation of silks have found that the peak intensities of the amide regions have been affected. The amide I peak, used as a marker of structural change, was reduced through increased irradiation exposure (Luo et al. 2012) and increase with natural ageing in parchment, which can also be applied to silk proteins (Derrick 1991; Vilaplana et al. 2015). An increase in vibration is thought to be due to an increase in O-H bending as a result of hydrolysis or an increase in carbonyl species (C=O stretching) as a result of oxidation and was identified in the case of *Aspergillus, Penicillium* and natural biofilm incubation. A reduction in amide I was observed for *Cladosporium* and is due to a reduction in the vibration of C-N stretching & C-H-N in-plane bending of the polymer backbone, indicating a loss of C-N/C-H-N groups, or an increase in secondary bonding. As a decrease in all amide bonds primary and secondary aliphatic amine regions, it is likely the latter is true. The production of aliphatic amines at a result of degradation was also observed in historic silk banners (Vilaplana et al. 2015) and was found after incubation with *Penicillium* and the natural biofilm. Although not highlighted as areas of significant change, the changes in the carbonyl region of silk post degradation were noted in other studies, signifying oxidative degradation and induced through UV and thermal oxidation. (Vilaplana et al. 2015; Nilsson et al. 2010). Exposure to high pH and RH did not cause changes in the carbonyl vibrations in these studies, indicating that the carbonyl peaks observed during this work are likely to be as a result of enzyme degradation, rather than chemical; supporting the specific protein assay findings (see 4.3.1.4) where fungi could reduce the long chain protein content of a silk media by over 30%. Evidence of chemical change is further supported by the differences in skeletal stretching and disulphide species throughout incubation. The fungal inoculums caused the greatest change to skeletal stretching, but only *Cladosporium* was able to significantly alter the S-S bonding of disulphide bonds between the fibroin proteins (Vilaplana et al. 2015; M. A. Koperska et al. 2015; Koperska et al. 2014).

4.4.3.8 Wool

Changes to the C-H and C-H$_2$ regions of wool FTIR spectra have not been reported potentially due to hydrogen bonding effects on protein spectra being weaker and are attributed to the methylamino bonds of protein (Coates 2000). As a reduction in vibrational intensity was seen, this may indicate degradation of the protein polymer backbone. In the untreated control wool, peaks centred at 1732cm^{-1} and 1716cm^{-1} could be attributed to fatty acids (Odlyha et al. 2007). A reduction in the intensity of these areas could therefore indicate degradation of the fatty acids in the wool by the fungi, which has been previously reported (Kavkler & Demšar 2012). Other small peaks and differences noted between the species could be attributed to products from polymer chain scission or derived from the degraded lipids of wool (Kavkler & Demšar 2012; Jones & Carr 1998). Kavkler (2011, 2012) reported that there were no distinctive changes to the amide I region of wool after fungal growth and Millington (1997) after photodegradation (Kavkler & Demšar 2012; Millington & Church 1997; Kavkler, Gunde-Cimerman, et al. 2011). However the findings of this study suggest that there was a significant difference to the amide I peak of wool after fungal growth and as there was an increase in intensity, this could be indicative of depolymerisation, the breaking of disulphide bonds and hydrolysis (Derrick 1991; Carr & Lewis 1993). As there were few new carbonyl peaks observed in the wool spectra, it is likely that hydrolysis, rather than oxidation is the primary method of deterioration (Derrick 1991). A similar result was also found in the study of photodegraded wool (Carr & Lewis 1993). Decreased intensity of the amide II region were observed in wool inoculated with *F. fomentarius* and was also attributed to hydrolysis (Kavkler & Demšar 2012). The amide III region is indicative of conformational changed in the wool (Wojciechowska et al. 1999). As the peak height reduced after fungal incubation and shifted towards lower wavenumbers, this is indicates an increase in structural order and may be due to hydrogen bonding (Jones & Carr 1998; Odlyha et al. 2007).

Changes to the region of 1102-1000cm^{-1} indicate changes in sulphur-oxygen species and that the cysteine derivatives of fibres have been altered as a result of fungal growth. This would have implications to the secondary structure of keratin due to the role of the di-sulphide bridge between cysteine residues as a stabilising intra and inter molecular bond (Jones & Carr 1998; Carr & Lewis 1993; Wojciechowska et al. 2004). A reduction of sulphur- oxygen species as a result of fungal growth was also observed with *A. clavatus* (Kavkler & Demšar 2012). The breaking of disulphide bonds is indicated by the production of *S*-sulphocysteine (Erra et al. 1997), which was observed during the first week of incubation with *Aspergillus*, *Cladosporium* and *Penicillium*, but not with the natural biofilm. A study of photo-degraded wool also found an initial increase in *S*-

sulphocysteine, but with prolonged treatment, this and the other sulphur-oxygen species (except cysteic acid) reduced, presumably due to hydrolysis (Carr & Lewis 1993).

4.4.3.9 Leather

As highlighted by Derrick (1991), the change in infrared spectra is indicative of difference in the particular area analysed, rather than the object as a whole (Derrick 1991). In the case of leather in particular, very distinct colonies could be seen to form, as well as a fine surface growth. If a large colony happened to have formed in the area sample, then this could influence the result. The PCA scores of leather indicated that there had been little change in the spectra of the natural biofilm samples and the *Aspergillus/Cladosporium* samples of weeks 6/3. These samples showed the least change in the amide I/II ratio so the PCA scores may therefore be linked to hydrolytic degradation of the leather. This is supported by the sample with the greatest peak height ratio (week 3 *Penicillium*), being one of the furthest from the control leather PCA scores. It can be seen from the peak height ratios of 1660/1630cm^{-1} and amide I and II bands that some of the fungal conditions have caused changes to the leather. However, it does not appear that denaturation of the collagen has occurred, as was found in thermally denatured & historic parchment and the Dead Sea Scrolls (Derrick 1991; Odlyha et al. 2009). The amide I/II height ratios in this study decreased, rather than the increases observed in other parchment degradation studies (Derrick 1991; Odlyha et al. 2009). This is likely due to the reduction in intensity of the amide I peak that was observed and a possible reduction in protein content for the leather inoculated with fungi. There were also changes to the C-H, C-H$_2$ and C-H$_3$, indicating changes in the inter/intra molecular bonding of the leather. No significant change to the free O-H region were found but there was a decrease of the O-H features associated with the amide I peak. This could mean that the changes are related to hydrogen bonds and cross linking (Larsen et al. 2005). These changes may also be changes in orientation of fibres, rather than degradation (Bicchieri et al. 2011). As there were no significant changes seen in the carbonyl region, it is unlikely that oxidative degradation has occurred (Dolgin et al. 2012), although there were changes in the 1100-910cm^{-1}, associated with the tanning components of tannin, esters and carboxylic acids. Decreased vibrational intensity in these regions has previously been noted in historic tanned parchments, although changes in this study were not consistent and likely caused by colony placement on the leather (Bicchieri et al. 2011). It has also been reported that there would be a loss of fatty compounds and tannins after fungal growth (Kowalik 1980).

4.4.3.10 Parchment

Fewer regions of the parchment spectra were significantly affected by fungal growth when compared to the leather. As there were changes to the C-H and C-H$_2$ regions, with the amide I peak, this may indicate changes to the hydrogen bonding of parchment, although this may also be related to fibre orientation (Bicchieri et al. 2011). Changes in the amide I and II regions were interrogated using indices but no significant degeneration or denaturation of the collagen triple helix were found in this study (Derrick 1991; Odlyha et al. 2009). Changes in the amide I peak height were inconsistent over the trial indicating that hydrolysis may have occurred, although this was not uniformly seen over the sample/sample positions of each week, again indicating that the damage is not homogenous and closely related to colony margins (Derrick 1991). Other changes to the spectra indicate stretching and bending of the fingerprint region indicate stretching and bending of the skeleton and functional groups with an increase in the aliphatic amine region (Derrick et al. 1999), although as no significant carbonyl product were detected, this does not indicate depolymerisation. Although changes to parchment have been found after fungal growth, there does not appear to have been significant depolymerisation of structural changes related to these species in the areas sampled. This is supported by the large number of protein degradation products that were found in the LC-MS extracts.

The three most commonly isolated fungi from UK heritage buildings and the natural biofilm of materials have shown the capability to chemically alter substrates through primary metabolic enzyme degradation and the production of secondary metabolic products, some of which can continue to degrade the polymer structure, change material properties, have toxic effects to humans and aesthetically alter objects.

5. Physical changes cause by fungal growth on organic materials

This chapter aims to assess the mechanical changes in materials after fungal growth has occurred and been treated. The tensile strength of whole materials was used to determine this and the implications of a change in tensile properties discussed. This work will inform the assessment of fungal outbreaks on historic objects and may influence prioritisation of treatment handling decisions and display of objects in a heritage environment.

5.1 Introduction

The mechanical properties of materials can be expressed as a stress, strain (elongation, load) curve and can be produced with weights, a tensile strength tester and dynamic mechanical analysis (DMA) (Odlyha et al. 2009; Kavkler & Demšar 2012; Garside & Wyeth 2004a). During the process of enzyme production and substrate deterioration, fungi can change the mechanical properties of materials through depolymerisation and a reduction in strength (Peacock 2005). Although a material may be weakened by fungal growth, the individual tensile properties (extension, the maximum load and the energy required to cause failure) are all important factors to consider in the future treatment, handling and storage or display of objects (France 2004). Testing the tensile strength properties of textiles and paper has been widely reported (Hackney & Hedley 1981; M.A. Koperska et al. 2015; British Standards Institution 1999; Błyskal 2015; Zou et al. 1994). There have also been studies investigating the tensile changes that occur after fungal growth (Magaudda 2004; Kavkler & Demšar 2012; Błyskal 2015; Kavkler et al. 2015; Abdel-kareem 2010).

This work aims to assess the mechanical changes after fungal growth as an expression of the degradative capabilities of fungi on a substrate, the secondary metabolic products produced and the physical and chemical changes that have occurred in the substrate. This work will be supported by the findings of Chapters 3 & 4. By considering the outcome of fungal growth on materials holistically, it is hoped that the risk to objects from fungi can be better understood.

5.2 Methods

The selection and preparation of organic substrates and inoculation techniques can be found in Chapter 3.2. Preliminary tensile strength tests determined that the wood and parchment samples could not be analysed using a tensile test machine due to limitations in the material available and inhomogeneity. DMA using a tensile clamp was found to be a suitable alternative but the equipment was not available at the time of this trial. It was therefore not possible to assess the mechanical properties of the wood or parchment samples.

The experimental samples were the whole material substrates used for the ATR-FTIR and HLPC-MS studies so the standard strip test method was used as the basis for testing (BS EN ISO 13934-1:1999 British Standards Institution, 1999). As detailed in Chapter 3.2, each sample was prepared to 115mm by 10mm, cut from the same length of material and in the same orientation. Sample deviations were recorded with digital callipers and can be found in Table 3.1. An Instron 5544 tensile tester, with Bluehill software version 1.4, with data acquisition every 100ms and when the load changed by one Newton or greater. Rubber faced serrated jaws were used to grip the samples, to prevent slippage, and a 1KN load cell. A constant force was applied to the test samples and the rate of extension (mm) and load (N) were recorded. This forms a standard tensile curve, from which can be calculated the energy at the point of rupture, the modulus of the curve, the percentage extension of the sample and the maximum load. All experiments were performed under ambient conditions as it was not possible to control the environment. Temperature fluctuated over the experimental period between 15-28°C with an average of 22.9°C and the relative humidity between 40-53% with an average of 47%.

Five repeat samples were prepared for each experimental condition and the variability of sample dimensions recorded. Each sample within a test group was cut adjacent to the next from the whole material to ensure that there were no samples that contained the same warp fibres or grain so that the tests would not be related. Optimisation was performed to determine the rate of extension, sample orientation and the gauge length (the initial distance) between the jaws. The rate of extension was tested at 1, 3, 5 and 10mm/min for each of the materials. Although the experimental time was reduced when the speed was 10 mm/min, there was a loss in tensile strength for some of the materials. As 1mm/min was more consistent, but took too long to run, a rate of 3mm/minute was chosen. The orientation of the samples was tested for each material. There was little difference for the paper, but the textiles were stronger and had less deviation in the warp direction so this was chosen as a parameter for all samples.

The sample size was limited, by the size of Petri dish available, a maximum of 11.5cm. As a result, gauge lengths of 50mm and 60mm were trialled, 2.75-3.25mm in each grip. A lower maximum load was recorded for the 60mm samples, likely due to the increase in fibre ends exposed as part of the sample. Although this is more realistic in terms of real life objects, there was also an increase in sample deviation and more grip slippage as less of the sample was held. It was therefore decided to test samples at 50mm gauge length with 3.25mm in each grip.

All samples were tested using an extension rate of 3mm/minute, in the warp direction (nose to tail for leather and along the length of the paper) with a sample size of 11.5cm and gauge length of 50mm. Samples that ruptured close to the holding grips were discounted from further calculations. Pre-loads were not applied to samples to ensure consistency, so the data points of the tensile curve before the point at which the sample became taught were also removed from calculations.

Figure 5.1 shows and example tensile strength curve and the data derived. The maximum load (N) and extension (mm) at the point of sample failure were recorded and the modulus of the curve/elasticity calculated between 0.1-.03mm of extension using Equation 5.1. The modulus indicated initial extensibility in fibres where stress is proportional to strain, with this reducing as fibres degrade and become less elastic (France 2004; Roylance 2001). As the tensile test continues, the stress/strain becomes disproportionate and once the proportional limit has been passed (the linear section of change in a tensile curve), there is an increased plastic flow in the material causing rearrangement of the fibres and their molecular structure (Roylance 2001). Materials with less plasticity will have a lower maximum extension. Plastic flow is largely
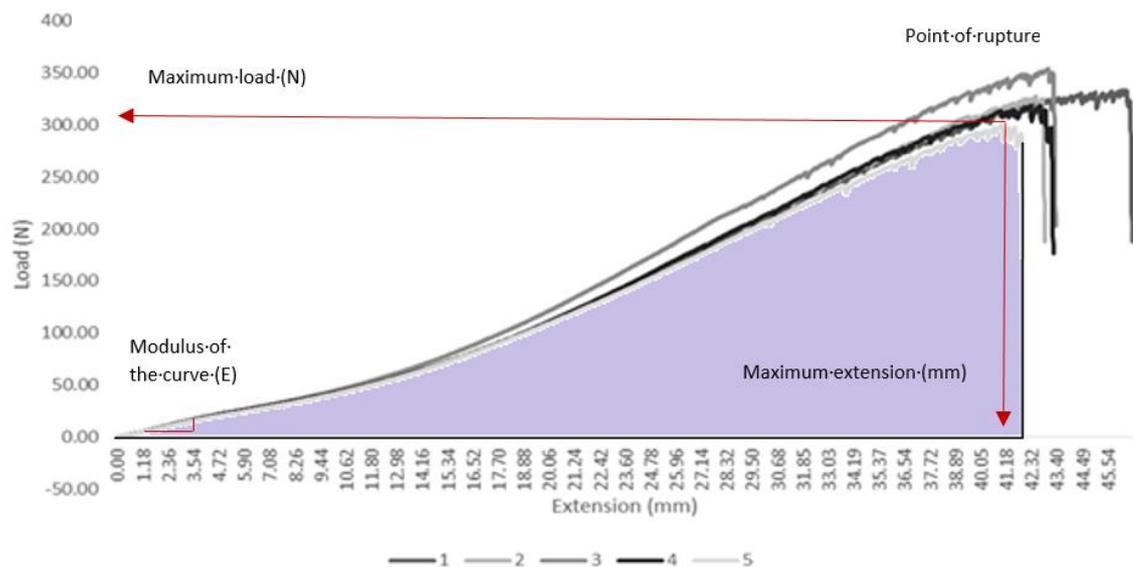
Figure 5.1- An example tensile strength cure for leather at 3mm/min extension rate detailing the key features of the curve, extension (mm) and load (N). From this the modulus of the curve (E) and the area under the curve which is equivalent to the energy required to rupture the sample (shaded area).

equivalent to the elastic limit and once a material has been taken beyond this point, the stretching effect is likely to be permanent and the material will not return to its original shape when the force is removed (Roylance 2001). The area under the tensile curve (shaded in Figure 5.1) is the equivalent to the energy of rupture of the sample (Roylance 2001). This was calculated from multiple trapezoidal areas (100 data points) and then summed. Equation 5.2 represents this calculation.

Equation 5.1- The modulus of elasticity (E) where Y is the load and X the extension. This was calculated between 0.1-0.3 of extension for all materials

$$E = \Delta Y / \Delta X$$

Equation 5.2- The energy of rupture, where e is extension and L1 & L2 are the first and last loads of the 100 data points used to calculate the area of the trapezoid. These re then summed and divided by 1000 to give and energy as Nm/J

$$\frac{\sum \frac{1}{2} * \Delta e \, (L1 + L2)}{1000}$$

As all samples were sourced from the same batch and prepared in the same way, differences in tensile properties are assumed to be as a result of incubation with fungi (Kavkler et al. 2015). All analysis was performed in SPSS and Microsoft Excel, according to protocols described by Field or Townend (Field 2009; Townend 2009).

5.3 Results

The results of mechanical analysis using tensile strength testing is reported below, organised by material. The maximum load and extension were recorded for each sample, along with the area under the tensile curve which is the equivalent to the energy required to rupture the material. The initial modulus of elasticity indicates the extensibility of fibres during the linear phase of a tensile curve where stress is proportional to strain. The pine, oak and parchment substrates could not be analysed, details can be found in section 5.2.

5.3.1 Cotton

The mean tensile properties of cotton after incubation under all fungal conditions can be seen in Table 5.1. *Aspergillus* caused a reduction in the initial modulus of cotton for all weeks of the trial, with the greatest change occurring in weeks 6-10 having an decrease of 44-49% and the lowest in week 12 (-22%). *Cladosporium* had a similar effect, although the greatest percentage changes were seen from weeks 3-10 (-28 to -41%). There was again a lesser reduction in week 12 (-12%). The *Penicillium* and the natural biofilm caused the greatest reduction in the modulus after 1 week of incubation (-49% & -46%) and the lowest reduction was again seen in week 12

(-9% & -16%). These results indicate that fungal growth increases the initial elasticity of cotton fibres, although the effect is lessened after 12 weeks of incubation.

The energy required to rupture cotton was reduced in all of the sample weeks after incubation with *Aspergillus*. There was a small change after 1 week (-1%) but then after 2 weeks the greatest reduction in strength was observed, with a 26% less energy required to cause failure in cotton. After 12 weeks of incubation 25% less energy was required to cause failure. *Cladosporium* initially cased an increase or little change in the energy to break cotton over the first 2 weeks of incubation. There was then a decrease in the energy requirements until week 10 when 38% less energy was required to cause failure in the cotton. A similar effect was seen for *Penicillium* with a small increase (0.6%) seen after 1 week but then by week 12, 72% less energy was needed to break the cotton samples. The natural biofilm caused a reduction in energy requirement each week, with the greatest occurring in week 10 where 27% less energy was required to cause failure. Fungal growth on cotton reduces the energy required to break the material, although *Penicillium* had the greatest effect.

As indicated by the reduction in energy required to rupture, the load that cotton was able to withstand before breaking was reduced after incubation with the fungi. The load that cotton could stand before failure with *Aspergillus* showed the least change after 1 weeks incubation (-3%) and the most in the week 2 samples (-18%). By the latter weeks (10-12), there was a 15% reduction in the force needed to break cotton. *Cladosporium* growth caused an increase (1%) in the load at failure, but then a decrease for the rest of the trial. The greatest effect was seen after 10 weeks of incubation, where the samples could stand 43% less force before breaking. *Penicillium* samples showed a similar pattern with a 1% increase in load after a week of incubation and then a 57% decrease in the force needed to break cotton after 12 weeks. The natural biofilm caused a reduction in the force needed to break cotton each week of incubation, with a reduction of 6% after 1 week and 63% after 10 weeks.

After an increase in extension after 1 week of incubation (0.2%), *Aspergillus* then caused a reduction each week until, in the week 12 samples, cotton samples were extended by 22% less before failure. *Cladosporium* cased little change and then an increase in extension (6%) over the first 2 weeks of incubation. The extension at the point of rupture then decreased over the rest of the incubation weeks until the samples in week 12 had a 20% reduction in extension. The *Penicillium* caused a 1% increase in extension after a 1 week incubation with cotton. There was then a decrease in the maximum extension of samples before breaking with a 47% reduction in the week 12 cotton. The natural biofilm showed a similar trend, with a 1% increase after 1 week

and then a decrease in the maximum extension. The greatest change was recorded in the samples of week 10 with a reduction of 33% in the extension of cotton.

Table 5.1- The mean tensile properties for cotton incubated with A. versicolor, C. cladosporiodes, P. brevicompactum *and the natural biofilm over 12 weeks. Mean calculated from 5 repeats with ± standard deviation*

Incubation time (weeks)	Fungal condition	Mean measurements ± standard deviation			
		Modulus of elasticity	Energy of rupture (Nm/J)	Breaking Load (N)	Breaking extension (mm)
0	Control	1.78±0.43	0.21±0.01	93.35±4.09	8.73±0.44
1	Aspergillus	1.21±0.13	0.20±0.02	90.55±5.71	8.74±0.27
	Cladosporium	1.51±0.15	0.22±0.00	94.59±6.44	8.67±0.20
	Penicillium	0.90±0.14	0.21±0.02	94.28±7.49	8.83±0.18
	Natural Biofilm	0.96±0.18	0.20±0.02	91.74±3.61	8.83±0.38
2	Aspergillus	1.30±0.04	0.15±0.01	76.14±3.51	7.83±0.57
	Cladosporium	1.61±0.15	0.21±0.02	86.36±5.32	9.22±0.36
	Penicillium	1.30±0.09	0.19±0.01	88.27±5.55	8.09±0.20
	Natural Biofilm	1.26±0.19	0.19±0.02	87.40±3.32	8.61±0.46
3	Aspergillus	1.17±0.11	0.17±0.00	84.89±3.82	7.60±0.39
	Cladosporium	1.25±0.08	0.18±0.01	80.32±5.34	8.47±0.31
	Penicillium	1.22±0.10	0.17±0.02	81.76±5.17	7.67±0.39
	Natural Biofilm	1.09±0.15	0.18±0.00	82.96±4.33	8.00±0.31
4	Aspergillus	1.20±0.11	0.17±0.02	78.01±5.02	7.46±0.31
	Cladosporium	1.27±0.17	0.19±0.01	85.74±5.48	7.73±0.33
	Penicillium	1.26±0.21	0.16±0.02	79.44±4.57	7.42±0.51
	Natural Biofilm	1.17±0.19	0.18±0.01	81.86±4.24	7.81±0.38
6	Aspergillus	0.91±0.16	0.17±0.01	85.17±5.46	7.75±0.40
	Cladosporium	1.19±0.16	0.16±0.01	75.51±7.80	7.59±0.29
	Penicillium	1.16±0.07	0.15±0.02	74.44±7.70	6.98±0.19
	Natural Biofilm	1.11±0.17	0.10±0.02	59.63±7.51	6.61±0.64
8	Aspergillus	1.00±0.15	0.18±0.02	82.90±5.68	7.69±0.30
	Cladosporium	1.05±0.11	0.14±0.02	70.26±8.24	7.30±0.26
	Penicillium	1.12±0.39	0.19±0.02	85.64±3.63	7.68±0.49
	Natural Biofilm	1.03±0.22	0.10±0.02	56.05±10.45	6.69±0.33
10	Aspergillus	0.93±0.14	0.16±0.02	79.11±5.94	7.62±0.37
	Cladosporium	1.12±0.17	0.13±0.04	60.27±9.69	7.32±0.73
	Penicillium	1.05±0.10	0.13±0.02	68.59±5.32	6.79±0.40
	Natural Biofilm	1.35±0.23	0.06±0.04	34.36±22.92	6.08±1.69
12	Aspergillus	1.39±0.30	0.15±0.01	79.01±3.95	6.81±0.21
	Cladosporium	1.57±0.18	0.16±0.02	80.00±6.83	7.02±0.28
	Penicillium	1.63±0.32	0.06±0.04	40.25±18.88	4.63±0.99
	Natural Biofilm	1.50±0.11	0.15±0.05	75.26±17.44	6.83±0.46

5.3.2 Linen

The mean tensile properties of linen after incubation under all fungal conditions can be seen in Table 5.2. Over the 12 weeks of incubation there was an increase in the modulus of elasticity for linen with *Aspergillus*. The least change was seen in the samples from week 2 (19%) but by the end of the trail, the week 12 samples showed a 127% increase in the modulus. Cladosporium had a similar effect, with the smallest change in the week 1 samples (17%) and the week 10 & 12 samples having an increase of 101-102%. The *Penicillium* caused a decrease in the elastic modulus after a week of incubation (-2%) but then further incubation time caused an increase, with the samples in week 12 having a 114% increase in the modulus. The natural biofilm caused the greatest initial decrease in the elastic modulus after 1 week of incubation (-33%). Further incubation then caused an increase in the modulus with a peak change of 114% in week 10. This indicates that linen incubated with fungi has a decreased elasticity when force is applied and may be more brittle.

After a decrease (-6%) in the samples of 1 weeks incubation, *Aspergillus* increased the energy required to rupture linen over the following weeks, with the greatest increase of 19% seen in week 8. Linen inoculated with *Cladosporium* had a more varied response with both increased and decreased energy requirements recorded throughout the incubation time with no clear trends. The greatest increase in energy needed was in the week 2 samples (18%) and the greatest decrease in week 12, with 16% less energy needed to cause failure. *Penicillium* caused an increase in the energy required to rupture linen in week 1 & 2 and week 12, with all other weeks reducing the required energy to break linen with the greatest reduction observed in week 10 (-34%). The natural biofilm caused an increase in energy needed for all weeks (7 to 20%) except 6, 10 and 12 where there was a reduction in the energy needed by between 5-11%.

The difference in the maximum load of linen was changed by *Aspergillus* and the natural biofilm, although there were no clear trends over the 12 weeks with both an increased and decreased force to break linen observed. After an initial increase in the maximum load, *Cladosporium* incubation then decreased this and by week 12 there was 16% less force required to break the linen. The same was also true of the linen with *Penicillium*, although for those samples the maximum decrease was seen in week 10 (-34%) and there was then an increased load needed to break linen in week 12, 9% more than that of the control.

The breaking extension of linen was increased for all weeks of incubation with *Aspergillus* (4 to 15%); with the exception of week 3, where no significant change was recorded and week 12, where there was a 6% decrease in the maximum extension at the point of failure for linen. *Cladosporium* caused an increase of 10% and a decrease of 9% in the maximum extension over

the incubation with linen, however there were no clear trends in the data. The same was true of *Penicillium* and the natural biofilm with increases of 16% & 11% after 1 week and decreases of 13% in week 10 for the *Penicillium* and week 6 for the biofilm.

Table 5.2- The mean tensile properties for linen incubated with A. versicolor, C. cladosporiodes, P. brevicompactum *and the natural biofilm over 12 weeks. Mean calculated from 5 repeats with ± standard deviation*

Incubation time (weeks)	Fungal condition	Mean measurements ± standard deviation			
		Modulus of elasticity	Energy of rupture (Nm/J)	Breaking Load (N)	Breaking extension (mm)
0	Control	0.59±0.27	0.23±0.06	145.67±23.34	7.55±0.66
1	Aspergillus	0.72±0.17	0.21±0.03	135.30±7.91	7.81±0.62
	Cladosporium	0.68±0.05	0.23±0.03	148.29±12.03	7.79±0.38
	Penicillium	0.57±0.15	0.29±0.04	161.90±12.02	8.78±0.44
	Natural Biofilm	0.39±0.15	0.24±0.05	144.92±15.59	8.40±0.62
2	Aspergillus	0.70±0.20	0.26±0.06	145.95±23.27	8.67±0.83
	Cladosporium	0.96±0.24	0.27±0.04	144.07±16.02	8.28±0.36
	Penicillium	0.81±0.11	0.25±0.03	143.17±6.38	7.95±0.37
	Natural Biofilm	0.99±0.45	0.25±0.02	132.61±8.74	7.98±0.53
3	Aspergillus	1.05±0.17	0.25±0.05	143.08±19.92	7.53±0.44
	Cladosporium	1.02±0.21	0.23±0.03	132.60±11.93	7.34±0.42
	Penicillium	0.72±0.23	0.23±0.05	141.96±28.64	7.28±0.31
	Natural Biofilm	1.01±0.15	0.27±0.04	153.56±26.67	7.62±0.44
4	Aspergillus	0.86±0.33	0.25±0.05	150.51±23.21	8.01±0.58
	Cladosporium	0.94±0.13	0.20±0.04	130.61±20.52	6.87±0.38
	Penicillium	1.06±0.20	0.20±0.04	131.07±20.91	6.91±0.22
	Natural Biofilm	0.90±0.23	0.26±0.04	144.33±5.16	7.80±0.33
6	Aspergillus	0.86±0.33	0.23±0.02	134.44±11.91	7.86±0.66
	Cladosporium	0.91±0.32	0.19±0.03	123.56±10.19	6.93±0.21
	Penicillium	0.72±0.17	0.21±0.01	135.74±3.04	7.76±0.34
	Natural Biofilm	1.00±0.26	0.20±0.03	136.23±11.97	6.54±0.23
8	Aspergillus	0.96±0.28	0.27±0.05	154.39±10.45	8.07±0.49
	Cladosporium	1.03±0.19	0.26±0.09	138.58±21.61	7.61±0.80
	Penicillium	1.07±0.37	0.22±0.05	122.43±36.41	7.26±0.29
	Natural Biofilm	0.85±0.09	0.25±0.04	153.17±15.34	7.97±0.67
10	Aspergillus	0.72±0.21	0.24±0.04	141.60±7.56	7.86±0.80
	Cladosporium	1.18±0.19	0.22±0.03	130.84±26.56	7.46±0.54
	Penicillium	1.01±0.12	0.15±0.06	109.33±41.65	6.57±0.47
	Natural Biofilm	1.25±0.44	0.22±0.06	152.24±25.28	6.81±0.93
12	Aspergillus	1.33±0.31	0.24±0.05	141.84±16.30	7.07±0.30
	Cladosporium	1.18±0.32	0.19±0.03	117.85±14.23	6.88±0.66
	Penicillium	1.26±0.24	0.25±0.05	150.76±10.91	7.13±0.80
	Natural Biofilm	1.19±0.22	0.21±0.05	137.70±22.20	6.68±0.84

5.3.3 Cotton and linen paper

The mean tensile properties of cotton and linen paper after incubation under all fungal conditions can be seen in Table 5.3. The incubation of *Aspergillus* on the paper cased a reduction in the modulus of elasticity for all weeks (-11 to -44%), with the greatest reduction occurring in the week 12 samples. *Cladosporium* produced a similar result (-27 to -48%), but with the greatest reduction seen in the week 1 samples. *Penicillium* caused the most significant change in modulus of elasticity, with reductions of 31% to 58%. The natural biofilm showed a reduction in the modulus for all weeks (-13% to -47%), except the samples incubated for 10 where an increase of 14% was recorded (due to a high load and low breaking extension of 3 samples). This indicates that the elasticity of the cotton and linen paper under low force would be increased after fungal growth.

The energy required to rupture the paper was increased for all of the incubation times by *Aspergillus* (8 to 74%). *Cladosporium* samples were increased for all measurement weeks (25 to 76%) except 6 and 12, due to a high maximum load in one repeat sample. The *Penicillium* inoculated paper had a greater variation in results (from -45% to 66%) and no trend to the changes. The paper grown with a natural biofilm showed an increase to the energy needed to rupture (4% to 48%) over all but weeks 6 and 12, due to variations in the breaking load of repeat samples.

The maximum load of paper was largely decreased after incubation with *Aspergillus* (-11% to -26%), excluding the samples from week 3, where four of the repeats had a higher maximum load than the other incubation samples. Incubation with *Cladosporium* reduced the maximum load of the paper by between 8% and 35%, with the greatest effects were observed in weeks 1, 6 and 12. The *Penicillium* also reduced the maximum force that paper could endure before failure by between 7% and 53%. Paper incubated with the natural biofilm also had a reduced maximum load (-17% to -34%), although as previously mentioned, the samples in week 10 appear to be an anomaly as there was an increase in the loads of three samples..

The growth of *Aspergillus* on cotton and linen paper caused an increase in the extension at breaking point of between 24% and 89%. The same was true for the *Cladosporium* (19%-80%) and the natural biofilm (2%-68%). The *Penicillium* inoculated paper samples had an increased extension at the point of rupture (2%-80%) until week 12, when there was a decrease of 6%.

Table 5.3- The mean tensile properties for cotton and linen paper incubated with A. versicolor, C. cladosporiodes*,* P. brevicompactum *and the natural biofilm over 12 weeks. Mean calculated from 5 repeats with ± standard deviation*

Incubation time (weeks)	Fungal condition	Mean measurements ± standard deviation			
		Modulus of elasticity	Energy of rupture (Nm/J)	Breaking Load (N)	Breaking extension (mm)
0	Control	30.20±2.34	0.01±0.00	16.45±0.48	1.18±0.11
1	Aspergillus	18.96±1.78	0.02±0.00	12.59±0.30	1.81±0.13
	Cladosporium	15.67±1.08	0.02±0.00	11.61±0.55	2.01±0.18
	Penicillium	15.40±2.31	0.02±0.01	11.80±1.92	2.14±0.49
	Natural Biofilm	15.91±1.07	0.01±0.00	10.88±0.77	1.78±0.43
2	Aspergillus	19.82±4.79	0.01±0.00	14.72±0.85	1.47±0.21
	Cladosporium	22.19±2.32	0.02±0.01	14.76±1.38	2.00±0.36
	Penicillium	15.74±1.04	0.02±0.00	12.26±0.62	2.23±0.28
	Natural Biofilm	18.67±0.56	0.02±0.00	13.65±0.64	1.98±0.22
3	Aspergillus	26.76±5.88	0.02±0.01	19.67±3.66	1.60±0.20
	Cladosporium	21.11±2.03	0.02±0.01	14.89±1.40	1.95±0.32
	Penicillium	16.68±2.57	0.01±0.01	11.73±3.18	1.49±0.71
	Natural Biofilm	19.46±1.89	0.02±0.00	13.03±0.84	1.77±0.28
4	Aspergillus	20.36±2.77	0.02±0.01	14.54±1.41	1.85±0.34
	Cladosporium	20.70±1.05	0.02±0.00	15.07±0.72	2.13±0.23
	Penicillium	20.98±1.58	0.02±0.01	15.30±1.37	2.01±0.31
	Natural Biofilm	16.96±3.44	0.02±0.01	11.64±2.47	1.85±0.68
6	Aspergillus	17.29±1.56	0.01±0.00	12.23±1.27	1.69±0.31
	Cladosporium	16.71±1.34	0.01±0.00	10.76±0.50	1.45±0.17
	Penicillium	12.61±1.46	0.01±0.00	7.77±1.57	1.20±0.49
	Natural Biofilm	16.52±1.17	0.01±0.00	10.86±0.63	1.50±0.16
8	Aspergillus	19.80±1.80	0.02±0.00	14.25±0.63	2.22±0.17
	Cladosporium	19.62±1.80	0.02±0.01	13.93±1.15	1.73±0.34
	Penicillium	15.30±1.69	0.02±0.01	11.28±1.35	2.05±0.51
	Natural Biofilm	18.01±2.13	0.02±0.00	12.44±1.05	1.84±0.39
10	Aspergillus	21.13±1.67	0.02±0.01	14.44±1.20	1.70±0.33
	Cladosporium	21.07±0.89	0.02±0.00	13.74±0.45	1.73±0.18
	Penicillium	20.84±2.27	0.01±0.01	12.62±2.37	1.43±0.47
	Natural Biofilm	34.55±15.31	0.02±0.00	21.81±8.75	1.20±0.30
12	Aspergillus	17.02±2.18	0.02±0.00	13.12±1.74	2.07±0.25
	Cladosporium	20.54±2.77	0.01±0.00	12.31±1.58	1.41±0.29
	Penicillium	16.23±1.11	0.01±0.00	9.72±0.83	1.10±0.19
	Natural Biofilm	20.81±3.27	0.01±0.00	12.63±1.57	1.39±0.20

5.3.4 Beech wood paper

The mean tensile properties of beech wood paper after incubation under all fungal conditions can be seen in Table 5.4. The paper inoculated with *Aspergillus* had a reduced modulus of elasticity after incubation, with decreases of 3% to 39% observed. The same effect was recorded for the *Cladosporium* (-14% to -49%), *Penicillium* (-16% to -52%) and the natural biofilm samples (-23% to -42%). Meaning that beech wood paper incubated with fungi is more elastic at low force.

The energy required to rupture beech wood paper increased after incubation with *Aspergillus* (22%-157%) with the greatest change found in the week 4 samples. *Cladosporium* also caused an increase in the energy required (39%-148%), with the exception of the samples in week 8, due to two of the samples having low breaking loads and extensions. The same was seen for *Penicillium* with two week 10 samples having a low breaking load, but other time intervals causing an increase (22%-180%). The natural biofilm samples showed an increased energy to rupture until week 12, where there was a decrease of 8%. As the greatest increase was seen in the week 2 samples (117%), the lowest in week 10 (24%) and it is three of the samples that have lower maximum loads and extensions, it is assumed that this result is not an anomaly.

The breaking load of the paper decreased after incubation with *Aspergillus* (-2% to -26%) except for weeks 4 and 10 where there was an increase in all samples (9% and 18% respectively). For the *Cladosporium* samples, all but those in week 2 (an increase of 15% with all samples at least 10%) had a decreased breaking load (-1% to -41%). *Penicillium* incubation reduced the maximum load of the paper (-3% to -39%), with the exception of weeks 2, 4 and 12 (15%, 15% and 1% increase). The natural biofilm caused a reduced breaking load in all (-1% to -35%) but the week 2 samples (6%).

The breaking extension of the paper was increased by incubation with *Aspergillus* (49%-106%) with the greatest increase occurring in the samples of weeks 3 and 4. The same was found for *Cladosporium* showing an increase of between 35% and 90%, with the greatest effect occurring on the week 2 samples. *Penicillium* also increased the maximum extension of the paper (22%-111%), with week 4 having the greater and week 10 the lesser difference from the control. An increased in breaking extension was also recorded for the natural biofilm samples (30%-90%), with those in week 4 having showing the greatest change and week 12 the least. These results indicate that fungal growth causes paper to elongate further before breaking.

Table 5.4- The mean tensile properties for beech wood paper incubated with A. versicolor, C. cladosporiodes, *P.* brevicompactum *and the natural biofilm over 12 weeks. Mean calculated from 5 repeats with ± standard deviation*

Incubation time (weeks)	Fungal condition	Mean measurements ± standard deviation			
		Modulus of elasticity	Energy of rupture (Nm/J)	Breaking Load (N)	Breaking extension (mm)
0	Control	63.82±5.19	0.01±0.00	32.09±1.84	0.70±0.07
1	Aspergillus	39.39±2.72	0.02±0.00	25.35±1.29	1.18±0.09
	Cladosporium	40.58±1.65	0.02±0.00	26.46±1.30	1.19±0.12
	Penicillium	35.20±6.80	0.02±0.00	23.31±2.81	1.46±0.13
	Natural Biofilm	36.98±4.34	0.02±0.00	21.92±1.35	1.14±0.12
2	Aspergillus	45.99±8.29	0.02±0.01	29.38±4.15	1.26±0.24
	Cladosporium	54.45±2.62	0.03±0.00	37.00±1.16	1.34±0.12
	Penicillium	53.32±5.26	0.04±0.00	36.95±1.99	1.45±0.07
	Natural Biofilm	48.11±4.41	0.03±0.00	33.88±1.61	1.30±0.14
3	Aspergillus	47.21±4.63	0.03±0.01	31.48±3.15	1.45±0.16
	Cladosporium	47.53±2.28	0.02±0.01	28.66±4.26	1.17±0.30
	Penicillium	47.53±2.28	0.03±0.00	31.16±1.58	1.25±0.09
	Natural Biofilm	49.20±2.96	0.02±0.00	31.61±1.65	1.21±0.05
4	Aspergillus	48.19±2.90	0.03±0.01	34.87±1.97	1.45±0.15
	Cladosporium	47.72±4.44	0.03±0.01	31.80±3.39	1.22±0.20
	Penicillium	52.54±3.52	0.04±0.00	36.95±2.33	1.48±0.09
	Natural Biofilm	45.03±2.58	0.03±0.00	29.94±1.31	1.34±0.10
6	Aspergillus	39.25±4.40	0.02±0.00	23.79±3.08	1.04±0.13
	Cladosporium	55.05±2.05	0.02±0.00	31.92±1.22	1.08±0.11
	Penicillium	43.10±1.51	0.02±0.00	29.92±0.99	1.28±0.07
	Natural Biofilm	42.99±4.99	0.02±0.00	24.96±2.62	1.14±0.09
8	Aspergillus	44.46±6.47	0.03±0.01	29.36±3.03	1.37±0.18
	Cladosporium	32.62±4.93	0.01±0.01	18.97±4.06	0.95±0.23
	Penicillium	30.81±14.35	0.02±0.01	19.67±10.77	1.03±0.49
	Natural Biofilm	44.02±3.29	0.02±0.00	27.42±2.11	1.17±0.14
10	Aspergillus	61.62±2.77	0.03±0.00	37.92±0.95	1.26±0.12
	Cladosporium	43.97±4.80	0.02±0.00	26.75±2.13	1.06±0.08
	Penicillium	43.04±6.40	0.01±0.01	21.24±3.55	0.85±0.20
	Natural Biofilm	44.08±3.48	0.02±0.00	26.94±2.73	0.96±0.16
12	Aspergillus	44.35±18.21	0.02±0.01	26.99±9.57	1.13±0.18
	Cladosporium	41.33±4.95	0.02±0.00	26.92±2.56	1.23±0.09
	Penicillium	50.99±4.51	0.02±0.01	32.31±3.49	1.17±0.20
	Natural Biofilm	37.62±2.77	0.01±0.00	20.91±2.04	0.91±0.16

5.3.5 Silk

The mean tensile properties of silk after incubation under all fungal conditions can be seen in Table 5.5. *Aspergillus* caused an increase in the modulus of elasticity after incubation which increase from 1-100% from weeks 1-2. There was then a decrease in this effect over the remaining weeks of the trial. This indicates that *Aspergillus* reduces the initial extensibility of silk, with the greatest effect occurring after 2 weeks. *Cladosporium* also caused an increase in the modulus compared with the control. The effect was larger over the first two weeks of incubation, reduced in the centre until week 12 when an increase of 112% was recorded.

Penicillium too increased the initial modulus of elasticity, although the effect was varied over the incubation time and in week 1 and 6 there was a reduction in the modulus of 13% & 1%. The greatest effect was observed in the week 4 samples with the modulus increasing by 185%, meaning that the silk was far less elastic. The natural biofilm had a similar effect on the silk with an increased modulus of 101-102% by the end of the trial, with the exception of the week 8 samples where there was a reduction.

After a decrease in week 1, the energy required to rupture silk increased with *Aspergillus* by 25% after 2 weeks of incubation. This effect after this point was lessened to 10-13% over the rest of the study, with the exception of the samples in week 6 (influenced by 2 samples having low maximum loads). *Cladosporium* also increased the energy of rupture of the silk over the trail with the greatest effect occurring after 2 weeks incubation where it increased by 25%. The same was true of *Penicillium* with the greatest increase of 35% seen in the week 2 samples. However, by week 12 of incubation, there was then a reduction in the mean energy required to rupture the silk, largely influenced by two much weakened samples. Samples incubated with the natural biofilm all increased the energy of rupture, however the greatest changes were seen towards the end of the trial in weeks 10-12 where the energy required to rupture silk increased by 35-27%.

The breaking load of silk largely increased after incubation with *Aspergillus*, with the samples in week 6 showing a reduction (influenced by 2 samples). The *Cladosporium* also increased the maximum loads of silk with the week 2 and 12 samples showing the greatest changes of 15% & 12% respectively. After an initial decrease in the maximum load was seen in the week 1 samples (-1%), *Penicillium* then also increase the maximum load of the silk with weeks 3 and 10 increasing the load by 17% & 15%. The natural biofilm showed a similar result, with an initial reduction in the maximum load of 2%. An increase in the load was then seen for all subsequent weeks with the latter two having an increase of 21% and 18% from the control.

The extension of silk after incubation with *Aspergillus* was greater than that of the control until week 12, when the extension was reduced by 2.5%. The same was seen for the *Cladosporium* samples with a maximum extension increase of 10% in week 8 but then by week 12 a decrease of 9%. The Penicillium was similar but with the greatest increase in extension found in the week 2 samples (22%) and the week 12 samples reducing the maximum extension of the silk by 6%. The natural biofilm increased the maximum extension of silk for all of the incubated samples, with increases of 12% to 15% between weeks 2-10. The week 1 and 12 samples had a lesser increase of 5-3%.

Table 5.5- The mean tensile properties for silk incubated with A. versicolor, C. cladosporiodes, P. brevicompactum *and the natural biofilm over 12 weeks. Mean calculated from 5 repeats with ± standard deviation*

Incubation time (weeks)	Fungal condition	Mean measurements ± standard deviation			
		Modulus of elasticity	Energy of rupture (Nm/J)	Breaking Load (N)	Breaking extension (mm)
0	Control	0.31±0.09	0.14±0.01	56.59±2.63	8.39±0.43
1	Aspergillus	0.31±0.06	0.13±0.01	56.18±2.01	8.73± 0.46
	Cladosporium	0.49±0.10	0.15±0.02	59.46±4.44	8.92± 0.51
	Penicillium	0.37±0.08	0.14±0.01	55.44±3.00	8.79± 0.43
	Natural Biofilm	0.27±0.09	0.14±0.02	55.99±5.16	9.21± 0.64
2	Aspergillus	0.62±0.04	0.17±0.01	63.28±2.75	9.75± 0.65
	Cladosporium	0.55±0.03	0.17±0.01	64.97±1.49	9.09± 0.66
	Penicillium	0.48±0.12	0.16±0.01	61.09±3.41	9.57± 0.67
	Natural Biofilm	0.51±0.05	0.18±0.01	62.22±2.89	10.26± 0.68
3	Aspergillus	0.56±0.04	0.15±0.01	59.75±2.47	9.25± 0.69
	Cladosporium	0.46±0.03	0.14±0.01	58.36±3.03	8.51± 0.70
	Penicillium	0.35±0.12	0.17±0.02	63.90±5.16	9.63± 0.71
	Natural Biofilm	0.35±0.05	0.16±0.03	66.28±5.32	8.41± 0.72
4	Aspergillus	0.54±0.13	0.15±0.01	60.03±3.43	9.31± 0.73
	Cladosporium	0.40±0.10	0.14±0.02	57.50±3.87	8.78± 0.74
	Penicillium	0.46±0.02	0.15±0.01	60.01±1.41	9.45± 0.75
	Natural Biofilm	0.87±0.08	0.17±0.00	61.26±1.27	9.92± 0.76
6	Aspergillus	0.36±0.07	0.13±0.03	55.66±6.61	8.79± 0.77
	Cladosporium	0.30±0.08	0.15±0.01	61.36±3.31	8.86± 0.78
	Penicillium	0.33±0.30	0.15±0.02	60.02±2.91	9.56± 0.79
	Natural Biofilm	0.30±0.21	0.15±0.02	57.77±4.40	8.95± 0.80
8	Aspergillus	0.30±0.12	0.15±0.01	57.17±2.24	9.35± 0.81
	Cladosporium	0.34±0.21	0.15±0.02	59.53±2.06	9.23± 0.82
	Penicillium	0.24±0.09	0.16±0.02	58.80±3.76	9.48± 0.83
	Natural Biofilm	0.34±0.10	0.17±0.01	60.49±2.50	9.90± 0.84
10	Aspergillus	0.47±0.18	0.15±0.02	62.24±3.63	9.37± 0.85
	Cladosporium	0.40±0.09	0.14±0.01	60.39±2.40	8.50± 0.86
	Penicillium	0.62±0.11	0.18±0.05	68.44±10.60	9.36± 0.87
	Natural Biofilm	0.47±0.11	0.16±0.02	65.15±3.79	9.15± 0.88
12	Aspergillus	0.37±0.07	0.15±0.01	63.01±1.91	8.18± 0.89
	Cladosporium	0.65±0.20	0.16±0.02	63.24±4.43	7.61± 0.90
	Penicillium	0.61±0.05	0.17±0.02	66.54±6.56	8.67± 0.91
	Natural Biofilm	0.36±0.17	0.13±0.02	59.54±3.84	7.89± 0.92

5.3.6 Wool

The mean tensile properties of silk after incubation under all fungal conditions can be seen in Table 5.6. The wool samples inoculated with *Aspergillus* showed a reduction in the modulus of elasticity (-24% to -55%), with a reduction of 41% after 1 week of incubation. *Cladosporium* had a greater effect on the wool with a reduction in the modulus of 54% after a week of incubation and between a 35% and 66% reduction over the other weeks of the trial. The *Penicillium* caused the greatest reduction in the modulus with a 78% decrease after the first week of incubation and between 51% and 81% reductions of the rest of the experiment. The wool incubated with

the natural biofilm again had a large decrease in the modulus of the tensile curve in the week 1 samples (-46%) and a reduction of between 13% and 63% for the others. This indicates that wool colonised by fungi will have a greater initial elasticity when low force is applied to it.

For the wool, there was a reduction in the energy required to cause failure in the material for all of the incubation conditions. *Aspergillus* had a greater effect on the week 4 samples with a 90% decrease in the energy needed to break the wool. For the other samples, the energy required was reduced by 42% to 90%. The *Cladosporium* had a greater effect in wool towards the end of incubation time with the largest decrease occurring in the week 10 samples (-97%). Over the rest of the trial, energy reductions ranged from 27% to 93% in weeks 2 and 8. The *Penicillium* showed a linear trend in reduction, with the smallest change in energy in week 1 (-35%) and the greatest in week 12 (-98%). The natural biofilm samples also had the greatest reduction in the energy required to break wool towards the end of the incubation times with the samples of week 1 being reduced by 14% and those in week 10 by 95% (week 12 samples had a reduced energy of 83%).

There was also a reduction in the maximum load at the point of breaking for all wool samples. The *Aspergillus* inoculated wool caused reductions in maximum force of 22% to 43% with the first two weeks of samples having a 24% decrease. The wool incubated with *Cladosporium* had reduction in maximum load of 18% to 69% with the greatest change occurring in week 10. The *Penicillium* samples again showed the greatest change in breaking load towards the end of the incubation trial, with reductions of 22% to 69%, the latter occurring in the week 12 wool. The greatest effect for the natural biofilm samples was seen in week 10, with decreases on 13% to 61% in the breaking load of wool observed.

The breaking extension of wool inoculated with *Aspergillus* was reduced for all samples by between 10% and 76%, with the latter occurring in the week 4 wool. *Cladosporium* caused the greatest changed in the breaking extension of wool in the week 10 samples with reductions of 11% to 84% over the trial. The wool inoculated with *Penicillium* showed a linear change in maximum extension with a 7% decrease in week 1 and 87% in week 12. The natural biofilm caused a 1% increase in the extension at breaking of the week 1 wool samples. After 2 weeks incubation though, there were decreases of between 31% and 83% in the maximum extension, with the greatest change occurring after 10 weeks.

Table 5.6- The mean tensile properties for wool incubated with A. versicolor, C. cladosporiodes, P. brevicompactum *and the natural biofilm over 12 weeks. Mean calculated from 5 repeats with ± standard deviation*

Incubation time (weeks)	Fungal condition	Mean measurements ± standard deviation			
		Modulus of elasticity	Energy of rupture (Nm/J)	Breaking Load (N)	Breaking extension (mm)
0	Control	2.94±0.66	0.32±0.05	24.61±2.59	16.87±1.45
1	Aspergillus	1.72±0.56	0.18±0.05	18.75±1.29	12.12±2.78
	Cladosporium	1.36±0.09	0.21±0.07	19.02±1.56	14.15±3.74
	Penicillium	1.00±0.41	0.21±0.06	18.02±1.60	15.68±3.83
	Natural Biofilm	1.59±0.52	0.28±0.05	20.76±2.13	17.11±1.45
2	Aspergillus	2.42±0.93	0.15±0.04	18.75±1.38	10.53±1.65
	Cladosporium	1.48±0.37	0.23±0.04	20.20±2.27	15.08±1.39
	Penicillium	1.45±0.75	0.18±0.06	18.09±2.96	13.22±3.06
	Natural Biofilm	2.55±1.09	0.19±0.07	21.46±2.12	11.60±2.79
3	Aspergillus	2.22±0.51	0.14±0.04	19.08±2.15	9.58±2.09
	Cladosporium	1.72±0.86	0.16±0.06	17.45±2.03	11.77±3.14
	Penicillium	2.04±1.08	0.20±0.01	19.20±1.26	13.74±1.42
	Natural Biofilm	2.35±1.03	0.14±0.01	18.46±0.93	10.39±0.54
4	Aspergillus	1.68±0.40	0.03±0.01	14.10±1.99	4.06±0.66
	Cladosporium	1.42±0.19	0.11±0.04	15.07±0.81	10.01±3.00
	Penicillium	2.25±0.49	0.15±0.04	17.25±1.72	11.12±1.86
	Natural Biofilm	1.46±0.40	0.06±0.02	15.72±0.86	5.81±1.11
6	Aspergillus	1.56±0.72	0.15±0.04	16.39±1.81	12.15±1.56
	Cladosporium	0.99±0.27	0.05±0.02	14.49±1.80	5.22±0.92
	Penicillium	1.76±0.92	0.03±0.01	12.19±1.97	4.16±1.05
	Natural Biofilm	1.19±0.34	0.09±0.05	15.70±1.44	7.69±3.44
8	Aspergillus	1.41±0.16	0.18±0.03	15.64±0.92	15.25±2.27
	Cladosporium	1.28±0.34	0.02±0.01	10.51±1.73	3.92±0.85
	Penicillium	1.18±0.27	0.01±0.00	9.92±1.40	3.08±0.39
	Natural Biofilm	1.30±0.49	0.11±0.06	15.07±1.26	9.92±3.87
10	Aspergillus	1.31±0.08	0.12±0.03	16.77±1.14	9.66±1.39
	Cladosporium	1.39±0.23	0.01±0.00	7.56±1.09	2.65±0.55
	Penicillium	0.58±0.36	0.03±0.03	11.90±4.01	4.42±1.94
	Natural Biofilm	1.09±0.25	0.02±0.01	9.61±4.43	2.85±1.26
12	Aspergillus	1.72±0.58	0.15±0.02	15.72±1.38	12.01±1.84
	Cladosporium	1.92±0.79	0.16±0.02	17.34±1.82	12.34±1.01
	Penicillium	1.31±0.45	0.01±0.00	7.61±2.34	2.16±0.50
	Natural Biofilm	2.06±0.48	0.05±0.02	15.47±0.79	5.34±0.95

5.3.7 Leather

The mean tensile properties of silk after incubation under all fungal conditions can be seen in Table 5.7. For all of the fungal treatments on leather there was an increase in the modulus of the tensile curve, meaning that the elasticity of the material under low force was reduced. The *Aspergillus* caused an increase of between 88% and 414% in the modulus of the leather with the greatest change occurring in the week 2 samples. *Cladosporium* had an even greater effect, with increases of 150% to 985% in the modulus of the week 6 samples. The leather inoculated with *Penicillium* had a 157% to 461% increase in modulus recorded with the week 8 samples showing

the greatest effect. The natural biofilm of leather also caused a large increase in the modulus of elasticity, with 220% to 953% changes measured in weeks 6 and 4.

The energy required to break leather was largely reduced for all incubation conditions over the trial, with the exception of samples in weeks 2. *Aspergillus* inoculated leather showed a reduction in the energy needed to rupture of 11% to 63% with the latter occurring in the week 10 samples. The leather of week 2 showed an increase in the mean energy needed of 23%, influenced by four samples with a result greater than those of the untreated leather. The *Cladosporium* samples also had a reduced energy requirement for all weeks (-7 to -67%), but those measured in the second week. Again and increase of 22% was recorded in this week with three samples needing more energy to cause failure. The same was true for the *Penicillium* week 2 samples where a mean increase of 19% was influenced by 3 samples. For the other weeks of the trail the leather inoculated with *Penicillium* showed reductions in the energy needed to break of 11% to 53%. The natural biofilm samples showed an increase of 8% in the energy required to break the leather in week 2, but then a decrease of between 18% and 51% for the rest of the trial with the latter recorded in the week 12 samples.

The maximum load of the leather samples inoculated with *Aspergillus* are varied throughout the trail and range from a 21% increase in the week 3 sampled to a 55% decrease in the week 10. There are no clear trends in the maximum force that the leather with *Aspergillus* can stand before failure. With the exception of weeks 6 and 8 (where a 6% and 55% decrease in max load were recorded), the leather inoculated with *Cladosporium* showed an increase in the force that could be applied before failure of between 6% and 26%. The leather inoculated with *Penicillium* showed an increase in the maximum load at the point of failure for the first 3 and weeks 8 and 12 (6%-32%). The leather samples of the other weeks had reduced maximum loads ranging between 16% and 38%. The samples incubated with the natural biofilm showed a decrease in the maximum load for weeks 3 and 12 (-3% and -4%) and not change for week 8. The samples from the other weeks had increased maximum loads (2%-20%) with the greatest increases occurring in the week 1 and 4 leather samples.

The maximum extension of the leather decreased after incubation with *Aspergillus* with the greatest change occurring in the week 1 and 12 samples (-47% and -50% respectively). The *Cladosporium* samples also showed a decrease in the extension before failure (-21% to -67%) with the exception of the week 8 samples where an increase of 14% was recorded which related to an increase in three samples. A similar result was seen for the *Penicillium* inoculated leather where the week 4 samples had an increase of 5% in the maximum extension, relating to three samples having an extension greater than that of the control. The other sample weeks all

showed a decrease in the maximum extension (-12 to -45%) with the week 12 leather showing the greatest change. The leather incubated with the natural biofilm shows a decreased maximum extension over the 12 weeks (-23% to -55%) with the greatest change occurring in the week 4 samples.

Table 5.7- The mean tensile properties for leather incubated with A. versicolor, C. cladosporiodes, P. brevicompactum *and the natural biofilm over 12 weeks. Mean calculated from 5 repeats with ± standard deviation*

Incubation time (weeks)	Fungal condition	Mean measurements ± standard deviation			
		Modulus of elasticity	Energy of rupture (Nm/J)	Breaking Load (N)	Breaking extension (mm)
0	Control	4.64±0.08	5.89±0.44	323.35±18.64	42.35±0.80
1	Aspergillus	22.18±3.67	3.57±0.84	346.92±52.45	22.32±2.70
	Cladosporium	16.44±2.54	4.30±0.48	347.51±20.31	28.77±1.88
	Penicillium	12.20±1.16	5.25±0.31	379.59±8.67	33.11±1.02
	Natural Biofilm	31.00±2.17	3.97±0.40	387.83±19.80	21.52±1.08
2	Aspergillus	23.83±0.42	7.26±1.59	315.96±44.35	32.02±5.82
	Cladosporium	23.42±4.81	7.19±1.59	396.89±52.42	23.77±5.06
	Penicillium	23.79±6.67	7.01±1.99	378.99±25.42	23.95±6.22
	Natural Biofilm	37.12±6.42	6.36±2.18	328.44±61.96	20.89±1.13
3	Aspergillus	12.48±2.08	4.84±0.52	392.82±83.02	31.74±5.88
	Cladosporium	14.70±1.50	5.47±0.56	354.38±36.73	33.65±1.39
	Penicillium	12.56±0.91	5.10±0.29	425.71±32.22	30.35±1.73
	Natural Biofilm	32.57±2.79	3.89±0.35	313.58±20.19	27.11±3.33
4	Aspergillus	10.48±0.98	4.12±0.36	271.27±20.41	36.71±0.92
	Cladosporium	35.99±3.27	3.37±0.57	357.11±29.54	18.64±2.00
	Penicillium	23.31±3.41	3.10±0.89	200.58±40.42	44.37±4.71
	Natural Biofilm	48.83±5.11	3.70±0.23	386.69±10.17	18.69±1.20
6	Aspergillus	8.84±0.69	4.02±0.49	291.52±20.81	38.20±4.20
	Cladosporium	50.33±5.55	2.18±0.28	302.94±30.21	13.76±0.50
	Penicillium	19.86±0.93	3.42±0.18	273.15±9.84	28.99±2.04
	Natural Biofilm	14.84±11.21	4.73±0.80	351.42±15.78	32.48±7.73
8	Aspergillus	9.49±1.15	5.25±0.57	384.08±25.61	34.37±1.49
	Cladosporium	11.58±3.99	2.72±0.35	145.94±17.11	48.41±6.43
	Penicillium	26.01±4.23	3.99±0.47	343.95±33.96	26.14±1.11
	Natural Biofilm	21.93±2.02	3.67±0.24	323.03±15.62	25.18±0.84
10	Aspergillus	8.72±1.13	2.20±0.43	144.69±44.30	39.39±5.92
	Cladosporium	27.34±4.29	3.80±0.20	407.33±7.60	19.64±1.13
	Penicillium	11.90±4.94	2.76±0.42	182.44±34.03	37.06±4.10
	Natural Biofilm	23.60±1.19	3.37±0.57	326.41±15.37	21.99±2.46
12	Aspergillus	22.43±2.96	3.41±0.44	343.71±14.86	21.25±1.82
	Cladosporium	39.97±4.80	2.87±0.49	341.17±75.14	16.32±1.24
	Penicillium	25.40±1.95	4.12±0.36	371.71±11.21	23.30±2.24
	Natural Biofilm	24.84±2.30	2.91±0.39	309.75±23.15	19.56±0.75

5.4 Discussion

Investigations into the effect of fungal growth on the tensile properties of materials have shown that significant changes can be made on most materials and the identification of fungal species growing on objects is therefore an important factor in risk assessments.

5.4.1 Cotton

Cotton incubated with all fungi exhibited significantly different tensile properties to the untreated control samples. A decrease in the modulus of elasticity means that with low force, there may be a greater elasticity in cotton fibres. This could have implications for objects that may naturally have cotton fibres under tension, such as upholstered furniture or framed textiles. As the natural biofilm of cotton contained examples of *Aspergillus* and *Cladosporium* species (Table 3.3), it is understandable that this incubation condition produced similar results. This result is contrary to other findings, where the initial modulus increased and was attributed to depolymerisation, increased intermolecular bonding and a higher crystallinity (Kavkler et al. 2015). Depolymerisation (an increase in carbonyl species at 1770-1700cm^{-1}) and an increase in crystallinity (investigated using the TCI and LOI) was also found during the FTIR work (4.3.3.1). In addition, HPLC-MS extracts highlighted the cellulose depolymerisation products of oligosaccharides and glycosides (Valaskova & Baldrian 2006; Szostak-Kotowa 2004) with carboxylic and carbonyl species. However, there was also an increase, despite drying, in the adsorbed water content of cotton (1635cm^{-1}) which could cause increased fibre slippage and act as a plasticiser (Garside & Wyeth 2004a; Timar-Balazsy & Eastop 2007). The energy required to cause failure in cotton was decreased after incubation with all of the fungal conditions, with the *Aspergillus* and natural biofilm having a similar effect with a reduction in energy of 26-27%. The *Cladosporium* had a greater effect with a reduction of 38%, but the *Penicillium* was by far the most degradative with a 72% reduction in the energy required to break cotton after 12 weeks of incubation. This is contrary to the result of the specific enzyme activity test for cellulose, in which the *Aspergillus* showed the greatest activity and the *Penicillium* the least (4.3.1.2). Although the CMC plate assay for endoglucanase activity indicated that *Penicillium* had the greater capability for enzyme production. The *Aspergillus* and *Penicillium* also produced a similar number of volatile compounds when extracts were analysed through HPLC-MS (4.3.2.1). This indicated that the limitations of the plate assay may better represent the capabilities of fungi to degrade whole cotton as a substrate. This is supported by the PCA results (Figure 4.23), showing that the *Aspergillus* and natural biofilm are more closely grouped and show less deviation from the control sample spectra than the *Cladosporium* and *Penicillium* samples. The load and the

extension of cotton at the point of breaking was reduced for all of the incubation conditions and this effect was greater the longer that the fungi were growing on the material. Kavkler (2015) found that cotton yarns incubated with *P. corylophilum* and *C. cladosporiodes* for 8-20 weeks also caused a decrease in breaking extension (strain) but an increase in the breaking load (stress). This was attributed to depolymerisation of the cotton and the filling effect of fungal growth in the cotton yarns (Kavkler et al. 2015). As this study has demonstrated depolymerisation and conformational change markers for cotton and the microbial deterioration of textiles reduces the tensile strength of fibres (Peacock 2005), it is assumed that these are the mechanisms for the deterioration of cotton in this case.

5.4.2 Linen

The tensile properties of linen were altered significantly after incubation with fungi, despite the chemical ones having been minimal (4.3.3.2). The initial modulus of the linen was increased in all cases but the first week of incubation with the natural biofilm. This indicates that the textile has become less elastic when put under low force and may be more brittle, also observed in cotton fibres after fungal inoculation (Kavkler et al. 2015). The reduction in elasticity could be attributed to increased inter/intra molecular bonding of the linen fibres (4.4.3.2). The increased in adsorbed water of linen ($1653cm^{-1}$) may also be a factor and wetting can increase the tenacity of linen (Garside & Wyeth 2004a). The energy required to rupture the linen increased for all inoculation conditions. As the only significant chemical effect of *Aspergillus* growth was the increase in the adsorbed water peak ($1653cm^{-1}$), which also occurred in the other incubations, this may have increased the tensile strength of the linen (Garside & Wyeth 2004a). Linen samples inoculated with *Aspergillus*, *Chaetomium* and *Penicillium* species in other work have shown a loss in tensile strength (Abdel-kareem 2010). There was largely a reduction in the maximum load of linen, with the *Penicillium* and *Cladosporium* having the most consistent effect. This is supported by the greater deviations from the control PCA scores indicating a greater change in the vibrational spectra of these species (Figure 4.24), indicating that the reduction is due to chemical changes in the linen. The maximum load of aged and degraded linen is expected to be significantly reduced, based on the findings of other studies (Garside & Wyeth 2004a; Abdel-Kareem 2005). The maximum extension of the linen was reduced by all incubation conditions by the end of the trial, as would be expected from other fungal growth studies of cellulosic materials (Kavkler et al. 2015; Abdel-kareem 2010). As few degradation products were found in the LC-MS extracts of linen and the content for all conditions was more volatile, in addition to the lack of degradation markers found in the FTIR study, it suggests that fungi were not able to successfully depolymerise linen. However, incubation still had effects on the

mechanical properties of the linen, with the elasticity being reduced and elongation after longer incubation.

5.4.3 Cotton and linen paper

The tensile properties of cotton and linen paper have been significantly altered after fungal growth, reflecting the chemical changes summarised in the PCA scores (Figure 4.25). The elastic modulus of paper was found to decrease in almost all cases, indicating that the paper extends more under low force after fungal growth. Under humidity cycling, a low elastic modulus (Alfthan 2004) and the tensile strength (Bogaard & Whitmore 2002) were observed for paper, with depolymerisation and an increase in carbonyl products attributed to the loss of strength (Bogaard & Whitmore 2002). This is consistent with the reduced maximum load that paper could withstand found during this study, however the extension of the paper increased, meaning that there was also an increase in the energy required to rupture the paper in most cases. The depolymerisation of the paper has been shown through the increase in carbonyl peaks observed during the FTIR study (Table 4.3) and there was a likely reduction in hydrogen bonding due to an increase in C-H species vibrations. The increase in maximum extension may therefore be explained by the increase in adsorbed water acting as a plasticiser (Timar-Balazsy & Eastop 2007; Garside & Wyeth 2004a). However it is difficult to attribute tensile changes in paper, due to the complexity of the cellulosic fibres and the matrix formed in paper (Bogaard & Whitmore 2002). The stress on individual fibres was found to vary during humidity cycle creep tests (Alfthan 2004), indicating that the same is likely true of a mixed fibre paper used in these tests. Particularly as cotton fibres have been found to be more susceptible to degradation than linen ones. As the woven fibres of both cotton and linen had reduced extensions after incubation, this indicates that changes in the tensile properties of paper occur in the matrix, rather than the fibres. These tests have shown that cotton and linen paper has a greater extensibility after growth but can withstand lower loads before breaking. This could have implications for the handling of library materials and paper under tension, such as wall coverings.

5.4.4 Beech wood paper

The anomalous results in the tensile strength tests are also reflected in the PCA scores of the FTIR spectra. The *Aspergillus* and to a greater extent *Cladosporium* and *Penicillium* had large deviations in scores with the same sample weeks that have tensile anomalies having either high or low PC1 and low PC2 scores. This indicates that the tensile strength differences are as a result of a chemical change in the paper. The beech wood paper exhibited the same trend for the decrease in initial modulus and increase in extension as the cotton and linen paper (with an

increase in the energy of rupture and decrease in maximum load). This further supports the hypothesis that it is the paper matrix, rather than the fibres that influence the tensile properties of paper.

5.4.5 Silk

The growth of all of the fungi on silk showed a marked decrease in the initial elasticity of the fibre, indicating that even with relatively low force on the material, it is less capable of extension and may be more brittle. The natural biofilm had a similar effect to the other fungal inoculums, potentially due to the presence of *Cladosporium* (Table 3.3). This change is unlikely due to changes in the conformation of silk as the I_β/I_α index indicated a decrease in crystallinity, meaning an increase in the more flexible amorphous random coil conformation (4.3.3.7). These findings are contrary to those of Nilsson (2010) who found that historic and artificially aged silk samples had a decreased modulus and overall extension (Nilsson et al. 2010). As the energy required to rupture silk also increased after incubation with the fungi (excepting the week 12 *Penicillium* samples), it is likely that the reduction in extensibility and increase in strength is due to cross liking in the protein polymer (France 2004). As there is evidence of hydrolysis and depolymerisation after fungal growth, this indicated that there would be shorter molecules with functional groups that could form cross links. This is supported by the increase in aliphatic amine vibrations in the *Aspergillus*, *Penicillium* & natural biofilm and the increased disulphide presence in *Cladosporium* samples. There was also no significant increase in water of the silk samples, meaning that the fibres are likely to me more closely packed and that there would be less slippage between them. The increase to the maximum load of silk is again indicative of greater cross linking in the structure. The increase in maximum extension indicates that the plastic properties of silk have been increased after fungal growth. Although the initial extensibility of the silk was reduced, as the load increased, it is likely that the fabric became taught (with a straightening of the warp yarns) fibre slippage and then changes to the polymer structure occurred (Garside & Wyeth 2004a). The mechanism for this may be strain induced crystallisation, as the fungi caused depolymerisation of the silk, there are likely more chemical species available for cross linking, increasing crystallinity (Richardson et al. 2013).

These findings are contrary to those of Nilsson (2010) who found that historic and artificially aged silk samples had a decreased modulus and overall extension (Nilsson et al. 2010). This indicated that fungi subject silk to different degradation pathways and that after 12 weeks of growth, fibre degradation is not as advanced as those of 16th-17th century silk and those artificially ages by UV, temperature, high pH/RH.

5.4.6 Wool

The mechanical properties of wool are intrinsically linked with the inter and intra-molecular disulphide bonds characteristically formed between cysteine residues (Wojciechowska et al. 1999). The extensibility of wool has been observed after photo-deterioration of wool, and was attributed to the breaking of disulphide bonds and changes in inter/intra-molecular forces (Jones & Carr 1998). As the initial elasticity of wool was increased and the FTIR study indicated an increase, then decrease in *S*-sulphocysteine (a product of disulphide cleavage) and a reduction in cysteine monoxide, this indicates degradation by hydrolysis (Carr & Lewis 1993). The difference in the week 2 samples of the wool is likely due to the breaking of disulphide bonds, shown in the increase of *S*-sulphocysteine and the isolation of these samples in the FTIR PCA scores. The presence of sulphur containing compounds in the HPLC extracts also supports this. The reduction in the energy required to rupture the wool, the maximum load and extension of the wool are likely due to hydrolytic degradation (5.1.3.8) and changes to the inter/intra-molecular bonds of the wool, also observed in other studies of wool inoculated with fungi (Błyskal 2015; Kavkler & Demšar 2012). The maximum load and extension of wool at breaking were both reduced after prolonged incubation, indicating that the wool would be more brittle and liable to bread under lower force. This would have implications for objects that are natural under tension, such as upholstery and hanging textiles like tapestries which typically have a high wool content.

5.4.7 Leather

The modulus of elasticity in leather was increased after all incubations, meaning that the initial elasticity of the leather was reduced after fungal growth, with the leather feeling more brittle. This may be due to a decrease in the fatty and tannin compounds of the leather (Kowalik 1980). This can be demonstrated by a peak height decrease in the tannin FTIR region (around $1030cm^{-1}$) and fatty acid compounds in the fungal LC-MS extracts (4.4.2.9), although these were only found for *Aspergillus* and the natural biofilm. There was generally a decrease in the energy require to rupture leather, contrary to the increase in tensile strength noted in bacterial degradation of leather (Hameed et al. 1996), although cited as a likely effect of fungal growth (Kowalik 1980). The leather samples of week 2 all showed an increase in the energy required to rupture. The RH of a test space may influence tensile properties (Richardson 2009). The mean RH and temperature in the tensile testing space for the time that measurements were taken was 47% & 23°C and on the day that the week 2 samples were tested, the RH was 45% & 21°C. It is therefore assumed that the difference in the tensile properties are due to chemical

variation, as the dimensional properties of the sample showed low deviation. The maximum load at rupture for leather was varied over the trial with each incubation condition. As the colonisation of leather was not uniform and distinct colonies formed, this may account for differences in the force that leather can withstand. This is supported by the variations in FTIR spectra over the trial and the wide spread of PCA scores (Figure 4.31). The maximum extension of leather largely decreased after incubation, as expected (Orlita 2004; Kowalik 1980), meaning that the leather was more brittle. This is again likely due to a reduction in tanning and fatty compounds in the leather (Kowalik 1980), but may also be due to changes in hydrogen bond/cross linking and fibre orientation (4.4.3.9). This could mean that leather post fungal growth might be less flexible and easier to break.

This work has shown that fungal growth on materials can affect the tensile properties differently, depending on their chemical structure and the ability of fungi to degrade them. All mechanical changes can have implications for future display, storage and handling, but particularly for materials that are inherently under tension. Fungal growth could lead to stretching or shrinkage and premature breaking of components.

6. The Treatment & Prevention of Fungal Growth

The treatment of fungal growth on historic objects is an area that is now being documented, but there is no standard treatment protocol and case studies are generally object/material specific. Unfortunately, historic house collections often contain a wide range of objects, not individually considered to be of economic significance individually, but as a whole collection in context (Appelbaum 1994). As a result, the collection as a whole, will be assessed specific cases of fungal contamination may not be identified until scheduled cleaning. Consequently, with large collections to care for, there is usually minimal funding for research into effective treatments on an individual object basis, unless deemed significant. The following work looks at some common treatments employed within conservation and their effectiveness on different organic materials. Biocide and chemical remediation treatments are evaluated and technologies from industry that may be applicable to the heritage sector assessed. The historic house environment, predictive models and climatic control are also considered in terms of fungal growth prevention.

6.1 The conservation cleaning of organic substrates

The degradation of organic materials by microorganisms is often both destructive and irreversible. Paper is particularly vulnerable to fungi, due to its hygroscopic nature and easily accessible nutrients (Sequeira et al. 2012), but textiles, wood and hide products are also at risk (Szostak-Kotowa 2004; Orlita 2004; Blanchette 2000; Kavkler, Šmit, et al. 2011; Abdel-kareem 2010; Sterflinger & Pinzari 2012). In addition to depolymerisation from enzymes, fungi produce secondary metabolic products that can contribute to chemical degradation after active growth has ceased (Florian 2007a; Sequeira et al. 2012; Szostak-Kotowa 2004) and pigments produced are aesthetically disturbing (Tiano 2001; Abdel-kareem 2010; Florian 2007a; Pinzari et al. 2006).

Therefore, for a conservation treatment to be effective, viable fungal material and secondary metabolic products (including pigments) should be removed prior to re-display or storage. The collective knowledge base of how to treat fungal outbreaks within the heritage sector is limited (Sterflinger 2010) and testing of treatment outcomes (beyond sensitivity tests on object materials) are not standard. There are published case studies, relating to specific objects and locations, although due to the specific conditions it is difficult to transfer methodology and predict the outcome. The important considerations for conservation cleaning are does the treatment remove current growth, prevent reoccurrence and reduce the rate of deterioration in the affected material? Treatments should also be minimally invasive and not unduly damage the substrate, a reason why the treatments selected are common practice.

Generalised protocols for object treatment often include the controlled drying of materials infected with fungi and vacuum cleaning to reduce the spore load of the material (Florian 2007a; Stavroudis 2012; Sterflinger & Pinzari 2012; Tiano 2001). Other dry cleaning methods including swabs, smoke sponges and products like Groom Stick may also be used (Sterflinger & Pinzari 2012; Tiano 2001). The aqueous washing of stable organic materials can be very effective at removing stains and soiling and has also been applied to objects after fungal growth, particularly in the case of textiles. Solvent treatments are commonly used for the treatment of water sensitive materials and 70% alcohol, specifically ethanol is one of the most effective treatment for the removal of fungi (Stavroudis 2012; Sterflinger & Pinzari 2012; Nitterus 2000; Konsa et al. 2014; Sterflinger 2010; Sequeira et al. 2012; BACÍLKOVÁ 2006), more so than pure alcohol (Sequeira et al. 2017). Nittérus describes that ethanol of above 80% can denature the lipid features of cells and create a coating, preventing further infiltration of the alcohol (Nitterus 2000). Alcohol treatments also act as membrane active compounds and denature proteins (Sequeira et al. 2012; BACÍLKOVÁ 2006). However, they have also been noted as having the potential for spore activation and the sporicidal effects questionable (Nitterus 2000; Florian 2007a), so they are therefore not yet proven as effective sterilisers for all materials (BACÍLKOVÁ 2006).

6.1.1 The effectiveness of conservation cleaning treatments

Preliminary work on conservation treatments were tested on textile samples infected with *Aspergillus*, *Chaetomium* and *Penicillium.* It was found that the use of solvents and freezing samples increased viability after incubation under the same conditions. Aqueous washing with a surfactant/repeated rinsing and a surface vacuum were the most effective at reducing re-growth, although none of the treatments prevented new growth within 1 month (Downes 2013). This study was performed using visual analysis of fungal growth on cotton, linen, silk & wool and ranking of growth into 5 categories (no growth, 25%, 50%, 75% and 100% surface coverage), similar to the system used for the VTT model fungal index (see section 6.6.1.3) (Viitanen et al. 2010). An extended methodology was developed to include the 10 organic materials and the 3 inoculated fungi used in chapters 3, 4 & 5, to provide quantitative data using spectrophotometry of broth solutions to determine the viable fungal matter that could be removed after the conservation treatments.

6.1.2 Methods

The selection and preparation of the organic material substrates can be found in Chapter 3. All work, including drying, was performed under a laminar flow hood to reduce contamination risk.

Each triplicate 1cm^2 of the ten substrates (cotton, linen, silk, wool, cotton and linen paper, beech wood paper, pine, oak, leather and parchment) was prepared for each of the eight cleaning treatments (control included). Cleaning treatments were designed to mimic those performed during interventive conservation. A 4% water agar (Oxoid) media was used to ensure a sustained moisture content within the materials, but without imparting nutrients.

Cultures of *A. versicolor*, *C. cladosporiodes* and *P. brevicompactum* (obtained during survey phase, see Chapter 2) were incubated on potato dextrose agar (PDA, Oxoid), at 20°C for 7 days prior to spore harvesting. Cultures were flooded with 5ml of de-ionised water, the suspension was centrifuged, cells isolated and rinsed with 2ml of saline solution (0.9% NaCl, 0.01% Tween 80) (Duncan et al. 2008). The clean cells were suspended in de-ionised water and the concentration determined by haemocytometer. The spore suspensions were then diluted to create a final concentration of 1-1.7x10^5. Material samples were inoculated with 100µl of spore suspension (approximately 1000-1700 cells) and distributed evenly with a disposable loop. Samples were sealed and incubated for 14 days at 20°C when growth was visible on all substrates. The materials were removed from the agar surface and dried for 48 hours in loosely covered Petri dishes, to reduce air movement from the laminar flow cabinet. Post drying, samples were brush vacuumed to remove particulate matter from the surface and treated on both sides using conservation treatments: a low powered suction micro-vacuum with a brush attachment, smoke sponge (vulcanised rubber) pressed onto the surface with light pressure and a sweeping motion, Groomstick (natural rubber) rolled over the surface with light pressure, 70% ethanol, 90% ethanol, industrial methylated spirits and de-ionised water were introduced via a single use saturated swab being rolled over the surface with light pressure. Aqueous swab treatments were repeated 3 times until the material was saturated and suspended in a film of liquid. A dry swab was then used to remove excess liquid. The materials were dried again prior to being placed into Flacon tubes and covered with 1ml of maximum recovery diluent (MRD, peptone 1g/l & NaCl 8.5g/l). Tubes were shaken for 30 minutes at room temperature and the material discarded. From the resulting suspension, 100µl was transferred to a 96 well plate and diluted with 100µl of potato dextrose broth (PDB, Oxoid). Figure 6.1 shows the plate layout with the treatment conditions running from A-E and the fungi running 1-12, with X marking the blanks that only contained MRD and PDB. These were included between each set of repeats for calibration and to identify any contamination.

Plates were then incubated at 20°C and 150rpm for 7 days before reading the optical density of the suspension 600nm using a plate reader (BioTek Synergy 2). Blank suspensions of MRD and PDB were used to calibrate. Spore suspensions were diluted from approximately 1700 cells per well to 1 cell per well across a 96 well plate in order to assess the optical density as an expression of cell count. Of the 5 repeat dilutions for each fungi, the median was selected and plotted so that curve could be fitted and expressed as an equation. The equation of each curve was used with the OD readings for each material and the approximate number of cells calculated.
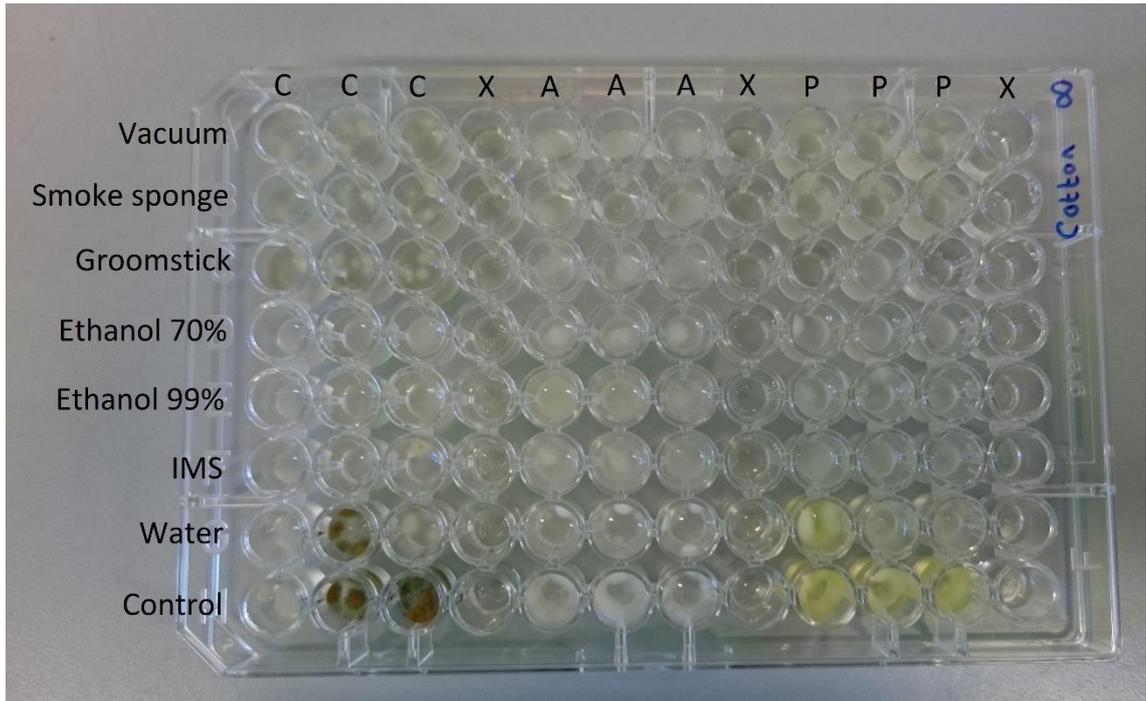
Figure 6.1- Plate layout for the cotton conservation cleaning growth assay, the treatments run (A-E) and the fungal inoculants (1-12). Triplicates of each condition were plated and blanks (X, MRD & PDB only) separate. The fungi used were Cladosporium (C), Aspergillus (A) and Penicillium (P)

6.1.3 Results

The viability of cells from the material suspensions was visible as colonies could be seen in the plate wells of the MRD extracts and not in the blank MRD/PDB wells. The more developed colonies produced pigmentation and sporulated, as can be seen in Figure 6.1 for the control and water cleaning of cotton. The serial spore dilution curves that were fitted to the median optical density readings were $R^2=0.63$ for *Aspergillus*, $R^2=0.90$ for *Cladosporium* and $R^2=0.71$ for *Penicillium*. Table 6.1 shows the results of the cleaning tests expressed as percentage increase/decrease in cell viability compared to the control.

Table 6.1- Percentage difference in viable cell numbers recovered from organic materials after conservation cleaning. Cell counts were calculated from optical densities of serial spore dilution curves for each fungal inoculum.

0-25% increase +	0-25% decrease -
26-50% increase ++	26-50% decrease --
51-100% increase +++	51-100% decrease ---
>100% increase ++++	>100% decrease ----
>200% increase +++++	>200% decrease -----

Blank shows no change from the control

Material	Fungus	Vacuum	Smoke sponge	Groomstick	70% ethanol	90% ethanol	IMS	Water
Cotton	Aspergillus	+++++	-	+++++	+++++	+++++	+++++	---
	Cladosporium	---	---	---	---	---	---	---
	Penicillium	+++++	+++++	+++++	+	++++	---	+
Linen	Aspergillus	---	---	---	+++++	+++++	+++++	+++++
	Cladosporium	---	---	---	---	---	---	---
	Penicillium	+++++	+++++	+++	---	+++	---	+++++
Cotton and linen paper	Aspergillus	---		---	---	---	++++	---
	Cladosporium	+++++	--	-	+++++	+	++++	-
	Penicillium	---	---	---	---	---	---	++++
Beech wood paper	Aspergillus	---	---	---	+++++	+++++	+++++	---
	Cladosporium	---	---	---	---	---	---	---
	Penicillium	+++++	+++++	+++++	---	++	---	+++++
Pine	Aspergillus	---	---	---	---	++	+++++	+++++
	Cladosporium	+++++	++++	+	+++++	+	+++	-
	Penicillium	---	---	---	+++++	+++++	+++++	---
Oak	Aspergillus	---	---	---	-	+++++	---	---
	Cladosporium	++	+++	-	++	+++++	+++	---
	Penicillium	+++++	+++++	-	+++++	+++++	+++++	++++
Silk	Aspergillus	---	---	---	+++++	+++++	+++++	---
	Cladosporium	---	---	---	+++	+++++	+	---
	Penicillium	---	+++++	++++	---	---	++	+++
Wool	Aspergillus	---	+++++	+++++	+++++	+++++	+++++	+++++
	Cladosporium	---	---	---	+	---	+++++	---
	Penicillium	+++++	+++++	+++++	---	---	+	+
Leather	Aspergillus	---	+	---	---	---	---	---
	Cladosporium	---		---	---	---	.	---
	Penicillium	+++++	+++++	+++++	+++++	+++++	+++++	+++++
Parchment	Aspergillus	---	---	---	---	---	+++++	---
	Cladosporium	---	---	---	---	---	---	---
	Penicillium	---	---	---	+++++	++	+++++	---

A positive outcome of a cleaning treatment would be a large decrease in the number of viable cells recovered from the materials post cleaning and drying, determined from the optical density of the spore dilutions. This occurred in the case of *Aspergillus* being vacuumed from pine, although not all viable cells were removed. Any treatment that had an increase in the viable cell count was deemed to be detrimental as the cell count was greater than when cleaning had not occurred. Figure 6.2 shows the number of viable cell reductions recorded for each treatment.
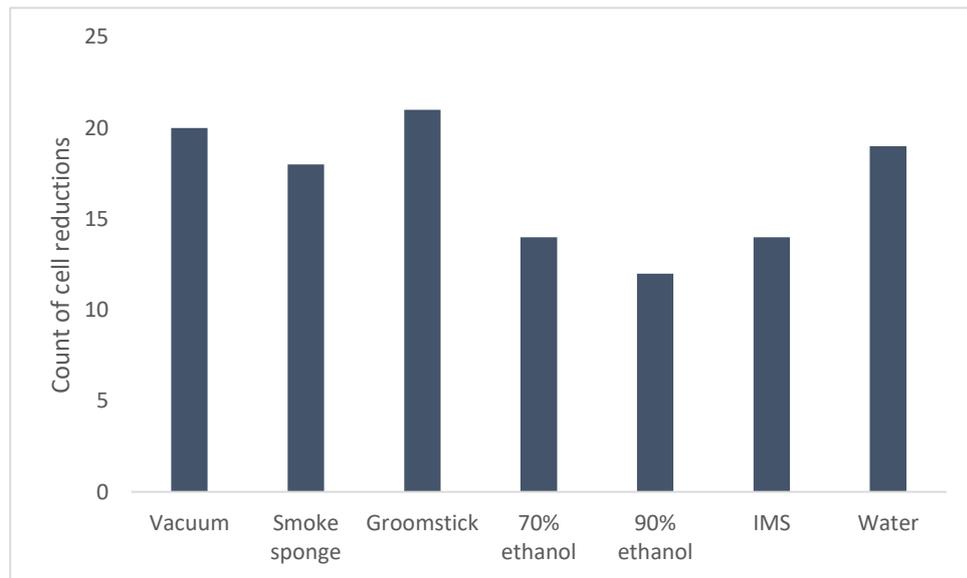
Figure 6.2- The instances of viability reduction post conservation cleaning for each treatment. Cell viability was calculated form the optical density of liquid cultures taken from the clean dry materials, in comparison to a control that was not cleaned.

The dry cleaning treatments (vacuuming, smoke sponge and Groomstick) and water had better outcomes than the aqueous solvent treatments and the 70% ethanol was more effective than the 90%. The effectiveness of cleaning treatments were not uniform for all materials and fungal species, the *Cladosporium* being reduced most widely, followed by *Aspergillus* and *Penicillium*.

The viability of *Aspergillus* was most successfully reduced by the dry cleaning treatments with 9/10 materials having fewer cells than the control, the exception being cotton. The smoke sponge and Groomstick showed a reduction in cells for 8/10 materials with the treatment being ineffective for leather and wool and cotton and wool respectively. Water was also one of the more effective treatments with reduction in *Aspergillus* cells on all but the linen, pine and wool. Solvent treatments were less effective at reducing viable cell transfer but the 70% ethanol was effective in the cases the cotton and linen paper, the leather, parchment and the two wood samples; the 90% ethanol only reduced cells on the first three and the IMS on the woods and leather.

For reducing the viability of *Cladosporium* spores, water was the most effective treatment with lower cell counts than the control on all materials. The Groomstick also reduced viability on all but the pine. The vacuum and smoke sponge treatments were effective on all but the cotton and linen paper and woods (vacuum) and the woods and leather for the sponge, where the leather showed no difference from the control. In the case of *Cladosporium* viability and solvent treatments, the 70% ethanol was the least effective of the solvents with positive outcomes for leather, parchment, beech wood paper, linen and cotton. The 90% ethanol was the same with the addition of wool and the IMS the wool and oak.

Of the three fungi, *Penicillium* was the most resilient and bad outcomes were seen in 65% of cases. Of the dry cleaning treatments, vacuuming reduced cells in the cotton and linen paper, pine, silk and parchment; the Groomstick was the same, with the oak instead of the silk; for the smoke sponge, only the paper, pine and parchment. The 70% ethanol was effective for both paper types, linen and silk, but the 90% only the cotton and linen paper, silk and wool. The IMS reduced cells in cotton, linen and both papers. Water was the least successful treatment and only improved the outcome of the pine and parchment samples. A summary of the cleaning treatments with the best outcome for each material can be seen in Table 6.2. The best outcomes were determined by the greatest reduction in viable cell count post cleaning, recovery and incubation. Where the percentage change was within 0.5%, two options have been presented.

6.1.4 Conclusions

Although there was a 100% decrease in viable calls after vacuum cleaning *Aspergillus* from pine, which showed the greatest reduction, growth did still occurred. This indicates that none of the conservation treatments tested under these conditions were fungicidal, rather than sporicidal and cannot prevent further germination occurring. Some treatments increased the cell count and may have increased germination as stated elsewhere (Nitterus 2000; Florian 2007a).

The combination of drying an vacuum cleaning and treatment (Florian 2007a; Sterflinger & Pinzari 2012; Stavroudis 2012) was effective at removing large particulate matter from the surface of the smoother materials. Although there is not one treatment that would be effective on all materials, generally the dry cleaning treatments seem to be most effective on the materials with a lesser surface texture; the papers, leather and parchment. The water was beneficial to cotton and silk, the two tighter weave textiles and the pine, potentially hydrating the fibres and enabling the suspension of more fungal matter. Solvent cleaning was broadly the better treatment for *Penicillium* on materials with the 70% ethanol being the most effective on paper, as found by Sequeira *et al*. (Sequeira et al. 2017).

Table 6.2- The best treatment outcomes for each material after treatment, determined from the greatest reduction in viable cell transfer. Cell content was calculated from the mean optical density of PDB broth and cell suspensions harvested from the treated materials after drying and median spore dilution curves. If the reduction in cells was within 0.5%, two options are shown. Blanks indicate no treatments caused a reduction in cells from the control which received no treatment.

Material	Fungi	Treatment
Cotton	*Aspergillus*	Water
	Cladosporium	Water
	Penicillium	IMS
Linen	*Aspergillus*	Smoke sponge
	Cladosporium	IMS/Groomstick
	Penicillium	70% ethanol
Cotton and linen paper	*Aspergillus*	Smoke sponge
	Cladosporium	Smoke sponge
	Penicillium	70% ethanol
Beech wood paper	*Aspergillus*	Groomstick
	Cladosporium	Smoke sponge/Groomstick
	Penicillium	70% ethanol
Pine	*Aspergillus*	Vacuum
	Cladosporium	Water
	Penicillium	Water
Oak	*Aspergillus*	Smoke sponge
	Cladosporium	IMS
	Penicillium	Groomstick
Silk	*Aspergillus*	Water
	Cladosporium	Vacuum
	Penicillium	99% ethanol
Wool	*Aspergillus*	Vacuum
	Cladosporium	99% ethanol
	Penicillium	99% ethanol
Leather	*Aspergillus*	99% ethanol
	Cladosporium	Groomstick
	Penicillium	-
Parchment	*Aspergillus*	Smoke sponge
	Cladosporium	Vacuum/Water
	Penicillium	Smoke sponge

It is also important to note that although the dry cleaning treatments may be effective at reducing the viable cell content in some cases, they will not remove metabolic products released during growth (detailed in Chapter 4). These products could continue to deteriorate materials and can be hazardous to human health, in the case of some of the mycotoxins that were identified during this work.

Although this study was small scale, it demonstrates the difficulty of finding treatments for historic objects, particularly those that are mixed media in nature. It would be of use to extend the research by trialling different culturing techniques as there are limitations to the visual ranking (Downes 2013) and liquid broth recover method used. This is due to the subjectivity in the visual and the difficulties in interpretation with the quantitative broth method. Although it was possible to fit curves to the optical densities of spore dilutions, the dark pigmentation and the sometimes globular colonies formed meant that there was variance in results and the

resulting equation models could only represent 63%, 90% & 71% of the results for *Aspergillus*, *Cladosporium* and *Penicillium* optical densities. It would therefore be beneficial to compare the visual, optical density and a digital image analysis (Sequeira et al. 2017) of cleaning experiments to determine the most accurate methodology.

By creating a simple protocol for testing the effectiveness of treatments, it would then be possible to determine the likelihood of re-growth when an object is re-displayed or stored; reducing repeat outbreaks and potential contamination of other materials. The introduction of standardised cleaning tests for fungal growth would also provide a greater industry knowledge and the potential for creating material specific treatment protocols.

6.2 Physical and chemical treatments for fungal growth

In addition to interventive conservation treatments, there are other potentially more invasive methods to remove and prevent fungal growth form occurring within heritage buildings and collections. Below is a summary of techniques that have been applied along with any limitations to general use.

6.2.1 Chemical, temperature based and irradiation cleaning

6.2.1.1 Ethylene oxide

Ethylene oxide vapour treatments are highly effective for the treatment of organic materials colonised by fungi, without damage to the underlying material (Sterflinger & Pinzari 2012). This gas disrupts the cellular metabolism of organisms by alkylation, but can therefore be toxic to humans; leading to its use being severely restricted (Michaelsen et al. 2013; Sequeira et al. 2012; Magaudda 2004). It has also been reported that some materials are more prone to subsequent fungal growth after treatment; potentially due to the production of ethylene glycol, which may influence spore activation (Florian 2007a; Michaelsen et al. 2013). However, when tested on library materials and viability determined through both DNA and culture techniques, Michaelsen *et al*. determined that ethylene oxide was completely effective at rendering the fungi non-viable. Although largely effective, due to the toxic nature and the need for specialist application this makes the approach impractical for general conservation treatments.

6.2.1.2 Ozone

Ozone has been used for the treatment of water and within the food industry for disinfection and the increase of shelf life for products (Guzel-seydim et al. 2004; Kim et al. 2003). Ozone has powerful oxidising properties and is therefore a powerful antimicrobial as well as being used to

remove tastes, odours and colour. It is considered safe for use with food because after exposure to the gaseous form, food will not be left with any residual chemicals and ozone decomposes to oxygen when used at room temperature (Savi & Scussel 2014). The study by Savi and Scussel found that ozone gas treatment (60 µmol/mol for 120 minutes) significantly reduced the growth of mature *Fusarium*, *Penicillium* and *Aspergillus* cultures (particularly the *Fusarium*), all exhibiting hyphal death and the *Penicillium* was unable to grow after further cultureing. The gaseous ozone treatment of conidia also reduced germination to between 3-39% from the 80-99% of the control spores (Savi & Scussel 2014). Ozone was also found to be particularly effective in the deactivation of fungal species found in barley including mycelium and spores, although the spores were more resistant. It was also found that in the case of barley grain, the ozone was more effective inder warmer conditions with a higher water activity (Allen et al. 2003). For wheat and contaminating *Aspergillus parasiticus,* it was found that exposure of ozone at 50ppm for 3 days in a 12.7 tonne grain bin reduced the germination of conidia by 63% and this was the most resistant fungi found (Kells et al. 2001). This shows that the use of ozone gas is effective as a fungistatic agent for some species and has potential as a fungicide. As it is also bacteriacidal and antiviral, without leaving a residue , it could be of potential use for the treatment of historic objects; provided that there is sufficient testing to ensure that degradative oxidation of materials cannot occur during the required treatment time.

6.2.1.3 Anoxia

Anoxic treatments have been used in food packaging and the treatment of insect pests within heritage collections (Appendini & Hotchkiss 2002; Valentin 1993). However, although fungi need oxygen for growth processes, a low oxygen environment does not completely inhibit growth of fungi on proteinaceous material (Valentin et al. 1990) and in fact the control of the RH has a greater effect on the rate of growth. The results of the Valentin study were dependant on the measurement of respiration and so couldn't account for non-respiring cells, like conidia. This indicates that an anoxic environment is likely to be fungistatic, but not fungicidal over time.

6.2.1.4 Temperature change

The thermal treatment of insect pests has been used within the heritage sector for some time (Nicholson & Von Rotberg 1996) and the temperatures used in this process (50-55°C) may remove active fungal growth through dehydration. However, these temperatures are not sufficient to be sporicidal and the change in temperature may in fact lead to the activation of germination in some spores (Florian 2007a). The use of moist heat at a higher temperature is considered to be a more effective treatment for the disinfection of books (95°C at 40%RH for 4

hours) (Tiano 2001). However, during this project, it was found that the use of higher temperatures (121°C) in an autoclave was very destructive to the mechanical properties of materials, particularly leather and parchment (Chapter 5). The reduced tensile strength may however have been due to the pressure or temperature and pressure of the autoclave.

The freezing of materials with fungal growth has been established as detrimental, due to the high water availability on the return to ambient temperatures and the survival rate of spores at the temperatures commonly used, -20-30°C (Downes 2013; Sequeira et al. 2012). Although the reduction of temperature will reduce the rate of growth on materials, the damage that can be caused to vulnerable materials through the freezing process (expansion of materials during the phase change of liquid to solid water), transport/packaging and the potential to induce germination during defrosting, this method is not recommended. The use of freeze drying however, removes the liquid water by reducing the pressure in the system and allowing the solid water to transition to gas phase; the gaseous water is then pumped out of the vacuum to leave the material dry. This reduces damage and dimensional changes within the material, along with the safe removal of water and the desiccation of hydrated fungal matter; however it does not reduce the viability of fungal material that may remain, just reduces the risk of germination (Florian 2007a; Michaelsen et al. 2013). This process is one of the most effective ways of treating organic material after an incident involving wetting (fire or flood) within a collection, where fungal growth can quickly occur with high levels of available water, particularly in the case of libraries where many objects can be affected (Michaelsen et al. 2013). However, materials would need to undergo decontamination post drying.

6.2.1.5 Irradiation

Ultraviolet (UV) radiation is commonly used for the sterilisation of industrial non-organic materials (Sequeira et al. 2012) and has been effectively trailed on stone and plaster within historic collections (Stewart et al. 2008; Lithgow & Stewart 2001; Stanley et al. 2016; Tiano 2001). However, the penetration of this form of radiation is limited, due to its low energy level, this form of radiation is less effective at sterilising thicker materials such as textiles and books (Sequeira et al. 2012; Merka-Richards 2015). The effects of UV light on organic materials are well documented and it is commonly used as an artificial ageing treatment (Luxford 2009; Luo et al. 2012; Colom et al. 2003; Dahlin 1995; Porck 2000) and as the level of disinfection is poor, it is not a suitable treatment for anything other than inorganic collections.

Gamma irradiation has been tested for the cleaning of textile, leather, wood and library materials as it has a good penetration of materials, due to having a short wavelength and

therefore high energy (Sequeira et al. 2012; Guiomar Carneiro Tomazello, M. WIENDL 1995; Sterflinger & Pinzari 2012; Michaelsen et al. 2013; Geba et al. 2014). However the application of this treatment to organic heritage collections is debated, due to the damage that can be caused by free radicalisation of the material, changes to the crystal structure and depolymerisation in high doses (Kasprzyk & Wichłacz 2004; Kugel et al. 2011; Sterflinger & Pinzari 2012; Gutarowska, Rembisz, et al. 2012). Using up to 20 kGy of radiation was shown to reduce the fungal load of library materials, however it was not completely fungicidal with some species being more resistant (Guiomar Carneiro Tomazello, M. WIENDL 1995) and those that were not removed has a tendency towards increased pigment production (Pavon Flores 1976; Sequeira et al. 2012). There was also greater fibre damage recorded with radiation of over 10kGy in proteins (Geba et al. 2014). Other studies have found that dosed below 10kGy were effective, but these were based on culture methods (Magaudda 2004; Nunes et al. 2013). Michaelsen *et al*. concentrated their work on the destruction of spores, as these are the most resistant to environmental change and found that through DNA extraction (rather than culture alone) gamma irradiation only reduced the short term recovery of fungal DNA (Michaelsen et al. 2013). Although research has been conducted into the effects of gamma radiation treatments on fungi, the work has been conducted on specific material classes, usually artificially aged and with a limited fungal population. Further work would need to be conducted in this area and for the treatment to become more widely available before it could have a positive impact of the treatment of fungi on collections.

6.2.2 Fungicides

The application of biocides, in this case fungicides, within historic buildings and on artefacts is accompanied by many risks including toxicity, short activity time and an unknown effect over time on the surface (Sedlbauer & Krus 2003; krus et al. 2007; Sterflinger 2010). A comprehensive review of the antimicrobial treatments used within the heritage profession can be found in Sequeira *et al.* particularly in reference to paper conservation (Sequeira 2016; Sequeira et al. 2012).

Fungicides can be incorporated into materials at the time of production (Orlita 2004), added to paints, sizes and coatings (Shirakawa et al. 2010), included as preventative agents in conservation adhesives and coatings (Kowalik 1984; Abdel-kareem 2010)and used as surface treatments as part of treating an outbreak of growth (Garg et al. 1995). It has been reported that the ineffective treatment of certain species with fungicides has led to an increase in spore toxicity (World Health Organization 2009; Murtoniemi et al. 2001; Murtoniemi et al. 2003).

Specifically in the case of plasterboard, surface fungicide treatment prevented growth, but when the fungicide was embedded within the core, it was ineffective at preventing growth. It did however reduce sporulation but the spores that were produced were highly cytotoxic, compared to the untreated spores. Due to the limitations of fungicides previously mentioned, it is not often that are used in the direct treatment of organic objects, more likely in the decontamination of building material and inorganics. As with conservation treatments, it should be noted that testing effectiveness of fungicides against the target species is recommended prior to treatment.

6.3 Antifungal compounds

Due to the threat of antibiotic resistance, research into the antimicrobial properties of plant based compounds has increased, usually in the form of essential oils (Holme 2007). The majority of research has related to the treatment of human pathogens, although studies into the use of volatile organic compounds and heritage collections have also been conducted (Rakotonirainy & Lavédrine 2005; Stupar et al. 2014). The concept of using plants to prevent pests in homes has been historically documented (Culpeper 1653; Gerard 1597; Pechey 1694) and can still be seen in the use of lavender bags in draws. A short study into the antifungal properties of 11 plants used in the treatment of infections and pests (Culpeper 1653; Hatfield 2009) were analysed to determine their antifungal properties against *Aspergillus versicolor, Cladosporium cladosporiodes* and *Penicillium brevicompactum*. The antimicrobial properties of the extracts selected have not been studied within a heritage context previously or within the Birkbeck research group.

6.3.1 Methods

Plant extracts were sourced in w/v alcohol suspensions from Rutland Biodynamics (Table 6.3). Due to time restrictions, pre-prepared extracts were used.

Table 6.3- The plant extracts sourced for antifungal assays in w/v alcohol suspensions

Name	Common name	Plant part	w/v
Dipsacus fullonum	Teasel	Root	1:3
Symphytum officianale	Comfrey	Root	1:5
Stellaria media	Chickweed	Whole herb	1:2
Arctium lappa	Burdock	Root	1:2
Solidago canadensis	Goldenrod	Flowering top	1:2
Hydrastis canadensis	Goldenseal	Root	1:4
Apium graveolens	Celery	Seed	1:2
Polygonatum biflorum	Solomon's-seal	Rhizome	1:1
Stachys betonica	Wood betony	Whole herb	1:2
Althaea officinalis	Marsh mallow	Root	1:2
Olea Europaea	Olive	Leaf	1:2
Filipendula ulmaria	Meadowsweet	Flowering herb	1:2

Initial screening of compounds was conducted using the poison food method (Shridhar et al. 2003; Abdollahi et al. 2011), in which the extract was added to potato dextrose agar (1% v/v) and poured into triplicate Petri dishes. A 7 day culture plug placed at the centre and radial growth was measured after 7 days incubation at 20°C. Any inhibition of growth was taken as a positive result. Active compounds in the extracts were separated by thin layer chromatography in a dichloromethane and methanol solvent system (7:3) before bands were visualised under short and longwave UV light (Yoon et al. 2013). The silica gel was sectioned into visible bands and scraped, before elution in 3ml of methanol, centrifugal separation and the removal of 1ml of the methanol fraction. The concentration was then increased by vacuum evaporation for 2 hours at 22°C and elution in 300ml of methanol. Extract fractions were then analysed by disc diffusion assay (Espinel-Ingroff et al. 2010; Fisher & Phillips 2008), sterile filter discs were impregnated with concentrations of the extracts and placed equidistant onto PDA plates spread with 100μL of a 10^5 spore suspension made from 7 day old PDA cultures (for method see 4.2.1.2). Three extract discs and a methanol control were used for each plate and zones of inhibition were measured after 7 days incubation at 20°C using digital callipers. Fractions with antifungal properties were then analysed by PDB broth dilution using 100μL of broth and in each well of the 96 well plate before serial dilution of 100μL of extract (Rex et al. 2008; Shehata, Mukherjee & Ghannoum 2008). Methanol controls were used and minimum inhibitory concentration (MIC) was compared to those after incubation for 7 days at 20°C, 150rpm. Plates were measured spectrophotometrically at 540nm and the MIC and those extract fractions that had a greater MIC than methanol were analysed with HPLC-MS (see 4.2.2 for methodology).

6.3.2 Results

The goldenseal (GS) celery seed (CS) and meadowsweet (MS) all showed inhibitory properties against the three fungi with the poison food plates and the bands found at 2cm, 7-10cm & 14cm for CS, 7-11 & 13-15cm for GS and 2-3cm, 7cm, 9cm & 11cm for MS were highlighted as bioactive in the disc diffusion assay. These were then used in the broth dilution assay and the inhibitory effects that were greater than the methanol on the three fungi can be seen in the MICs of Table 6.4.

Table 6.4-Minimum inhibitory concentration of concentrated plant extracts, separated by TCL and eluted in methanol, on Aspergillus, Cladosporium *and* Penicillium *in PDB broth plate dilutions with a methanol control. Plates were incubated for 7 days at 20°C, 150rpm prior to reading at 540nm.*

Extract	TLC fraction	MIC µl/ml of concentrated extract		
		Aspergillus	*Cladosporium*	*Penicillium*
Celery seed	2 cm	41.7	83.3	83.3
	7 cm	41.7	83.3	83.3
	8 cm	41.7	83.3	83.3
	9 cm	41.7	83.3	83.3
	10 cm	41.7	83.3	83.3
	14 cm	41.7	83.3	83.3
Goldenseal	7 cm			
	8 cm			
	9 cm			
	10 cm			
	11 cm			
	13 cm	31.3		31.3
	14 cm	31.3		31.3
	15 cm		62.5	
Meadowsweet	2 cm		83.3	83.3
	3 cm	41.7	83.3	83.3
	7 cm	41.7	83.3	83.3
	9 cm	41.7	83.3	83.3
	11 cm	41.7		83.3

The celery seed extract was the most effective as a broad spectrum fungal growth inhibitor, however the Goldenseal fractions at 13-14 cm were effective at lower concentration with the *Aspergillus* and *Penicillium*. The *Aspergillus* was the fungi most easily inhibited due to the lower concentrations of extract required. Table 6.5 shows the identified compounds from the extract fractions. As can be seen, the meadowsweet fractions were all found to contain a predominant naphthacene carboxylic acid methyl ester.

Table 6.5- *The significant features from the total ion chromatogram for celery seed, goldenseal and meadowsweet TLC fractions; identified using XC-MS and the chemical taxonomy of the compound from METLIN. M/z =the median mass over charge ratio of the feature peak, RT= median retention time, Max Int= the maximum intensity recorded for the feature.*

Extract	TLC fraction	m/z	RT	Max Int	Adduct	Chemical taxonomy
Celery seed	2 cm	796.25	21.73	36838	M+Na	Pressinamide
	7 cm	923.00	23.69	36997	M+K	Benzenesulfonic acid, 4,4',4'',4'''-(2,3-pyridinediyldi-1,2,4-triazine-3,5,6-triyl)tetrakis-
	8 cm	642.56	23.90	2693	M+H	1-Naphthacenecarboxylic acid, 4-(((2''',3'''-anhydro)-O-3,6-dideoxy-alpha-L-erythro-hexopyranos-4-ulosyl-(1-4)-O-2,6-dideoxy-alpha-L-lyxo-hexapyranosyl-(1-4)-2,3,6-trideoxy-3-(dimethylamino)-alpha-L-lyxo-hexopyranosyl)oxy)-1,2,3,4,6,11-hexahydro-2,5,7-trihydroxy-2-methyl-6,11-dioxo-, methyl ester
	9 cm	923.00	23.69	36997	M+Na	1,1',1''-(Ethane-1,1,1-triyl)tris{4-[2-(1-iodoethoxy)ethoxy]benzene}
	10 cm	907.06	23.69	96605	M+K	2-Naphthalenecarboxamide, N,N'-(3,3'-dichloro[1,1'-biphenyl]-4,4'-diyl)bis[4-[(2-chlorophenyl)azo]-3-hydroxy-
	14 cm	907.06	23.69	96605	M+K	2-Naphthalenecarboxamide, N,N'-(3,3'-dichloro[1,1'-biphenyl]-4,4'-diyl)bis[4-[(2-chlorophenyl)azo]-3-hydroxy-
Goldenseal	13 cm	405.94	4.712	2703050	M+K	4-[(2,6-Difluoropyrimidin-4-yl)amino]benzene-1,3-disulfonic acid
	14 cm	340.06	5.666	2224191	M+H-2H$_2$O	1-Methyl-3,4-bis(phenylsulfanyl)quinolin-2(1H)-one
	15 cm	340.06	5.666	2224191	M+H-2H$_2$O	1-Methyl-3,4-bis(phenylsulfanyl)quinolin-2(1H)-one
Meadowsweet	2 cm	796.31	21.65	55184	M+H	1-Naphthacenecarboxylic acid, 4-(((2''',3'''-anhydro)-O-3,6-dideoxy-alpha-L-erythro-hexopyranos-4-ulosyl-(1-4)-O-2,6-dideoxy-alpha-L-lyxo-hexapyranosyl)oxy)-1,2,3,4,6,11-trideoxy-3-(dimethylamino)-alpha-L-lyxo-hexopyranosyl)oxy)-1,2,3,4,6,11-hexahydro-2,5,7-trihydroxy-2-methyl-6,11-dioxo-, methyl ester
	3 cm	796.31	21.65	55184	M+H	1-Naphthacenecarboxylic acid, 4-(((2''',3'''-anhydro)-O-3,6-dideoxy-alpha-L-erythro-hexopyranos-4-ulosyl-(1-4)-O-2,6-dideoxy-alpha-L-lyxo-hexapyranosyl)oxy)-1,2,3,4,6,11-trideoxy-3-(dimethylamino)-alpha-L-lyxo-hexopyranosyl)oxy)-1,2,3,4,6,11-hexahydro-2,5,7-trihydroxy-2-methyl-6,11-dioxo-, methyl ester
	7 cm	796.31	21.65	55184	M+H	1-Naphthacenecarboxylic acid, 4-(((2''',3'''-anhydro)-O-3,6-dideoxy-alpha-L-erythro-hexopyranos-4-ulosyl-(1-4)-O-2,6-dideoxy-alpha-L-lyxo-hexapyranosyl)oxy)-1,2,3,4,6,11-trideoxy-3-(dimethylamino)-alpha-L-lyxo-hexopyranosyl)oxy)-1,2,3,4,6,11-hexahydro-2,5,7-trihydroxy-2-methyl-6,11-dioxo-, methyl ester
	9 cm	796.31	21.65	55184	M+H	1-Naphthacenecarboxylic acid, 4-(((2''',3'''-anhydro)-O-3,6-dideoxy-alpha-L-erythro-hexopyranos-4-ulosyl-(1-4)-O-2,6-dideoxy-alpha-L-lyxo-hexapyranosyl)oxy)-1,2,3,4,6,11-trideoxy-3-(dimethylamino)-alpha-L-lyxo-hexopyranosyl)oxy)-1,2,3,4,6,11-hexahydro-2,5,7-trihydroxy-2-methyl-6,11-dioxo-, methyl ester
	11 cm	796.31	21.65	55184	M+H	1-Naphthacenecarboxylic acid, 4-(((2''',3'''-anhydro)-O-3,6-dideoxy-alpha-L-erythro-hexopyranos-4-ulosyl-(1-4)-O-2,6-dideoxy-alpha-L-lyxo-hexapyranosyl)oxy)-1,2,3,4,6,11-trideoxy-3-(dimethylamino)-alpha-L-lyxo-hexopyranosyl)oxy)-1,2,3,4,6,11-hexahydro-2,5,7-trihydroxy-2-methyl-6,11-dioxo-, methyl ester

6.3.3 Conclusions

The antimicrobial properties of these plants have been previously evaluated, with the active compounds of alkaloids, phenols, flavonoids organic acids, amides and hydrocarbons identified

(Scazzocchio et al. 2001; Krasnov et al. 2006; Momin & Nair 2001) and have been found to have antimicrobial and insecticidal properties (Synowiec et al. 2014; Boziaris et al. 2011; Eddy Knight 1999; Momin & Nair 2001; Villinski et al. 2003). For the fungi tested here, the antimicrobial properties were found to be varied, with different MICs required and not being effective on all fungi. The celery seed shows the most promise of having broad spectrum antifungal properties, although due to the colour and smell of the plant extract, further refinement and treatment applications would need to be extensively explored for the heritage sector.

6.4 Microencapsulation of bioactive compounds

Microencapsulated compounds have been used for the controlled release of active compounds within the cosmetic, food and pharmaceutical industries. Encapsulated compounds, usually volatile, are protected from degrading factors like oxygen, their properties can be preserved for longer and then delivered at the desired time and location (Pham-hoang & Romero-guido 2013). The application of polymer capsule technology is now being applied as a coating to various substrates, particularly textiles as a delivery system for fragrance, moisturisers, insecticides and drug release (Holme 2007).

There are a wide range of materials that have been used to encapsulate volatile and poorly soluble compounds. Encapsulation can be achieved by methods including liposome entrapment, spray drying, fluidised-bed coating and emulsion in polymer spheres (Holme 2007). The aim of microencapsulation is to impart the desirable properties of the encased compound, without changing the nature of the substrate to which it is applied and to have a long activity (Nelson 2002). Those techniques and polymers which are well documented and may have applications for heritage materials are discussed in the following sections.

6.4.1 Yeast cell encapsulation

The mono-cellular structure of yeasts, particularly the Ascomycete *Saccharomyces s cerevisiae,* make them well designed as vectors for essential oils and sensitive compounds. The cell wall is composed largely of polysaccharides, crosslinked glucans and mannans with some chitin and protein, which comprise of approximately 20% of the dry cell weight. There is then a plasma membrane, lipid bilayer (Nelson et al. 2006; Pham-hoang & Romero-guido 2013). The process of encapsulation involves the removal of the cytoplasm of the yeast cell and the absorption/insertion of the target compound, with the uptake of some chemicals being through simple diffusion. Yeast cells can be modified by increasing the lipid content of the cell (>40%) on high nitrogen based media, in order to incorporate lipophilic compounds (Shank 1977; Nelson

et al. 2006). As yeast cells (of the same species) are a relatively homogenous in size, a constant product can be achieved that will not be detected in the final substrate due to their small size of 5-10μm (Pham-hoang & Romero-guido 2013).

Although the use of yeast cells is a relatively simple process, due to the pre-formed nature of the structure and diffusion being viable for the chemical uptake, the delivery method may not be suitable for a heritage context. One of the most common ways for chemical release within the cosmetic, paper and food industry was through pressure and the bursting of the yeast cell (Nelson et al. 2006). A similar effect can be achieved by the encapsulation of chemicals in gelatin (Nelson 2002), which has been used with pressure release microcapsules on paper and textiles. Although the use of yeast cells would be a cost effective way of delivering a fungicidal chemical to historic buildings, the use of pressure of abrasion as a release mechanism could only be applied in specific situations. It is also possible to gain a controlled release from yeast cells through the gradual lysis of the cell (Pham-hoang & Romero-guido 2013). However, the residual effect of lysed cells and the remaining encapsulated, potentially lipid based, compounds could be deleterious to many historic surfaces.

6.4.2 Cyclodextrin

Cyclodextrins (β-cyclodextrin being the most widely used) are cyclic oligosaccharides with the inside of the molecule being hydrophobic and the outside hydrophilic (Dastjerdi & Montazer 2010), meaning that chemical release can be moisture dependant (Wacker Chemie AG 2009). Although the use of cyclodextrin as and encapsulation method is restricted in some countries (Pham-hoang & Romero-guido 2013), it is still widely used for the preservation and delivery of volatile compounds in the food, medical and cosmetics industries (Gutarowska & Michalski 2012; Holme 2007; Appendini & Hotchkiss 2002; Gerhardt et al. 2013; Wacker Chemie AG 2009). Cyclodextrins have an inclusion forming capability with a wide range of volatile plant based compounds with a high residual activity when applied to cotton and wool (Shahid & Mohammad 2013) and has many applications as a coating for substrates due to its crosslinking and covalent bond capabilities (Holme 2007; Dastjerdi & Montazer 2010). Due to the bonding of the cyclodextrin capsule to substrates, it means that this treatment is resistant to washing and has the potential of a long delivery when moisture conditions would allow the growth of fungi. As this encapsulation method has been proven to work effectively as a textile coating and there is a lot of published work in this area (Dastjerdi & Montazer 2010; Holme 2007), there is a potential to develop textiles for conservation treatments, like linings and support fabrics. However, extensive longevity and degradation studies would need to be performed.

6.4.3 Chitin/chitosan

Chitin and chitosan have been used as polymer nanocomposites in the food packaging industry and can be dispersed within a compatible polymer, usually plastic (Duncan 2011; Lagaron et al. 2007). They are a biodegradable, edible and will retain lipid based compounds (such as essential oils) in films and capsules and has been found to be effective against fungal developement (Lagaron et al. 2007). They have also been used in conjunction with silver to create capsules and films for drug delivery and biomedical application (Dastjerdi & Montazer 2010) and have been developed for antimicrobial packaging (Muñoz-Bonilla & Fernández-García 2012). Bioactive textiles have also been created using chitosan encapsulation which will withstand washing (Holme 2007). As chitosan is inherently antimicrobial and can be used to encapsulate bioactive compounds, it has potential applications for heritage film and coating based treatments, such as adhesives and waxes.

6.4.4 Silk

Silk has been used as a novel biomaterial for the controlled release of drugs and as biomaterial scaffolds (Wang et al. 2007; Vepari & Kaplan 2007; Mandal et al. 2009). In multilayer coatings, the target release compound is coated in silk fibroin layers and relies on diffusion. During release, there is an initial burst in the released drug concentration, followed by a slower release (14-35 days till total release, depending on target compound). The initial concentration burst can be moderated by changing the number of fibroin layers (Wang et al. 2007). Controlled release can also be modulated with self-degrading polymers, such as gelatin (Mandal et al. 2009). The release rate of drugs trialled for silk are in the region of days, which would mean that this may be a suitable method of delivery for the interventive treatment of fungal growth, but would not be suitable for a long term delivery system unless modifications to the fibroin layers could be developed for slower diffusion rates.

6.4.5 Conclusions

There is scope for the development of controlled release systems within the heritage industry, although extensive testing would be required. A suitable fungicide of an appropriate molecular weight would need to be identified, a suitable control mechanism found and long term studies into the degradation of the fungicide and delivery system evaluated. It is unlikely that a fungicide delivery system would be employed on historic object surfaces, but for a matrix within conservation materials, adhesive treatments and surface coating that are sensitive to fungal degradation. Another application of encapsulation technology could be in the development of

antifungal packaging materials for archives and storage. Nanoparticles have already been proved effective for the long term storage of food products (Duncan 2011), and if an acid free polymer, card or paper matrix could be developed then this could help to prevent widespread outbreaks in storage areas that are not subjects to regular monitoring.

6.5 Non-organic nanoparticles

Nano (in Greek meaning dwarf), refers to particles that are 10^{-9}m (Holme 2007), or from 100nm – 0.2nm. The result of such small particles is a relatively large surface area, which can increase the reactivity of materials (Gutarowska & Michalski 2012). Coatings of this type are already widely used within the sporting textile and medical industry for antimicrobial effects (Holme 2007). Metallic compound nanoparticles have been created from gold, silver, copper, zinc oxide (ZnO), titanium dioxide (TiO_2) have been used to create novel coatings with antimicrobial properties (Dastjerdi & Montazer 2010). The antibacterial properties of nanoparticles have been more widely studied, but the effect on fungi less so, although some results have been described within the textile, medical and food packaging industries (Dastjerdi & Montazer 2010; Duncan 2011; Wu et al. 2013).

Gold nanoparticles are reported to be an effective antimicrobial against bacteria and fungi (Dastjerdi & Montazer 2010; Gutarowska & Michalski 2012). However, due to the expense of gold and the effectiveness of cheaper metals, they do not appear to have been tested for heritage applications. Silver is a broad spectrum antimicrobial and have been found to be toxic to fungi (Duncan 2011; Sharma et al. 2013; Wu et al. 2013). Silver can cause enzyme disruption, promote cellular oxidation, protein denaturation and respiration blocking in microorganisms, but have minimal effects on humans; although this is dependent on dispersal method and particle size (Dastjerdi & Montazer 2010). Silver nanoparticles have been investigated for antimicrobial activity on microorganisms isolated from heritage environments (Gutarowska, Skora, et al. 2012). Their activity when misted onto historic materials was also assessed, where their effect on fungi was greatest for the wood and paper, but less so for canvas and parchment (Gutarowska, Skora, et al. 2012). Minimal changes were recorded for colour after application and there were no significant differences in the tensile properties of cotton or silk (Gutarowska, Rembisz, et al. 2012). However, the long term effect of silver nanoparticle misting was not investigated, although considered. The effect of silver nanoparticles on building materials was investigated and found that *Penicillium* and *Aspergillus sp*. were inhibited on materials incubated at 85% RH for 35 days, with the exception of a wooden floor sample and calcium silicate board for the *Aspergillus* (Huang et al. 2015). Copper nanoparticles have been used for

textile applications and tested for antifungal capacity when applied to building materials, but are considered to be less effective than silver (Huang et al. 2015; Dastjerdi & Montazer 2010). For building materials there was some resistance to *Aspergillus sp*. growth on calcium silicate board, gypsum board and mineral fibre ceiling; wooden flooring and calcium silicate boarding showed some improved resistance to *Penicillium sp* (Huang et al. 2015)*. This indicates that copper nanoparticles would be fungistatic, to a certain degree, with some materials in heritage buildings, although it would depend on the material and fungal species. Zinc oxide has been used for UV protection and antimicrobial coating of textiles, food packaging and building materials (Dastjerdi & Montazer 2010; Saravanan 2007; Gutarowska & Michalski 2012; Duncan 2011; Huang et al. 2015). The zinc nanoparticle coating of building materials was more effective against *Penicillium* and *Aspergillus sp*. that copper, with improved fungal resistance on all materials except mineral fibre ceiling (Huang et al. 2015). However, although the nanoparticles improved resistance, growth still occurred within 35 days of incubation at 85% RH (Huang et al. 2015). TiO_2 nanoparticles have been used for UV protection of textiles and display antimicrobial properties due to its reactive oxygen species (Dastjerdi & Montazer 2010). Their use on paper materials as an antifungal agent was assessed with *Aspergillus* and *Penicillium sp*. and indicated that when applied as a solvent and solvent/adhesive mist, the TiO_2 acted as a fungistatic, not fungicidal agent. There were also physical and chemical changes to the paper observed after artificial ageing. (Afsharpour et al. 2011). Their application was found to be more effective as an antibacterial coating for marble (La Russa et al. 2014).

Nanoparticles have been proved to be effective in certain circumstances against fungi found within heritage buildings. However, results are varied across the nanoparticle, application, substrate and fungal species. The longevity of activity and the potential detrimental effect to the substrate have also not fully been investigated. This means that application of nanoparticles would likely be a specialised treatment option, rather than a widespread treatment plan for a fungal outbreak.

6.6 Environmental control as a prevention of fungal growth

The control of fungal growth within buildings has been a key topic for research, particularly within historic buildings. There are a number of projects that have looked at the prediction of future climate patterns within buildings and the effect that this may have on collections, with particular attention being paid to fungal growth (Thelandersson et al. 2009; Camuffo et al. 2013; Martens 2012; Saunders 2008; Thelandersson & Isaksson 2013; Antretter 2013; Isaksson et al. 2010; Lankester & Brimblecombe 2012b; Huijbregts et al. 2012; Camuffo et al. 2001; Sedlbauer

& Krus 2003; Krus et al. 2010; krus et al. 2007; Sedlbauer 2001). A number of these projects look at future climate patterns and how these will affect the internal climatic conditions of properties.

In-vitro studies of fungi can indicate the boundaries in which fungi can grow and therefore model the risk of infection for properties and surfaces (Sedlbauer & Krus 2003; Krus et al. 2010; Sedlbauer 2001). This is largely achieved by the use of isopleth, biohygrothermal or VTT models.

6.6.1 Isopleth models

The simplest isopleth models use growth curves to indicate favourable from unfavourable temperature and humidity conditions (Vereecken & Roels 2012).The more complex involve a graphical representation of the germination time and growth rate of fungi under different temperature and humidity conditions; the growth substrate and available nutrition is also considered (Sedlbauer 2001). The isopleth models developed by Sedlebauer are based on the published growth parameters of 150 species (divided into classes based on risk) and the lowest isopleths for growth used, along with 4 different nutritional conditions for substrates (Sedlbauer & Krus 2003). The ESP-r model (Clarke and Rowan) divides the indoor fungi in terms of their water requirements; from hydrophilic to xerophilic (Vereecken & Roels 2012) and defines the growth curves by polynomial function.

Using the Sedlebauer isopleths for substrate category II (biologically recyclable building materials) as a representative for organic collections within heritage buildings, the environmental data recorded from buildings during this survey was analysed. It was found that the only spaces that were predicted to contain fungal growth were those with extreme environments, such as those that were subterranean or had a high air exchange rate with outside (data not shown). This underestimation of growth was also observed by Vereecken et al. (2012) and this can be associated with the fact that the growth curves were derived from closed system laboratory experiments.

6.6.2 Transient Biohygrothermal models

This model takes into account the potential desiccation of fungal spores that may occur from the point of deposition, to the development of a microclimate suitable for germination (Sedlbauer & Krus 2003; krus et al. 2007). The moisture content of the spore is predicted from the surrounding climatic conditions, according to the moisture storage capacity of the spore and its resistance to vapour diffusion. An example of this type of model is the WUFI Bio platform, which can be used to assess the risk of fungal growth (mm) based on the temperature and RH

of a room and the substrate class, giving a potential moisture storage function of the spore and a mould index. The specific water content of spores is based on the experimental work associated with the lowest growth isopleth. In order to be able to assess the critical moisture content of spores, it is really necessary to have constant climatic monitoring within the space. The model also does not account for the moisture regain of specific materials, only general substrate classes. It can therefore be a useful tool to be used as part of general environmental monitoring, but further investigation of the collection would still be necessary. As the model is not based on visual analysis of growth, but growth functions, it is also not possible to tell when growth would become visible to the naked eye (Viitanen et al. 2015).

6.6.3 The Viitanen model (VTT)

This model works from regression analysis of *in-vitro* experiments using Scots Pine and Norway Spruce sapwood as a substrate and monitoring the time for germination and growth of fungi under specific humidities and temperatures (Vereecken & Roels 2012). The output works on a mould index system with a scale of 0 (no growth) to 6 (dense coverage 100%) (Viitanen et al. 2010; Krus et al. 2010; Viitanen et al. 2015). The index system means that results are more easily interpreted by heritage professionals, but only differentiates between two wood and one mineral substrate classes, meaning that a large proportion of materials found within heritage buildings would not be accounted for by the model (Krus et al. 2010).

There has since however been a collaboration and the VTT and biohygrothermal approach have been found to have comparable predictive outcomes. WUFI Bio now produces fungal growth predictions (mm) and a mould index score, along with a traffic light system for risk interpretation (Krus et al. 2010; Viitanen et al. 2015).

Future climate simulations for historic buildings in Europe indicate that the internal environment will have a higher relative humidity, be warmer and be less stable with greater fluctuations in conditions (Huijbregts et al. 2012). This study also predicted that buildings with some, even if limited HVAC systems, will be less likely to suffer from an increase in fungal growth. It is also indicated that changes in meteorological patterns (high winds etc.) may increase the surface wetness of buildings and increase damp penetration, meaning that collections within historic buildings may become more vulnerable to external conditions (Brimblecombe 2014; Brimblecombe & Brimblecombe 2016). It is also likely that the growth of fungi will increase, although due to an increase in temperature, rather than moisture (Brimblecombe 2014).

6.6.4 Heating, ventilation and cooing in historic buildings

Most damage to collections within historic buildings is caused by unfavourable or unstable internal climatic conditions and this is particularly the case in buildings that are being used for purposes other than the original construction (krus et al. 2007). This is the case with a lot of historic buildings in the United Kingdom that are now used to house collections and as a visitor attraction. With changes to the building envelope, introduction of modern facilities (kitchens/bathrooms etc.), comfort heating through extended open seasons and changes made through security considerations (keeping windows closed, solar protection blinds, restricted visitor routes etc.) there may be microclimates in which the dew point for condensation is reached. The standard conditions for the protection of historic collections is between 40-60% RH and 16-25°C, with minimal fluctuations (British Standards Institution 2012); conditions that are largely in line with other European and world standards (Atkinson 2014).

Many modern options to control the RH of the historic house environment are not often feasible, such as installing a HVAC systems, alterations to the building envelope and justifying the expense of energy outlays in order to control the environment (Staniforth 2010; Kerschner 1992). Many of the buildings used as heritage attractions used to be heated by open fires , local heating systems (such as hot air or portable heaters) or (depending on age and retro-fitting) central heating (Neuhaus & Schellen 2007). The continued use of antiquated heating systems can lead to pollution, health and safety issues and unintended damage to the building structure if current environmental standards are to be achieved (Kerschner 1992). It is important that the structure of the historic building should be considered and the limitations to any environmental control mechanisms in the space understood. By monitoring the temperature and RH, the normal conditions for the building can be understood and any deviations investigated. Common sources for deviations have been identified as water, vegetation, dust, heat and the use of a historic building as an exhibition space (Kerschner 1992); all of which can be mediated in some way before further damage occurs, including fungal growth.

The concept of conservation heating is now being used within many historic buildings in the UK, in order to control the RH in spaces to below 60% by the controlled heating of spaces by a humidistat (Staniforth et al. 1994); it has also been found to be effective in Dutch historic buildings (Neuhaus & Schellen 2007). However using this system, in order to maintain an RH within the British standard, it is often necessary to heat during the summer and not during the winter and with the climatic control usually in a single location within a space, it is difficult to prevent microclimates. Conservation heating will however help to mitigate fluctuations in RH,

which can be important for the initial growth of fungi. Johansson et al. found that the lower the temperature in which wood was stored, the lower the rate of fungal growth. It was also observed that the average recorded RH may not be an effective gauge of fungal growth as an average 75% RH with short fluctuations outside of favourable moisture conditions did not affect fungal growth as much as a mean 75% RH with longer periods of fluctuation (Johansson et al. 2013). This means that the minimum and maximum range of RH should be considered, rather than the mean.

It is also important to note the comfort heating of buildings and the role which this can play in fungal growth. As buildings are opening during the colder months, comfort heating is considered necessary for staff and guests, but this can lead to condensation build up exterior walls and windows and very damp microclimates forming. Brimblecombe (2016) also notes that comfort heating can cause damage by lowering the humidity. Ventilation of buildings is also an important factor in the prevention of fungal growth and the dispersal of heat and humidity during the summer months (Kerschner 1992). It is also possible to use heat convection and fans to promote air movement and surface evaporation.

6.7 Conclusions

The treatment of fungal growth on objects is complex issue and from the cleaning trials (6.1.1), it is clear that current conservation cleaning techniques may not be effective in all cases. It is also important to understand the genera of the colonising fungi as it has been demonstrated in the work of Chapters 3-5 that this can have important implications for the cleaning requirements (removal of secondary metabolic products) and handling (changes in chemical and mechanical properties). The genera and substrate to be cleaned are also important factors in cleaning decisions (6.1.1). The introduction of more testing when fungal growth is treated would improve the long term condition of objects through damage risk assessments, improved treatment outcome and understanding future degradation mechanisms and risks of growth reoccurring. Although there are techniques of disinfection that could be transferrable and more widely used for the treatment of fungal growth on heritage objects, these often require specialist equipment and would not be viable in most cases.

The use of natural products for disinfection has been proven to be effective on fungi found in historic buildings, both in-vitro (6.3) and on objects (Rakotonirainy and Lavédrine, 2005), however a broad spectrum antifungal has not yet been found and tested over all common heritage fungi and the effects on materials determined through ageing studies. The time of antifungal activity has also not been investigated and as repeated treatment of historic objects

does not commonly occur, longevity of fungal prevention would be a key factor. There is the possibility of encapsulating bioactive compounds for controlled release, however there would again need to be extensive ageing studies performed on a range of materials to determine decomposition and future degradation risks to the substrate. The same is true for non-organic nanoparticles.

The most effective method of fungal prevention within heritage collections seems to be the control of the environment and ensuring that water and nutrients are not available. Growth prediction models are a useful tool for indicating spaces where fungal growth may occur. However, they should be used in conjunction with physical examination and testing as models have a tendency to under predict growth levels. The model developed from building data and growth observations on collections during this study has the capacity to be developed by training and testing on new data sets, in the hope of producing a simple and reliable prediction tool for UK heritage buildings.

7. General conclusions

This work has been concerned with the fungi found in UK heritage buildings, what building features can promote fungal growth on objects and the damage that can be caused to different substrates. The cleaning of objects, antifungal treatments and methods of control were then evaluated.

The fungi found within heritage buildings are predominantly from an outside source and colonisation of historic objects and surfaces appears to be opportunistic, with the exception of some extreme environments. The building features that are significant for fungal growth to occur are related to the geographical position, building type, the level of furnishing & organic collections and the environmental conditions. High internal CFU counts are influenced by geographical location, external water features, the type of building and whether it has multiple floors & windows, the external temperature & CFU count and whether fungal growth has been observed in the space. The CFU counts and diversity in buildings are greater in the summer, least in the winter and are largely influenced by external conditions. However, if the external conditions are accounted for, then the winter season has the highest instances of CFU counts that are 100 or greater than those of the external. As the outside conditions of properties are so influential, the air exchange with the outside could be considered as a method of control for spores entering buildings and increasing the regularity of surface cleaning would mean that settled spores would be less likely to be able to germinate. *Aspergillus versicolor, Cladosporium cladosporiodes* and *Penicillium brevicompactum* were found in all properties, over all seasonal surveys and are considered to be the most abundant fungi in UK heritage buildings.

The three most abundant fungi have the ability to grow on all of the organic substrates tested when water availability is not an obstacle. There are also diverse natural biofilms that form on substrates, not restricted to fungi. Permanent damage can occur as a result of fungal staining, which cannot be removed through conservation style solvent cleaning. The HPLC-MS results indicate that pigments are removed from some materials, but localised colour change was significant for most materials after cleaning. *Cladosporium* caused the most widespread and aesthetically damaging colour change on most materials. Growth is not restricted to the surface of substrates and the fungi were all able to penetrate through surface matrices and into the fibre/cellular structures of the materials. Confocal laser scanning fluorescence microscopy was a useful technique for live cell imaging and differentiation between the fungi/substrate and whether fungi were still viable. Depending on the density of the material (leather could not be

imaged), orthogonal slices of the image stack enabled the depth of fungal growth to be determined below the surface.

The primary metabolism was assessed through enzyme assays, which indicated that the fungi are capable of depolymerisation of complex polymers, although activity was shown to be low for the digestion of long chain cellulose and proteins in plate assays. However the specific enzyme activity assays indicate that activity is increased in liquid suspension. The fungi all showed a greater capacity for the digestion of shorter chain cellulose and hemicellulose substrates. These assays did not indicate the ability to digest pectin or lignin substrates. HPLC-MS extracts of the growth materials showed that secondary metabolic products were produced, along with evidence of substrate degradation. Although degradation had occurred, some of the volatile and potentially toxic products also be indicative of nutrient distress along with the production of lipid storage compounds. This results of this study indicate that the surface cleaning of fungal growth is likely insufficient and aqueous treatments would be recommended for secondary product removal to prevent auto hydrolysis and oxidation of the substrate from these volatile compounds. FTIR indicated that significant changes to the chemical structure and conformation of materials is possible after relatively short periods of fungal growth. This was largely evidenced by depolymerisation markers, the production of carbonyl compounds and the likelihood of structural cross linking. As the chemical changes were so variable (largely associated with colony formation and sample location), this highlights the importance of understanding which genera of fungi is colonising materials so that the risks of chemical change (along with volatile compounds) can be qualified. Closely related to the chemical changes, the mechanical properties of materials were significantly altered after fungal growth, although this was dependant on colony formation and results were variable over the replicates. However, the changes observed mean that the handling properties and physical state of materials would change which would have particular implications for materials that are naturally under tension and mixed media objects.

The cleaning of fungal growth and future control is a complex issue that is not close to being solved. Particularly as the findings of this work indicate that effective conservation cleaning is dependent on the colonising species and the substrate being cleaned. Although there are control methods from other industries that seem viable (bioactive compounds and nanoparticles), the treatment of historic surfaces with them and the long term effects have not been widely explored. Their use in conservation materials hold more promise though. The most available and effective prevention of fungal growth appears to be environmental control, although this needs to be considered on an individual basis as the likelihood fungal growth

occurring in spaces is different, as shown in this study. Predictive models are a useful tool for assessing the risk of fungal growth, however there are issues with under prediction and the complex nature of the historic house environment.

This study was limited to only twenty historic buildings and four survey visits with spot monitoring. Accuracy could have been improved through focussing on fewer properties, installing radio-telemetric monitoring and sampling more frequently. However, the geographical differences and influence of different building features in the CFU count and growth occurrence may not have been detected. The study was also performed early in the research and due to climatic changes, the results may be different if performed now. This study could be repeated and extended to more properties in order to see how the fungal populations have changed and whether there are other building features that are significant to the fungal content of historic properties. This work would also facilitate the improvement of the predictive models. This work was also limited by the quantity of materials, time and the analytical equipment available for the material analysis phase. The study could easily be extended to include more of the common fungi found during the survey and the range of materials broadened. It would also be beneficial to include artificially aged and historic samples to compare the differences after fungal growth. However, with artificial ageing and historic samples, it is difficult to attribute an accurate age and with the historic samples there is often little documentary evidence of previous conditions that may affect the way in which fungi grow on them. The use of GC-MS and DMA that were tested during this trial would have been used had time permitted and would have provided useful and complimentary information about the gaseous products of fungi and the mechanical properties of the denser materials that could not be analysed through the tensile strength testing. Future work on conservation cleaning and an appropriate test of effectiveness would be a useful development for conservators. This study only looked at a small selection of organic materials and could be extended to include a wider range of materials and include complex surfaces such as painted and varnished ones. Research into the disinfection and protection of surfaces from fungal growth is ongoing in many fields. The heritage sector would benefit from the application of techniques to historic materials and longevity testing to determine potential effects of ageing on these surface active agents.

Bibliography

Abdel-kareem, O., 2010. Fungal Deterioration of Historical Textiles and Approaches for Their Control in Egypt. *e-PreservationScience*, 7, pp.40–47.

Abdel-kareem, O. & Morsy, M., 2004. The effect of accelerated ageing on properties of Egyptian cotton textiles treated with fungicides. In R. Janaway & P. Wyeth, eds. *Scientific Analysis of Ancient and Historic Textiles*. Butterworth Heinemann, pp. 57–65.

Abdel-Kareem, O.M. a., 2005. The long-term effect of selected conservation materials used in the treatment of museum artefacts on some properties of textiles. *Polymer Degradation and Stability*, 87(1), pp.121–130. Available at: http://linkinghub.elsevier.com/retrieve/pii/S0141391004002496 [Accessed January 28, 2014].

Abdollahi, A. et al., 2011. Screening of Antifungal Properties of Essential Oils Extracted From Sweet Basil , Fennel , Summer Savory and Thyme Against Postharvest Pathogenic Fungi. *Journal of Food Safety*, 31, pp.350–356.

Afsharpour, M., Rad, F.T. & Malekian, H., 2011. New cellulosic titanium dioxide nanocomposite as a protective coating for preserving paper art-works. *Journal of Cultural Heritage*, 12, pp.380–383.

Agrawal, O.P., 1981. "Appropriate" Indian Technology for the Conservation of Museum Collections. In *"Appropriate technologies" in the conservation of cultural property*. Unesco Press, pp. 70–77.

Akerholm, M., Hinterstoisser, B. & Salmen, L., 2004. Characterization of the crystalline structure of cellulose using static and dynamic FT-IR spectroscopy. *Carbohydrate Research*, 339, pp.569–578.

Alfthan, J., 2004. The effect of humidity cycle amplitude on accelerated tensile creep of paper. *Mechanics of Time-Dependent Materials*, 8(4), pp.289–302.

Allen, B., Wu, J. & Doan, H., 2003. Inactivation of fungi associated with barley grain by gaseous ozone. *Journal of environmental science and health Part B: Pesticides, food contaminants and agricultural wastes*, B38(5), pp.617–630.

Aluigi, A. et al., 2007. Study on the structure and properties of wool keratin regenerated from formic acid. *International journal of biological macromolecules*, 41, pp.266–273.

Antretter, F., 2013. *Multi - zone hygrothermal building simulation tools*,

Appelbaum, B., 1994. Criteria for Treatment of Collections Housed in Historic Structures. *Journal of the American Institute for Conservation*, 33(2), pp.185–191.

Appendini, P. & Hotchkiss, J.H., 2002. Review of antimicrobial food packaging. *Innovative Food Science & Emerging Technologies*, 3(2), pp.113–126. Available at: http://linkinghub.elsevier.com/retrieve/pii/S1466856402000127.

Arai, H., 2000. Foxing caused by Fungi : twenty-five years of study. , 46, pp.181–188.

Arenz, B.E. & Blanchette, R. a., 2011. Distribution and abundance of soil fungi in Antarctica at sites on the Peninsula, Ross Sea Region and McMurdo Dry Valleys. *Soil Biology and Biochemistry*, 43(2), pp.308–315. Available at: http://linkinghub.elsevier.com/retrieve/pii/S0038071710003998 [Accessed January 21, 2014].

Atkinson, J.K., 2014. Environmental conditions for the safeguarding of collections : A background to the current debate on the control of relative humidity and temperature. *Studies in Conservation*, 59(4), pp.205–212.

BACÍLKOVÁ, B., 2006. Study on the Effect of Butanol Vapours and other Alcohols on Fungi. *Restaurator*, 27, pp.186–199.

Badea, E. et al., 2008. Study of deterioration of historical parchments by various thermal analysis techniques complemented by SEM, FTIR, UV-Vis-NIR and unilateral NMR investigations. *Journal of Thermal Analysis and Calorimetry*, 91(1), pp.17–27.

Beeton, I., 1890. *Beeton's Housewife's Treasury of Domestic Information*, Ward Lock and Co.

Beisel, J.N. et al., 2003. A comparative analysis of evenness index sensitivity. *International Review of Hydrobiology*, 88(1), pp.3–15.

Bellemain, E. et al., 2010. ITS as an environmental DNA barcode for fungi: an in silico approach reveals potential PCR biases. *BMC microbiology*, 10, p.189.

Bensch, K. et al., 2005. The Genus cladosporium. *Studies in Mycology*, 72, pp.1–401.

Beyrouty, K. El & Tessler, A., 2013. *The Economic Impact of the UK Heritage Tourism Economy*,

Bicchieri, M. et al., 2011. Non-destructive spectroscopic characterization of parchment documents. *Vibrational Spectroscopy*, 55(2), pp.267–272. Available at: http://dx.doi.org/10.1016/j.vibspec.2010.12.006.

Bicchieri, M. et al., 2002. Study of foxing stains on paper by chemical methods, infrared spectroscopy, micro-X-ray fluorescence spectrometry and laser induced breakdown spectroscopy. *Spectrochimica Acta - Part B Atomic Spectroscopy*, 57(7), pp.1235–1249.

Blades, W., 2013. The Enemies of Books (1881). In S. Staniforth, ed. *Historical Perspectives on Preventive Conservation*. The Getty Conservation Institute, pp. 68–77.

Blanchette, R.A., 2000. A review of microbial deterioration found in archaeological wood from different environments. In *International Biodeterioration and Biodegradation*. pp. 189–204.

Blyskal, B., 2014. Gymnoascus arxii's potential in deteriorating woollen textiles dyed with natural and synthetic dyes. *International Biodeterioration and Biodegradation*, 86, pp.349–357.

Błyskal, B., 2015. Fungal deterioration of a woollen textile dyed with cochineal. *Journal of Cultural Heritage*, 16(1), pp.32–39. Available at: http://dx.doi.org/10.1016/j.culher.2014.01.008.

Bogaard, J. & Whitmore, P.M., 2002. Explorations of the Role of Humidity Fluctuations in the Deterioration of Paper. *Studies in Conservation*, 47(sup3), pp.11–15. Available at: http://www.tandfonline.com/doi/full/10.1179/sic.2002.47.s3.003.

Borrego, S. et al., 2012. Determination of Indoor Air Quality in Archives and Biodeterioration of the Documentary Heritage. *ISRN Microbiology*, 2012, pp.1–10. Available at: http://www.hindawi.com/journals/isrn/2012/680598/.

Borrego, S. et al., 2010. The quality of air at archives and the biodeterioration of photographs. *International Biodeterioration & Biodegradation*, 64(2), pp.139–145. Available at: http://linkinghub.elsevier.com/retrieve/pii/S0964830510000041 [Accessed January 28, 2014].

Boziaris, I.S. et al., 2011. Antimicrobial effect of filipendula ulmaria plant extract against selected foodborne pathogenic and spoilage bacteria in laboratory media, fish flesh and fish roe product. *Food Technology and Biotechnology*, 49(2), pp.263–270.

Bradner, J.R., Sidhu, R.K., et al., 1999. Hemicellulase Activity of Antarctic Microfungi. *Journal of Applied Microbiology*, 87, pp.366–370.

Bradner, J.R., Gillings, M. & Nevalainen, K.M.H., 1999. Qualitative assessment of hydrolytic activities in antarctic microfungi grown at different temperatures on solid media. *Journal of Microbiology*, 1, pp.131–132.

Brimblecombe, P., 2014. Refining climate change threats to heritage. *Journal of the Institute of Conservation*, 37(2), pp.85–93.

Brimblecombe, P. & Brimblecombe, C., 2016. Climate Change and Non-mechanically Ventilated Historic Interiors. *The Journal of Preservation Technology*, 47(1), pp.31–38.

British Standards Institution, 2012. *PAS 198:2012 Specification for Managing Environmental Conditions for Cultural Collections*,

British Standards Institution, 1999. *Tensile Properties of Fabrics Part I: Determination of Maximum Force and Elongation at Maximum Force Using the Strip Method*, British Standards Institute.

Buroker-kilgore, M. & Wang, K.K., 1993. A Coomassie brilliant blue G-250-based colorimetric assay for measuring activity of calpain and other proteases. *Analytical biochemistry*, 208, pp.387–392.

Cabral, J.P.S., 2010. Can we use indoor fungi as bioindicators of indoor air quality? Historical perspectives and open questions. *Science of the Total Environment*, 408(20), pp.4285–4295. Available at: http://dx.doi.org/10.1016/j.scitotenv.2010.07.005.

Camuffo, D. et al., 2001. Environmental monitoring in four European museums. *Atmospheric Environment*, 35(1), pp.127–140.

Camuffo, D. et al., 2013. Past, present and future effects of climate change on a wooden inlay bookcase cabinet: A new methodology inspired by the novel European Standard EN 15757:2010. *Journal of Cultural Heritage*. Available at: http://linkinghub.elsevier.com/retrieve/pii/S1296207413000022 [Accessed January 28, 2014].

Cardamone, J.M., 2010. Investigating the microstructure of keratin extracted from wool: Peptide sequence (MALDI-TOF/TOF) and protein conformation (FTIR). *Journal of Molecular Structure*, 969(1–3), pp.97–105. Available at: http://dx.doi.org/10.1016/j.molstruc.2010.01.048.

Cardinali, G. et al., 2002. Multicenter Comparison of Three Different Analytical Systems for Evaluation of DNA Banding Patterns from Cryptococcus neoformans. *Society*, 40(6), pp.2095–2100.

Carr, C.M. & Lewis, D.M., 1993. An FTIR spectroscopic study of the photodegradation and thermal degradation of wool. *Journal of the Society of Dyers and Colourists*, 109(1), pp.21–24.

Coates, J., 2000. Interpretation of Infrared Spectra, A Practical Approach. In R. A. Meyers, ed. *Encyclopedia of Analytical Chemistry*. John Wiley & Sons Ltd, pp. 10815–10837. Available at: http://doi.wiley.com/10.1002/9780470027318.a5606.

Cogliati, M. et al., 2007. Cryptococcus neoformans typing by PCR fingerprinting using (GACA) 4 primers based on C. neoformans genome project data. *Journal of Clinical Microbiology*, 45(10), pp.3427–3430.

Colom, X. et al., 2003. Structural analysis of photodegraded wood by means of FTIR spectroscopy. *Polymer Degradation and Stability*, 80(3), pp.543–549.

Corte, A.M., Ferroni, a. & Salvo, V.S., 2003. Isolation of fungal species from test samples and maps damaged by foxing, and correlation between these species and the environment. *International Biodeterioration & Biodegradation*, 51(3), pp.167–173. Available at: http://linkinghub.elsevier.com/retrieve/pii/S0964830502001373.

Culpeper, N., 1653. *Culpeper's Complete Herbal: A Book of Natural Remedies for Ancient Ills*, Ware: Wordsworth Editions (1995).

Dahlin, E., 1995. Preventive conservation strategies for organic objects in museums , historic buildings and archives Plenary sessions. , pp.57–60.

Dastjerdi, R. & Montazer, M., 2010. A review on the application of inorganic nano-structured materials in the modification of textiles: focus on anti-microbial properties. *Colloids and surfaces. B, Biointerfaces*, 79(1), pp.5–18. Available at: http://www.ncbi.nlm.nih.gov/pubmed/20417070 [Accessed January 23, 2014].

Davis, A.J. et al., 1998. Making mistakes when predicting shifts in species range in response to global warming. *Nature*, 391, pp.783–786.

Deacon, J., 2006. *Fungal Biology* 4th ed., Blackwell Publishing.

Degano, I. et al., 2011. Historical and archaeological textiles: an insight on degradation products of wool and silk yarns. *Journal of chromatography. A*, 1218(34), pp.5837–47. Available at: http://www.ncbi.nlm.nih.gov/pubmed/21774938 [Accessed January 28, 2014].

Derrick, M.., Stulik, D. & Landry, J.., 1999. *Infrared Spectroscopy in Conservation Science* T. Ball & S. Tidwell, eds., Los Angeles: The Getty Conservation Institute.

Derrick, M., 1991. Evaluation of the state of degradation of dead sea scroll samples using FT-IR spectroscopy. *Book Paper Group Annual*, 10(2).

Dey, P., Banerjee, J. & Maiti, M.K., 2011. Comparative lipid profiling of two endophytic fungal isolates--Colletotrichum sp. and Alternaria sp. having potential utilities as biodiesel feedstock. *Bioresource technology*, 102(10), pp.5815–23. Available at: http://www.ncbi.nlm.nih.gov/pubmed/21414775 [Accessed January 15, 2015].

Dickson, S. & Kolesik, P., 1999. Visualization of mycorrhizal fungal structures and quantification of their surface area and volume using laser scanning confocal microscopy. *Mycorrhiza*, (9), pp.205–213.

Dolgin, B. et al., 2012. Assessment of damage in old parchment by DSC and SEM. *Journal of Thermal Analysis and Calorimetry*, 104(1), pp.487–492. Available at: http://www.morana-rtd.com/e-preservationscience/2012/Badea-31-12-2012.pdf%5Cnhttp://www.cyf-kr.edu.pl/~ncbratas/pdf/full_larsen.pdf.

Dornieden, T., Gorbushina, A.A. & Krumbein, W.E., 2001. Biodecay of cultural heritage as a space / time-related ecological situation — an evaluation of a series of studies. , 46(2000), pp.261–270.

Downes, S., 2013. In Training, Removing Mould from Historic Textiles. *ICON News*, p.32.

Duncan, S.M. et al., 2006. Endoglucanase-producing fungi isolated from Cape Evans historic expedition hut on Ross Island, Antarctica. *Environmental Microbiology*, 8(7), pp.1212–1219.

Duncan, S.M. et al., 2010. Monitoring and identification of airborne fungi at historic locations on Ross Island, Antarctica. *Polar Science*, 4(2), pp.275–283. Available at: http://linkinghub.elsevier.com/retrieve/pii/S1873965210000162 [Accessed January 26, 2014].

Duncan, S.M. et al., 2008. Screening fungi isolated from historic Discovery Hut on Ross Island, Antarctica for cellulose degradation. *Antarctic Science*, 20(05), pp.1–8.

Duncan, T. V, 2011. Applications of nanotechnology in food packaging and food safety: barrier materials, antimicrobials and sensors. *Journal of colloid and interface science*, 363(1), pp.1–24. Available at: http://www.ncbi.nlm.nih.gov/pubmed/21824625 [Accessed January 22, 2014].

Dunin-Borkowski, S., 2013. On the Duties of a Librarian (1827). In S. Staniforth, ed. *Historical Perspectives on Preventive Conservation*. The Getty Conservation Institute, pp. 65–67.

Eddy Knight, S., 1999. Goldenseal (Hydrastis canadensis) versus Penicillin : A Comparison of Effects on Staphylococcus aureus , Streptococcus pyogenes , and Pseudomonas aeruginosa. *Bios*, 70(1), pp.3–10.

Erra, P. et al., 1997. FTIR analysis to study chemical changes in wool following a sulfitolysis treatment. *Textile Research Journal*, 67(6), pp.397–401.

Espinel-Ingroff, A. et al., 2010. M51-A Method for Antifungal Disk Diffusion Susceptibility Testing of Nondermatophyte Filamentous Fungi; Approved Guideline. *Clinical and Laboratory Standards Institute*, 30(11), pp.1–29.

Fackler, K. et al., 2007. Qualitative and quantitative changes of beech wood degraded by wood-rotting basidiomycetes monitored by Fourier transform infrared spectroscopic methods and multivariate data analysis. *FEMS Microbiology Letters*, 271(2), pp.162–169.

Faggi, E. et al., 2001. Application of PCR to Distinguish Common Species of Dermatophytes. , 39(9), pp.3382–3385.

Falcão, L. & Araújo, M.E.M., 2014. Application of ATR-FTIR spectroscopy to the analysis of tannins in historic leathers: The case study of the upholstery from the 19th century Portuguese Royal Train. *Vibrational Spectroscopy*, 74, pp.98–103. Available at: http://dx.doi.org/10.1016/j.vibspec.2014.08.001.

Field, A., 2009. *Discovering Statistics Using SPSS* Third Edit.,

Fisher, K. & Phillips, C., 2008. Potential antimicrobial uses of essential oils in food: is citrus the answer? *Trends in Food Science & Technology*, 19(3), pp.156–164. Available at: http://linkinghub.elsevier.com/retrieve/pii/S0924224407003548 [Accessed January 25, 2014].

Flannigan, B., 1997. Air sampling for fungi in indoor environments. *Journal of Aerosol Science*, 28(3), pp.381–392.

Florian, M., 2007a. *Fungal Facts*, Archetype Books.

Florian, M., 2007b. *Protein Facts Fibrous proteins in cultural and natural history artifacts*, Archetype Publications.

Florian, M.E. & Manning, L., 2000. SEM analysis of irregular fungal fox spots in an 1854 book : population dynamics and species identication. , 46, pp.205–220.

Fog Nielsen, K., 2002. *Mould growth on building materials: Secondary metabolites , mycotoxins and biomarkers*. Danish Building Research Institute.

Fog Nielsen, K., 2003. Mycotoxin production by indoor molds. *Fungal Genetics and Biology*, 39(2), pp.103–117. Available at: http://linkinghub.elsevier.com/retrieve/pii/S1087184503000264 [Accessed March 13, 2015].

Fog Nielsen, K. & Smedsgaard, J., 2003. Fungal metabolite screening: database of 474 mycotoxins and fungal metabolites for dereplication by standardised liquid chromatography–UV–mass spectrometry methodology. *Journal of Chromatography A*, 1002, pp.111–136.

France, F.G., 2004. Scientific analysis in the identification of textile materials. In R. Janaway & P. Wyeth, eds. *Scientific Analysis of Ancient and Historic Textiles*. Archetype Publications, pp. 3–11.

Garg, K.L., Jain, K.K. & Mishra, a. K., 1995. Role of fungi in the deterioration of wall paintings. *Science of The Total Environment*, 167(1–3), pp.255–271. Available at: http://linkinghub.elsevier.com/retrieve/pii/004896979504587Q.

Garrod, B. & Fyall, A., 2000. Managing heritage tourism. *Annals of Tourism Research*, 27(3), pp.682–708. Available at: http://www.sciencedirect.com/science/article/pii/S0160738399000948 [Accessed January 29, 2014].

Garside, P. & Wyeth, P., 2004a. Assessing the physical state of the fore topsail of HMS Victory. In R. Janaway & P. Wyeth, eds. *Scientific Analysis of Ancient and Historic Textiles*. Archetype Publications, pp. 118–125.

Garside, P. & Wyeth, P., 2006. Identification of Cellulosic Fibres by FTIR Spectroscopy Differentiation of flax and hemp by polarized ATR FTIR. *Studies in Conservation*, 51(3), pp.205–211.

Garside, P. & Wyeth, P., 2003. Identification of cellulosic fibres by FTIR spectroscopy Thread and single fibre analysis by attenuated total reflectance. *Studies in Conservation*, 48(4), pp.269–275.

Garside, P. & Wyeth, P., 2004b. Polarised-ATR-FTIR Characterisation of Cellulosic Fibres in Relation To Historic. *Restaurator*, 25, pp.249–259.

Garside, P. & Wyeth, P., 2007. Use of polarized spectroscopy as a tool for examining the microstructure of cellulosic textile fibers. *Applied Spectroscopy*, 61(5), pp.523–529.

Geba, M. et al., 2014. Gamma irradiation of protein-based textiles for historical collections decontamination. *Journal of Thermal Analysis and Calorimetry*, 118(2), pp.977–985.

Gerard, J., 1597. *The herball or generall history of plantes*, London: John Norton, 1974.

Gerhardt, L.-C. et al., 2013. Tribological investigation of a functional medical textile with lubricating drug-delivery finishing. *Colloids and surfaces. B, Biointerfaces*, 108, pp.103–9. Available at: http://www.ncbi.nlm.nih.gov/pubmed/23524083 [Accessed January 23, 2014].

Giorni, P. et al., 2008. Effect of aw and CO_2 level on Aspergillus flavus growth and aflatoxin

production in high moisture maize post-harvest. *International Journal of Food Microbiology*, 122, pp.109–113.

Giorni, P. et al., 2014. Influence of water activity and anti-fungal compounds on development and competitiveness of Fusarium verticillioides. *Phytopathologia Mediterranea*, 53(3), pp.459–469.

Goddard, D. & Michaelis, L., 1935. A Study on Keratin. *Journal of the American Leather Chemists Association*, 30, pp.557–568.

Goodell, B., 2003. Brown-rot fungal degradation of wood: Our evolving view. In *Wood Deterioration and Preservation, Advances in our changing world*. Washington, DC: American Chemical Society, pp. 97–118.

Górny, R.L. et al., 2002. Fungal fragments as indoor air biocontaminants. *Applied and Environmental Microbiology*, 68(7), pp.3522–3531.

Green, B.J., Sercombe, J.K. & Tovey, E.R., 2005. Fungal fragments and undocumented conidia function as new aeroallergen sources. *Journal of Allergy and Clinical Immunology*, 115(5), pp.1043–1048.

Guiomar Carneiro Tomazello, M. WIENDL, F., 1995. The Applicability of Gamma Radiation to the Control of Fungi in Naturally Contaminated Paper. *Restaurator*, 16(2), pp.93–99.

Gutarowska, B., Skora, J., et al., 2012. Analysis of the sensitivity of microorganisms contaminating museums and archives to silver nanoparticles. *International Biodeterioration & Biodegradation*, 68, pp.7–17. Available at: http://linkinghub.elsevier.com/retrieve/pii/S0964830511002538 [Accessed January 27, 2014].

Gutarowska, B., Rembisz, D., et al., 2012. Optimization and application of the misting method with silver nanoparticles for disinfection of the historical objects. *International Biodeterioration & Biodegradation*, 75, pp.167–175. Available at: http://linkinghub.elsevier.com/retrieve/pii/S0964830512002715 [Accessed January 28, 2014].

Gutarowska, B. & Michalski, A., 2012. Microbial Degradation of Woven Fabrics and Protection Against Biodegradation. In H.-Y. Jeon, ed. *Woven Fabrics*. InTech, pp. 267–296.

Guzel-seydim, Z.B., Greene, A.K. & Seydim, A.C., 2004. Use of ozone in the food industry. *LWT-Food Science and Technology*, 37, pp.453–460.

Hackney, S. & Hedley, G., 1981. Measurements of the ageing of linen canvas. *Studies in conservation*, 26(1), pp.1–14.

Haleem Khan, a a & Mohan Karuppayil, S., 2012. Fungal pollution of indoor environments and its management. *Saudi journal of biological sciences*, 19(4), pp.405–26. Available at: http://www.pubmedcentral.nih.gov/articlerender.fcgi?artid=3730554&tool=pmcentrez&rendertype=abstract [Accessed January 21, 2014].

Hallett, K. & Howell, D., 2005. Size exclusion chromatography as a tool for monitoring silk degradation in historic tapestries. In R. Janaway & P. Wyeth, eds. *Scientific Analysis of Ancient and Historic Textiles*. Archetype Publications, pp. 143–150.

Hameed, A., Natt, M.A. & Evans, C.S., 1996. Short communication: Production of alkaline protease by a new Bacillus subtilis isolate for use as a bating enzyme in leather treatment. *World Journal of Microbiology and Biotechnology*, 12(3), pp.289–291.

Hankin, L. & Anagnostakis, S.., 1975. The use of solid media for detection of enzyme production by fungi. *Mycologia*, 67, pp.597–607.

Hatfield, G., 2009. *Hatfield's Herbal: The Curious Stories of Britain's Wild Plants*, Penguin UK.

Held, B.W. et al., 2005. Environmental factors influencing microbial growth inside the historic expedition huts of Ross Island, Antarctica. *International Biodeterioration & Biodegradation*, 55(1), pp.45–53. Available at: http://linkinghub.elsevier.com/retrieve/pii/S0964830504000952 [Accessed January 28, 2014].

Hibbett, D.S.H. et al., 2014. The Mycota VII Part A. In D. J. M. and J. W. S. (Eds.), ed. *Systematics and Evolution*. Springer-Verlag Berlin Heidelberg, pp. 373–429.

Hickey, P.C. et al., 2004. Live-cell Imaging of Filamentous Fungi Using Vital Fluorescent Dyes and Confocal Microscopy. *Methods in Microbiology*, 34(Microbial Imaging), pp.63–87.

Hirooka, Y. et al., 2013. Species delimitation for Neonectria coccinea group including the causal agents of beech bark disease in Asia, Europe, and North America. *Mycosystema*, 32(May), pp.485–517.

Holme, I., 2007. Innovative technologies for high performance textiles. *Coloration Technology*, 123(2), pp.59–73. Available at: http://doi.wiley.com/10.1111/j.1478-4408.2007.00064.x [Accessed August 20, 2013].

Hori, R. & Sugiyama, J., 2003. A combined FT-IR microscopy and principal component analysis on softwood cell walls. *Carbohydrate Polymers*, 52(4), pp.449–453.

Huang, H., Lin, C. & Hsu, K., 2015. Comparison of resistance improvement to fungal growth on green and conventional building materials by nano-metal impregnation. *Building and Environment*, 93, pp.119–127. Available at: http://dx.doi.org/10.1016/j.buildenv.2015.06.016.

Huijbregts, Z. et al., 2012. A proposed method to assess the damage risk of future climate change to museum objects in historic buildings. *Building and Environment*, 55, pp.1–14. Available at: http://linkinghub.elsevier.com/retrieve/pii/S0360132312000170 [Accessed January 28, 2014].

Humphrey, J.W. et al., 2000. The importance of conifer plantations in northern Britain as a habitat for native fungi. *Biological Conservation*, 96(2), pp.241–252.

Iamanaka, B.T. et al., 2014. Potential of volatile compounds produced by fungi to influence sensory quality of coffee beverage. *Food Research International*, 64, pp.166–170. Available at: http://linkinghub.elsevier.com/retrieve/pii/S0963996914004098 [Accessed March 13, 2015].

Ingold, C.T., 1953. *Dispersal in Fungi*, Oxford University Press.

Isaksson, T. et al., 2010. Critical conditions for onset of mould growth under varying climate conditions. *Building and Environment*, 45(7), pp.1712–1721. Available at: http://linkinghub.elsevier.com/retrieve/pii/S0360132310000351 [Accessed January 29, 2015].

Janiskee, R.L., 1996. Historic houses and special events. *Annals of Tourism Research*, 23(2), pp.398–414. Available at: http://www.sciencedirect.com/science/article/pii/0160738395000690 [Accessed January 29, 2014].

Johannesson, H., Renvall, P. & Stenlid, J., 2000. Taxonomy of Antrodiella inferred from morphological and molecular data. *Mycological research*, 104, pp.92–99.

Johansson, P., Bok, G. & Ekstrand-tobin, A., 2013. The effect of cyclic moisture and temperature on mould growth on wood compared to steady state conditions. *Building and Environment*, 65, pp.178–184. Available at: http://dx.doi.org/10.1016/j.buildenv.2013.04.004.

Jones, D. & Carr, C., 1998. Investigating the photo-oxidation of wool using FT-Raman and FT-IR spectroscopies. *Textile research journal*, p.739. Available at: http://trj.sagepub.com/content/68/10/739.short.

Kalogerakis, N. et al., 2005. Indoor air quality—bioaerosol measurements in domestic and office premises. *Journal of Aerosol Science*, 36(5–6), pp.751–761. Available at: http://linkinghub.elsevier.com/retrieve/pii/S0021850205000340 [Accessed February 9, 2015].

Karbowska-Berent, J. et al., 2011. Airborne and dust borne microorganisms in selected Polish libraries and archives. *Building and Environment*, 46(10), pp.1872–1879. Available at: http://linkinghub.elsevier.com/retrieve/pii/S0360132311000783 [Accessed January 28, 2014].

Kasprzyk, H. & Wichłacz, K., 2004. Some aspects of estimation of the crystallinity of gamma radiation wood cellulose by FTIR spectroscopy and X-ray diffraction techniques. *Acta Scientiarum Polonorum Silvarum Colendarum Ratio et Industria Lignaria*, 3(1), pp.73–84.

Katajamaa, M., Miettinen, J. & Orešič, M., 2006. MZmine: Toolbox for processing and visualization of mass spectrometry based molecular profile data. *Bioinformatics*, 22(5), pp.634–636.

Kavkler, K. et al., 2015. Deterioration of contemporary and artificially aged cotton by selected fungal species. *Polymer Degradation and Stability*, 113, pp.1–9.

Kavkler, K., Gunde-Cimerman, N., et al., 2011. FTIR spectroscopy of biodegraded historical textiles. *Polymer Degradation and Stability*, 96(4), pp.574–580. Available at: http://linkinghub.elsevier.com/retrieve/pii/S0141391011000103 [Accessed January 28, 2014].

Kavkler, K., Šmit, Ž., et al., 2011. Investigation of biodeteriorated historical textiles by conventional and synchrotron radiation FTIR spectroscopy. *Polymer Degradation and Stability*, 96(6), pp.1081–1086. Available at: http://linkinghub.elsevier.com/retrieve/pii/S0141391011001273 [Accessed January 28, 2014].

Kavkler, K. & Demšar, A., 2011. Examination of cellulose textile fibres in historical objects by micro-Raman spectroscopy. *Spectrochimica Acta - Part A: Molecular and Biomolecular Spectroscopy*, 78(2), pp.740–746.

Kavkler, K. & Demšar, A., 2012. Impact of fungi on contemporary and accelerated aged wool fibres. *Polymer Degradation and Stability*, 97(5), pp.786–792. Available at: http://linkinghub.elsevier.com/retrieve/pii/S0141391012000523 [Accessed January 28, 2014].

Kells, S.A. et al., 2001. Efficacy and fumigation characteristics of ozone in stored maize. *Journal of Stored Products Research*, 37, pp.371–382.

Kerschner, R.L., 1992. A Practical Approach to Environmental Requirements for Collections in Historic Buildings. *Journal of the American Institute for Conservation*, 31(1), pp.65–76.

Kim, J.G., Yousef, A.E. & Khadre, M.A., 2003. Ozone and its current and future application in the food industry. In S. L. TAYLOR, ed. *ADVANCES IN FOOD AND NUTRITION RESEARCH 45*. Academic Press, pp. 167–218.

Kong, R.Y.. et al., 2000. Relationships of Halosarpheia, Lignincola and Nais inferred from partial 18s rDNA. *Mycological research*, 104, pp.35–43.

Konsa, K., Tirrul, I. & Hermann, A., 2014. Wooden objects in museums: Managing biodeterioration situation. *International Biodeterioration & Biodegradation*, 86, pp.165–170. Available at: http://linkinghub.elsevier.com/retrieve/pii/S0964830513002485 [Accessed January 28, 2014].

Koperska, M.A. et al., 2014. Degradation markers of fibroin in silk through infrared spectroscopy. *Polymer Degradation and Stability*, 105(1), pp.185–196.

Koperska, M.A. et al., 2015. Fibroin degradation - Critical evaluation of conventional analytical methods. *Polymer Degradation and Stability*, 120, pp.357–367.

Koperska, M.A., Łojewski, T. & Łojewska, J., 2015. Evaluating degradation of silk's fibroin by attenuated total reflectance infrared spectroscopy: Case study of ancient banners from Polish collections. *Spectrochimica Acta - Part A: Molecular and Biomolecular Spectroscopy*, 135, pp.576–582. Available at: http://dx.doi.org/10.1016/j.saa.2014.05.030.

Korpi, A. et al., 1997. Microbial Growth and Metabolism in House Dust. *International Biodeterioration & Biodegradation*, 40(1), pp.19–27.

Korpi, A., Järnberg, J. & Pasanen, A.-L., 2009. Microbial volatile organic compounds. *Critical reviews in toxicology*, 39(2), pp.139–93. Available at: http://www.ncbi.nlm.nih.gov/pubmed/19204852.

Kowalik, R., 1984. Microbiodeterioration of Library Materials Part 2 Microbiodecomposition of Auxiliary Materials Chapter 5-9. *Restaurator*, 6, pp.61–115.

Kowalik, R., 1980. Microbiodeterioration of Library Materials Part 2 Microbiodecomposition of Basic Organic Library Materials Chapter 4. *Restaurator*, 4, pp.135–219.

Koziróg, A. et al., 2014. Colonising organisms as a biodegradation factor affecting historical wood materials at the former concentration camp of Auschwitz II – Birkenau. *International Biodeterioration & Biodegradation*, 86, pp.171–178. Available at: http://linkinghub.elsevier.com/retrieve/pii/S0964830513002989 [Accessed January 28, 2014].

Krasnov, E.A. et al., 2006. Phenolic compounds from Filipendula ulmaria. *Chemistry of Natural Compounds*, 42(2), pp.148–151.

krus, M., Kilian, R. & Sedlbauer, K., 2007. Mould growth prediction by computational simulation on historic buildings. In T. Padfield & K. Borchersen, ed. *Museum microclimates*. National Museum of Denmark, pp. 185–189.

Krus, M., Michael, S. & Sedlbauer, K., 2010. Comparative Evaluation of the Predictions of Two Established Mold Growth Models. In *Thermal Performance of the Exterior Envelopes of Whole Buildings XI International Conference*.

Kugel, A., Stafslien, S. & Chisholm, B.J., 2011. Antimicrobial coatings produced by "tethering" biocides to the coating matrix: A comprehensive review. *Progress in Organic Coatings*, 72(3), pp.222–252. Available at: http://linkinghub.elsevier.com/retrieve/pii/S0300944011002220 [Accessed January 28,

2014].

Lagaron, J.M., Fernandez-Saiz, P. & Ocio, M.J., 2007. Using ATR-FTIR spectroscopy to design active antimicrobial food packaging structures based on high molecular weight chitosan polysaccharide. *Journal of Agricultural and Food Chemistry*, 55(7), pp.2554–2562.

Lammers, K., Arbuckle-Keil, G. & Dighton, J., 2009. FT-IR study of the changes in carbohydrate chemistry of three New Jersey pine barrens leaf litters during simulated control burning. *Soil Biology and Biochemistry*, 41(2), pp.340–347. Available at: http://dx.doi.org/10.1016/j.soilbio.2008.11.005.

Lankester, P. & Brimblecombe, P., 2012a. Future thermohygrometric climate within historic houses. *Journal of Cultural Heritage*, 13(1), pp.1–6. Available at: http://linkinghub.elsevier.com/retrieve/pii/S1296207411000598 [Accessed January 28, 2014].

Lankester, P. & Brimblecombe, P., 2012b. The impact of future climate on historic interiors. *The Science of the total environment*, 417–418, pp.248–54. Available at: http://www.ncbi.nlm.nih.gov/pubmed/22239966 [Accessed January 28, 2014].

Larsen, R. et al., 2005. Damage assessment of parchment : complexity and relations at different structural levels Giuseppe Della Gatta , Elena Badea and Admir Mas Soghomon Boghosian. *14th triennial meeting of ICOM-CC*, pp.199–208.

Lee, T. et al., 2006. Culturability and concentration of indoor and outdoor airborne fungi in six single-family homes. *Atmospheric Environment*, 40(16), pp.2902–2910.

Leene, J.E., 1972. *Textile Conservation* J. E. Leene, ed., Leene, Jentina Emma. Textile conservation. Butterworths and Smithsonian Institution (for IIC).

Leissner, J. et al., 2015. Climate for Culture : assessing the impact of climate change on the future indoor climate in historic buildings using simulations. *Heritage Science*, pp.1–15.

Li, D.-W. & Kendrick, B., 1996. Functional and causal relationships between indoor and outdoor airborne fungi. *Canadian Journal of Botany*, 74(2), pp.194–209.

Li, D.W. & Kendrick, B., 1995. A year-round study on functional relationships of airborne fungi with meteorological factors. *International journal of biometeorology*, 39(2), pp.74–80.

Lithgow, K. & Stewart, J., 2001. Strategies for Damp Buildings and Plaster : Lacock Abbey in Wiltshire. *Journal of Architectural Conservation*, 7(2), pp.7–26.

López-ribot, J.L., Mcatee, R.K. & Richard, W., 2000. Comparison of DNA-based typing methods to assess genetic diversity and relatedness among Candida albicans clinical isolates. , pp.49–54.

Luciana, C., Dallagnol, A. & Ponsone, L., 2014. Ochratoxin A production by Aspergillus niger : Effect of water activity and a biopreserver formulated with Lactobacillus plantarum CRL 778. , 45.

Luo, X. et al., 2012. Study on Light Aging of Silk Fabric by Fourier Transform Infrared Spectroscopy and Principal Component Analysis. *Analytical Letters*, 45(10), pp.1286–1296. Available at: http://www.tandfonline.com/doi/abs/10.1080/00032719.2012.673098.

Luxford, N., 2009. *Reducing the Risk of Open Display: Optimising the Preventive Conservation of Historic Silks*. University of Southampton.

Magaudda, G., 2004. The recovery of biodeteriorated books and archive documents through

gamma radiation : some considerations on the results achieved. *Journal of Cultural Heritage*, 5, pp.113–118.

Mandal, B.B., Mann, J.K. & Kundu, S.C., 2009. Silk fibroin/gelatin multilayered films as a model system for controlled drug release. *European journal of pharmaceutical sciences : official journal of the European Federation for Pharmaceutical Sciences*, 37(2), pp.160–71. Available at: http://www.ncbi.nlm.nih.gov/pubmed/19429423 [Accessed January 28, 2014].

Mandrioli, P. & Saiz-Jimenez, C., 1997. Biodeterioration: Macromonitoring and Microeffects on Cultural Heritage and the Potential Benefits of Research to Society. In *EC Advanced Study Course, Technical Notes for Sessions 7–8*. pp. 1–15.

Manso, M. & Carvalho, M.L., 2009. Application of spectroscopic techniques for the study of paper documents: A survey. *Spectrochimica Acta - Part B Atomic Spectroscopy*, 64(6), pp.482–490. Available at: http://dx.doi.org/10.1016/j.sab.2009.01.009.

Marshall, M.N., 1996. Sampling for qualitative research Sample size. *Family Practice*, 13(6), pp.522–525.

Martens, M., 2012. *Climate Risk Assessment in Museums*. Technische Universiteit Eindhoven.

Martin, K.J. & Rygiewicz, P.T., 2005. Fungal-specific PCR primers developed for analysis of the ITS region of environmental DNA extracts. *BMC microbiology*, 5, p.28.

Matysik, S., Herbarth, O. & Mueller, A., 2009. Determination of microbial volatile organic compounds (MVOCs) by passive sampling onto charcoal sorbents. *Chemosphere*, 76(1), pp.114–9. Available at: http://www.ncbi.nlm.nih.gov/pubmed/19289243 [Accessed March 13, 2015].

McDonald, B. a, 1997. The population genetics of fungi: tools and techniques. In *Population Genetics of Soilborne Fungal Plant Pathogens*. pp. 448–453.

Medrela-Kuder, E., 2003. Seasonal variations in the occurrence of culturable airborne fungi in outdoor and indoor air in CracÃ ow. , 52, pp.203–205.

Menart, E., De Bruin, G. & Strlič, M., 2011. Dose–response functions for historic paper. *Polymer Degradation and Stability*, 96(12), pp.2029–2039. Available at: http://linkinghub.elsevier.com/retrieve/pii/S0141391011002977 [Accessed January 28, 2014].

Merka-Richards, K., 2015. *Insights into the fungal infestation of heritage materials, the optimal sterilisation methods for inoculation and the production of metabolites and enzymes by substrate and fungal type*. Birkbeck, University of London.

Michaelsen, A. et al., 2013. Monitoring the effects of different conservation treatments on paper-infecting fungi. *International Biodeterioration & Biodegradation*, 84, pp.333–341. Available at: http://dx.doi.org/10.1016/j.ibiod.2012.08.005.

Micheluz, A. et al., 2015. The extreme environment of a library: Xerophilic fungi inhabiting indoor niches. *International Biodeterioration & Biodegradation*, 99, pp.1–7. Available at: http://linkinghub.elsevier.com/retrieve/pii/S0964830514003813 [Accessed March 13, 2015].

Millington, K.R. & Church, J.S., 1997. The photodegradation of wool keratin. II. Proposed mechanisms involving cystine. *Journal of Photochemistry and Photobiology B: Biology*, 39(3), pp.204–212.

Mohebby, B., 2005. Attenuated total reflection infrared spectroscopy of white-rot decayed beech wood. *International Biodeterioration and Biodegradation*, 55(4), pp.247–251.

Möhlenhoff, P. et al., 2001. Molecular approach to the characterisation of fungal communities: Methods for DNA extraction, PCR amplification and DGGE analysis of painted art objects. *FEMS Microbiology Letters*, 195(2), pp.169–173.

Momin, R.A. & Nair, M.G., 2001. Mosquitocidal, nematicidal, and antifungal compounds from Apium graveolens L. seeds. *Journal of Agricultural and Food Chemistry*, 49(1), pp.142–145.

Müller, A. et al., 2013. Volatile profiles of fungi--chemotyping of species and ecological functions. *Fungal genetics and biology : FG & B*, 54, pp.25–33. Available at: http://www.ncbi.nlm.nih.gov/pubmed/23474123 [Accessed February 26, 2015].

Muñoz-Bonilla, A. & Fernández-García, M., 2012. Polymeric materials with antimicrobial activity. *Progress in Polymer Science*, 37(2), pp.281–339. Available at: http://linkinghub.elsevier.com/retrieve/pii/S0079670011001079 [Accessed January 22, 2014].

Murtoniemi, T. et al., 2001. Induction of cytotoxicity and production of inflammatory mediators in RAW264. 7 macrophages by spores grown on six different plasterboards. *Inhalation Toxicology*, 13, pp.233–247.

Murtoniemi, T., Nevalainen, A. & Hirvonen, M., 2003. Effect of Plasterboard Composition on Stachybotrys chartarum Growth and Biological Activity of Spores. *Applied and Environmental Microbiology*, 69(7), pp.3751–3757.

Naumann, A. et al., 2005. Fourier transform infrared microscopy and imaging: Detection of fungi in wood. *Fungal Genetics and Biology*, 42(10), pp.829–835.

Nelson, G., 2002. Application of microencapsulation in textiles. *International Journal of Plharmaceutics*, 242(1), pp.55–62.

Nelson, G. et al., 2006. Microencapsulation in Yeast Cells and Applications in Drug Delivery. Chapter 19. In S. Svenson, ed. *In Polymeric Drug Delivery I*. ACS Symposium Series; American Chemical Society: Washington, DC, 2006, pp. 268–281.

Neuhaus, E. & Schellen, H.L., 2007. Conservation Heating for a Museum Environment in a Monumental Building. In *Proceedings of the 10th Conference on the thermal performance of the exterior envelopes of whole buildings*. pp. 2–7.

Nicholson, M. & Von Rotberg, W., 1996. CONTROLLED ENVIRONMENT HEAT TREATMENT AS A SAFE AND EFFICIENT METHOD OF PEST CONTROL. In *Proceedings of 2nd international conference of insect pests in the urban environment*.

Nielsen, K.F. et al., 1998. Production of mycotoxins on artificially and naturally infested building materials. *International Biodeterioration & Biodegradation*, 42, pp.9–16.

Nielsen, K.F. & Fog Nielsen, K., 2003. Mycotoxin production by indoor molds. *Fungal Genetics and Biology*, 39(2), pp.103–117. Available at: http://linkinghub.elsevier.com/retrieve/pii/S1087184503000264 [Accessed March 13, 2015].

Nilsson, J. et al., 2010. The Validation of Artificial Ageing Methods for Silk Textiles Using Markers for Chemical and Physical Properties of Seventeenth-century Silk. *Studies in Conservation*, 55(March), pp.55–65.

Nilsson, R.H. et al., 2009. The ITS region as a target for characterization of fungal communities

using emerging sequencing technologies. *FEMS Microbiology Letters*, 296(1), pp.97–101.

Nitterus, M., 2000. Ethanol as Fungal Sanitizer in Paper Conservation. *Restaurator*, 21(2), pp.101–115.

Nunes, I. et al., 2013. Bioburden assessment and gamma radiation inactivation patterns in parchment documents. *Radiation Physics and Chemistry*, 88, pp.82–89. Available at: http://dx.doi.org/10.1016/j.radphyschem.2013.03.031.

O'Brien, M. et al., 2006. Mycotoxins and Other Secondary Metabolites Produced in Vitro by Penicillium paneum Frisvad and Penicillium roqueforti Thom Isolated from Baled Grass Silage in Ireland. *Society*, (23), pp.9268–9276.

Odlyha, M., Theodorakopoulos, C. & Campana, R., 2007. Studies on Woollen Threads from Historical Tapestries. , 7(1).

Odlyha, M., Theodorakopoulos, C. & Groot, J. De, 2009. Fourier Transform Infra-Red Spectroscopy (ATR/FTIR) and Scanning Probe Microscopy of Parchment. *e-PreservationScience*, 6, pp.138–144.

Oh, S.Y., Dong, I.Y., et al., 2005. Crystalline structure analysis of cellulose treated with sodium hydroxide and carbon dioxide by means of X-ray diffraction and FTIR spectroscopy. *Carbohydrate Research*, 340(15), pp.2376–2391.

Oh, S.Y., Yoo, D. Il, et al., 2005. FTIR analysis of cellulose treated with sodium hydroxide and carbon dioxide. *Carbohydrate Research*, 340(3), pp.417–428.

Orlita, A., 2004. Microbial biodeterioration of leather and its control: A review. *International Biodeterioration and Biodegradation*, 53(3), pp.157–163.

Ortiz, R. et al., 2014. Deterioration, decay and identification of fungi isolated from wooden structures at the Humberstone and Santa Laura saltpeter works: A world heritage site in Chile. *International Biodeterioration & Biodegradation*, 86, pp.309–316. Available at: http://linkinghub.elsevier.com/retrieve/pii/S0964830513003454 [Accessed January 28, 2014].

Oxford & Economics, 2016. *THE IMPACT OF HERITAGE TOURISM FOR THE UK ECONOMY*,

Palacios, S. et al., 2014. Impact of water potential on growth and germination of Fusarium solani soilborne pathogen of peanut. , 1112, pp.1105–1112.

Pandey, K.K. & Pitman, A.J., 2003. FTIR studies of the changes in wood chemistry following decay by brown-rot and white-rot fungi. *International Biodeterioration and Biodegradation*, 52(3), pp.151–160.

Pangallo, D. et al., 2013. Disclosing a crypt: microbial diversity and degradation activity of the microflora isolated from funeral clothes of Cardinal Peter Pázmány. *Microbiological research*, 168(5), pp.289–99. Available at: http://www.ncbi.nlm.nih.gov/pubmed/23305771 [Accessed January 28, 2014].

Park, S. et al., 2009. Measuring the crystallinity index of cellulose by solid state C13 nuclear magnetic resonance. *Cellulose*, 16, pp.641–647.

Pasanen, P. et al., 1997. Growth and Volatile Metabolite Production of Aspergillus Versicolor in House Dust. *Environment International*, 23(4), pp.425–432.

Pavon Flores, S.C., 1976. Gamma Radiation as Fungicide and Its Effects on Paper. *Bulletin of the American Institute for Conservation of Historic and Artistic Works*, 16(1), pp.15–44.

Peacock, E.E., 1996. Biodegradation and characterization of water-degraded archaeological textiles created for conservation research. *International Biodeterioration & Biodegradation*, 38(1), pp.49–59. Available at: http://linkinghub.elsevier.com/retrieve/pii/S0964830596000236.

Peacock, E.E., 2005. The biodeterioration of textile fibres in wet archaeological contexts with implications for conservation choices. *Incontri di Restauro*, 4, pp.46–61.

Pearce, J. & Ferrier, S., 2000. Evaluating the predictive performance of habitat models developed using logistic regression. *Ecological Modelling*, 133(0000), pp.225–245.

Pechey, J., 1694. *The Compleat Herbal of Physical Plants*,

Pei-chih, W., U, S.H. & Chia-yin, L., 2000. Characteristics of indoor and outdoor airborne fungi at suburban and urban homes in two seasons.

Pessoa, O.D.L. et al., 2005. Antibacterial activity of the essential oil from Lippia aff. gracillis. *Fitoterapia*, 76(7–8), pp.712–4. Available at: http://www.ncbi.nlm.nih.gov/pubmed/16233961 [Accessed January 28, 2014].

Pham-hoang, B.N. & Romero-guido, C., 2013. Encapsulation in a natural , preformed , multi-component and complex capsule : yeast cells. *Applied Microbiology and Biotechnology*, 97(15), pp.6635–6645.

Pinzari, F., Pasquariello, G. & Mico, A. De, 2006. Biodeterioration of Paper : A SEM Study of Fungal Spoilage Reproduced Under Controlled Conditions. *Macromolecular Symposia*, 238(1), pp.57–66.

Pitkäranta, M. et al., 2008. Analysis of fungal flora in indoor dust by ribosomal DNA sequence analysis, quantitative PCR, and culture. *Applied and Environmental Microbiology*, 74(1), pp.233–244.

Pitt, J.I., 1975. Xerophilic fungi and the spoilage of foods of plant origin. In *Water relations of foods*. pp. 273–307.

Pluskal, T. et al., 2010. MZmine 2: modular framework for processing, visualizing, and analyzing mass spectrometry-based molecular profile data. *BMC bioinformatics*, 11, p.395. Available at: http://www.pubmedcentral.nih.gov/articlerender.fcgi?artid=2918584&tool=pmcentrez&rendertype=abstract.

Pointing, S.B., 1999. Qualitative methods for the determination of lignocellulolytic enzyme production by tropical fungi. *Fungal Diversity*, 2(March), pp.17–33.

Polizzi, V. et al., 2012. Identification of volatile markers for indoor fungal growth and chemotaxonomic classification of Aspergillus species. *Fungal biology*, 116(9), pp.941–53. Available at: http://www.ncbi.nlm.nih.gov/pubmed/22954337 [Accessed March 13, 2015].

Porck, H.J., 2000. *Rate of Paper Degradation The Predictive Value of Artificial Aging Tests*, Amsterdam.

Pose, G. et al., 2010. Water activity and temperature effects on mycotoxin production by Alternaria alternata on a synthetic tomato medium. *International Journal of Food Microbiology*, 142, pp.348–353. Available at: http://dx.doi.org/10.1016/j.ijfoodmicro.2010.07.017.

Proniewicz, L.M. et al., 2001. FT-IR and FT-Raman study of hydrothermally degradated cellulose. *Journal of Molecular Structure*, 596(1–3), pp.163–169.

Puică, N.M., Pui, A. & Florescu, M., 2006. FTIR Spectroscopy for the analysis of vegetable tanned ancient leather. *European Journal of Science and Theology*, 2(4), pp.49–53.

Rakotonirainy, M.S. & Lavédrine, B., 2005. Screening for antifungal activity of essential oils and related compounds to control the biocontamination in libraries and archives storage areas. *International Biodeterioration & Biodegradation*, 55(2), pp.141–147. Available at: http://linkinghub.elsevier.com/retrieve/pii/S0964830504001313 [Accessed January 28, 2014].

Rao, C.Y., Burge, H. a & Chang, J.C., 1996. Review of quantitative standards and guidelines for fungi in indoor air. *Journal of the Air & Waste Management Association (1995)*, 46(9), pp.899–908.

Reis-Menezes, A.A. et al., 2011. Accelerated testing of mold growth on traditional and recycled book paper. *International Biodeterioration & Biodegradation*, 65(3), pp.423–428. Available at: http://linkinghub.elsevier.com/retrieve/pii/S0964830511000102 [Accessed January 28, 2014].

Rex, J.H. et al., 2008. M38-A2 Reference Method for Broth Dilution Antifungal Susceptibility Testing of Filamentous Fungi; Approved Standard—Second Edition. *Clinical and Laboratory Standards Institute*, 28(16), pp.1–35.

Richardson, E., 2009. *Investigating the Characterisation and Stability of Polyamide 6,6 in Heritage Artifacts*. University of Southampton.

Richardson, E., Martin, G. & Wyeth, P., 2013. Effects of heat on new and aged polyamide 6,6 textiles during pest eradication. *Polymer Degradation and Stability*, pp.6–13. Available at: http://linkinghub.elsevier.com/retrieve/pii/S0141391013004138 [Accessed January 28, 2014].

Rittenour, W.R. et al., 2014. Internal transcribed spacer rRNA gene sequencing analysis of fungal diversity in Kansas City indoor environments. *Environ Sci Process Impacts*, 16(1), pp.33–43.

Roylance, D., 2001. Stress-Strain Curves. , pp.1–14.

La Russa, M.F. et al., 2014. Testing the antibacterial activity of doped TiO 2 for preventing biodeterioration of cultural heritage building materials. *International Biodeterioration & Biodegradation*, 96, pp.87–96. Available at: http://dx.doi.org/10.1016/j.ibiod.2014.10.002.

Sabatini, L., Sisti, M. & Campana, R., 2018. Evaluation of fungal community involved in the biODerioration process of wooden artworks and canvases in Montefeltro area (Marche, Italy). *Microbiological Research*, 207(September 2017), pp.203–210.

Sackville-West, R., 1998. *Knole*, The National Trust.

Saraf, A. et al., 1997. Quantification of ergosterol and 3-hydroxy fatty acids in settled house dust by gas chromatography-mass spectrometry: Comparison with fungal culture and determination of endotoxin by a Limulus amebocyte lysate assay. *Applied and Environmental Microbiology*, 63(7), pp.2554–2559.

Saravanan, D., 2007. UV Protection Textile Materials. *AUTEX Research Journal*, 7(1), pp.53–62.

Sato, Y., Aoki, M. & Kigawa, R., 2014. Microbial deterioration of tsunami-affected paper-based objects: A case study. *International Biodeterioration & Biodegradation*, 88, pp.142–149. Available at: http://linkinghub.elsevier.com/retrieve/pii/S0964830513004459 [Accessed January 28, 2014].

Saunders, D., 2008. Climate Change and Museum Collections. *Studies in conservation*, 3, pp.287–297.

Savi, G.D. & Scussel, V.M., 2014. Effects of Ozone Gas Exposure on Toxigenic Fungi Species from Fusarium , Aspergillus , and Penicillium Genera. *Ozone: Science & Engineering*, 36, pp.144–152.

Scazzocchio, F. et al., 2001. Anti-bacterial activity of Hydrastis canadensis Extract and its Major Isolated Alkaloids. *Planta Med Letters*, 67, pp.561–564.

Schabereiter-Gurtner, C. et al., 2001. Analysis of fungal communities on historical church window glass by denaturing gradient gel electrophoresis and phylogenetic 18S rDNA sequence analysis. *Journal of Microbiological Methods*, 47(3), pp.345–354.

Schmidt, O. & Moreth, U., 2000. Species-specific PCR primers in the rDNA-ITS region as a diagnostic tool for Serpula lacrymans. *Mycological research*, 104, pp.69–72.

Schoch, C.L. et al., 2012. Nuclear ribosomal internal transcribed spacer (ITS) region as a universal DNA barcode marker for Fungi. *Proceedings of the National Academy of Sciences*, 109(16), pp.6241–6246.

Scott, J.A., 2001. *Studies on indoor fungi*. University of Toronto. Available at: http://search.proquest.com/docview/304761835?accountid=14553%5Cnhttp://openurl.library.uiuc.edu/sfxlcl3?url_ver=Z39.88-2004&rft_val_fmt=info:ofi/fmt:kev:mtx:dissertation&genre=dissertations+&+theses&sid=ProQ:ProQuest+Dissertations+&+Theses+Full+Text&atitle=.

Sebestyén, Z. et al., 2015. Thermal characterization of new, artificially aged and historical leather and parchment. *Journal of Analytical and Applied Pyrolysis*, 115, pp.419–427.

Sedlbauer, K. et al., 2001. Mold growth prediction by computational simulation. *IAQ Conference*, (auf CD).

Sedlbauer, K., 2001. *Prediction of mould fungus formation on the surface of and inside building components* .,

Sedlbauer, K. & Krus, M., 2003. A new Model for Mould Prediction and its Application in Practice. *Research in Building Physics*, pp.921–927.

Sequeira, S., Cabrita, E.J. & Macedo, M.F., 2012. Antifungals on paper conservation: An overview. *International Biodeterioration & Biodegradation*, 74, pp.67–86. Available at: http://linkinghub.elsevier.com/retrieve/pii/S0964830512001904 [Accessed January 28, 2014].

Sequeira, S.O. et al., 2017. Ethanol as an antifungal treatment for paper: short-term and long-term effects. *Studies in Conservation*, 62(1), pp.33–42.

Sequeira, S.O., 2016. *Fungal biodeterioration of paper : Development of safer and*. Universidade Nova de Lisboa.

Seves, A. et al., 1998. The microbial degradation of silk: a laboratory investigation. *International Biodeterioration & Biodegradation*, 42, pp.203–211.

Shahid, M. & Mohammad, F., 2013. Perspectives for natural product based agents derived from industrial plants in textile applications – a review. *Journal of Cleaner Production*, 57, pp.2–18. Available at: http://linkinghub.elsevier.com/retrieve/pii/S0959652613003855 [Accessed January 28, 2014].

Shank, J.L., 1977. Encapsulation process utilizing microorganisms and products produced thereby.

Sharma, G., Wu, W. & Dalal, E.N., 2005. The CIEDE2000 color-difference formula: Implementation notes, supplementary test data, and mathematical observations. *Color Research & Application*, 30(1), pp.21–30. Available at: http://doi.wiley.com/10.1002/col.20070 [Accessed January 29, 2015].

Sharma, V.K. et al., 2013. Organic-coated silver nanoparticles in biological and environmental conditions: Fate, stability and toxicity. *Advances in colloid and interface science*, 204, pp.15–34. Available at: http://www.ncbi.nlm.nih.gov/pubmed/24406050 [Accessed January 22, 2014].

Shehata, A.S., Mukherjee, P.K., Aboulatta, H.N., et al., 2008. Single-Step PCR Using (GACA) 4 Primer : Utility for Rapid Identification of Dermatophyte Species and Strains. *Journal of Clinical Microbiology*, 46(8), pp.2641–2645.

Shehata, A.S., Mukherjee, P.K. & Ghannoum, M.A., 2008. Comparison between the Standardized Clinical and Laboratory Standards Institute M38-A2 Method and a 2 , 3-Bis (2-Methoxy-4-Nitro-5- [(Sulphenylamino) Carbonyl] -2 H -Tetrazolium Hydroxide- Based Method for Testing Antifungal Susceptibility of Dermatop. *Journal of Clinical Microbiology*, 46(11), pp.3668–3671.

Shelton, B.G. et al., 2002. Profiles of Airborne Fungi in Buildings and Outdoor Environments in the United States Profiles of Airborne Fungi in Buildings and Outdoor Environments in the United States. *Applied and Environmental Microbiology*, 68(4), pp.1743–1753.

Shirakawa, M.A. et al., 2010. Climate as the most important factor determining anti-fungal biocide performance in paint films. *The Science of the total environment*, 408(23), pp.5878–86. Available at: http://www.ncbi.nlm.nih.gov/pubmed/20869099 [Accessed January 28, 2014].

Shridhar, S.R. et al., 2003. Antifungal Activity of Some Essential Oils. *Journal of Agricultural and Food Chemistry*, 51, pp.7596–7599.

Simon, B., 2013. The Seven Golden Rules for Archivists (1761-1781). In S. Staniforth, ed. *Historical Perspectives on Preventive Conservation*. The Getty Conservation Institute, pp. 63–64.

Smith, B. & Wilson, J.B., 1996. A Consumer's Guide to Evenness Indices. *Oikos*, 76(Fasc. 1), pp.70–82.

Smith, C.A. et al., 2006. XCMS: Processing Mass Spectrometry Data for Metabolite Profiling Using Nonlinear Peak Alignment, Matching, and Identification. *Anal. Chem*, 78(3), pp.779–787.

Souza, J.V. et al., 2003. Screening of fungal strains for pectinolytic activity: endopolygalacturonase production by Peacilomyces clavisporus 2A. UMIDA. 1. *Process Biochemistry*, 39, pp.455–458.

Staniforth, S., 2010. Slow conservation. *Studies in conservation*, 55(2), pp.74–80.

Staniforth, S., Hayes, B. & Bullock, L., 1994. Appropriate technologies for relative humidity control for museum collections housed in historic buildings. *Studies in Conservation*, 39(2), pp.123–128.

Stanley, B. et al., 2016. A Challenging Conservations Environment: Climate Change and Innovative Mould Treatments. In *ICON 2016, CCG and Historic Interiors session*.

Stavroudis, C., 2012. Superstorm Sandy: Frontline Advice for Dealing with Mold and Salvaging Electronic Devices. *WAAC Newsletter*, 34(3), pp.19–21.

Sterflinger, K., 2010. Fungi: Their role in deterioration of cultural heritage. *Fungal Biology Reviews*, 24(1–2), pp.47–55. Available at: http://linkinghub.elsevier.com/retrieve/pii/S1749461310000278 [Accessed January 28, 2014].

Sterflinger, K. & Pinzari, F., 2012. The revenge of time: fungal deterioration of cultural heritage with particular reference to books , paper. , 14(3), pp.559–566.

Stetzenbach, L.., 1998. Microorganisms and Indoor Air Quality. *Clinical Microbiology Newsletter*, 20(19). Available at: http://scholar.google.com/scholar?hl=en&btnG=Search&q=intitle:Clinical+Microbiology+ Newsletter#1 [Accessed March 13, 2015].

Stewart, J., More, A. & Simpson, P., 2008. TH E USE O F ULTRAVIOLET ERRADLVTION T O CONTROL MICROBIOLOGICAL GROWTH O N MOSAIC PAVEMENTS: A PRELIMINARY ASSESSMENT AT NEWPORT ROMAN VILLA. In *THE 10th CONTERENCE OF THE INTERNATIONAL COMMITTEE FOR THE CONSERVATION OF MOSAICS (ICCM)*. pp. 296–305.

Stummer, B.. et al., 2000. Genetic diversity in populations of Uncinula necator: comparison of RFLP- and PCR-based approaches. *Mycological research*, 104, pp.44–52.

Stupar, M. et al., 2014. Antifungal activity of selected essential oils and biocide benzalkonium chloride against the fungi isolated from cultural heritage objects. *South African Journal of Botany*, 93, pp.118–124.

Synowiec, A. et al., 2014. Effect of meadowsweet flower extract-pullulan coatings on rhizopus rot development and postharvest quality of cold-stored red peppers. *Molecules*, 19(9), pp.12925–12939.

Szostak-Kotowa, J., 2004. Biodeterioration of textiles. *International Biodeterioration & Biodegradation*, 53(3), pp.165–170. Available at: http://linkinghub.elsevier.com/retrieve/pii/S0964830503000908 [Accessed January 28, 2014].

Tautenhahn, R. et al., 2007. XC-MS Online: A Web-Based Platform to Process Untargeted Metabolomic Data. *Analytical Chemistry*, pp.10–13.

Taylor, J. et al., 2011. Flood management: prediction of microbial contamination in large-scale floods in urban environments. *Environment international*, 37(5), pp.1019–29. Available at: http://www.ncbi.nlm.nih.gov/pubmed/21481472 [Accessed January 28, 2014].

Thelandersson, S. et al., 2009. Modelling of onset of mould growth for wood exposed to varying climate conditions. *The International Reserarch Group on Wood Protection, Section 2; Test Methodolgy and Assessment. 40th Annual Meeting, Beijing China, 24-28 May 2009.*, pp.1–17.

Thelandersson, S. & Isaksson, T., 2013. Mould resistance design (MRD) model for evaluation of risk for microbial growth under varying climate conditions. *Building and Environment*, 65, pp.18–25. Available at: http://dx.doi.org/10.1016/j.buildenv.2013.03.016.

Tiano, P., 2001. Biodegradation of Cultural Heritage: Decay Mechanisms and Control Methods. *CNR-Centro di Studio Sulle Cause Deperimento e Metodi Conservazione Opere d'Arte*, 9, pp.1–37. Available at: http://www.arcchip.cz/w09/w09_tiano.pdf.

Timar-Balazsy, A. & Eastop, D., 2007. *Chemical Principles of Textile Conservation*, Butterworth Heinemann.

Tondi, G. et al., 2015. ATR FTIR Mapping of Leather Fiber Panels. *Journal of Applied Spectroscopy*, 81(6), pp.1078–1080.

Townend, J., 2009. *Practical statistics for Environmental and Biological Scientists*, Wiley.

Trovão, J. et al., 2013. Can arthropods act as vectors of fungal dispersion in heritage collections? A case study on the archive of the University of Coimbra, Portugal. *International Biodeterioration and Biodegradation*, 79, pp.49–55. Available at: http://dx.doi.org/10.1016/j.ibiod.2012.10.015.

Valaskova, V. & Baldrian, P., 2006. Degradation of cellulose and hemicelluloses by the brown rot fungus Piptoporus betulinus – production of extracellular enzymes and characterization of the major cellulases. *Microbiology*, 152, pp.3613–3622.

Valentin, N., 1993. Comparative Analysis of Insect Control by Nitrogen , Argon and Carbon Dioxide in Museum, Archive and Herbarium Collections. *International Biodeterioration & Biodegradation*, 32, pp.263–278.

Valentin, N., Lidstrom, M. & Preusser, F., 1990. Microbial Control by Low Oxygen and Low Relative Humidity Environment. *Studies in Conservation*, 35(4), pp.222–230.

Vaskainen, O., Hottola, J. & Siitonen, J., 2010. Modeling species co-occurrence by multivariate logistic regression generates new hypotheses on fungal interactions Reports. , 91(9), pp.2514–2521.

Vepari, C. & Kaplan, D.L., 2007. Silk as a Biomaterial. *Progress in polymer science*, 32(8–9), pp.991–1007. Available at: http://www.pubmedcentral.nih.gov/articlerender.fcgi?artid=2699289&tool=pmcentrez& rendertype=abstract [Accessed January 21, 2014].

Vereecken, E. & Roels, S., 2012. A Review of mould prediction models and their influence on mould risk evaluation. *Building and Environment*, 51, pp.296–310. Available at: http://dx.doi.org/10.1016/j.buildenv.2011.11.003.

Viitanen, H. et al., 2010. Moisture and Bio-deterioration Risk of Building Materials and Structures. *Journal of Building Physics*, 33(3), pp.201–224.

Viitanen, H. et al., 2015. Mold Risk Classification Based on Comparative Evaluation of Two Established Growth Models. *Energy Procedia*, 78, pp.1425–1430. Available at: http://dx.doi.org/10.1016/j.egypro.2015.11.165.

Vilaplana, F. et al., 2015. Analytical markers for silk degradation: comparing historic silk and silk artificially aged in different environments. *Anal Bioanal Chem*, 407, pp.1433–1449.

Villinski, J.R. et al., 2003. Antibacterial activity and alkaloid content of Berberis thunbergii, Berberis vulgaris and Hydrastis canadensis. *Pharmaceutical Biology*, 41(8), pp.551–557.

Wacker Chemie AG, 2009. New Applications for the Aboriginal Rem- edy: Tea Tree Oil – Wrapped up in Sugar Molecules. *Features Wacker Chemie AG*, pp.1–10.

Wang, X. et al., 2007. Nanolayer biomaterial coatings of silk fibroin for controlled release. *Journal of controlled release : official journal of the Controlled Release Society*, 121(3), pp.190–9. Available at: http://www.pubmedcentral.nih.gov/articlerender.fcgi?artid=2695962&tool=pmcentrez& rendertype=abstract [Accessed January 28, 2014].

Warscheid, T. & Braams, J., 2001. Biodeterioration of stone : a review. , 46(2000), pp.343–368.

Was-Gubala, J. & Salerno-Kochan, R., 2000. The biodegradation of the fabric of soldiers' uniforms. *Science & justice : journal of the Forensic Science Society*, 40(1), pp.15–20. Available at: http://www.ncbi.nlm.nih.gov/pubmed/10795424.

Watanabe, A. et al., 2006. Drying process of microcrystalline cellulose studied by attenuated total reflection IR spectroscopy with two-dimensional correlation spectroscopy and principal component analysis. *Journal of Molecular Structure*, 799(1–3), pp.102–110.

van der Werf, I.D. et al., 2017. Chemical characterization of medieval illuminated parchment scrolls. *Microchemical Journal*, 134, pp.146–153. Available at: http://linkinghub.elsevier.com/retrieve/pii/S0026265X17303296.

White, M.M. et al., 2006. Phylogeny of the Zygomycota based on nuclear ribosomal sequence data. *Mycologia*, 98(6), pp.872–884.

Wihlborg, R., Pippitt, D. & Marsili, R., 2008. Headspace sorptive extraction and GC-TOFMS for the identification of volatile fungal metabolites. *Journal of Microbiological Methods*, 75(2), pp.244–250. Available at: http://linkinghub.elsevier.com/retrieve/pii/S0167701208002303 [Accessed March 13, 2015].

Wilson, R.. et al., 2005. Changes to the elevational limits and extent of species ranges associated with climate change. *Ecology Letters*, 8, pp.1138–1146.

Wojciechowska, E. et al., 2002. The application of Fourier-transform infrared (FTIR) and Raman spectroscopy (FTR) to the evaluation of structural changes in wool fibre keratin after deuterium exchange and modification by the orthosilicic acid. *Journal of Molecular Structure*, 614(1–3), pp.355–363.

Wojciechowska, E. et al., 2004. The use of Fourier transform-infrared (FTIR) and Raman spectroscopy (FTR) for the investigation of structural changes in wool fibre keratin after enzymatic treatment. *Journal of Molecular Structure*, 704(1–3), pp.315–321.

Wojciechowska, E., Włochowicz, A. & Wesełucha-Birczyńska, A., 1999. Application of Fourier-transform infrared and Raman spectroscopy to study degradation of the wool fiber keratin. *Journal of Molecular Structure*, 511–512, pp.307–318.

World Health Organization, 2009. *WHO guidelines for indoor air quality- Dampness and Mould*,

Wu, C. & Hsiang, T., 2000. Genetic relationships of pathogenic Typhula species assessed by RAPD, ITS-RFLP and ITS sequencing. *Mycological research*, 104, pp.16–22.

Wu, J. et al., 2013. In situ synthesis of silver-nanoparticles/bacterial cellulose composites for slow-released antimicrobial wound dressing. *Carbohydrate Polymers*. Available at: http://linkinghub.elsevier.com/retrieve/pii/S0144861713011223 [Accessed January 28, 2014].

X-rite, 2007. *A Guide to Understanding Colour Communication*,

Xiao, L. et al., 2014. HS-SPME GC/MS characterization of volatiles in raw and dry-roasted almonds (Prunus dulcis). *Food chemistry*, 151, pp.31–9. Available at: http://www.ncbi.nlm.nih.gov/pubmed/24423498 [Accessed January 28, 2015].

Yamada, H. et al., 2001. Preparation of undegraded native molecular fibroin solution from silkworm cocoons. *Materials Science and Engineering*, 14, pp.41–46.

Yoon, Y.K. et al., 2013. Synthesis and evaluation of antimycobacterial activity of new benzimidazole aminoesters. *European Journal of Medicinal Chemistry*. Available at: http://linkinghub.elsevier.com/retrieve/pii/S0223523413003930 [Accessed January 28, 2014].

Zhao, H. et al., 2007. Studying cellulose fiber structure by SEM, XRD, NMR and acid hydrolysis. *Carbohydrate Polymers*, 68, pp.235–241.

Zotti, M., Ferroni, a. & Calvini, P., 2008. Microfungal biodeterioration of historic paper: Preliminary FTIR and microbiological analyses. *International Biodeterioration & Biodegradation*, 62(2), pp.186–194. Available at: http://linkinghub.elsevier.com/retrieve/pii/S0964830508000103 [Accessed January 28, 2014].

Zotti, M., Ferroni, A. & Calvini, P., 2011. Mycological and FTIR analysis of biotic foxing on paper substrates. *International Biodeterioration and Biodegradation*, 65(4), pp.569–578. Available at: http://dx.doi.org/10.1016/j.ibiod.2010.01.011.

Zou, X. et al., 1994. Accelerated aging of papers of pure cellulose: mechanism of cellulose degradation and paper embrittlement. *Polymer Degradation and Stability*, 43, pp.393–402.

Zyska, B., 1997. Fungi isolated from library materials: A review of the literature. *International Biodeterioration & Biodegradation*, 40(1), pp.43–51. Available at: http://linkinghub.elsevier.com/retrieve/pii/S0964830597000619.

Appendices – Chapter 2

	A	B	C	D	E	F	G	H	I	J	K	L	M	N
1		CFU risk calculator												
3		This tool is designed to help interpret the results of indoor air sampling and whether there is a risk of an internal fungal source. All of the fields must be completed												
5		Elevation above sea level	50		This can be found at: https://www.freemaptools.com/elevation-finder.htm									
7		Water features	Fountain or less		Any water features that are close to the property									
9		Building classification			The type of building in which air samples were taken									
11		Floor level			Negative values are basement levels									
13		Windows	No windows		The type of glazing in the air sample location									
15		Mean outdoor temperature (Max (°C))	0		This can be found using the local weather station data for the time that air sampling took place (http://www.metoffice.gov.uk/public/weather/climate-									
17		Mean CFU m³	1		Calculated from the average colony count of triplicate indoor air samples									
19		Fungal growth observed	No		Whether fungal growth has been observed on collections or the building fabric									
21		High internal CFU - further investigation required	No		Result: If yes, the colony forming unit count is over 100 higher than the external air. This could indicate and internal spore source and should be investigated further. If no, the colony forming unit count is less than that of the external and any CFU/m³ counts over 600 are likely to be due to the external environment.									

Dropdown list in C7: Fountain or less / Pond / Stream / Water storage / Lake / River / Coastal

Data form

Screen shot of an example user form in Excel for the prediction of whether an area within a building will be at risk. The image shows the example for the colony forming units, but one has also been created for the risk of fungal growth.

Appendices – Chapter 3

Material	Supplier	Product code (if available)
Silk Cotton linen	Whaleys Bradford Ltd	Fuji Silk Natural Calico Light A2085 Linen Scrim Natural (Loomstate)
Wool	Rainbow Silks	Fine Wool Natural Loomstate
Cotton and linen paper Beech wood paper Goat skin parchment	Shepherds London	RM 1790's Wove Shepherds Age Compatible (SMAC) Pergamena Goat Vellum
Pine veneer Oak veneer	Vale Veneers	

Suppliers of organic materials used in experimental work

Appendices- Chapter 4
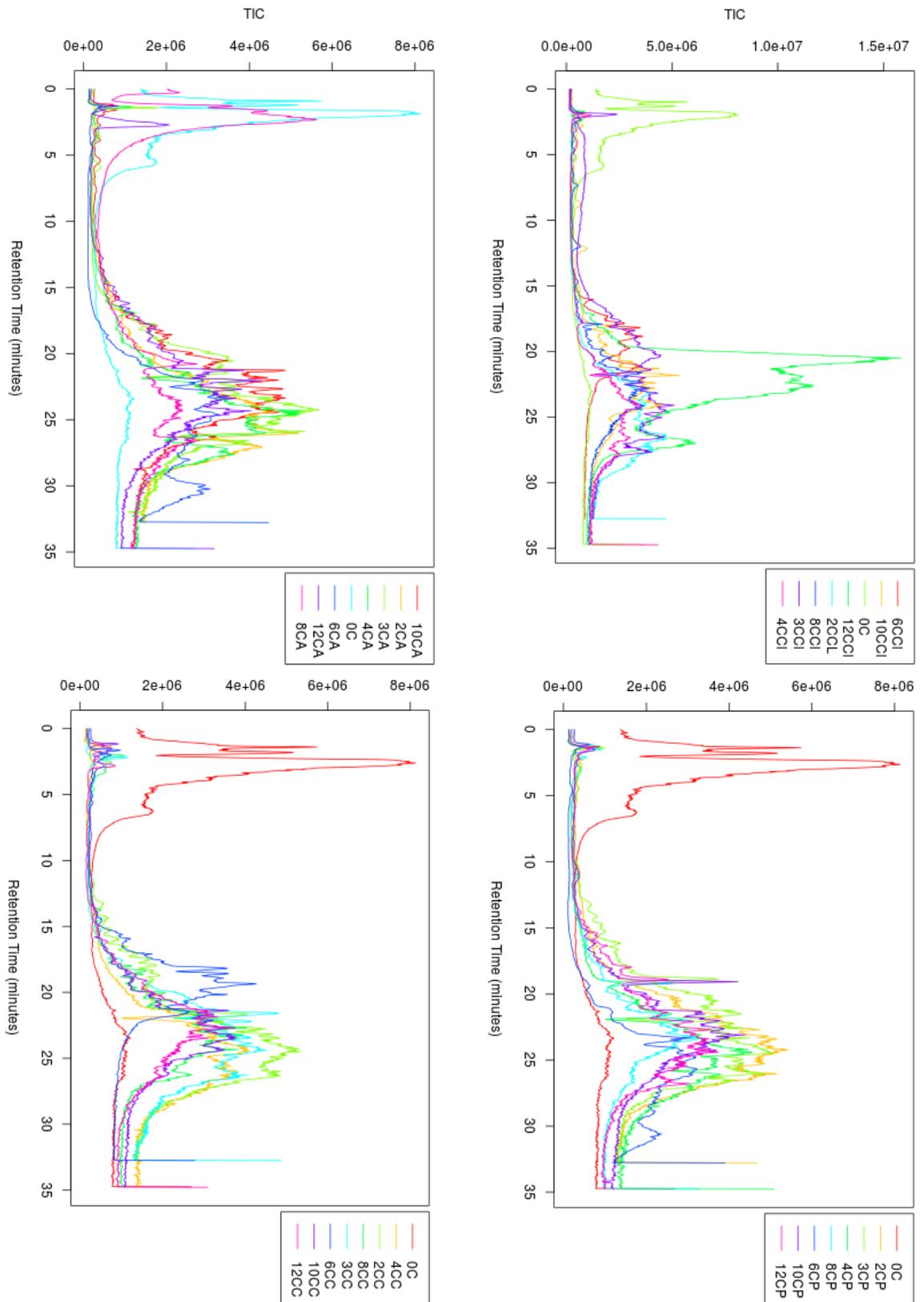
Retention time & baseline corrected total ion chromatogram for cotton under each condition, produced by XC-MS. The key shows the sample code as the number of weeks incubated, C for cotton and the inoculation condition (A= Aspergillus, *Cl*=Cladosporium, *C=control/natural biofilm & P*=Penicillium*)*

276

The significant features from the total ion chromatogram for cotton under each incubation condition that were not found in the control; identified using XC-MS and the chemical taxonomy of the compound from METLIN. M/z =the median mass over charge ratio of the feature peak, RT= median retention time, Max Int= the maximum intensity recorded for the feature.

Fungi	m/z	RT	Max Int	Adduct	Chemical taxonomy	Information
Aspergillus	845.3	23.3	29075	M+Na	Flavonoid	Pigment
	933.3	25.3	14982	M+K	Triazine	Toxin
	794.8	25.6	9812	M+	Organonitrogen compound	
	773.8	24.7	6644	M+2Na	Azaspirodecane derivative	
	373.7	24.2	4786	M+2Na	Aminoglycoside	Toxin
	696.8	25.4	3562	M+H-2H$_2$O	Benzoic acid ester	
Cladosporium	640.9	20.5	43654	M+k	Alkanolamine	
	1173.3	22.9	23642	M+K	Oligosaccharide	
	448.5	22.8	16040	M+H-2H$_2$O	Triazine	Toxin
	615.8	23.3	15222	M+Na	Benzene & substituted derivatives	
	586.3	22.5	14145	M+H	Carboxylic acids & derivatives	
	706.3	23.4	11813	M+H	Oligopeptide	
	587.1	22.5	10195	M+NH$_4$	Glycoside	
	888.1	22.7	9156	M+K	Fatty Acyl	
	551.5	22.6	8886	M+NH$_4$	Fatty Acyl	
	1021.7	27.5	4064	M+K	Tetraterpene	Aromatic
Natural Biofilm	905.5	26.6	123353	M+H-2H$_2$O	Glycerophospholipid	
	787.3	24.9	26436	M+K	Fatty acid ester	
	891.2	21.8	24196	M+NH$_4$	Fatty Acyl	
	478.8	21.2	13479	M+Na	Oxepane	
	622.3	23.5	10424	M+K	Oligopeptide	
	1013.3	23.0	8025	M+Na	Oligosaccharide	
	562.8	22.6	7504	M+2Na-H	Thioester	
	1176.3	22.0	6746	M+H	Anthocyanidin	Pigment
	1186.6	23.5	6150	M+H-2H$_2$O	Oligopeptide	
	954.3	22.8	5824	M+NH$_4$	Triterpene saponin	Aromatic
	836.0	24.0	3428	M+Na	Azonaphthalene	Pigment
Penicillium	597.1	20.2	35128	M+2Na-H	Galloyl ester	
	890.3	22.0	29636	M+2Na-H	Indoles and derivatives	Aromatic
	770.3	22.3	5731	M+NH$_4$	Flavones and Flavonols	Pigment
	435.3	23.3	5477	M+Na	Prenol lipid	
	476.9	21.2	5153	M+K	Pyrazine	Aromatic
	409.9	21.3	4318	M+H-2H$_2$O	Phenol ether	
	1123.4	22.5	2615	M+K	Oligosaccharide	Toxin
	576.4	26.5	2322	M+	Sterol	
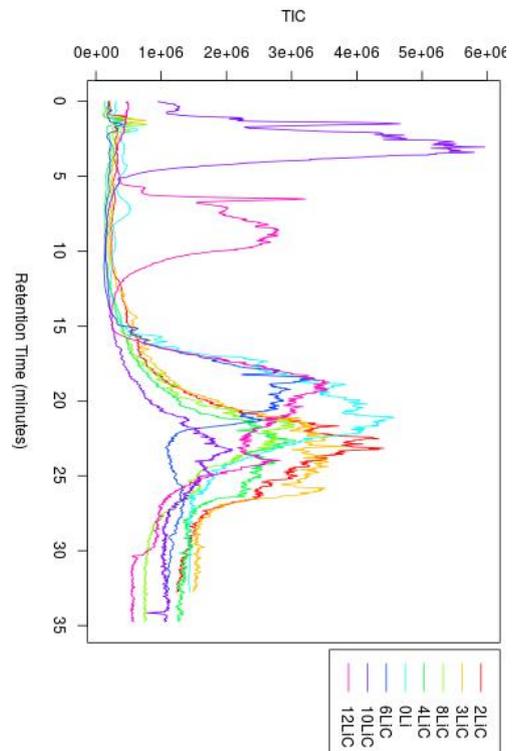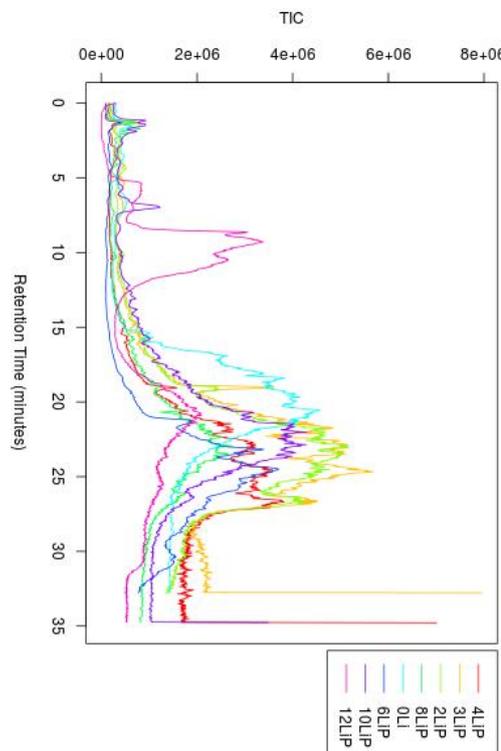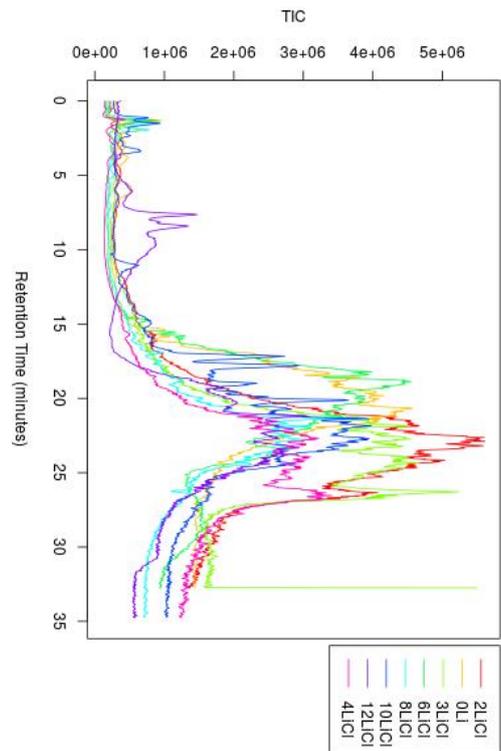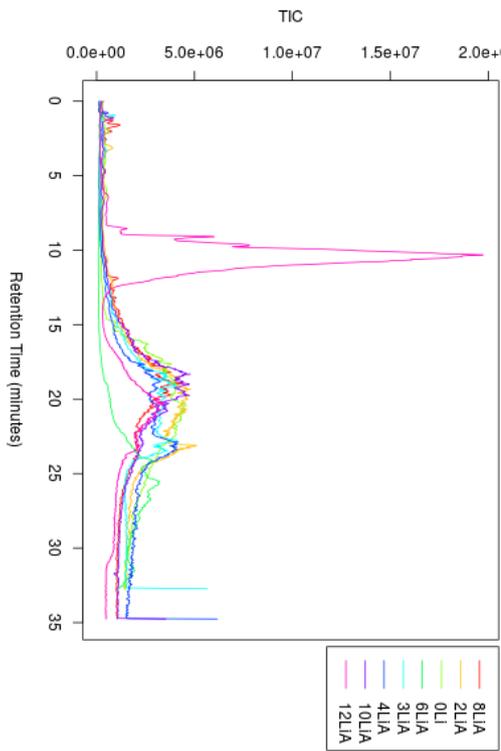
Retention time & baseline corrected total ion chromatogram for Linen under each condition, produced by XC-MS. The key shows the sample code as the number of weeks incubated, Li for linen and the inoculation condition (A= Aspergillus, *Cl*=Cladosporium, *C=control/natural biofilm & P*=Penicillium*)*

The significant features from the total ion chromatogram for linen under each incubation condition that were not found in the control; identified using XC-MS and the chemical taxonomy of the compound from METLIN. M/z =the median mass over charge ratio of the feature peak, RT= median retention time, Max Int= the maximum intensity recorded for the feature.

| Fungi	m/z	RT	Max Int	Adduct	Chemical taxonomy	Information
Aspergillus	858.3	18.8	42758	M+H-H_2O	Quinoline/derivative	Toxin
	902.7	23.3	20678	M+H-H_2O	Phosphosphingolipid	
	430.1	18.3	6576	M+H	Benzoic acid ester	Aromatic
	811.3	22.7	4197	M+2Na-H	Sterol	
	553.3	18.5	3264	M+NH_4	Oligopeptide	Toxin
Cladosporium	454.8	21.4	20242	M+K	Benzoic acid ester	Aromatic
	783.3	21.3	14896	M+H	Flavone/Flavonol	Pigment
	464.3	21.9	13567	M+H-H_2O	Pyrimidine nucleoside	
	283.1	1.8	5855	M+NH_4	Hexose	
	824.9	23.4	5602	M+H	Anthocyanidin	Pigment
	1175.3	22.0	2656	M+Na	Benzene/substituted derivatives	Aromatic
Natural Biofilm	415.7	21.2	6816	M+2Na	Aminoglycoside	
	1086.2	22.9	6211	M+K	Azine/derivative	
	681.3	23.0	4713	M+2Na-H	Cyclic amide	
	670.1	23.3	4202	M+NH_4	Tannin	Pigment
Penicillium	475.0	22.7	29032	M+K	Benzene/substituted derivatives	
	820.3	20.9	4567	M+Na	Aminoglycoside	
	899.4	26.4	3826	M+2Na-H	Oligopeptide	
	763.8	2.1	2825	M+	Benzene/substituted derivatives	
	415.4	21.4	2359	M+NH_4	Fatty amide	
	881.4	26.6	2242	M+Na	Cardenolide glycoside/derivatives	
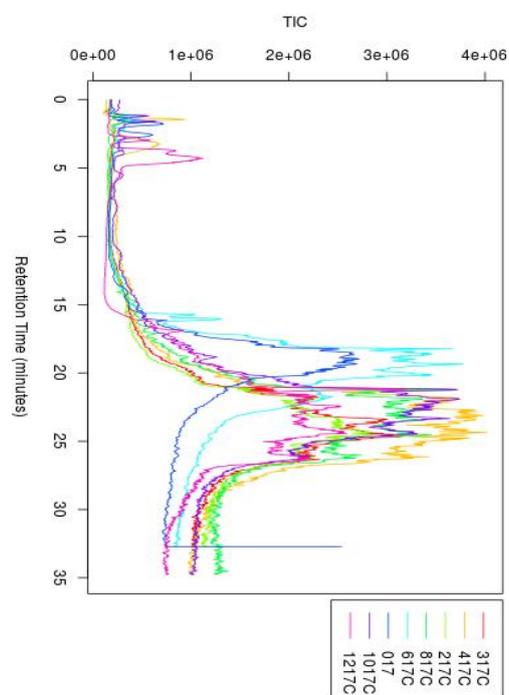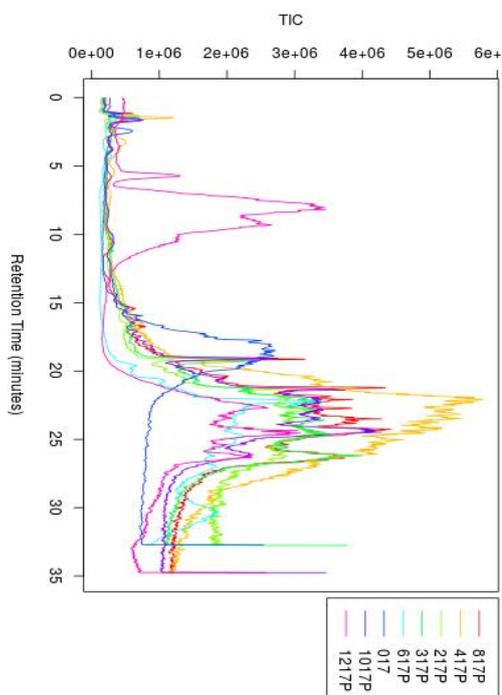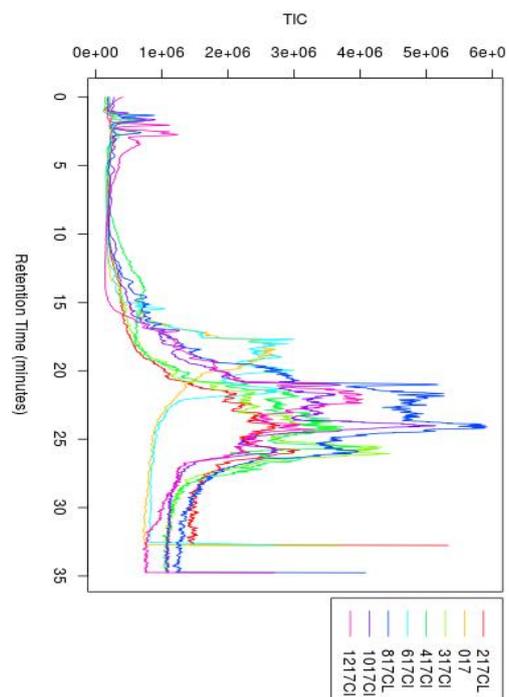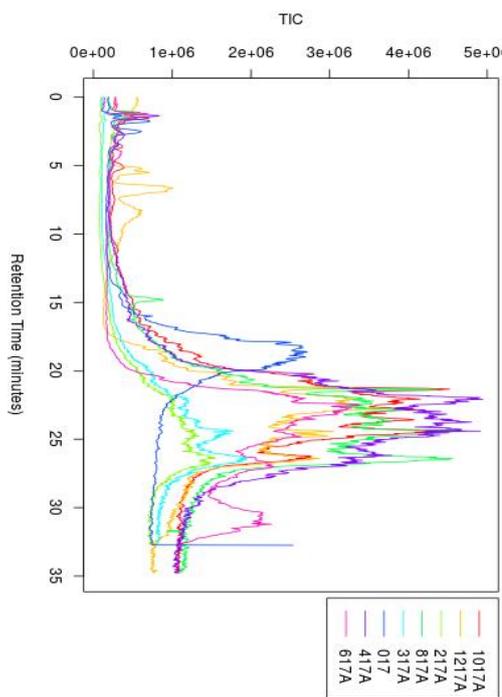
Retention time & baseline corrected total ion chromatogram for cotton and linen paper (17) under each condition, produced by XC-MS. The key shows the sample code as the number of weeks incubated, 17 for the paper and the inoculation condition (A= Aspergillus, Cl=Cladosporium, C=control/natural biofilm & P=Penicillium)

The significant features from the total ion chromatogram for cotton and linen paper under each incubation condition that were not found in the control; identified using XC-MS and the chemical taxonomy of the compound from METLIN. M/z =the median mass over charge ratio of the feature peak, RT= median retention time, Max Int= the maximum intensity recorded for the feature.

| Fungi	m/z	RT	Max Int	Adduct	Chemical taxonomy	Information
Aspergillus	781.2	21.9	170465	M+Na	Phenylacetamide	
	825.2	22.0	118942	M+H-H$_2$O	Anthocyanidin	Pigment
	901.5	26.3	97258	M+Na	Oligopeptide	
	864.2	22.2	77217	M+NH$_4$	Naphthol/derivatives	Aromatic
	876.7	26.4	49687	M+H-H2O	Glycerophospholipid	
	443.3	22.0	26027	M+H	Benzene/substituted derivative	
	841.1	22.0	20646	M+K	Quinoline/derivative	Aromatic
	884.3	26.8	19985	M+NH$_4$	Benzene/substituted derivative	Aromatic
	963.5	27.6	18030	M+Na	Glycerophospholipids	
	1084.2	22.7	15450	M+K	Glycerolipid	
Cladosporium	910.4	26.4	105066	M+H-H$_2$O	Oligopeptide	
	901.4	25.8	77763	M+Na	Benzimidazole	
	783.3	24.0	67570	M+H	Flavone/Flavonol	Pigment
	1001.2	22.1	50041	M+2Na-H	Terpene glycoside	Aromatic
	816.3	22.4	33403	M+H-H$_2$O	Benzenesulfonic acid/derivatives	
	954.2	22.1	33041	M+Na	Fatty Acyl	
	641.0	23.2	26160	M+2Na-H	Alpha amino acid/derivative	
	553.4	22.6	24522	M+H	Benzene/substituted derivative	
	1090.2	22.3	21991	M+2Na-H	Amine	
	640.8	23.2	21179	M+K	Glycerolipid/derivative	
Natural Biofilm	869.2	22.1	74851	M+K	Anthocyanidin	Pigment
	913.3	22.1	62696	M+H-H$_2$O	Anthocyanidin	Pigment
	906.5	26.5	50417	M+H	Oligopeptide	
	687.3	23.4	47195	M+K	Amino acids/peptides/analogues	
	903.4	26.3	39071	M+2Na-H	Oligopeptide	
	873.8	26.2	27841	M+Na	Fatty acyl glycoside	
	906.6	26.6	22901	M+K	Diacylglycerophosphoserine	
	856.3	21.9	19922	M+2Na-H	Oligosaccharide	Toxin
	828.2	22.0	10034	M+NH$_4$	Benzene/substituted derivative	
	799.3	25.5	8237	M+	Oligopeptide	
Penicillium	1002.1	22.5	127833	M+2Na-H	Acyl CoA	
	554.3	22.8	107167	M+K	Long-chain fatty alcohol	
	878.5	26.2	101891	M+	Steroidal glycoside	Toxin
	825.2	22.0	81247	M+H-H$_2$O	Anthocyanidin	Pigment
	1046.2	22.6	80006	M+Na	Acyl CoA	
	1017.2	22.4	28837	M+2Na-H	Anthocyanidin	Pigment
	1152.3	24.7	23077	M+H	Alkane	
	866.4	22.7	9534	M+Na	Carboxylic acid ester	
	586.7	22.8	8737	M+2Na-H	Biphenyl/derivative	Toxin
	396.4	21.5	7029	M+	Aromatic hydrocarbon	
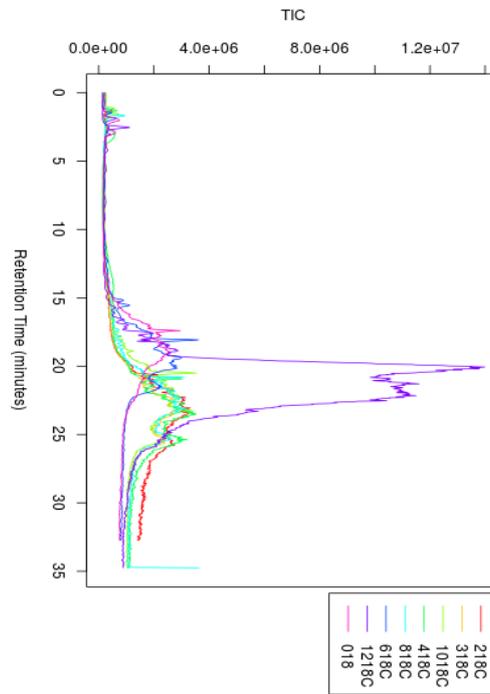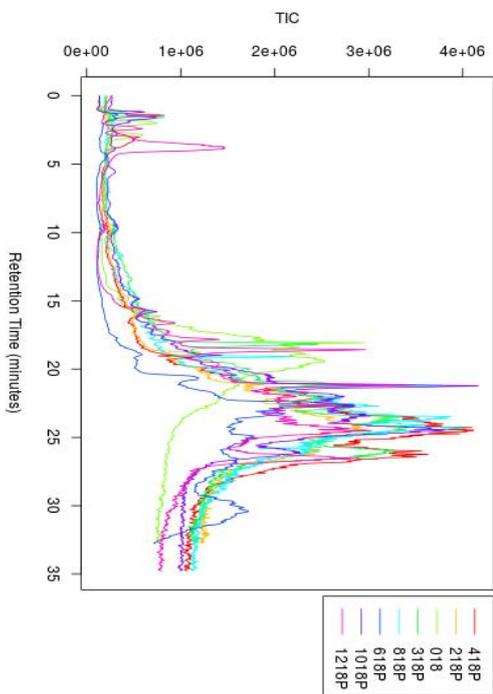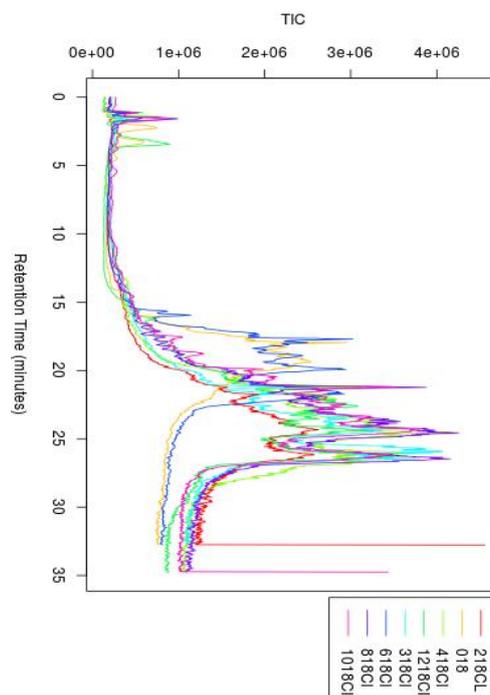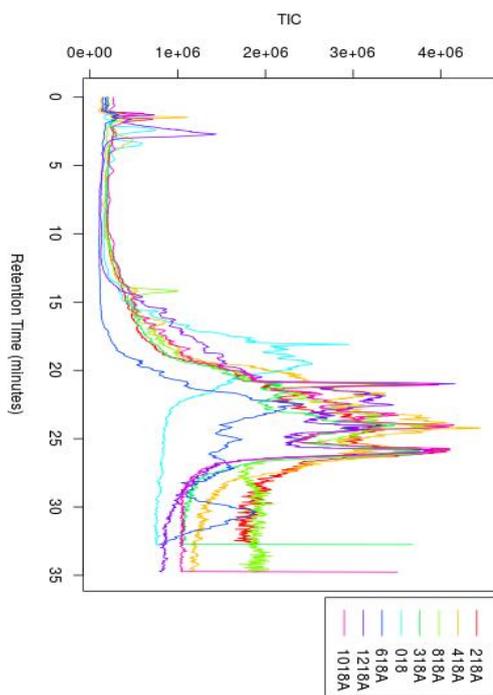
Retention time & baseline corrected total ion chromatogram for beech wood paper (18) under each condition, produced by XC-MS. The key shows the sample code as the number of weeks incubated, 18 for the paper and the inoculation condition (A= Aspergillus, Cl=Cladosporium, C=control/natural biofilm & P=Penicillium)

The significant features from the total ion chromatogram for beech wood paper under each incubation condition that were not found in the control; identified using XC-MS and the chemical taxonomy of the compound from METLIN. M/z =the median mass over charge ratio of the feature peak, RT= median retention time, Max Int= the maximum intensity recorded for the feature.

Fungi	m/z	RT	Max Int	Adduct	Chemical taxonomy	Information
Aspergillus	393.3	21.0	2149663	M+H	Fatty acid esters	
	879.7	26.0	207744	M+H-H$_2$O	Triradylglycerol	
	876.7	26.0	87403	M+H-H$_2$O	Glycerophospholipids	
	910.5	26.5	52424	M+H	Oligopeptide	
	893.4	25.4	40140	M+H	Purines/purine derivative	
	567.7	24.4	28243	M+Na	Substituted pyrrole	Pigment
	857.5	25.9	24476	M+NH$_4$	Oligopeptide	
	510.9	21.7	19768	M+Na	Quinazoline	Toxin
	885.3	26.3	14438	M+K	Cycloalkene	
	927.4	26.6	13255	M+K	Glycerophospholipid	
Cladosporium	903.5	26.2	114129	M+Na	Glycerophospholipid	
	762.8	24.6	56683	M+Na	Alcohol/polyol	
	884.8	26.6	55559	M+H-H$_2$O	Glycerophospholipid	
	873.4	26.1	42500	M+Na	Carboxylic acid ester	Aromatic
	895.9	26.5	30247	M+Na	Carboxylic acid/derivative	Pigment
	851.3	21.9	11275	M+Na	Glycosyl compound	
	849.9	25.9	8049	M+H	Fatty amide	
	548.1	24.0	7155	M+NH$_4$	Acetamide	
	646.6	24.2	6775	M+H-H$_2$O	Fatty acid amide	
	630.3	23.7	6638	M+	Coumarin/derivative	Pigment
Natural Biofilm	413.2	20.7	253210	M+Na	Carbonyl compound	Aromatic
	554.8	21.8	62257	M+K	Quinazoline	Aromatic
	636.0	20.0	29955	M+NH$_4$	Benzene/substituted derivative	Aromatic
	904.3	20.5	17764	M+NH$_4$	Flavone/Flavonol	Pigment
	860.1	21.1	14152	M+	Naphthalene	Pigment
	649.4	23.2	12661	M+H	Anthracene	Pigment
	511.0	21.1	10543	M+Na	Fatty acid ester	Aromatic
	590.3	23.3	9611	M+H-H$_2$O	Peptoid-peptide hydrid	Toxin
	784.2	20.7	6950	M+2Na-H	Pyrimidine nucleotide sugar	
	815.6	24.7	6761	M+NH$_4$	Glycerophospholipids	
Penicillium	393.3	21.2	2089100	M+H	Phosphoric acid ester	Toxin
	876.3	26.0	47679	M+H	Quinoline/derivative	Aromatic
	574.0	23.9	23939	M+K	Naphthalene sulfonic acid/derivative	Pigment
	586.1	9.3	13244	M+H-H$_2$O	Organoheterocyclic compound	Aromatic
	708.6	23.4	12683	M+NH$_4$	Phosphosphingolipid	
	590.3	22.3	8112	M+H-H$_2$O	Peptoid-peptide hydrid	Toxin
	997.4	22.9	7138	M+Na	Indoles/derivative	Aromatic
	533.4	23.9	7072	M+H-H$_2$O	Piperazine/derivative	
	635.2	23.6	6970	M+2Na-H	Acetamide	
	530.6	16.9	6550	M+H-H$_2$O	Fatty acid ester	
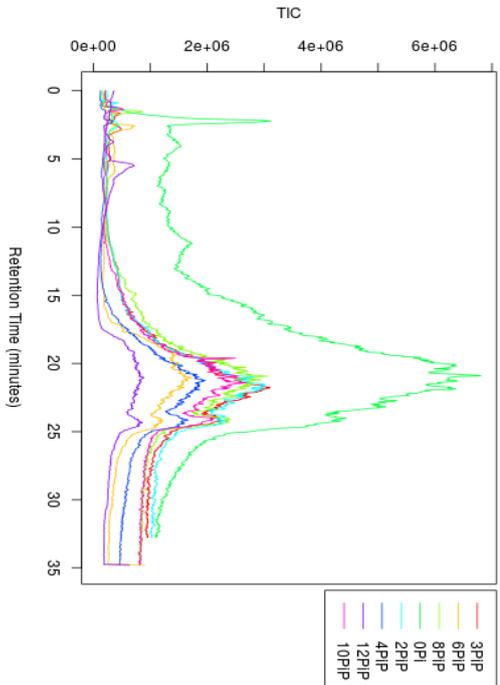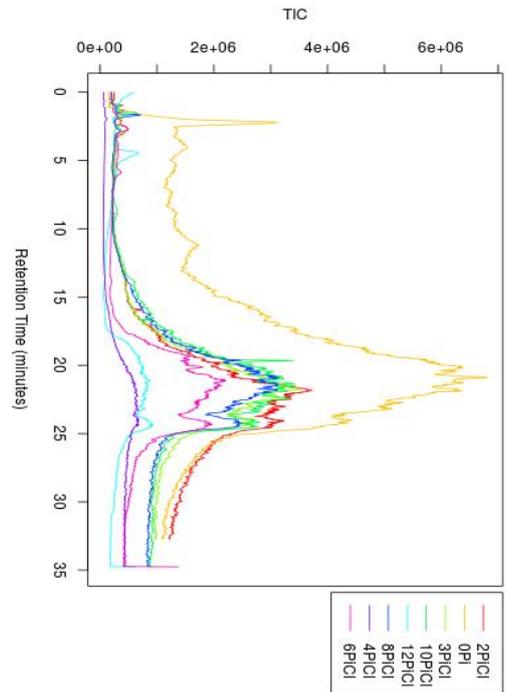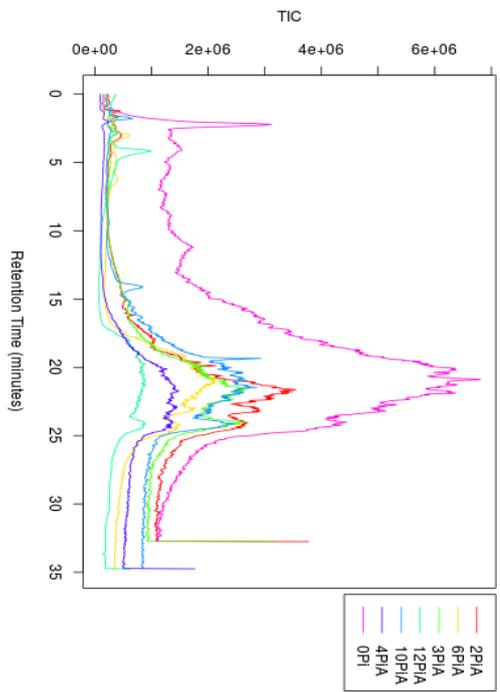
Retention time & baseline corrected total ion chromatogram for pine under each condition, produced by XC-MS. The key shows the sample code as the number of weeks incubated, Pi for pine and the inoculation condition (A= Aspergillus*, Cl=*Cladosporium*, & P=*Penicillium*)*

The significant features from the total ion chromatogram for pine under each incubation condition that were not found in the control; identified using XC-MS and the chemical taxonomy of the compound from METLIN. M/z =the median mass over charge ratio of the feature peak, RT= median retention time, Max Int= the maximum intensity recorded for the feature.

Fungi	m/z	RT	Max Int	Adduct	Chemical taxonomy	Information
Aspergillus	872.1	24.1	5495	M+H-H_2O	Acyl CoA	
Cladosporium	921.4	23.9	69433	M+Na	Oligopeptide	
	922.4	24.0	52280	M+2Na-H	Oligopeptide	
	658.1	21.4	28031	M+Na	Cyclic nucleotide	
	935.4	23.4	20573	M+H-H_2O	Organoheterocyclic compound	
	692.8	20.2	19591	M+K	Benzofuran	Aromatic
	644.5	21.9	18673	M+Na	Glycerophospholipid	
	920.3	20.9	8007	M+NH_4	Oligosaccharide	
	744.3	20.5	5927	M+NH_4	Chalcone/dihydrochalcone	Aromatic
	916.2	22.6	5386	M+NH_4	Biflavonoid/polyflavonoid	Pigment
	831.6	19.6	2953	M+H-$2H_2O$	Triacylglycerol	
Penicillium	921.4	23.9	58935	M+Na	Oligopeptide	
	901.5	24.5	40021	M+Na	Oligopeptide	
	924.4	23.4	36753	M+NH_4	Oligolactosamines	
	813.3	20.2	19043	M+H-H_2O	Fatty acid ester	
	884.3	24.4	13046	M+NH_4	Benzene/substituted derivative	
	860.3	21.1	7058	M+H-H_2O	Carbohydrate/ conjugate	
	870.6	23.9	6760	M+H	Glycerophosphoserine	
	653.5	20.6	5723	M+H	Dicarboxylic acid ester	
	830.4	22.5	4672	M+H-H_2O	Terpenoid	Toxin
	1086.4	21.3	3979	M+K	Xanthene	Pigment
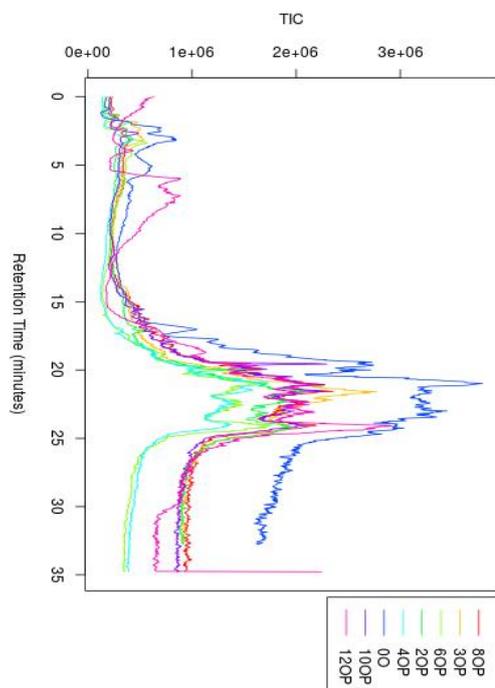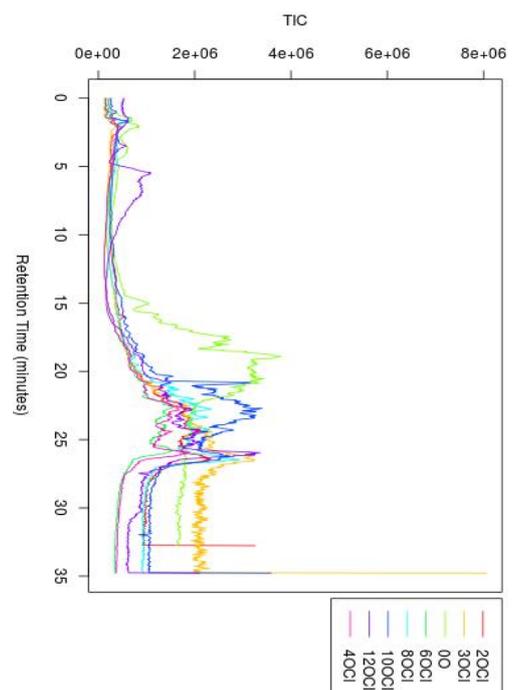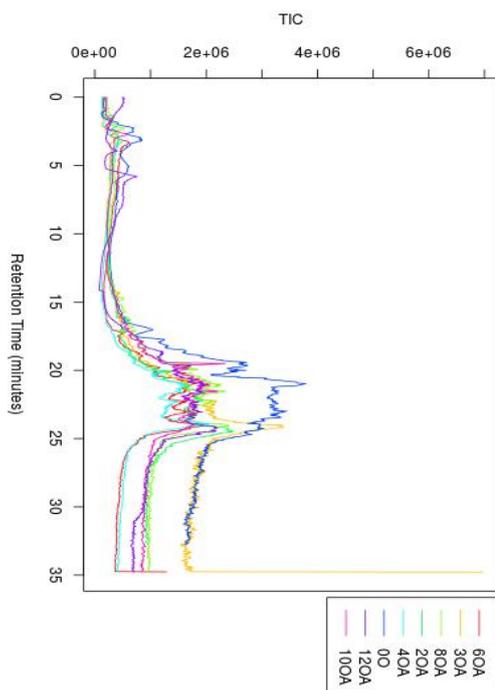
Retention time & baseline corrected total ion chromatogram for oak under each condition, produced by XC-MS. The key shows the sample code as the number of weeks incubated, O for oak and the inoculation condition (A= Aspergillus, Cl=Cladosporium, & P=Penicillium)

The significant features from the total ion chromatogram for oak under each incubation condition that were not found in the control; identified using XC-MS and the chemical taxonomy of the compound from METLIN. M/z =the median mass over charge ratio of the feature peak, RT= median retention time, Max Int= the maximum intensity recorded for the feature.

Fungi	m/z	RT	Max Int	Adduct	Chemical taxonomy	Information
	903.6	24.3	124353	M+H	Oligopeptide	
	905.6	24.4	96282	M+H-2H$_2$O	Cyclic Peptide	
	901.5	24.1	84035	M+	Diterpenoid	
	903.5	24.2	83675	M+Na	Glycerophospholipid	
	873.6	24.0	43211	M+Na	Glycerophospholipid	
Aspergillus	736.3	20.5	35657	M+H-H$_2$O	Diterpenoid	
	876.7	24.3	32287	M+H-H$_2$O	Glycerophospholipid	
	855.1	24.1	25270	M+K	Purine nucleotide	
	921.5	24.4	24000	M+Na	Oligopeptide	
	909.5	24.5	20569	M+H-2H$_2$O	Triterpenoid	
	782.4	24.3	90274	M+K	Monosaccharide derivative	Toxin
	736.3	22.0	86258	M+H-H$_2$O	Diterpenoid	
	659.4	20.9	83880	M+NH$_4$	Phenolic glycoside	
	875.4	26.0	56727	M+2Na-H	Cucurbitacin glycoside	
Cladosporium	878.6	26.1	42562	M+	Glycerophospholipid	
	904.4	22.7	35351	M+H-2H$_2$O	Oligopeptide	
	902.4	25.7	34568	M+K	Naphthalene	Aromatic
	854.8	26.2	14008	M+Na	Fatty Acyl	
	612.3	19.7	10926	M+Na	Oligopeptide	
	895.8	26.5	9872	M+H-H$_2$O	Triradylglycerol	
	901.6	24.2	110130	M+K	Glycerophospholipid	
	901.5	24.0	75972	M+Na	Oligopeptide	
	899.6	24.1	71858	M+Na	Glycerophospholipid	
	494.3	21.1	46233	M+NH$_4$	Oligopeptide	
	917.5	24.0	40346	M+H	Benzothiazole	
Penicillium	630.6	20.5	24172	M+H	Pyrazole	
	750.3	20.5	19404	M+H	Alkyl-phenylketone	
	664.5	21.5	18229	M+2Na-H	Diacylglycerol	
	470.2	20.7	17940	M+NH$_4$	Isoquinoline/derivative	Aromatic
	554.2	21.1	13454	M+H	Piperidine	
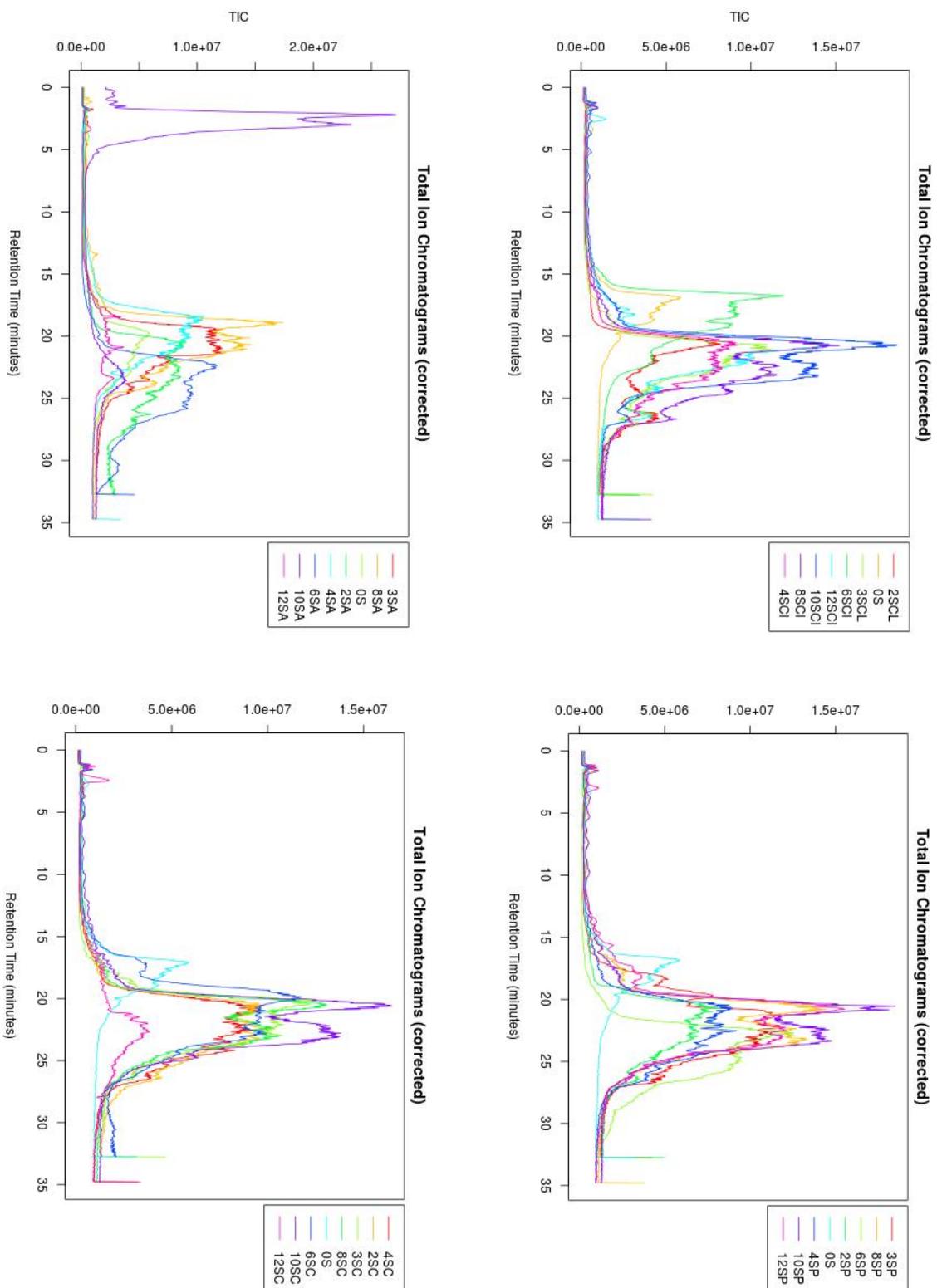
Retention time & baseline corrected total ion chromatogram for silk under each condition, produced by XC-MS. The key shows the sample code as the number of weeks incubated, S for silk and the inoculation condition (A= Aspergillus, Cl=Cladosporium, C=control/natural biofilm & P=Penicillium)

The significant features from the total ion chromatogram for silk under each incubation condition that were not found in the control; identified using XC-MS and the chemical taxonomy of the compound from METLIN. M/z =the median mass over charge ratio of the feature peak, RT= median retention time, Max Int= the maximum intensity recorded for the feature.

Fungi	m/z	RT	Max Int	Adduct	Chemical taxonomy	Information
Aspergillus	683.3	20.1	286419	M+H	Aromatic protein derivative	
	854.7	25.9	105133	M+NH$_4$	Lipid sterol	
	1068.5	21.9	73442	M+H	Cyclic peptide	
	659.7	20.0	62812	M+NH$_4$	Amino acid derivative	
	665.4	20.2	60710	M+H	Glycerophosphoglycerol	
	877.1	26.1	58560	M+H-2H$_2$O	Sesquiterpene	Aromatic
	875.0	26.1	56995	M+K	Nucleoside, nucleotide/analogue	
	820.1	23.8	50154	M+K	Napthalene	Pigment
	537.3	21.9	42573	M+Na	Oligopeptide	
	1076.8	24.9	30882	M+Na	Diacylglcerol	
Cladosporium	758.9	24.2	411657	M+	Alkane	
	596.6	19.8	194495	M+H	Fatty acid derivative	
	679.9	20.3	150622	M+H-H$_2$O	Fatty acid amide	
	883.3	21.1	135942	M+NH$_4$	Heterocyclic amine	
	703.9	20.4	104324	M+NH$_4$	Organic acid ester	
	574.3	19.7	101125	M+Na	Glycophospholipid	
	911.3	21.8	95665	M+2Na-H	Pyran	Mycotoxin
	659.6	20.2	92792	M+	Amino acid derivative	
	935.5	26.8	92449	M+H-H$_2$O	Triterpene saponin	
	747.9	20.8	88991	M+K	Amino acid derivative	
Natural Biofilm	683.3	20.4	318693	M+H	Aromatic protein derivative	
	953.4	22.9	186135	M+K	Phenylpropanoid/polyketide	Aromatic
	870.3	23.8	116850	M+K	Proline/derivative	
	911.3	22.0	78743	M+2Na-H	Pyran	Mycotoxin
	636.6	20.4	54703	M+H-H$_2$O	Pyridine/derivative	
	854.7	26.3	40866	M+NH$_4$	Lipid sterol	
	845.8	23.8	40579	M+H-H$_2$O	Triacylglycerol	
	878.9	26.2	35128	M+H	Naphthalene sulfonate	Pigment
	89.2	22.7	30108	M+H-2H$_2$O	Heterocyclic amine	
	687.5	23.5	27993	M+H	Diglyceride	
Penicillium	683.3	20.4	527805	M+H	Oligopeptide	
	797.4	24.4	159775	M+H	Alpha amino acid/derivative	
	965.3	22.6	149581	M+H	Flavonol glycoside	Pigment
	943.3	21.2	134493	M+H	Pyridinium	
	1168.3	23.5	83583	M+K	Oligosaccharide	
	692.9	23.6	81414	M+2Na-H	Acyclic alkane	
	754.1	24.0	77267	M+Na	Fatty acid/conjugate	
	693.6	23.3	72562	M+K	Coumarin/derivative	Aromatic
	769.0	23.6	62725	M+H-2H$_2$O	Glycerophospholipid	
	1018.8	25.0	58925	M+2Na-H	Hydroxycoumarin	Toxin
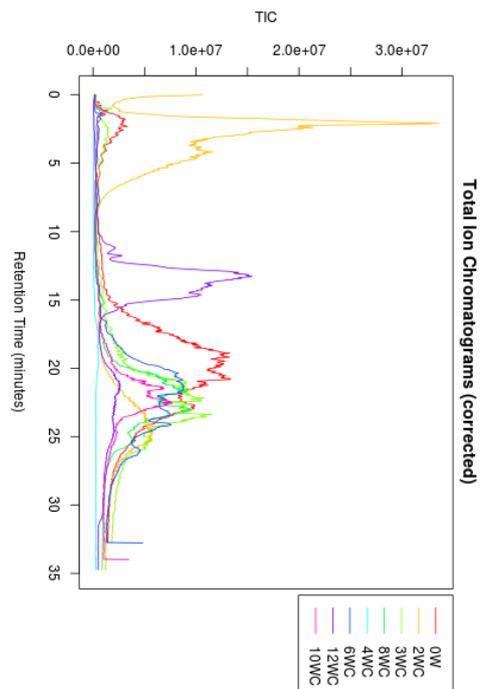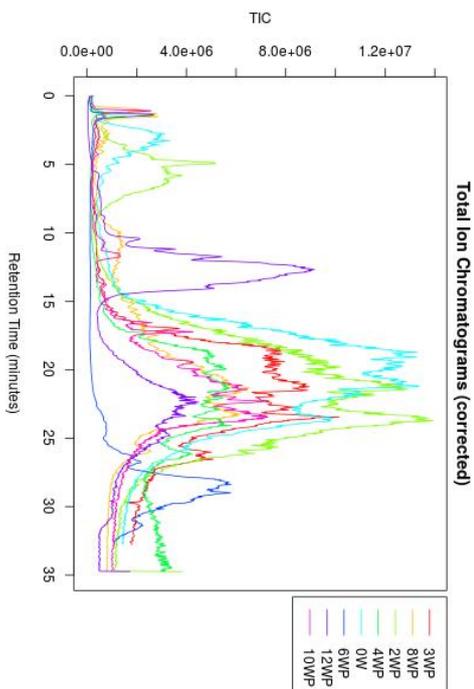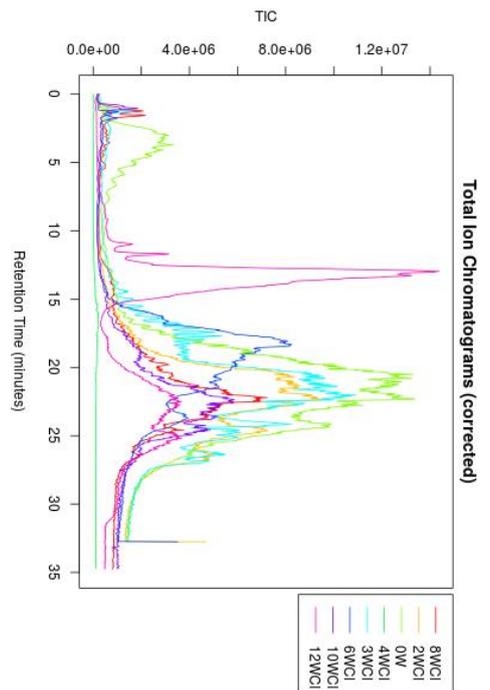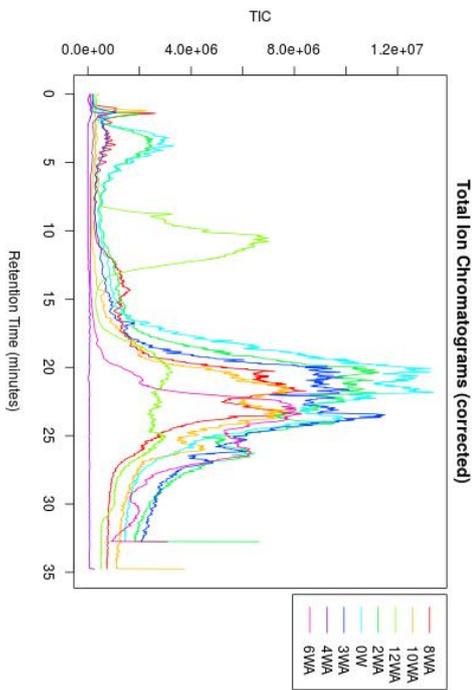
Retention time & baseline corrected total ion chromatogram for Wool under each condition, produced by XC-MS. The key shows the sample code as the number of weeks incubated, W for wool and the inoculation condition (A= Aspergillus, *Cl=*Cladosporium*, C=control/natural biofilm & P=*Penicillium*)*

The significant features from the total ion chromatogram for wool under each incubation condition that were not found in the control; identified using XC-MS and the chemical taxonomy of the compound from METLIN. M/z =the median mass over charge ratio of the feature peak, RT= median retention time, Max Int= the maximum intensity recorded for the feature.

Fungi	m/z	RT	Max Int	Adduct	Chemical taxonomy	Information
	821.3	21.9	117812	M+K	Steroid/steroid derivative	
	664.4	20.6	60571	M+H-2H$_2$O	Amino acid/peptide/analogue	
	1079.3	22.9	14848	M+H-2H$_2$O	Anthocyanidin	Pigment
	435.5	22.0	6292	M+H-H$_2$O	Fatty acid amide	
Aspergillus	942.7	22.0	5228	M+2Na-H	Glycerophospholipid	
	449.3	22.8	4773	M+H-2H$_2$O	Acridine	Pigment
	389.7	23.0	4461	M+2Na-H	Amino acid/peptide/analogue	
	1077.4	22.0	3571	M+H-2H2O	Naphthalene sulfonic acid/derivative	Pigment
	851.4	21.8	95884	M+NH$_4$	Amino acid/peptide/analogue	
	764.4	25.0	59573	M+NH$_4$	Aniline/substituted aniline	Aromatic
	1113.4	22.8	57831	M+2Na-H	Isothiocyanate	Aromatic
	1026.4	22.6	49214	M+2Na-H	Phenylalanine/derivative	
Cladosporium	963.3	18.5	37110	M+Na	Phenylalanine/derivative	
	969.3	19.1	9211	M+2Na-H	Hydroxycinnamic acid glycoside	Aromatic
	439.9	21.7	7839	M+K	Aniline/substituted aniline	Aromatic
	498.4	24.6	6164	M+K	N-acyl amine	
	412.7	22.7	5295	M+H-H$_2$O	Benzene/substituted derivative	
	470.2	22.1	5215	M+	Ogliopeptides	
	909.4	21.7	41633	M+H	Polyamine	
	1394.3	23.7	30041	M+NH$_4$	Steroid/steroid derivative	Toxin
	407.4	22.2	14876	M+NH$_4$	Carboximidic acid/derivative	Toxin
	421.3	21.3	11526	M+K	Phenylpropane	Aromatic
Natural Biofilm	1231.4	22.7	7789	M+Na	Naphthalene sulfonic acid/derivative	Pigment
	999.5	22.0	6722	M+H	Glycerophospholipid	
	895.5	23.3	6270	M+NH$_4$	Amino acid/peptide/analogue	
	1120.3	22.8	5038	M+H-H$_2$O	Fatty acid ester	
	497.2	22.9	4735	M+H	Polypeptide	
	499.8	23.4	4223	M+H-H$_2$O	Diphenylether	
	1069.4	22.0	58915	M+2Na-H	Oligopeptide	
	842.3	19.3	44524	M+	Organoheterocyclic compound	Aromatic
	924.4	21.5	36113	M+NH$_4$	Oligolactosamine	
	1055.4	21.7	28858	M+NH$_4$	Protein derivative	
Penicillium	785.1	21.3	27888	M+H-2H$_2$O	Anthocyanidin	Pigment
	765.0	23.9	23886	M+H	Benzophenone	
	1020.3	22.2	22968	M+	Flavonoid	Pigment
	906.4	21.1	21925	M+K	Amino acid/peptide/analogue	
	845.8	23.3	21214	M+H-H$_2$O	Triradylglycerol	
	1395.4	23.3	19432	M+2Na-H	Penicillanic acid ester	Toxin
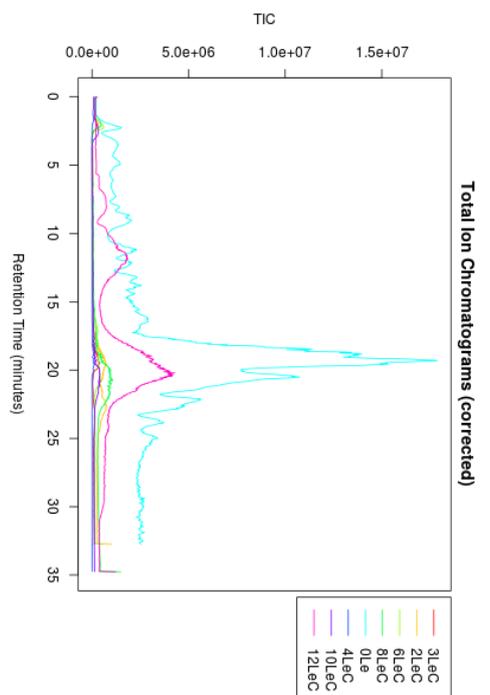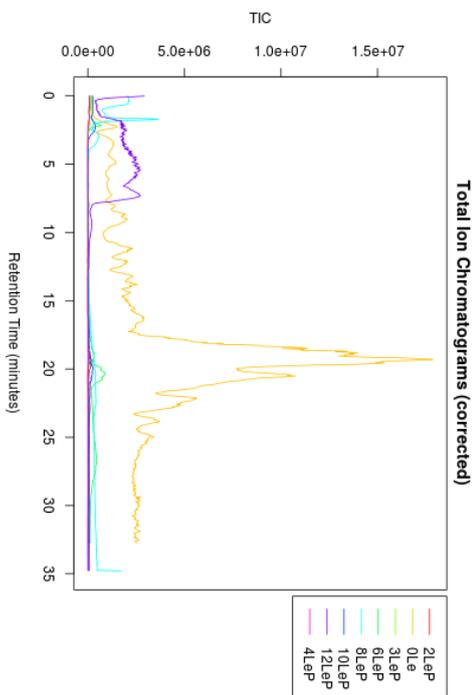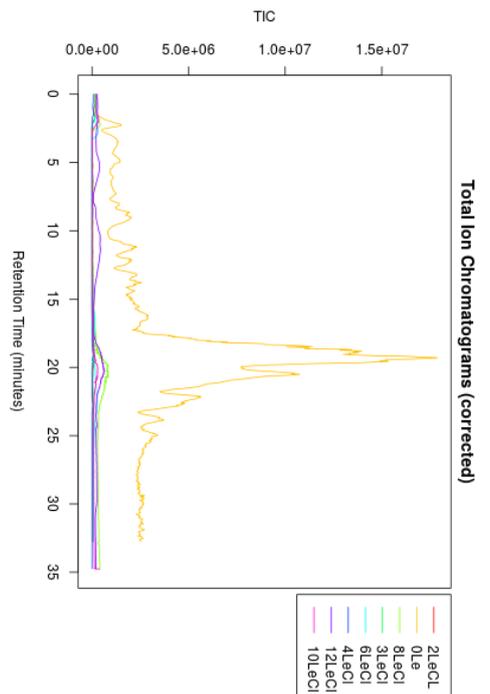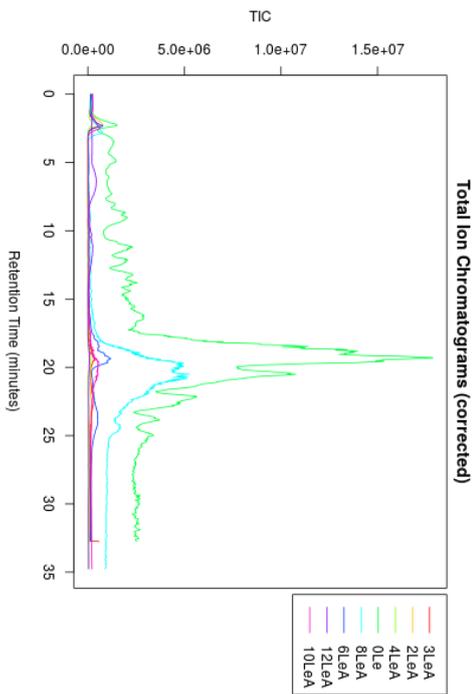
Retention time & baseline corrected total ion chromatogram for leather under each condition, produced by XC-MS. The key shows the sample code as the number of weeks incubated, Le for leather and the inoculation condition (A= Aspergillus*, Cl=*Cladosporium*, C=control/natural biofilm & P=*Penicillium*)*

The significant features from the total ion chromatogram for leather under each incubation condition that were not found in the control; identified using XC-MS and the chemical taxonomy of the compound from METLIN. M/z =the median mass over charge ratio of the feature peak, RT= median retention time, Max Int= the maximum intensity recorded for the feature.

Fungi	m/z	RT	Max Int	Adduct	Chemical taxonomy	Information
Aspergillus	1054.5	1054.5	208205	M+K	Steroidal saponin	
	709.4	709.4	110881	M+H-H$_2$O	Oligopeptide	
	870.1	870.1	81256	M+Na	Long-chain fatty acyl CoA	
	958.1	958.1	70941	M+K	Fatty acyl CoA	
	649.4	649.4	47986	M+H	Anthraquinone	Pigment
	666.1	666.1	47452	M+NH$_4$	Naphthalene/derivatives	Aromatic
	621.9	621.9	43596	M+H	Benzene/substituted derivative	
	578.2	578.2	41067	M+NH$_4$	Phenothiazine	Toxin
	754.2	754.2	39403	M+NH$_4$	Anthracene	Aromatic
	693.8	693.8	30621	M+2Na-H	Benzoic acid/derivative	
Cladosporium	973.3	19.5	6511	M+NH$_4$	Benzamide	Aromatic
	924.1	19.3	2701	M+K	Naphthalene sulfonate	Pigment
	1367.3	20.6	1684	M+K	Anthocyanidin	Pigment
	822.8	19.0	1157	M+NH$_4$	Triterpenoid	Aromatic
Natural Biofilm	930.1	20.3	30792	M+NH$_4$	Benzene/substituted derivative	Pigment
	1179.1	21.3	27498	M+Na	Naphthalene sulfonate	Pigment
	621.3	18.6	23308	M+H-2H$_2$O	Oligopeptide	
	666.8	19.0	20470	M+K	Fatty acid ester	
	913.2	20.0	19245	M+Na	Benzene/substituted derivative	
	870.9	20.0	12057	M+H-2H$_2$O	Steroid/steroid derivative	
	561.3	19.5	9518	M+H-2H$_2$O	Oligopeptide	
	885.5	20.2	9446	M+K	Glycerophosphoglycerol	
	988.3	18.9	9390	M+Na	Quinoline/derivative	Aromatic
	790.3	19.8	8277	M+K	Oligopeptide	
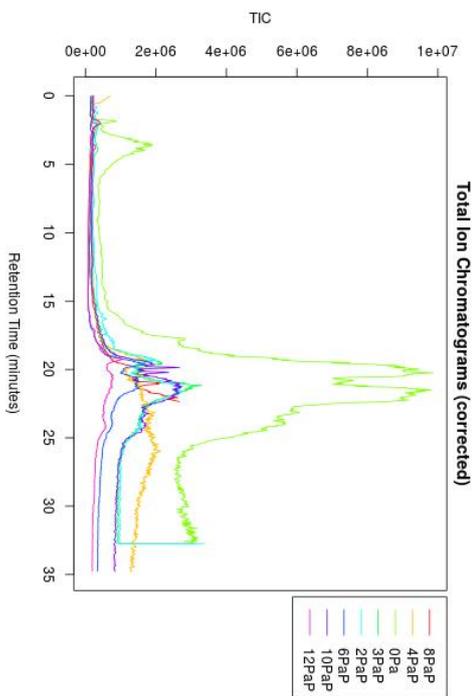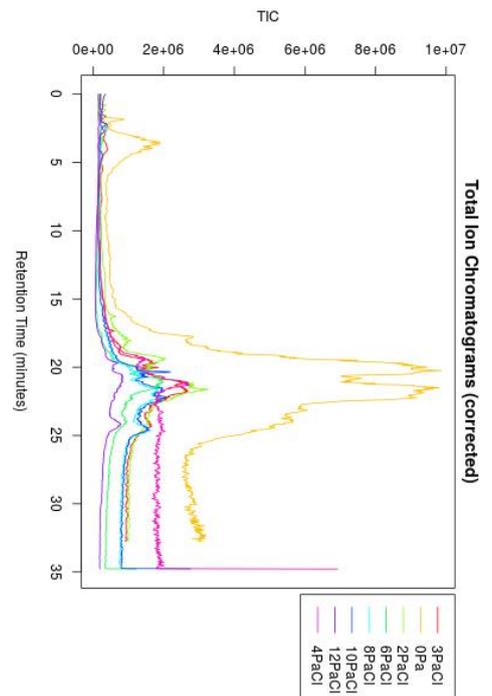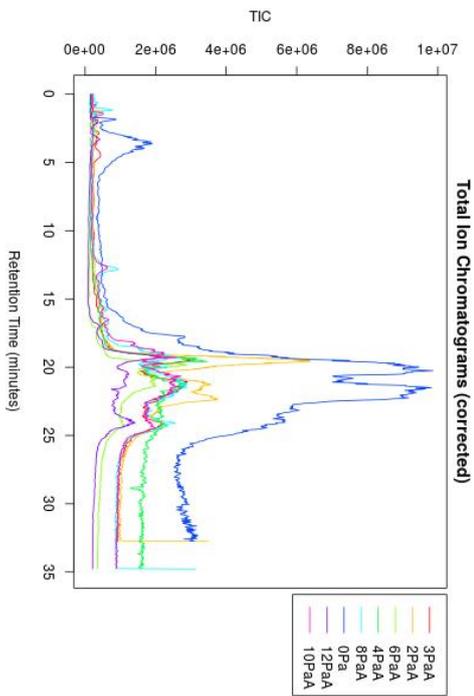
Retention time & baseline corrected total ion chromatogram for parchment under each condition, produced by XC-MS. The key shows the sample code as the number of weeks incubated, Pa for parchment and the inoculation condition (A= Aspergillus, Cl=Cladosporium & P=Penicillium)

The significant features from the total ion chromatogram for parchment under each incubation condition that were not found in the control; identified using XC-MS and the chemical taxonomy of the compound from METLIN. M/z =the median mass over charge ratio of the feature peak, RT= median retention time, Max Int= the maximum intensity recorded for the feature.

| Fungi	m/z	RT	Max Int	Adduct	Chemical taxonomy	Information
	413.4	20.0	110944	M+Na	Oxygenated hydrocarbon	
	913.3	20.6	103284	M+H-2H$_2$O	Anthocyanidin	Pigment
	1089.2	20.9	50368	M+H-H$_2$O	Triazines	Aromatic
	1085.2	20.9	47385	M+H-2H$_2$O	Benzofuran	Aromatic
	561.4	20.9	35482	M+NH$_4$	Ogliopeptide	
Aspergillus	1133.1	21.1	30663	M+H	Aromatic organonitrogen compound	
	910.5	24.9	25207	M+H	Ogliopeptide	
	791.3	19.5	21725	M+K	Ogliopeptide	
	824.3	20.1	21545	M+K	Heteroaromatic compound	Aromatic
	414.3	19.7	18288	M+Na	Alkanolamines	
	1133.2	21.0	28989	M+K	Volatile amine	
	683.8	19.6	11476	M+	Acetamides	
	953.3	21.1	10696	M+2Na-H	5'-deoxy-5'-thionucleosides	
Cladosporium	1099.4	20.8	10035	M+H	Tryptamine/derivative	
	909.3	21.0	9232	M+	Triazines	
	1085.3	21.5	6161	M+Na	Flavone/Flavonol	Pigment
	852.5	24.1	2132	M+K	Ceramide phosphoinositol	
	533.2	20.6	2090	M+2Na-H	Ogliopeptide	
	623.0	21.2	114043	M+H	Flavone/Flavonol	Pigment
	723.7	19.7	15605	M+NH$_4$	Bipyridine/oligopyridine	Pigment
	818.3	23.9	11596	M+H	Oligolactosamines	
	547.1	19.2	8253	M+H-2H$_2$O	Flavone/Flavonol	
Penicillium	666.9	21.5	7750	M+Na	Organic acid ester	
	547.0	19.0	5917	M+NH$_4$	Purine ribonucleoside triphosphates	
	791.3	19.5	5421	M+K	Ogliopeptide	
	638.4	19.4	4828	M+H-H$_2$O	Cyclic depsipeptide	

Baseline corrected mean ATR-FTIR absorbance spectra of cotton with Aspergillus *(a),* Cladosporium *(b),* Penicillium *(c) and the natural biofilm (d) taken over 12 weeks of incubation. Spectra formed from an average of 32 scans, between 4000-400cm^{-1}, at a resolution of 4cm^{-1}. Key features include:*

2930-2910 – C-H stretching

2860-2840 – C-H$_2$ symmetrical stretching

1750-1720 – C=O carbonyl stretching

1635 – adsorbed water

1155 – C-C ring breathing, asymmetric stretch

1025– C-OH stretch, alcohol

980 – C-H wagging in-plane

Baseline corrected mean ATR-FTIR absorbance spectra of linen with Aspergillus (a), Cladosporium (b), Penicillium (c) and the natural biofilm (d) taken over 12 weeks of incubation. Spectra formed from an average of 32 scans, between 4000-400cm⁻¹, at a resolution of 4cm⁻¹. Key features include:

3340-3310 - O-H stretching
2935-2900 - C-H stretching
2860-2845 - C-H₂ stretching
1635 - adsorbed water
1095-1060 - C-OH stretching secondary alcohols
970-920 - C-H wagging in-plane

Baseline corrected mean ATR-FTIR absorbance spectra of cotton and linen paper with Aspergillus *(a),* Cladosporium *(b),* Penicillium *(c) and the natural biofilm (d) taken over 12 weeks of incubation. Spectra formed from an average of 32 scans, between 4000-400cm^{-1}, at a resolution of 4cm^{-1}. Key features include:*

3340-3310 - O-H stretching

2935-2900 - C-H stretching

2860-2845 - C-H$_2$ stretching

1750-1720 - C=O stretching of carbonyls

1635 - adsorbed water

1326-1301 - C-H wagging deformation

1081-1032 - C-OH stretching primary & secondary alcohols

970-920 - C-H wagging in-plane

Baseline corrected mean ATR-FTIR absorbance spectra of beech wood paper with Aspergillus *(a),* Cladosporium *(b),* Penicillium *(c)* and the natural biofilm *(d)* taken over 12 weeks of incubation. Spectra formed from an average of 32 scans, between 4000-400cm⁻¹, at a resolution of 4cm⁻¹. Key features include:

3340-3310 - O-H stretching
2935-2900 - C-H stretching
2860-2845 - C-H_2 stretching
1635 - adsorbed water
1326-1301 - C-H wagging deformation
1150-1140 - C-C ring breathing & C-O-C stretching
1081-1032 - C-OH stretching primary & secondary alcohols
970-920 - C-H wagging in-plane

Baseline corrected mean ATR-FTIR absorbance spectra of pine with Aspergillus (a), Cladosporium (b) and Penicillium (c) taken over 12 weeks of incubation. Spectra formed from an average of 32 scans, between 4000-400cm⁻¹, at a resolution of 4cm⁻¹. Key features include:

3340-3310 - O-H stretching
2935-2900 - C-H stretching
2860-2845 - C-H$_2$ stretching
1746-1705 - C=O stretching of carbonyls
1635 - adsorbed water
1580-1540 - C=C aromatic ring stretching
1510-1505 - C=O aromatic ring stretching
1087-1067 - C-OH stretching of secondary alcohols
1015-966 - C-H wagging in-plane

Baseline corrected mean ATR-FTIR absorbance spectra of oak with *Aspergillus (a)*, Cladosporium *(b)* and Penicillium *(c)* taken over 12 weeks of incubation. Spectra formed from an average of 32 scans, between 4000-400cm^{-1}, at a resolution of 4cm^{-1}. Key features include:

3340-3310 - O-H stretching
2935-2900 - C-H stretching
2860-2845 - C-H$_2$ stretching
1746-1705 - C=O stretching of carbonyls
1635 - adsorbed water
1246-1226 - C-O stretch of lignin
1085-1065 - C-OH stretching of secondary alcohols
970-920 - C-H wagging in-plane

Baseline corrected mean ATR-FTIR absorbance spectra of silk with Aspergillus *(a)*, Cladosporium *(b)*, Penicillium *(c) and the natural biofilm (d) taken over 12 weeks of incubation. Spectra formed from an average of 32 scans, between 4000-400cm^{-1}, at a resolution of 4cm^{-1}. Key features include:*

1605-1579 - Amide I- C=O stretching, C-N stretching & C-H-N in-plane bending

1526-1477 - Amide II- N-H in-plane bending, C-N stretching & C=O in plane bending

1151-1116 - Primary & secondary aliphatic amine
C-N stretching

1100-973 - C-N & C-C skeletal stretching

685-406 - S-S stretching

Legend (each panel a, b, c, d):
- Control
- 2 weeks
- 3 weeks
- 4 weeks
- 6 weeks
- 8 weeks
- 10 weeks
- 12 weeks

Baseline corrected mean ATR-FTIR absorbance spectra of wool with Aspergillus *(a)*, Cladosporium *(b)*, Penicillium *(c)* and the natural biofilm *(d)* taken over 12 weeks of incubation. Spectra formed from an average of 32 scans, between 4000-400cm^{-1}, at a resolution of 4cm^{-1}. Key features include:

2942-2897 - C-H stretching
2862-2844 - C-H$_2$ stretching
1754-1738 - C=O stretching of carbonyls
1677-1590 - Amide I- C=O stretching, C-N stretching &
 C-H-N in-plane bending
1580-1477 - Amide II- N-H in-plane bending, C-N stretching
 & C=O in plane bending
1273-1218 - Amide III- 1260–1300 α-helix, 1240–1250
 disordered structure, 1230–1240 β-pleated sheet
1102-1000 - S-O stretching resulting from cysteine

303

Baseline corrected mean ATR-FTIR absorbance spectra of leather with Aspergillus *(a),* Cladosporium *(b),* Penicillium *(c) and the natural biofilm (d) taken over 12 weeks of incubation. Spectra formed from an average of 32 scans, between 4000-400cm^{-1}, at a resolution of 4cm^{-1}. Key features include:*

2958-2889 - C-H stretching
2870-2842 - C-H$_2$ stretching
1675-1590 - Amide I- C=O stretching, C-N stretching & C-H-N in-plane bending
1569-1536 - Amide II- N-H in-plane bending, C-N stretching & C=O in plane bending
1465-1436 - C-H3 in-plane bending
1153-1134 - Amide III- 1260–1300 α-helix, 1240–1250 disordered
 structure, 1230–1240 ß-pleated sheet
1100-959 - C-O-C, C-O, C-H and C-N stretch (s)/ bend (b) in
 primary/secondary alcohols (s), alkenes (b) & aliphatic
 amines (s)
916-910 - O-H bending of carboxylic acids
561-518 - Torsional N-H oscillation (525cm-1)
479-414 - N-H wagging
 in-plane

304

Baseline corrected mean ATR-FTIR absorbance spectra of Parchment with Aspergillus *(a)*, Cladosporium *(b)* and Penicillium *(c)* taken over 12 weeks of incubation. Spectra formed from an average of 32 scans, between 4000-400cm^{-1}, at a resolution of 4cm^{-1}. Key features include:

2923-2911 - C-H stretching

2850-2848 - C-H$_2$ stretching

1652-1612 - Amide I- C=O stretching, C-N stretching & C-H-N in-plane bending

1581-1512 Amide II- N-H in-plane bending, C-N stretching & C=O in plane bending

1112-983 - C-O-C, C-O, C-H and C-N stretching (s)/ bending (b) in primary/secondary alcohols (s), alkenes (b) and aliphatic amines (s)

655-443 - N-H torsional oscillation/wagging in-plane

305